ALMA MATER STUDIORUM
UNIVERSITÀ DI BOLOGNA

DOTTORATO DI RICERCA IN

ONCOLOGIA, EMATOLOGIA e PATOLOGIA

Ciclo XXXVII

Settore Concorsuale: 06/MEDS-02 PATOLOGIA GENERALE E PATOLOGIA CLINICA

Settore Scientifico Disciplinare: MEDS-02/A Patologia generale

Resistance to targeted therapy and immunotherapy in Non-Small Cell Lung Cancer (NSCLC) and development of novel therapeutic approaches

Presentata da: Dott.ssa Stefania Angelicola

Coordinatore Dottorato

Prof.ssa Manuela Ferracin

Supervisore

Prof. Pier-Luigi Lollini

Co-Supervisore

Dott.ssa Arianna Palladini

Esame finale anno 2025

Table of Contents

Abstract

Lung cancer is the first cause of cancer death worldwide and has been recently declared the most common tumor in the world. Non-small cell lung cancer (NSCLC) accounts for 85-90% of all lung cancers and it is unfortunately characterized by poor prognosis and late diagnosis. The introduction of tyrosine kinase inhibitors (TKIs) specifically targeting oncogenic mutations, including *EGFR*, *BRAF*, *ALK* and *ROS1*, in clinical practice has redefined treatment options for oncogene-driven NSCLC. On the other hand, the use of immune checkpoint inhibitors (ICIs) has provided an important breakthrough in the treatment of patients with unknown or undruggable oncogene-driven tumors. However, the emergence of therapeutic resistance remains a critical challenge. Tumor heterogeneity and the presence of resistant tumoral subclonal populations often lead to disease progression despite initial responses to TKIs or ICIs. Additionally, certain mutations–like *BRAF* class III and other "orphan mutations"–are currently lacking effective targeted therapies, leaving patients with these mutations underserved by available treatment options.

The aim of this PhD project was to investigate the mechanisms of resistance to the current therapeutic approaches, identify prognostic markers of response to therapy and explore novel therapeutic strategies for the treatment of NSCLC by directly analyzing tumors from therapy-resistant patients. To achieve these goals, we established a panel of primary cell cultures and patient-derived xenografts (PDXs) from tumor specimens of patients receiving TKI- or ICI-based therapies, whose disease progressed during treatment.

Within this panel, which included cases with rare clinical and molecular features, we concentrated our investigations on specific cell models, each offering unique insights into critical aspects of NSCLC resistance. First, these models enabled us to explore the role of tumor heterogeneity in TKI resistance by characterizing the *ROS1*-rearranged ADK-VR2 cell line and the *EGFR*-mutated LIBM-ADK-11 cell line. We also explored novel therapeutic strategies for tumors harboring orphan mutations that currently lack effective treatment options, utilizing the *BRAF* class III-mutated ADK-14 and PDX-ADK-36 cell lines. Moreover, we examined the mechanisms underlying resistance or adverse responses to ICI therapy, such as hyperprogressive disease (HPD), utilizing the *KRAS*-mutated ADK-17 and ADK-18 cell lines. To further investigate the molecular mechanisms driving hyperprogression and ICI resistance, we also employed a preclinical *in vivo* model of ICI resistance developed in syngeneic immunocompetent mice, using the transgenic murine BoLC.8M3 cell line, which carries a *KRAS* mutation and is *p53* knock-down.

Together, these models create a comprehensive platform to advance our understanding of resistance mechanisms in NSCLC and support the development of more effective targeted therapies.

Introduction

1. AN OVERVIEW ON LUNG CANCER

Lung cancer holds an unfortunate double record in cancer global burden, as it is not only the first cause of cancer death worldwide, accounting for the 18.7% of the total cancer deaths, with an estimated 1.8 million deaths in 2022, but it has also recently surpassed breast cancer as the most commonly diagnosed neoplasm in the world (12.4% of cases *vs* 11.6%) (Bray et al., 2024).

Despite men are twice as likely to be diagnosed with lung cancer, incidence and mortality among women is continuing to rise, unlike men (Bray et al., 2024; International Agency for Research on Cancer - World Health Organization, Cancer Today). The reasons of this trend are probably multifactorial, and may include increased tobacco consumption by women over the years, biological factors, genetics and sex differences in tolerability to therapies (Florez et al., 2024). Additionally, low-income countries report the highest mortality rates for lung cancer due to limited access to healthcare and cancer treatment, as well as inadequate public health initiatives for smoking cessation and early detection, despite generally lower incidence rates compared to high-income countries (Leiter et al., 2023; Bray et al., 2024). Indeed, despite environmental and occupational factors have been reported to contribute to lung cancer incidence, including exposure to secondhand smoke, asbestos, radon and air pollution, smoking tobacco remains the predominant risk factor for lung cancer, being responsible for about 85% of all cases (Leiter et al., 2023). Interestingly, the remaining cases of lung cancer are diagnosed in patients who never smoked and, contrarily to smoking-related lung tumors, their incidence is increasing, according to cancer statistics (de Alencar et al., 2022; LoPiccolo et al., 2024). Smoking-related and non-smoking related lung tumors are considered two totally distinct entities in terms of biological, genetic and epidemiological features, leading to important implications regarding the choice of the optimal therapeutic approach (Yano et al., 2008; de Alencar et al., 2022).

2. LUNG CANCER SCREENING

Regardless of the risk factors, lung cancer shows a tremendous mortality rate due to the absence of adequate screening programs which inevitably leads to late-stage diagnosis. Indeed, it has been estimated that only 15% of lung cancer patients are still alive 5 years after the diagnosis and that about 70% of patients show advanced, metastatic disease at the time of the diagnosis (de Koning et al., 2020). Conversely, patients with early-stage lung cancer have been reported to have a >75% chance of survival over 5 years (Goldstraw et al., 2016). It is clear that implementing screening programmes able to identify patients affected with lung cancer at earlier stages can be considered a significant public health concern, since it would significantly improve lung cancer patients' survival

chances. Currently, the only available existing screening approach for the early diagnosis of lung cancer is the low-dose computed tomography (LDCT)-based screening in asymptomatic individuals, which is still in an experimental phase and whose risk and benefits are still under evaluation. LDCT is the only approach that has demonstrated a significant reduction of mortality rates in patients who were at high risk of developing lung cancer (*e.g.*, current and former heavy smokers, ≥ 30 or more pack-years of cigarette smoking history), as reported by two major, independent, large randomized controlled trials, the US National Lung Screening Trial (NLST) and the NELSON trial (Aberle 2011; de Koning et al. 2020). The NLST reported that subjects undergoing annual LDCT-based screenings for three years showed a 20% relative reduction in mortality from lung cancer, as compared to subjects undergoing chest radiography-based screenings with the same frequency, after a median follow up of about 7 years (Aberle et al., 2011). Accordingly, the NELSON trial reported that lung cancer-related mortality had reduced by a quarter in patients that had undergone LDCT-based screening procedures (executed four times in six years), as compared to patients that had not been screened (Ru Zhao et al., 2011; de Koning et al., 2020).

Despite the evidence about the impact that LDCT-based screening programmes may have on lung cancer-related mortality reduction, the compliance to this procedure is still suboptimal (Pham et al., 2020). In the United States of America (USA), lung cancer LDCT-based screening is annually performed in high-risk patients, according to the U.S. Preventive Services Task Force (USPSTF) recommendations (*i.e.*, annual screening for adults aged 50-80 years with a smoking history of at least 20 pack-years or that have quit within the last 15 years) (Bandi et al., 2024). Nevertheless, a report from the American Lung Association estimated that only about 6% of eligible Americans underwent LDCT-based screening in 2021 (American Lung Association, 2022).

Similarly, United Kingdom (UK) is also implementing lung cancer early detection through LDCT-based screening programmes, inviting adults aged 55-74 with an history of smoking in their GP health record to be assessed for their risk and eventually be screened (Oudkerk et al., 2021; Mahase, 2023). Nevertheless, even among the most efficient centers of the UK in terms of recruitment of high-risk adults for lung cancer screening, very few have reported a percentage of participation rate that reaches 50% (Crosbie et al., 2019; Ghimire et al., 2019; Bartlett et al., 2020).

It is clear that the real-world effectiveness of lung cancer screening is still very far from the one reached by other screening programmes, including breast, cervical and colorectal cancer screening programmes (Armstrong et al., 2016). The reasons are to be found in several factors, including inadequate awareness about the topic, stigma associated with smoking, financial concerns, cost-effectiveness, lack of knowledge among physicians regarding screening guidelines and recommendations and geographic disparities in healthcare access (van der Aalst et al., 2021; Amicizia

et al., 2023). By the way, the implementation of LDCT-based screening is still ongoing and it will presumably become standard clinical practice in the next years. In this context, the parallel implementation of smoking cessation interventions should be integrated into lung screening programmes, in order to achieve the best possible results in terms of patients'survival.

3. LUNG ANATOMY AND LUNG CANCER HISTOLOGY

The lung is a complex organ used for multifaced primary and secondary functions, which include not only efficient gas exchange (Haddad, 2024), but also blood pH and blood pressure regulation (Takase et al., 2023), filtering and excretion of substances from the bloodstream (Joseph et al., 2013), metabolic roles (Alvarado & Arce, 2016; Liu & Summer, 2019), protection and temperature and humidity regulation (Haut et al., 2023; Haddad, 2024). The lungs are two paired, cone-shaped organs within the thoracic cavity, separated by the mediastinum and covered by double-layered pleural membranes, which secrete a certain amount of pleural fluid that lubricates the pleural surfaces reducing friction during breathing (Chaudhry, 2024). Structurally, the lung consists of respiratory bronchioles leading to alveolar ducts, which open into clusters of alveoli (Nanjwade et al., 2011). Bronchi and alveoli are surrounded by a connective tissue, enriched not only of lymphatic vessels, blood vessels and nerves, but also of several cell types, including macrophages, fibroblasts, and other immune cells (Ruge et al., 2013; Patel et al., 2015).

Considering its primary function of gas exchange, the lung is constituted of more than 40 cell types, which form a unique architecture necessary to guarantee its functioning (Cunniff et al., 2021).

The main types of cell types found in the lung are listed below (**Figure I**):

1. **Epithelial Cells**:
    - **Basal cells:** progenitors for other epithelial cell types, located in the airway epithelium (Cardoso & Whitsett, 2008);
    - **Goblet cells:** responsible for mucus production (D. F. Rogers, 1994);
    - **Ciliated cells:** endowed cilia that facilitate the moving of mucus and debris out of the airways (Gohy et al., 2019);
    - **Club cells:** responsible for surfactants secretion, involved in detoxification and located in the bronchioles (Cardoso & Whitsett, 2008);
    - **Pulmonary neuroendocrine cells (PNECs):** involved in airway-nerve communication, airway oxygen sensing, regulation of pulmonary blood flow, control of bronchial tonus, modulation of immune responses (Song et al. 2012);

- **Type I pneumocytes:** extremely thin cells that line the alveoli, facilitating gas exchange between the alveoli and blood (Song et al., 2012);
- **Type II pneumocytes:** responsible for surfactant secretion, they can differentiate into type I pneumocytes (Song et al., 2012).

2. **Immune cells:**
   - **Alveolar macrophages (AMs):** involved in innate defense mechanism, located within the alveoli (Chang et al., 2023);
   - **Dendritic cells:** responsible for the recognition and internalization of microbial antigens and the initiation of specific immune responses, located within the epithelium and interstitium of the lung (Lambrecht et al., 2001).

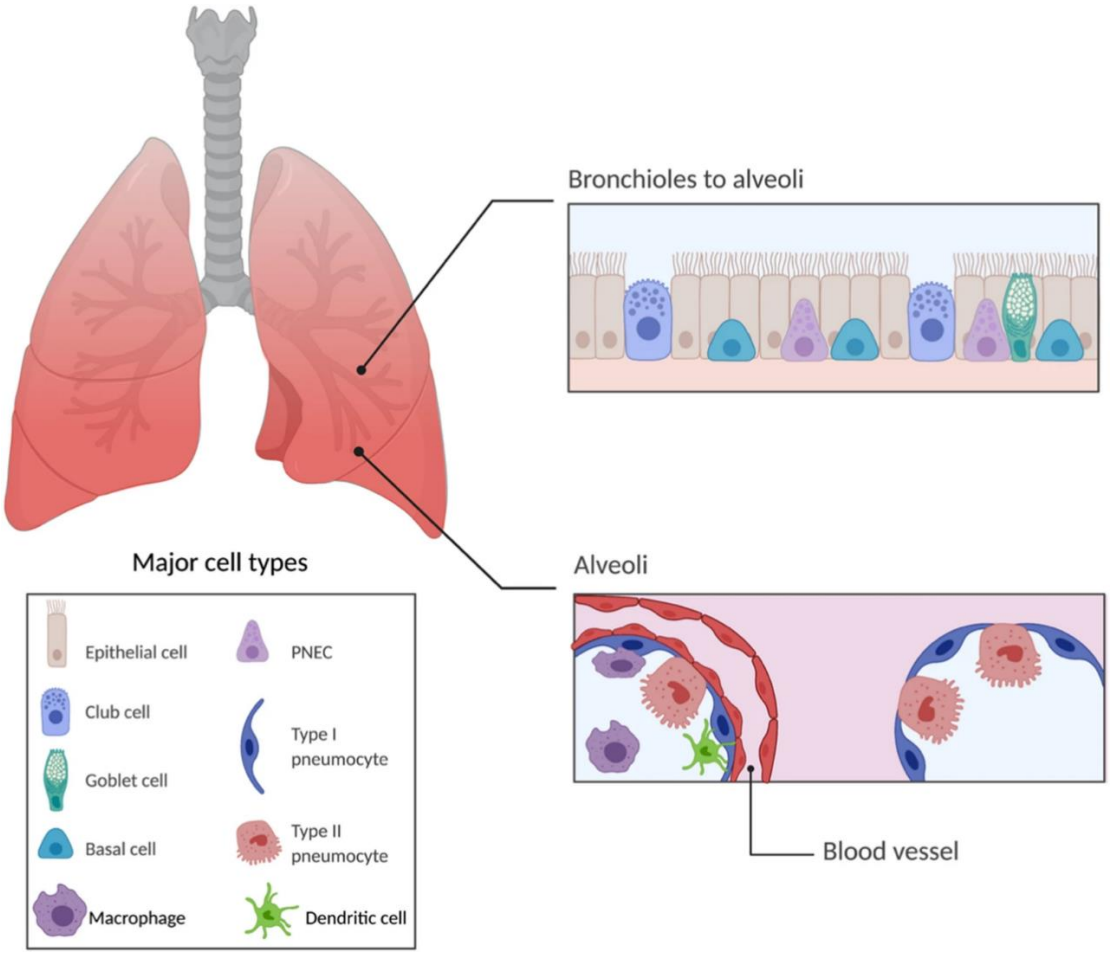

Figure I. The main types of cell lines found in the lung – from He et al., 2022.

In addition, bronchioalveolar stem cells (BASCs) have been also identified at the interface between the bronchioles and alveoli. These epithelial progenitor cells possess a bipotent nature, enabling them to differentiate into both Club cells and type II pneumocytes (Jones-Freeman & Starkey, 2020).

The origin of lung cancer can involve different types of cells among the ones described above. This type of malignancy is indeed highly heterogenous and, as described by the World Health Organization (WHO), can be characterized by widely variable clinicopathological features (Travis, Brambilla, Nicholson, et al., 2015). A histological classification of lung cancer is essential not only for the diagnosis, but also for the choice of adequate treatment planning.

Lung cancer can be classified in two major histological subgroups: Non-Small Cell Lung Cancer (NSCLC), which accounts for 85-90% of all lung cancer cases, and Small Cell Lung Cancer (SCLC), which is less common, making up about 10-15% of all lung cancer cases (**Figure IIA**).

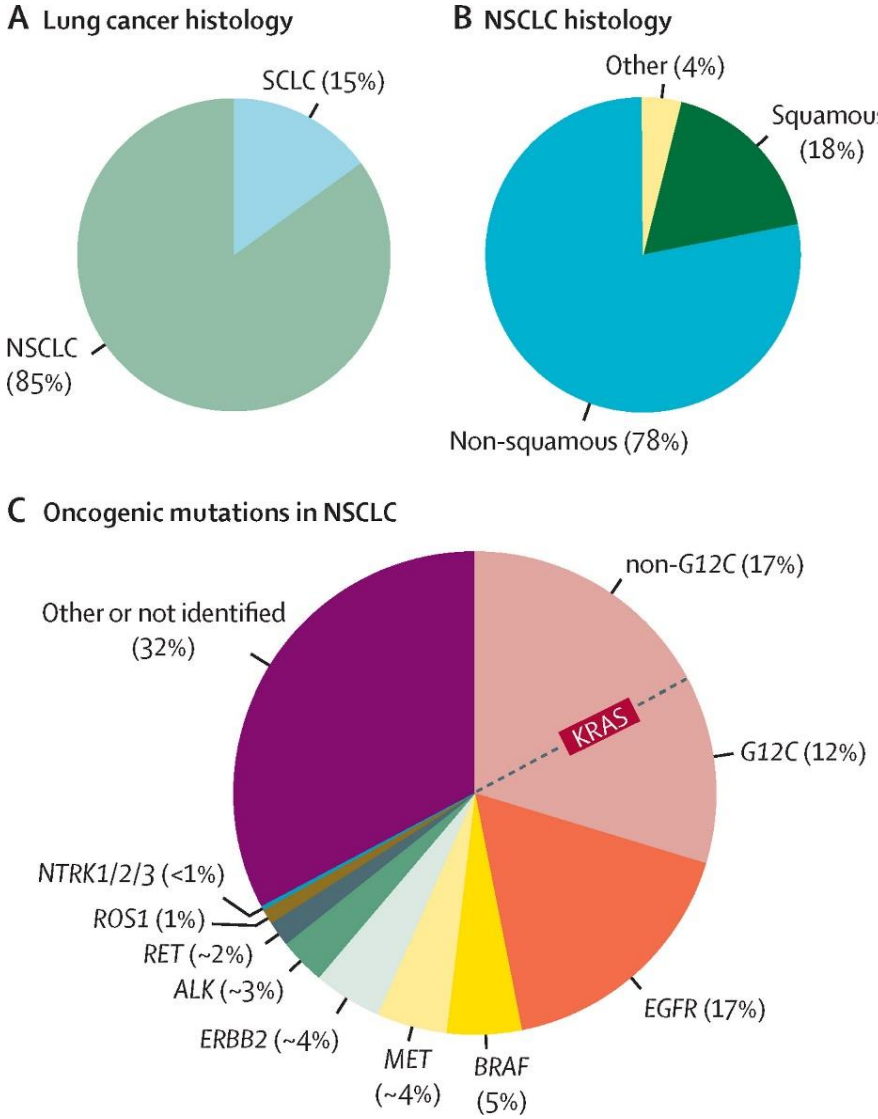

Figure II. Lung cancer histology and NSCLC molecular classification – from Thai et al., 2021. (A) Frequency of lung cancer histologies. **(B)** Frequency of NSCLC histologies. **(C)** Frequency of oncogenic driver mutations in NSCLC.

The names of the two subgroups refer to the microscopic appearance of the cancer cells, which allows to distinguish the type of lung cancer based on cell size and morphology (Nicholson et al., 2022).

SCLC is thought to arise from PNECs, it is more aggressive and faster-growing as compared to NSCLC and its treatment is mainly based on chemotherapy combined with radiation therapy (Karachaliou, 2016). Differently, NSCLC is thought to originate from epithelial cells, including basal cells, BASCs or type II pneumocytes (Sutherland & Berns, 2010; Semenova et al., 2015). This type of lung tumor is generally less aggressive as compared to SCLC and shows a wider range of therapeutic options, including surgery, chemotherapy, radiation therapy, immunotherapy, and targeted therapy (Lemjabbar-Alaoui et al., 2015).

NSCLC can be further histologically subdivided into non-squamous lung adenocarcinoma (LUAD), which is the most common subtype of NSCLC, particularly in non-smokers (78% of NSCLC cases), lung squamous cell carcinoma (LUSC), strongly associated with cigarette smoking (18% of cases), and other rare types of NSCLC tumors, which include large cell carcinoma, adenosquamous carcinoma and sarcomatoid carcinoma (about 4% of cases) (Pelosi et al., 2015; Li & Lu, 2018; Li et al., 2020; Chen & Dhahbi, 2021) (**Figure IIB)**.

4. NSCLC MOLECULAR CLASSIFICATION

The recent advances in the field of molecular pathology, including the advent of sequencing technologies such as next-generation sequencing (NGS), have allowed the identification of specific molecular profiles within NSCLC, enhancing the understanding of the molecular pathology of this malignancy. The 2015 WHO Classification included a description of these novel NSCLC molecular profiles, based on the identification of potentially targetable driver genetic alterations in lung cancer (Travis, Brambilla, Burke, et al., 2015; Inamura, 2017). Later, the 2021 WHO Classification further updated these classifications, giving insights into the clinical management of NSCLC cases based on their molecular characteristics (Nicholson et al., 2022). These advances allowed to discover that approximately half of NSCLC adenocarcinomas shows actionable genetic mutations, paving the way for personalized therapeutic options (Navani et al., 2022; Friedlaender et al., 2024).

Since the identification of the epidermal growth factor receptor (EGFR) as the first gene carrying oncogenic driver alterations in NSCLC in 2004 (Lynch et al., 2004), several additional oncodriver genes have been identified to carry targetable mutations. These include Kirstin rat sarcoma virus (*KRAS*), v-raf murine sarcoma viral oncogene homolog B (*BRAF*), c-MET proto-oncogene (*MET*), human epidermal receptor 2 (*HER2* or ErbB2), anaplastic lymphoma kinase (*ALK*), rearranged during transfection (*RET*), ROS proto-oncogene 1 (*ROS1*) and rearranged neurotrophic receptor tyrosine kinase (*NTRK*) genes (Le et al., 2023), as well as newly emerging targets such as phosphatidylinositol-3 kinase (*PIK3CA*) and fibroblast growth factor receptors (*FGFR1-3*), which are

expanding the landscape of actionable mutations in NSCLC (Scheffler et al., 2015; Tan, 2020; Zhou et al., 2021).

KRAS mutations are the most common alterations found in about 25% of NSCLC patients, followed by *EGFR* (~17% of cases), *BRAF* (~5%), *MET* and *HER2* (~4% each), *ALK* (~3%), *RET* (~2%), *ROS1* and *NTRK* (~1% each) (Thai et al., 2021) (**Figure IIC**).

The identification of actionable oncogenic driver mutations associated with NSCLC in routine clinical practice is mainly executed through the use of high-throughput sequencing methods such as NGS, as recommended by oncology societies such as ESMO and ASCO (Singh et al., 2022). Polymerase chain reaction (PCR) techniques are also often used in conjunction with sequencing methods (Sholl, 2017). Additionally, fluorescence in situ hybridization (FISH) is employed to detect genetic rearrangements and amplifications, such as those involving *ALK* or *ROS1* genes (Conde et al., 2022).

4.1 Targetable oncogenic drivers in NSCLC

4.1.1 EGFR

EGFR is a transmembrane protein belonging to the ErbB family of tyrosine kinase receptors, which include ErbB1 (EGFR), ErbB2 (HER2), ErbB3 (HER3) and ErB4 (HER4) receptors (Hynes & Lane, 2005). EGFR is a receptor tyrosine kinase (RTK) constituted of an extracellular ligand binding domain, a transmembrane portion, and an intracellular tyrosine kinase domain, responsible for the initiation of the intracellular signaling pathway triggered by the receptor activation. Upon binding with a specific ligand, such as the epidermal growth factor (EGF), transforming growth factor alpha (TGF-α) or others (Singh et al., 2016), EGFR undergoes dimerization, forming homodimers with other EGFR proteins or heterodimers with other members of the ErbB family. EGFR dimerization stimulates its intrinsic tyrosine kinase activity, resulting in autophosphorylation of its intracellular domains. This, in turn, activates several pro-growth signaling pathways, including the RAS−mitogen-activated protein kinase (MAPK), PI3K/AKT/mTOR and JAK-STAT pathways (Wee & Wang, 2017).

In lung adenocarcinoma, *EGFR* mutations have been reported to be more common among Asian, young, female, non/light-smokers (Rosell et al., 2009). The majority of *EGFR* somatic mutations identified in NSCLC are defined as “activating mutations”, since the alteration frequently occurs into the adenosine triphosphate (ATP)-binding pocket of the intracellular tyrosine kinase domain of the receptor, resulting in a ligand-independent, constitutive activation of EGFR signaling (Gazdar, 2009).

The most common *EGFR* mutations identified in NSCLC are exon 19 deletions and exon 21 L858R point mutations, which account for 90% of *EGFR* alterations (Zhang et al., 2019). Patients carrying these mutations have been reported to show a good response to targeted, tyrosine kinase inhibitors (TKIs)-based therapy (Rosell et al., 2009; Mitsudomi et al., 2010; Fukuoka et al., 2011; Lee et al., 2013). Nevertheless, a subset of patients harbors uncommon *EGFR* alterations, which comprise an heterogenous group of alterations representing about 10% of all the *EGFR*-mutated NSCLC cases (Bar et al., 2023; Borgeaud et al., 2024). The most frequent uncommon *EGFR* mutations are *EGFR* exon 20 insertions (2.5% of all lung adenocarcinoma cases), which include more than 100 distinct variants and constitute 6% of *EGFR*-mutations in NSCLC (Yasuda, Kobayashi, et al., 2012; Friedlaender et al., 2022). These mutations are generally associated with worse prognosis in advanced NSCLC as compared to other *EGFR* mutations and low response to EGFR-targeted therapy (Oxnard et al., 2013; Gristina et al., 2020).

The current standard of care for *EGFR*-mutated NSCLC is osimertinib, a third-generation EGFR-TKI, which is used both as a first-line treatment or for the treatment of patients who develop resistance to earlier-generation EGFR-TKIs. As will be discussed in *Section 6.4*, osimertinib has demonstrated remarkable superiority over first- and second-generation TKIs, not only in terms of progression-free survival (PFS) and overall survival (OS), but also in its ability to penetrate the central nervous system (CNS) (Miles & Mackey, 2021; Zhang et al., 2023).

4.1.2 KRAS

KRAS is a protein involved in the transducing signaling of activated RTKs and in the consequent activation of intracellular signaling pathways. Specifically, KRAS is a GTPase protein, responsible for the conversion of guanosine triphosphate (GTP) to guanosine diphosphate (GDP). The switch between GTP and GDP, and vice versa, acts as a molecular switch. KRAS protein can indeed be found in two functional forms: the active GTP-bound state and the inactive GDP-bound one (Cascetta et al., 2022). When activated and bound to GTP, KRAS activates downstream effectors such as RAF and PI3K, leading to the activation of the RAS/RAF/MEK/ERK MAPK pathway, the PI3K/AKT/mTOR pathway or the RAS-like (RAL) pathway, which regulate cell division, proliferation, differentiation, and survival (Lambert et al., 2002; Hancock, 2003).

KRAS is the most frequently mutated oncogene in human cancer and also in NSCLC, in which *KRAS* mutations occur in about 30% of cases (Friedlaender, Drilon, Weiss, et al., 2020; Huang et al., 2021). Generally, *KRAS* mutations show higher frequency among Caucasian, female smokers (Judd et al., 2021). The most common alterations identified in NSCLC consists in substitution mutations in codon 12 (about 90% of *KRAS*-mutated NSCLCs), followed by mutations in codon 13 (6% of cases) and 61 (1% of cases) (Kalemkerian et al., 2018).

The most common mutations involving *KRAS* codon 12 are the following (Xie et al., 2021; Cascetta et al., 2022):

- G12C mutation (40% of *KRAS*-mutated NSCLCs), in which a residue of glycine is substituted by a residue of cysteine;
- G12V mutation (18-21% of *KRAS*-mutated NSCLCs), in which a residue of glycine is substituted by a residue of valine;
- G12D mutation (17-18% of *KRAS*-mutated NSCLCs), in which a residue of glycine is substituted by a residue of aspartic acid.

KRAS has been long considered an undruggable target due to its intrinsic characteristics, thus the development of KRAS-targeting agents has been and continues to be quite challenging. Despite this limitation, targeted therapies specific for the $KRAS^{G12C}$ mutation, *e.g.*, sotorasib and adagrasib, have been successfully developed and approved for clinical use, making G12C the most well-characterized and targetable *KRAS* mutation (Addeo et al., 2021).

4.1.3 BRAF

BRAF is a serine/threonine kinase involved in the signal transduction downstream of RAS, playing a crucial role in the activation of the MAPK signaling pathway, cell growth, differentiation and apoptosis (Zaman et al., 2019). The activation of RAS GTPases after the binding of a RTK by one of its ligands, leads to the dimerization and activation of RAF family members, which include ARAF, BRAF and CRAF (Malumbres & Barbacid, 2003). When activated, BRAF starts a cascade of kinase activation, phosphorylating MEK1/2, which in turn activates ERK1/2 proteins. This signaling cascade ends with the stimulation of transcription factors which modulate the activation of genes involved in several cellular processes (Hussain et al., 2015). In physiological conditions, the activation of the MAPK pathway is tightly regulated through mechanisms of negative feedback (Lake et al., 2016). Nevertheless, mutations in the *BRAF* gene result in persistent, uncontrolled activation of the RAS/RAF/MEK/ERK pathway, leading to cell proliferation and survival (Dankner et al. 2018).

BRAF mutations are rare in NSCLC, accounting for 2-5% of lung adenocarcinoma cases and are more frequent in never-smokers, women and aggressive histological types (Nguyen-Ngoc et al., 2015; Thai et al., 2021).

Based on the site of mutation, kinase activity, RAS-dependency and dimerization status, *BRAF* oncogenic mutations have been categorized in three classes (Yao et al., 2015):

- Class I *BRAF* mutations: this class includes V600E/K/D/R point mutations, which occur in the valine residue at codon 600. These mutations lead to a constitutive, RAS-independent stimulation of BRAF kinase activity, which has been reported to be 500–700-fold enhanced as compared to wild type form of BRAF (Wan et al., 2004). In this

class of mutations, BRAF signals as a monomer (Dankner et al., 2018; Yan et al., 2022). $BRAF^{V600E}$ is the most frequent class I mutation and accounts for 30–50% of all *BRAF* mutations in NSCLC (Planchard et al., 2024);

- Class II *BRAF* mutations: this class includes non-V600 mutations located in the activation segment (K601 and L597 mutations) or P-loop (G464 and G469 mutations), which are *BRAF* gene regions involved in the maintenance of the inactive BRAF conformation (Karoulia et al., 2016). These mutations lead to impaired RTK and RAS signaling by negative feedback and constitutive, RAS-independent, high or intermediate stimulation of BRAF kinase activity. In this class of mutations, BRAF requires dimerization with other BRAF proteins to activate the MAPK pathway (Dankner et al., 2018);
- Class III *BRAF* mutations: this class also includes non-V600 mutations located in the P-loop (G466), catalytic loop (N581) or the activation segment with Asp-Phe-Gly (DFG motif) (D594, G596) (Śmiech et al., 2020). These mutations lead to impaired or dead BRAF kinase activity, which in this case is RAS-dependent. In addition, in this class of mutations, BRAF requires CRAF to form heterodimers in order to activate MAPK signaling pathway (Dankner et al. 2018).

Non-V600 mutations are the most common mutations in *BRAF*-mutated NSCLC, accounting for 50-80% of the cases (Paik et al., 2011; Litvak et al., 2014; The Cancer Genome Atlas Research Network, 2014). While the dual inhibition of the MAPK pathway through BRAF and MEK inhibitors turned out to be an efficient therapeutic approach for $BRAF^{V600}$-mutated NSCLC, $BRAF^{non\text{-}V600}$-mutated NSCLC remain orphan of targeted therapies and their treatment currently remains challenging (Di Federico et al., 2022).

4.1.4 MET

The MET protein, also known as c-Met or hepatocyte growth factor receptor (HGFR), is a transmembrane RTK, which, upon binding to its ligand (hepatocyte growth factor, HGF), dimerizes, autophosphorylates specific tyrosine residues located within its intracellular kinase domain and initiates a downstream signaling cascade that ends with the activation of several intracellular pathways involved in cell growth and survival, including RAS-MAPK, PI3K/AKT/mTOR, FAK, STAT, RAC/PAK and Wnt/β-catenin signaling pathways (Kim & Salgia, 2009; Recondo et al., 2020). Alterations in the *MET* gene are highly heterogenous and comprise protein overexpression, gene amplifications, gene fusions and activating point mutations, which lead to aberrant, constitutive MET receptor activation (Frampton et al., 2015; Friedlaender, Drilon, Banna, et al., 2020).

In NSCLC, the main identified *MET*-associated alterations are *MET* exon 14 skipping (METex14, 3-4% of cases) and *MET* amplifications (MET-amp, 1-5% of cases), which have been more frequently reported in older, smoking patients and have been associated with poor prognosis (Friedlaender, Drilon, Banna, et al., 2020; Remon et al., 2023; Spitaleri et al., 2023).

METex14 alterations are generated by the aberrant splicing and skipping of exon 14 in MET messenger RNA transcript, resulting in missense mutations, insertions and/or gene deletions. Of note, exon 14 contains the binding site for a ubiquitin ligase, thus its skipping results in impaired MET ubiquitination and persistent activation (Kong-Beltran et al., 2006; Awad et al., 2016). METex14 mutations are actionable oncogenic alterations in NSCLC as they show good sensitivity to MET inhibitors (Santarpia et al., 2021). For instance, capmatinib and temotinib are two selective MET inhibitors that have shown marked efficacy in *MET*-mutated NSCLC, leading to their approval for the treatment of patients harboring *MET* exon 14 mutations (Mathieu et al., 2022)

4.1.5 HER2

HER2 is a transmembrane RTK which, unlike other ErbB family members, does not directly bind to any known ligands (Yarden, 2001). The activation of HER2 receptor indeed occurs in a ligand-independent manner, through its heterodimerization with other ligand-activated members of the ErbB family, *i.e.* EGFR, HER3 or HER4, or through its homodimerization with other HER2 receptors (Hsu & Hung, 2016; Friedlaender et al., 2022). In the first case, the binding of the ligands with the other ErbB receptors facilitates a conformational change in HER2, inducing its dimerization, autophosphorylation and downstream signaling cascades, similarly to other RTKs (Gutierrez & Schiff, 2011). In the second case, the formation of HER2 homodimers results in trans-phosphorylation between the receptors' kinase domains, leading to the activation of the downstream pathways (Santhanakrishnan et al., 2024). HER2 activation triggers intracellular signaling pathways, including MAPK, STAT and PI3K/AKT/mTOR pathways, which regulate cell proliferation, survival and anti-apoptotic signals (Mazières et al., 2013).

Alterations in *HER2* gene or in the number of HER2 copies can lead to constitutive activation of the receptor. In NSCLC these kinds of alterations have been reported to be more frequent in female, Asian, non-smoking patients with moderate or poorly differentiated adenocarcinomas (Arcila et al., 2012). Specifically, the main mechanisms of aberrant activation of HER2 identified in NSCLC are *HER2* gene mutations (1-4% of cases) or *HER2* amplifications (2-5% of cases) (Mazières et al., 2013; Yu et al., 2013). For what concerns *HER2* mutations, in-frame insertions in exon 20, located in the kinase domain of the receptor, are the most common *HER2* alterations in NSCLC, accounting for 3% of cases. This mutation is particularly frequent among younger non-smokers patients affected with adenocarcinoma (Mazières et al., 2013). Regarding *HER2* amplifications, these have been reported

to rarely occur as *de novo* alterations (only 2% of NSCLC cases), but rather frequently arise as a mechanism of acquired resistance to TKIs-based therapies (13% of cases) (Yu et al., 2013). Currently, the only Food and Drug Administration (FDA) approved targeted therapy for *HER2*-altered, metastatic NSCLC patients is the antibody-drug conjugate (ADC) Trastuzumab–Deruxtecan (T-DXd) (Vathiotis et al., 2023).

4.1.6 ALK

ALK is a transmembrane RTK which, upon binding with its ligands, *i.e.* ALKAL1 and ALKAL2, triggers the classical cascade of signal transduction described for other RTKs, resulting in the activation of RAS-MAPK, P3K/AKT/mTOR and JAK-STAT pathways (Reshetnyak et al., 2021). ALK expression is generally suppressed post-natally, as its role is predominantly associated with the fetal development of the nervous system (Chiarle et al., 2008). Therefore, its post-natally expression is frequently considered aberrant and disease-associated.

In general, the most common *ALK* alterations are gene rearrangements, which result in the expression of fusion ALK proteins that constitutively dimerize, inducing the aberrant activation of ALK kinase and downstream signaling pathways (Chiarle et al., 2008). Of note, more than 90 fusion partners for ALK have been described (Chiarle et al., 2008). Approximately 3-5% of NSCLC cases harbor *ALK* gene rearrangements, specifically *ALK* translocations involving the Echinoderm Microtubule-associated protein Like 4 (*EML4*) gene (McKeage et al., 2020). In general, *ALK* rearrangements show higher frequency in younger, light or never-smoker patients with adenocarcinoma and are mutually exclusive with *EGFR* or *KRAS* activating mutations (Shaw et al., 2009; Cognigni et al., 2022).

Other than rearrangements, *ALK* amplifications have also been reported in some cases of NSCLC, while *ALK* point mutations mainly arise as a mechanism of resistance to TKIs-based therapies (Wu et al., 2016).

Currently, several TKIs have received approval for the treatment of *ALK*-rearranged NSCLC. The first approved targeted therapy for *ALK*-rearranged, advanced NSCLC was the multikinase inhibitor crizotinib, whose use demonstrated improvement in progression-free survival (PFS) as compared to traditional chemotherapy (Shaw et al., 2013; Solomon et al., 2014). Second-generation multikinase inhibitors, including ceritinib, brigatinib, alectinib and ensartinib, were later approved for the treatment of crizotinib-resistant patients and were successful in overcoming acquired resistance to crizotinib (Peters et al., 2017; Camidge et al., 2020; Mok et al., 2020; Horn et al., 2021). Finally, the third-generation TKI lorlatinib, targeting ALK and ROS1, was approved to overcome the acquired resistance induced by previous TKIs-based therapies, and to improve intracranial therapeutic efficacy, as *ALK*-rearranged NSCLCs are known to have high risk for developing brain metastases,

which are already detectable in about 30% of patients at the time of diagnosis (Rangachari et al., 2015; Zou et al., 2015; Solomon et al., 2018; Allen et al., 2021).

4.1.7 RET

RET is a transmembrane RTK activated by the binding with ligands belonging to the glial cell line-derived neurotrophic factor (GDNF) family of ligands (GFLs) (Takahashi, 2022). Ligand-induced activation of RET results in dimerization and autophosphorylation of its kinase domains, leading to the activation of RAS-MAPK, PI3K/AKT/mTOR and JAK-STAT pathways (Ferrara, Auger, et al., 2018). Interestingly, RET intracellular kinase domain shares 37% of homology with the one of the ALK receptor (Ferrara, Auger, et al., 2018). Also, similarly to *ALK*, the most common *RET* alterations include *RET* gene rearrangements, which lead to the production of a chimeric RET fusion protein responsible for the aberrant and constitutive activation of RET downstream signaling pathways (Gainor & Shaw, 2013).

In NSCLC, *RET* rearrangements are detected in 1-2% of cases and are more frequent in younger, non-smoker patients affected with adenocarcinomas (Ferrara, Auger, et al., 2018). Additionally, these rearrangements are mutually exclusive with *EGFR*, *KRAS*, *BRAF* mutations and *ALK* and *ROS1* translocations (Takeuchi et al., 2012).

Kinesin family 5B (KIF5B) and coiled coil domain containing-6 (CCDC6) are the two most common RET fusion proteins (detected in 70-90% and 10-30% of *RET*-rearranged NSCLCs, respectively) (Sarfaty et al., 2017). Since the treatment of *RET*-rearranged NSCLC with multikinase inhibitors, including cabozantinib, sunitinib and vandetanib, revealed limited efficacy and significant toxicity, the therapy of *RET*-mutated NSCLC has recently shifted towards the use of two RET-selective TKIs, selpercatinib and pralsetinib, which have demonstrated high response rates, good safety profiles and high CNS penetrance, which is fundamental in tumors characterized by high risk of brain metastases such as *RET*-rearranged NSCLC (Drilon et al., 2018; Drilon et al., 2020; Gainor et al., 2021; Andrini et al., 2022).

4.1.8 ROS1

ROS1 is a transmembrane RTK whose specific physiological roles in human remain controversial. Despite the identification of the neural epidermal growth factor-like like 2 (NELL2) as a specific physiological ligand of ROS1 in mice, no ligand for the ROS1 receptor in human has still been identified so far (Kiyozumi et al., 2020; Drilon et al., 2021). Nevertheless, this protein is believed to act as a receptor for growth factors and differentiation signals. Evidence from several studies has demonstrated that ROS1 activation results in autophosphorylation of its intracellular tyrosine residues, which recruit specific adaptor proteins that stimulate the activation of pathways involved in

cell survival, growth and proliferation, including RAS-MAPK, PI3K/AKT/mTOR and JAK-STAT3 pathways (Drilon et al., 2021).

Similarly to *ALK* and *RET*, *ROS1* alterations mainly consist in *ROS1* rearrangements, which lead to the presence of a constitutively activated chimeric ROS1 fusion protein (Drilon et al., 2021). The demographic distribution of *ROS1* rearrangements resembles the one of *ALK* alterations, as these mutations are more frequent in female, Asian, younger, non-smoker patients affected with adenocarcinoma (Zhu et al., 2015; Park et al., 2018). Additionally, *ROS1*-rearranged NSCLC also show increased risk of brain metastases as compared to other oncogenic-driven tumors (incidence of about 35%) (Friedlaender et al., 2024).

ROS1 rearrangements can involve at least 26 different partner genes, including *CD74* (44% of *ROS1*-rearranged NSCLCs), *SDC4* (14%) and *EZR* (16%), and have been reported to be mutually exclusive with other oncogenic driver mutations, such as *EGFR*, *KRAS* and *ALK* alterations (Lin et al., 2017; Li et al., 2018; Neel et al., 2019; Ou & Nagasaka, 2020; Drilon et al., 2021).

Considering that the kinase domains of *ALK* and *ROS1*-rearranged proteins share a high grade of homology (> 80% of the sequence in the ATP-binding sites), crizotinib has also shown a good affinity and activity in *ROS1*-rearranged NSCLC, enough to be approved by the FDA as the first TKI for the treatment of *ROS1*-rearranged NSCLC (Shaw et al., 2019; Guaitoli et al., 2021). Nevertheless, crizotinib showed the therapeutic limitations of low intracranial penetration and induction of on-target *ROS1* mutations, causing acquired resistance to therapy (Gainor et al., 2017). For this reason, the multikinase inhibitors entrectinib and reprotrectinib have been approved as preferred therapeutic options for patients with intracranial dissemination, due to their superior CNS penetration and efficacy as compared to crizotinib (Almquist & Ernani, 2021; Parisi et al., 2022; ten Berge et al., 2023; Drilon et al., 2024). Lorlatinib has also been approved for the treatment of *ROS1*-rearranged NSCLC, demonstrating promising results regarding its intracranial penetrance and its capacity to overcome resistance in patients who have progressed on earlier TKI-based therapies (Girard et al., 2022; Testa et al., 2023; Ahn et al., 2024).

4.1.9 NTRK 1/2/3

The neurotrophic receptor tyrosine kinase (NTRK), also known as tropomyosin receptor kinase (TRK) proteins, are a family of RTKs, encoded by the *NTRK1*, *NTRK2* and *NTRK3* genes. The ligands of NTRK consist in four neurotrophic factors, *i.e.*, nerve growth factor (NGF), brain-derived neurotrophic factor (BDNF), neurotrophin 3 (NT-3) and neurotrophin 4 (NT-4), involved in the development and survival of neurons (Skaper, 2012; Amatu et al., 2019). Upon ligand binding, NTRK receptor undergoes dimerization, which induces the autophosphorylation of residues located in the kinase domain and the typical signaling cascade described for other RTKs, which lead to the

activation of downstream pathways, including RAS-MAPK, PI3K/AKT/mTOR, PKC and PLCγ pathways, all involved in neuronal development and function (Amatu et al., 2019).

NTRK translocations are quite rare alterations, detected in less than 1% of NSCLC cases (F. Liu et al., 2022). More than 25 fusion partners have been identified for *NTRK*, including *ETV6*, *LMNA* and *TPM3* (Vaishnavi et al., 2013; Marchiò et al., 2019). The result of *NTRK* fusions is the production of chimeric NTRK proteins characterized by constitutive activation of downstream signaling pathways, which promote tumor growth and survival. Generally, *NTRK* translocations in NSCLC are mutually exclusive with other common oncogenic alterations, including *KRAS*, *EGFR*, *ALK* and *ROS1* mutations or rearrangements (F. Liu et al., 2022).

For NSCLC patients harboring *NTRK* fusions, the fist-generation TKIs larotrectinib and entrectinib have been approved as first-line treatments (F. Liu et al., 2022; Friedlaender et al., 2024). Nevertheless, the development of resistance to these therapies remains a major limitation, necessitating the finding of alternative therapeutic options for this subset of patients (F. Liu et al., 2022).

5. NSCLC STAGING

Adequate tumor staging is crucial for determining the prognosis of the disease and the planning of better treatment options. Guidelines recommend the combined use of imaging methods, including fluorodeoxyglucose positron emission tomography (FDG-PET) and computed tomography (CT) (Heineman et al., 2017), while other techniques such as magnetic resonance imaging (MRI), provide better information about the extent of tumor invasion (Kajiwara et al., 2010). In case of identification of mediastinal nodes on scans, considering the low sensitivity of FDG-PET for lesions < 1 cm, minimally invasive procedures can be performed to confirm the presence of cancer cells, including endobronchial ultrasound and mediastinoscopy (Heineman et al., 2017; Thai et al., 2021).

In general, the most widely used system for tumor staging is the tumor, node and metastasis (TNM) staging system. This classification system, jointly developed by the American Joint Commission on Cancer (AJCC) and the Union for International Cancer Control (UICC), is a globally recognized method of classification of solid tumors based on three components: size and extent of the primary tumor (T, classification from T0 to T4), involvement of regional lymph nodes (N, from N0 to N3) and the presence of distant metastases (M, M0 or M1) (Lababede & Meziane, 2018; Rosen & Sapra, 2024).

Based on the information provided by the TNM staging system, the stages of NSCLC range from 0 to IV, indicating the extent of the spread (Quint, 2007; Heineman et al., 2017):

- **Stage 0**: also referred to as "carcinoma in situ" (CIS). Cancer cells are present only in the top lining of the lung or bronchus but have not spread over deeper lung tissues;
- **Stage I**: the cancer is localized to the lung and has not spread to the lymph nodes. It is further divided into two sub-stages (IA and IB), based on tumor dimensions;
- **Stage II**: the cancer may have spread to nearby lymph nodes, but not to distant organs. It is further divided into two sub-stages (IIA and IIB), based on tumor dimensions and the extent of lymph nodes involvement;
- **Stage III**: the cancer may have spread to lymph nodes in the mediastinum. This stage is sub-categorized into three sub-stages (IIIA, IIIB or IIIC), depending on tumor size, location and extent of spreading;
- **Stage IV**: the most advanced form of cancer. In this stage, the tumor has spread beyond the lung with metastases to distant organs. This stage is sub-divided into two sub-stages (IVA and IVB), depending on the extent of the spreading.

As previously mentioned, the 5-year survival rates of NSCLC patients vary significantly depending on the tumor stage at the time of the diagnosis, with a dramatic decline as cancer progresses. While 5-year survival for patients with stage I NSCLC is approximately 80%, it declines to 16-60% in patients with stage II-III NSCLC, reaching barely 10% in advanced NSCLC (Jeon et al., 2023). These rates highlight the difference that early lung cancer diagnosis and treatment can make in patients' chances of survival.

6. NSCLC TREATMENT APPROACHES

The choice of the optimal therapeutic approach for treating NSCLC cases is closely dependent on several variables, including tumor stage, molecular features, patient's clinical history and overall condition. By and large, the therapeutic landscape of NSCLC encompasses surgery, radiotherapy, chemotherapy, targeted therapy or immunotherapy, either as part of combined treatment regimens or as monotherapies.

6.1 Surgery

Surgical resection remains the preferred therapeutic approach for treating patients with early-stage, localized disease, eventually followed by adjuvant chemotherapy or radiotherapy. Assessing the involvement of draining lymph nodes is an integral part of surgery in NSCLC, given its critical role in defining the stage of the disease (Lackey & Donington, 2013; Heineman et al., 2017; Indini et al., 2020).

Lobectomy, accompanied by lymph node dissection (LND), is the gold standard for the treatment of early-stage NSCLC patients (Montagne et al., 2021). This procedure, in which the entire lung lobe containing the tumor is resected, has shown important advantages in terms of survival and local recurrence as compared to sublobar resections (Raman et al., 2018). For compromised patients with poor lung function and not eligible for lobectomy, segmentectomy is recommended (Ettinger et al., 2015; Macke et al., 2015). This procedure allows to reduce the extent of resection, removing only part of a lobe (Montagne et al., 2021). Nevertheless, sublobar resections are recommended only if safe margins can be obtained, in order to avoid local recurrence.

More drastic approaches, such as pneumonectomy, which consists in removing the entire lung, or sleeve resection, which entails removing only a cancerous lung lobe along with a part of the bronchus, may be necessary for centrally located tumors, advanced tumors or those that have extended into the bronchi, where a lobectomy would be insufficient (Yan et al., 2020; Dai et al., 2022; Wang et al., 2022; Lee & Razi, 2024).

While traditional open thoracotomy is the main chosen approach for lobectomy, segmentectomy and sleeve resection, today less invasive techniques are also being increasingly adopted, including video-assisted thoracoscopic surgery (VATS) and robotic-assisted thoracoscopic surgery (RATS), because of their proven advantages in terms of short-term outcomes, adverse events, hospitalization, postoperative complications, recovery times, morbidity and mortality rates (Montagne et al., 2021). Despite ongoing questions about the effectiveness of nodal assessment with these novel techniques, no difference in nodal upstaging or overall survival has been reported in the literature between open approaches and less invasive techniques, supporting the adoption of these new methods in clinical practice (Raman et al., 2018).

For advanced or metastatic NSCLC, surgery can be considered within the context of multimodality therapy (MMT), which also includes radiotherapy and systemic treatments such as chemotherapy, targeted therapy and immunotherapy as either adjuvant or neoadjuvant approaches (König et al., 2022; Petrella et al., 2023).

6.2 Chemotherapy

Chemotherapy is a common treatment approach for NSCLC, and it is often used in various stages and contexts. Currently, the main chemotherapeutic agents used in clinical practice include cisplatin and carboplatin together with gemcitabine, taxanes and pemetrexed, usually in association with some targeted therapy drugs (Ramalingam & Belani, 2008). While cisplatin, carboplatin and gemcitabine act by disrupting the DNA repair system, which result in DNA damage cancer cell apoptosis (Mini et al., 2006; Dasari & Bernard Tchounwou, 2014), taxanes show a different mechanism of action based on the disruption of microtubule formation dynamics, consequent cell

cycle arrest and cancer cell apoptosis (Zhao et al., 2005; Tan et al., 2011). Differently, pemetrexed acts by inhibiting the enzymes involved in the metabolism of folate, resulting in cell cycle arrest in the S phase (Guo et al., 2022).

In early-stage NSCLC, chemotherapy is either used in an adjuvant setting to lower the risk of disease relapse after surgical resection (Arriagada et al., 2004; Indini et al., 2020), or in the neoadjuvant setting before surgery resection, in case of resectable NSCLC or in node-positive disease, in combination or not with radiotherapy, in order to shrink the tumor mass and facilitate its surgical removal (Aguado et al., 2022; Kalvapudi et al., 2023).

Historically, before the discovery of immunotherapy and targeted therapies, platinum-based chemotherapy has been the standard first-line treatment for advanced NSCLC (Sculier & Moro-Sibilot, 2009; Kim & Halmos, 2020). Nevertheless, the current recommendations for advanced NSCLC often suggest an approach based on the combination of chemotherapy with other agents, such as platinum-based chemotherapy combined with pemetrexed or targeted agents or chemotherapy plus immunotherapy, depending on patient and tumor's characteristics (Sculier & Moro-Sibilot, 2009; Kim & Halmos, 2020; Lee & Razi, 2024).

6.3 Radiotherapy

Radiotherapy (RT), alongside surgery and systemic agents, is one of the three key components of the multidisciplinary therapeutic approach adopted for NSCLC treatment. It is estimated that more than half of NSCLC patients receive a radiotherapeutic treatment across all stages of the disease, with either curative or palliative intent (Rodríguez De Dios et al., 2022). Broadly, radiotherapy consists in the irradiation of tumor cells with high doses of ionizing radiation, which results in irreversible DNA damage and, consequently, in cell cycle arrest and tumor shrinkage (Sia et al., 2020). In recent years, technological advances have greatly improved this therapeutic approach, allowing a more precise targeting of tumors, maximizing tumor control and reducing treatment-related toxicities or incidental irradiation of peripheral healthy tissues (Vinod & Hau, 2020).

Stereotactic body radiation therapy (SBRT), also known as stereotactic ablative radiation therapy (SABR), is the strategy of choice for early-stage NSCLC patient ineligible for surgery (Rodríguez De Dios et al., 2022). This radiation strategy allows the delivery of high radiation doses to specific target volumes with extreme precision in few sessions, typically one to five, unlike conventional radiation therapy which often requires several sessions over multiple weeks (Jeppesen et al., 2013; Tsang, 2016; Giaj-Levra et al., 2020). SBRT has been reported to be well tolerated and to yield efficient local control rates (> 90%) in both operable and inoperable early-stage NSCLC

patients (Timmerman et al., 2018) and to better improve overall survival as compared to traditional radiation strategies (Palma et al., 2010; Giaj-Levra et al., 2020).

As for unresectable, locally-advanced NSCLC patients, the concurrent combination of chemotherapy, especially platinum-based therapy, and radiotherapy (chemoradiotherapy), followed by adjuvant durvalumab-based immunotherapy, is the standard of care and has demonstrated significantly improvement in the OS of this class of patients (Chaft et al., 2021; Dohopolski et al., 2021; Łazar-Poniatowska et al., 2021; Rodríguez De Dios et al., 2022). Nevertheless, while this approach has improved the control of local disease, it has not demonstrated to significantly reduce the risk of distant metastases, indicating the need of improve the therapeutic schedule of this subset of patients (Xu & Le Pechoux, 2015). Novel techniques, including intensity modulated radiation therapy (IMRT) or proton treatment with concurrent chemotherapy, have demonstrated to improve the outcome of patients with locally advanced NSCLC, as these approaches manage to maximize tumor delineation and treatment delivery and reduce off target irradiation (Giaj-Levra et al., 2020). These achievements are feasible thanks to the concurrent use of image-guided radiotherapy (IGRT), which includes, for example, four-dimensional computed tomography (4DCT), which allows to accurately assess tumor movements during respiration, reducing radiation exposure to surrounding healthy tissues (Khan et al., 2009). For what concerns advanced metastatic NSCLC treatment, for which the standard of care remains the use of targeted therapies or immunotherapy, radiation therapy has been historically used as a palliative tool aimed at alleviating tumor-associated symptoms (Faria, 2014; Zhou et al., 2020; Zhu et al., 2022). Of note, over the last decades, the therapeutic use of SBRT has been extended to the subclass of patients with limited metastatic disease, *i.e.* oligometastatic disease, for which it has been reported to significantly improve OS, tumor local control and PFS compared to conventional treatment approaches (Faria, 2014; Wujanto et al., 2019; Chai et al., 2020; Virbel et al., 2021).

6.4 Targeted therapy

The discovery of targeted therapies employing TKIs and small molecule inhibitors has profoundly transformed the clinical landscape of NSCLC. Prior to the advent of TKIs, NSCLC patients were largely restricted to conventional chemotherapy as their primary treatment option, which frequently resulted in limited therapeutic outcomes and significant adverse effects (Li & Kwok, 2020; Araghi et al., 2023). The use of TKIs has revolutionized treatment by selectively targeting specific molecular alterations within tumors, inhibiting signaling pathways that drive cancer cell proliferation and providing a more effective personalized therapeutic approach for NSCLC. Generally, TKIs function by selectively binding the ATP-binding site of specific RTKs, preventing their phosphorylation and activation. This inhibition disrupts downstream signaling cascades

essential for tumor growth and survival, ultimately reducing cancer cell proliferation and promoting apoptosis (Pottier et al., 2020).

To date, over a dozen TKIs have been approved for the treatment of NSCLC, with gefitinib marking a significant milestone as the first TKI introduced into clinical practice (Kazandjian, Blumenthal, et al., 2016). This groundbreaking therapy not only established *EGFR* as the first targeted oncogene in NSCLC, but also paved the way for subsequent targeted therapies, ultimately enabling the targeting of all other oncogenes (**Figure III**).

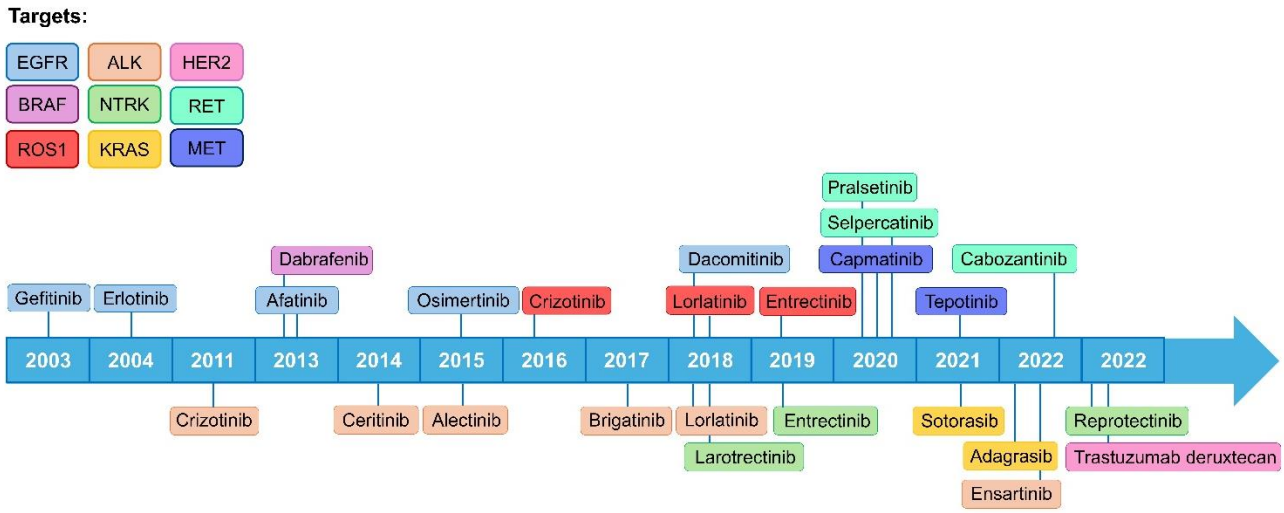

Figure III. Timeline detailing FDA approvals for TKIs in the clinical treatment of NSCLC.

As advancements in cancer treatment have progressed over time, the development of TKIs has also evolved, leading to their classification into three generations. Each generation is designed to enhance efficacy and overcome the limitations of its predecessors. In particular, next-generation TKIs have been specifically engineered to address the resistance issues commonly associated with this class of drugs (Yang et al., 2022; Attili et al., 2023). For instance, the third-generation EGFR-TKI osimertinib has been developed to specifically recognize the $EGFR^{T790M}$ mutation, which is an acquired resistance mutation that develops in 50-60% of patients who initially respond to first- (gefitinib, erlotinib) or second-generation (afatinib, dacomitinib) EGFR-TKIs, but that later progress (Imamura et al., 2020). The FLAURA trial has demonstrated a significant superiority of osimertinib over first- and second-generation TKIs in terms of PFS (18.9 months *vs* 10.2 months) and OS (38.6 months *vs* 31.8 months) (Gen et al., 2022). In addition, the high specificity of osimertinib, which allows the targeting of the T790M resistance mutation while sparing wild-type EGFR, also minimizes toxicity and adverse events as compared to early TKIs (Liu et al., 2020). Adding to its advantages, osimertinib also demonstrated the ability to penetrate the blood-brain barrier, enabling effective treatment of brain metastases, which represents a significant improvement over its predecessor drugs (Hui et al., 2022).

Using osimertinib as a representative example, early and next-generation TKIs targeting other oncogenes have also been developed, exhibiting similar characteristics and developmental trajectories to EGFR-directed TKIs. For instance, next generation ALK-TKIs, including alectinib, brigatinib, and lorlatinib, have also demonstrated improved PFS compared to earlier generation TKIs such as crizotinib (lorlatinib *vs* crizotinib, 12.5 months *vs* 9.2 months) (Tan et al., 2023), together with enhanced OS, intracranial efficacy and improved safety profiles (Wu et al., 2016; Cooper et al., 2022). Similar advantages have been observed in the use of ROS1-directed next generation TKIs (lorlatinib and entrectinib) as compared to the first-generation drug crizotinib (Boulanger et al., 2024).

Next-generation TKIs targeting MET (capmatinib and tepotinib), RET (selpercatinib and pralsetinib) and NTRK (larotrectinib and entrectinib), have similarly demonstrated superior efficacy compared to their early counterparts (Olmedo et al., 2022; Attili et al., 2023).

In other cases, the combination of different TKIs has led to significant clinical benefits in the treatment of NSCLC. A key example is the co-targeting of *BRAF* mutations with the combination of dabrafenib (a BRAF inhibitor) and trametinib (a MEK inhibitor), which has demonstrated remarkable efficacy in NSCLC patients harboring $BRAF^{V600E}$ mutations (Yan et al., 2022). This combined inhibition strategy has indeed significantly improved patients'clinical outcomes, as demonstrated by the pivotal phase II BRF113928 trial, in which patients with previously treated BRAF V600E-mutant NSCLC receiving the combination of dabrafenib and trametinib exhibited an objective response rate (ORR) of 64%, as compared to patients receiving dabrafenib monotherapy, who exhibited an ORR of 33% (Anguera & Majem, 2018).

For what concerns the targeting of *KRAS* mutations, this topic has to be addressed separately from other oncogenic targets, as the landscape surrounding KRAS has historically been different. Indeed, for several years KRAS has been considered an "undruggable" target due to its challenging structure as a GTPase protein (Huang et al., 2021). However, recent advancements have led to the approval of sotorasib and adagrasib, able to specifically target $KRAS^{G12C}$ mutation (Jänne et al., 2022; Nakajima et al., 2022). In the CodeBreaK 100 pivotal trial, treatment with sotorasib for patients with $KRAS^{G12C}$-mutated NSCLC demonstrated an ORR of 37% and a PFS of 6.8 months (Skoulidis et al., 2021). Similarly, the KRYSTAL-1 study reported an ORR of 43% and a PFS of 6.9 months for patients receiving adagrasib within the same $KRAS^{G12C}$-mutated NSCLC cohort (Jänne et al., 2022).

Despite the significant impact of TKIs in the treatment of NSCLC, their clinical efficacy remains heavily constrained by the development of resistance, which continues to be a major challenge in achieving sustained long-term responses, as we will discuss in the following sections.

6.5 Immunotherapy

The importance of immunotherapy in cancer treatment has grown exponentially in recent years, emerging as an innovative approach that harnesses the body's immune system to combat malignancies (Y. Zhang & Zhang, 2020). Among these innovative strategies, immune checkpoint inhibitors (ICIs) have revolutionized the treatment landscape for NSCLC, marking a significant shift in therapeutic strategies over the past decade (Tang et al., 2022).

Immune checkpoints are key modulators of the immune response and consist of a sophisticated system of receptor-ligand interactions expressed on the surface of immune cells, playing a crucial role in inhibiting and regulating the magnitude of the immune response. All types of immune responses, including antitumor immunity, rely on a delicate balance between the recognition of non-self and the regulation of both the duration and intensity of the immune response. An uncontrolled immune response can be harmful to the body, as it may damage surrounding tissues or lead to autoimmune reactions (Maleki et al., 2022). For this reason, throughout evolution, the immune system has developed a variety of inhibitory mechanisms aimed at controlling immune activity, including immune checkpoints (Sperk et al., 2018). One notable example is the ligand-receptor system of the Programmed cell Death Protein 1 and its ligand (PD1/PD-L1), where PD-L1 is primarily expressed by antigen-presenting cells (APCs), while PD-1 is expressed on T lymphocytes, regulating immune responses (Ortega et al., 2024). The inhibitory role of PD-1 upon interaction with its ligands, PD-L1 and PD-L2, disrupts the stimulatory signaling pathways initiated by the T-cell receptor (TCR), which recognizes antigens presented by other cells, and by CD28, a crucial co-stimulatory receptor necessary for T-cell activation. This disruption hinders the signaling pathways that regulate T-cell survival, function, and activation (Sharpe & Pauken, 2018).

Unfortunately, tumor cells have adapted to exploit these modulatory pathways, enabling them to evade antitumor immune responses. Tumor cells can indeed express PD-L1 ligand to engage PD-1 receptors on infiltrating T lymphocytes, thereby inhibiting T-cell activation and proliferation. This interaction effectively dampens the antitumor immune response, allowing cancer cells to escape immune surveillance (Juneja et al., 2017). The upregulation of tumoral PD-L1 can be induced by IFN-γ and other cytokines secreted by tumor-infiltrating lymphocytes (TILs) and cancer cells within the tumor microenvironment (TME), along with various inflammatory mediators (Benci et al., 2016; Garcia-Diaz et al., 2017; Cui et al., 2024) (**Figure IV**).

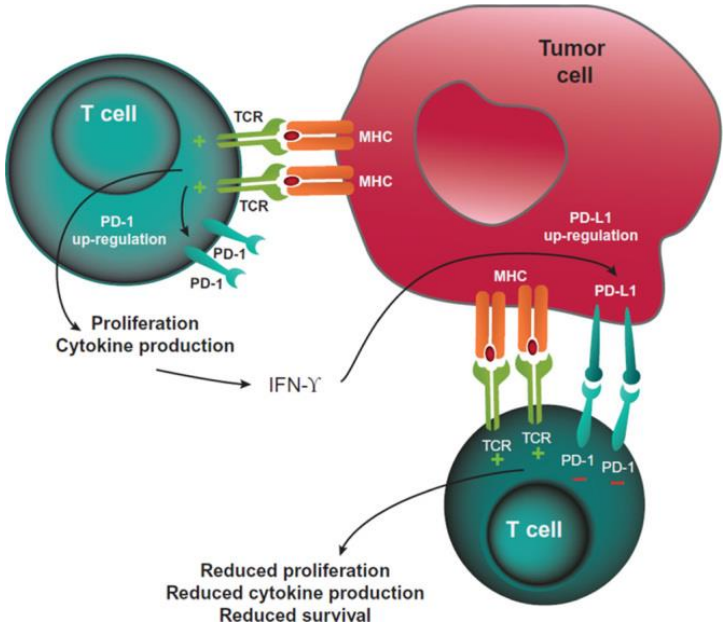

Figure IV. Mechanism of immune evasion mediated by PD-L1 expression on tumor cells – from Buchbinder & Desai, 2016. Prolonged stimulation of the T-cell receptor (TCR) during the antitumor response leads to increased expression of PD-1 on the lymphocyte membrane. Tumor cells can upregulate PD-L1 (or PD-L2, not shown) in response to stimulation by inflammatory cytokines produced by activated T lymphocytes. The PD-1/PD-L1 interaction inhibits the stimulatory signal from the TCR, resulting in reduced cytokine production, decreased proliferation, and diminished survival of T lymphocytes.

ICIs have been developed with the aim of reactivating the immune system against tumors. Among the various immune checkpoints, which also include TIM-3 (T-cell immunoglobulin mucin-3), LAG-3 (lymphocyte activation gene 3), and BTLA (B and T lymphocyte attenuator), particular focus has been placed on PD-1 and PD-L1, together with CTLA-4 (Cytotoxic T lymphocyte–associated protein 4), as these modulators have proven especially relevant in clinical applications for NSCLC. This new class of immunotherapeutic agents comprises a series of monoclonal antibodies that specifically target key immune checkpoints. Their mechanism of action involves binding to these checkpoints, which disrupts the pathways that suppress lymphocytic activity. This disruption enables tumor-infiltrating T lymphocytes to restore their natural antitumor effector function (Wei et al., 2018) (**Figure V**).

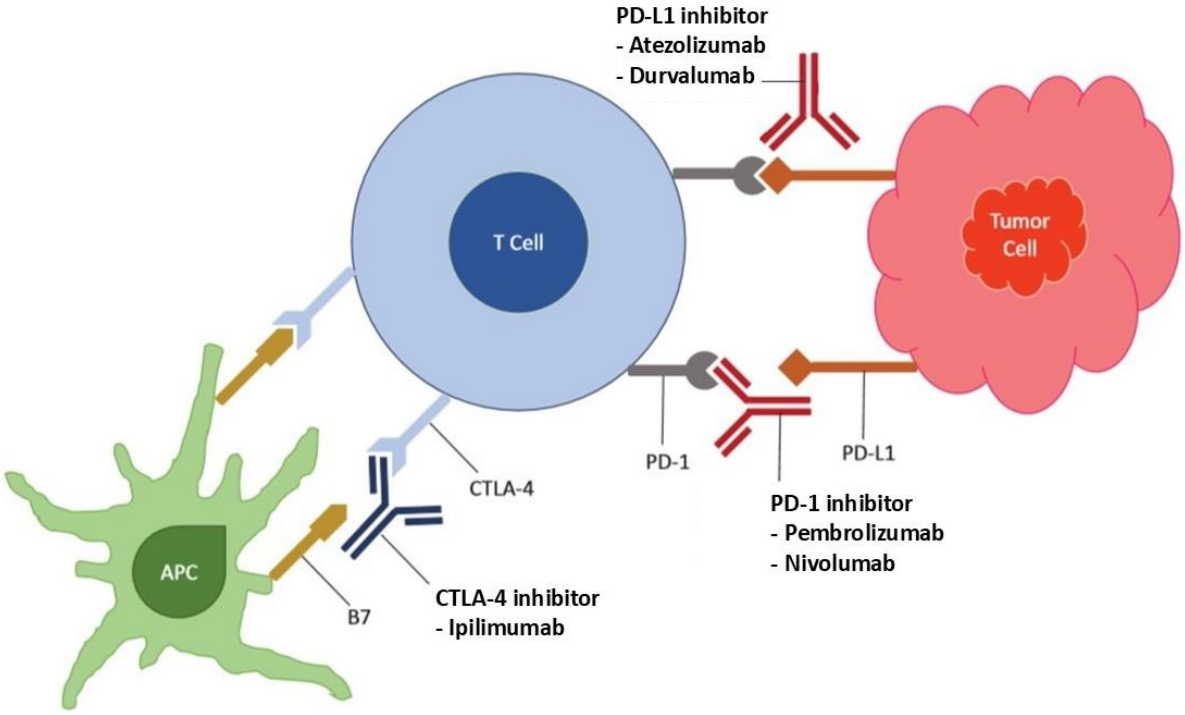

Figure V. Inhibition of immune checkpoints by ICIs – modified from Ahmed et al., 2019. The CTLA-4 inhibitor (ipilimumab) prevents the binding between CTLA-4 and the B7 ligand expressed on antigen-presenting cells (APCs), blocking the inhibitory signal to T lymphocytes. PD-1 inhibitors (*e.g.*, pembrolizumab and nivolumab) and PD-L1 inhibitors (*e.g.*, atezolizumab) prevent the binding of PD-1 and PD-L1, blocking the signaling pathway that inhibits T lymphocyte activity.

Currently, ICIs have become essential components of the clinical management of NSCLC and are utilized in both first-line and subsequent treatment settings (Olivares-Hernández et al., 2023). Agents such as pembrolizumab, nivolumab, atezolizumab, durvalumab and ipilimumab have also demonstrated substantial efficacy when administered as part of combination therapies with chemotherapy, significantly enhancing patient outcomes (Olivares-Hernández et al., 2023).

6.5.1 Approved ICIs targeting PD-1 for clinical application in NSCLC

Nivolumab (Opdivo) was the first ICI approved for clinical use in the treatment of NSCLC. The FDA granted this approval in March 2015, specifically for patients with advanced NSCLC who had progressed after platinum-based chemotherapy (Kazandjian, Suzman, et al., 2016). This decision was based on the findings of the phase III CheckMate-017 clinical trial, which demonstrated that nivolumab significantly improved the OS compared to standard chemotherapy. Specifically, patients treated with nivolumab experienced an average increase in survival of 3.2 months compared to those receiving docetaxel (Raedler, 2015; NCI Staff, 2015). Following its initial approval, the indications for nivolumab have expanded, and it is now also approved for first-line treatment in combination with chemotherapy for the treatment of patients with metastatic NSCLC (Lu et al., 2023).

In the same year, pembrolizumab (Keytruda) also received FDA approval for the treatment of advanced NSCLC patients whose tumors expressed high levels of PD-L1 and who had experienced disease progression following standard chemotherapy (Reck et al., 2016). The approval was primarily based on the results of the phase III KEYNOTE-010 trial, which demonstrated that pembrolizumab significantly improved OS compared to docetaxel (one-year OS of about 69% *vs* 49% in the chemotherapy group) (Herbst et al., 2021). Currently, pembrolizumab is also indicated as a first-line treatment in combination with chemotherapy for patients with metastatic NSCLC (Liu et al., 2023).

Most recently, Cemiplimab-rwlc (Libtayo) became the latest PD-1 targeting ICI approved by the FDA for NSCLC treatment (Ahn & Nagasaka, 2023). Approved in 2021, cemiplimab was initially indicated for patients with advanced NSCLC who have not received prior systemic therapy. This approval was supported by the results of the phase II EMPOWER-Lung 1 trial, which demonstrated a significant improvement in OS for patients treated with cemiplimab compared to standard chemotherapy (Sezer et al., 2021). In this trial, patients treated with cemiplimab achieved a median OS of 22.1 months, compared to the group receiving chemotherapy alone, who showed an OS of only 13.3 months. Cemiplimab is now also indicated as a first-line therapy for patients with locally advanced or metastatic NSCLC (Özgüroğlu et al., 2023).

6.5.2 Approved ICIs targeting PD-L1 for clinical application in NSCLC

Two monoclonal antibodies targeting PD-L1 have also been approved for the treatment of NSCLC. Atezolizumab (Tecentriq) was the first PD-L1 inhibitor to receive FDA approval in 2016, initially designated for patients with advanced NSCLC who had previously undergone at least one treatment (Cancer Discovery, News in Brief, 2016). This approval was based on the results of the phase II OAK clinical trial, which demonstrated a significant improvement in one-year OS compared to standard chemotherapy (50% *vs* 42%) (Rittmeyer et al., 2017). Today, atezolizumab is also indicated as a first-line therapy in combination with chemotherapy for patients with metastatic NSCLC, with data from the IMpower150 trial revealing a median OS of 19.2 months for patients receiving this combination versus just 14.7 months for those treated with chemotherapy alone (Ryu & Ward, 2018).

Following this, durvalumab (Imfinzi) was also approved in 2017 for patients with advanced NSCLC who showed response or stable disease after chemotherapy and radiation therapy (Syed, 2017). Its approval was based on the results of the phase III PACIFIC trial, which showed a significant improvement in PFS (16.8 months) compared to the control group (5.6 months) (Spigel et al., 2022). Currently, durvalumab is uniquely approved for consolidation therapy following platinum-based chemotherapy and radiation in unresectable stage III NSCLC (Moore et al., 2023).

6.5.3 Approved ICIs targeting CTLA-4 for clinical application in NSCLC

Ipilimumab (Yervoy) is a monoclonal antibody targeting CTLA-4, approved for the treatment of NSCLC in combination with nivolumab. This combination received FDA approval in 2021 for patients with advanced NSCLC who had previously undergone at least one line of therapy (Puri & Shafique, 2020). This approval was based on the results obtained from the phase III CheckMate 227 clinical trial, in which the combination therapy with ipilimumab and nivolumab demonstrated a significant improvement in the OS of NSCLC patients, especially those with high PD-L1 expression, compared to chemotherapy alone (17.1 months *vs* 14.9 months) (Hellmann et al., 2019). Subsequently, two randomised phase III trials, namely CheckMate 9LA and POSEIDON, evaluated the efficacy of the triplet combination of ipilimumab, nivolumab, and chemotherapy in untreated metastatic NSCLC. Results indicated that this combination significantly improved OS and PFS compared to chemotherapy alone, further supporting the role of ipilimumab in enhancing treatment outcomes for patients with advanced disease (Li et al., 2024).

6.5.4 Predictive biomarkers of response to ICIs

Despite ICIs have revolutionized the treatment landscape of NSCLC, providing new therapeutic opportunities for patients previously deemed inoperable, not all patients exhibit favorable responses, underscoring the critical need for the identification of reliable predictive biomarkers. Currently, PD-L1 expression is the only validated predictive biomarker used to guide ICI therapy in clinical practice (Doroshow et al., 2021). Nevertheless, its use is heavily limited and for this reason it is considered an incomplete biomarker. The assessment of PD-L1 expression is primarily conducted through immunohistochemistry (IHC), a technique that utilizes specific antibodies to detect PD-L1 protein levels on the surface of tumor cells or tumor infiltrating immune cells (Phillips et al., 2015; Dolled-Filhart et al., 2016). In clinical practice, PD-L1 expression is measured using two main scoring systems, which are often used interchangeably: the tumor proportional score (TPS) and the tumor cell (TC) expression. Both the scoring systems indicate the percentage of viable tumor cells with PD-L1 staining on the membrane, relative to all the viable tumor cells of the sample (Kerr et al., 2015; Kerr & Hirsch, 2016). Nevertheless, while TPS may encompass both tumor cells and immune cells, the TC percentage specifically refers to the proportion of tumor cells expressing PD-L1 (C.-E. Wu et al., 2020). The potential utility of PD-L1 expression as a predictive biomarker was highlighted in some of the early clinical trials that led to ICIs approval. Indeed, even though these studies were enrolled patients regardless of their tumoral PD-L1 expression, post hoc analyses showed that higher PD-L1 levels were associated with improved clinical outcomes. An example is the KEYNOTE-010 trial, evaluating pembrolizumab efficacy, in which it was observed that higher PD-L1 expression

(TPS ≥ 50%) correlated with better PFS and OS (Garon et al., 2015). Nevertheless, subsequent studies failed in demonstrating a sufficiently strong association between PD- L1 tumoral status and patients' clinical outcomes and, on the contrary, provided demonstration that subsets of patients with tumors negative for PD-L1 expression could as well benefit from ICI therapy (Brahmer et al., 2015; Reck et al., 2016; Rittmeyer et al., 2017). Currently, the majority of ICIs have been approved for patients with a TPS of PD-L1 greater than 50%. However, the conflicting data raise important questions about the adequacy of using PD-L1 as the sole criterion for patient selection. In addition to this, another key issue is the heterogeneous expression of PD-L1 within tumors, which can result in inconsistent assessments when based on a single biopsy. Furthermore, the lack of standardization in PD-L1 detection assays–due to variations in diagnostic kits, antibodies, and testing methodologies–makes it difficult to reliably compare results across different settings. This challenge is compounded by the absence of universally accepted cut-off values for PD-L1 positivity, further complicating the accuracy and consistency of the biomarker's clinical use (Mathew et al., 2017; Li et al., 2022; Catalano et al., 2023). All the limitations of PD-L1 as a predictive biomarker of response to ICIs have spurred the search for additional biomarkers. For instance, a promising biomarker is the tumor mutational burden (TMB), which measures the total number of somatic mutations per megabase (mut/Mb) in the tumor genome, reflecting the overall mutational landscape of the cancer (Chan et al., 2019). The rationale behind the use of TMB as a predictive biomarker is that higher TMB likelihood results in increased tumor expressing neoantigens, which may enhance tumor's immunogenicity and improve response to ICI therapy (Greillier et al., 2018; Scobie et al., 2023). Retrospective analyses have indeed demonstrated that patients with high TMB (often defined as ≥ 10 mut/Mb) exhibit improved ORR, OS and PFS when treated with ICIs, compared to patients with low TMB levels (Ma et al., 2021). For the same rationale, tumor microsatellite instability (MSI), which reflects defects in DNA repair mechanisms, has also garnered attention as a potential predictive biomarker for the efficacy of ICIs (Dempke et al., 2018; Mino-Kenudson et al., 2022). The evaluation of TILs, which reflect an "hot" TME, is also being investigated for its predictive potential (Mino-Kenudson et al., 2022; Ushio et al., 2022; Catalano et al., 2023). Alle these emerging biomarkers hold promises for refining patient selection and optimizing therapeutic strategies, but further validation and standardization are required before they can be integrated into routine clinical practice alongside PD-L1 testing.

6.5.5 Clinical responses to ICIs

ICIs exhibit response patterns that are unprecedented when compared to conventional chemotherapy or targeted therapies. These kinds of responses, which include durable complete response (Durable CR), durable partial responses (Durable PR), durable stable disease (Durable SD), pseudoprogression and hyperprogression, are summarized in **Figure VI**.

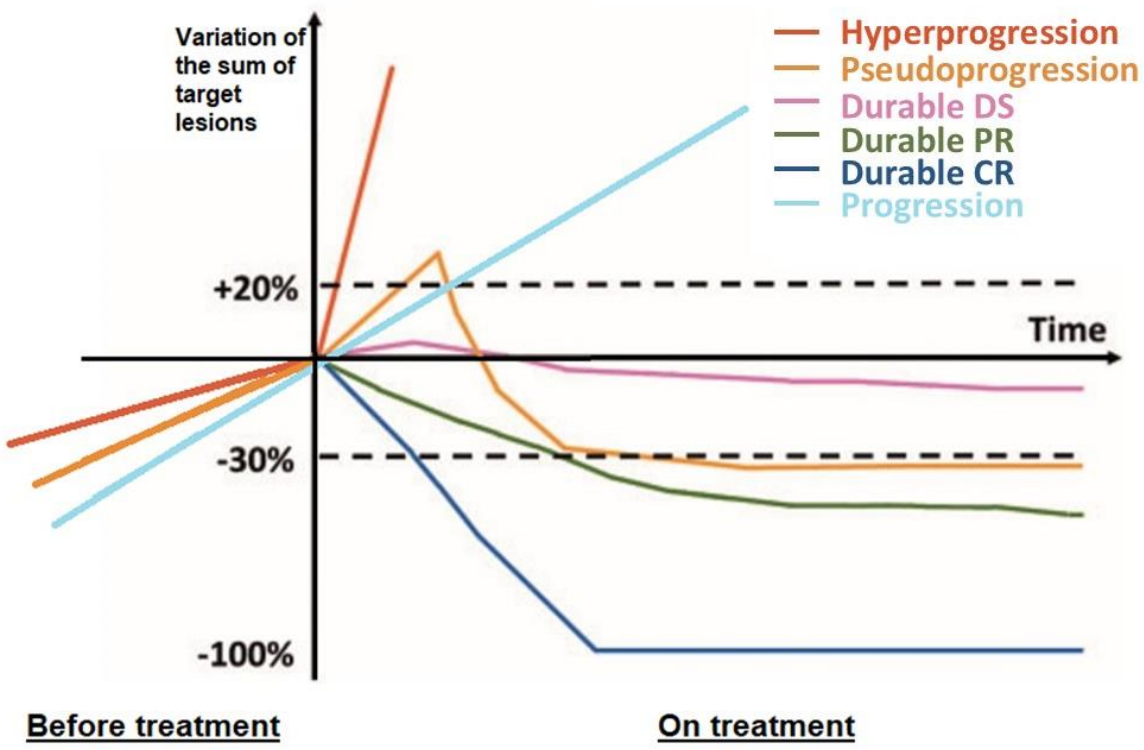

Figure VI. Response and progression patterns during ICI treatment – modified from Borcoman et al., 2019. SD: stable disease; PR: progression disease; CR: complete response.

The first type of ICI-related response is durable complete response (durable CR), in which the patient benefits from prolonged periods of disease control and, in some cases, long-lasting remissions, which can persist also after therapy discontinuation. Unlike traditional chemotherapy, which often results in short-term responses followed by relapses, ICIs can indeed induce sustained immune activation, leading to persistent anti-tumor effects (Borcoman et al., 2019; Pons-Tostivint et al., 2019; Johnson et al., 2022).

Differently, durable partial responses (durable PRs) are characterized by a significant reduction in tumor burden without achieving complete remission. Although the patients experiencing this kind of response do not achieve complete disease eradication, durable PRs also play an important role in enhancing patient outcomes, stabilizing the disease and improving patients' quality of life. Additionally, durable PRs may also transition into durable CRs over time, especially when patients continue to receive ICI therapy or experience immune-mediated effects that further reduce tumor size (Borcoman et al., 2019; Pons-Tostivint et al., 2019).

Durable stable disease (durable SD) refers to a situation in which the tumor does not progress or regress significantly over an extended period. Despite the disease not being eradicated, this kind of response offers an important period of disease stabilization in which tumor growth is controlled.

This stabilization can be particularly beneficial for those class of tumors that do not respond to other types of therapies, as frequently happens with advanced NSCLC (Borcoman et al., 2019).

Pseudoprogression refers to a phenomenon in which, during ICI therapy, there is a transient increase in the size of the primary tumor or the appearance of new lesions, followed by tumor regression (Borcoman et al., 2019). This response may be misleading, as it may result in the premature discontinuation of the therapy. Several mechanisms have been proposed to explain pseudoprogression, including a strong activation of the immune system, which may lead to an influx of immune cells into the TME, temporarily increasing the size of tumor due to inflammation and edema (Di Giacomo et al., 2009; Chiou & Burotto, 2015). Another hypothesis suggests that the release of tumor antigens into circulation due to tumor death and necrosis during ICI treatment may provoke a systemic immune response, attracting additional immune cells to the tumor site and leading to localized swelling (Jia et al., 2019).

As for hyperprogression, it is considered the most detrimental type of response to ICIs and it is characterized by an accelerated tumor growth that often leads to rapid clinical deterioration (Adashek et al., 2020). This phenomenon poses significant challenges in the management of cancer patients, as it contrasts sharply with the intended therapeutic outcomes of ICIs, which aim to induce durable tumor regression or stabilization. The implications of hyperprogression are profound, affecting treatment decisions and patient prognosis. For this reason, a comprehensive description of this phenomenon is provided in the following section.

6.5.5.1 Hyperprogression Disease (HPD)

Hyperprogression, also referred to as hyperprogressive disease (HPD), is described as a paradoxical, accelerated growth pattern of tumors following ICI therapy. Unlike typical disease progression, where tumors gradually increase in size or spread, hyperprogression is characterized by a rapid deterioration in patient's condition, often observed within weeks from therapy initiation (Borcoman et al., 2019; Angelicola et al., 2021). The phenomenon was initially documented in retrospective studies, in which a subset of patients exhibited rapid disease advancement following the initiation of ICI therapy (Chubachi et al., 2016; Saada-Bouzid et al., 2016; Saâda-Bouzid et al., 2017). Based on these observations, it was noted that the manifestation of hyperprogression did not correlate with specific tumor types, although some retrospective analyses suggest a higher frequency of the phenomenon in patients with NSCLC, where the incidence ranges from 8% to 21%, and in patients with head and neck tumors, where an incidence of 29% has been observed (Saada-Bouzid et al., 2016; Ferrara, et al., 2018). Nevertheless, the phenomenon of hyperprogression is challenging to define due to the variety of criteria used in its assessment. Indeed, after Champiat and collegues introduced for the first time the concept of hyperprogression in a retrospective study of cancer patients treated with

PD-1/PD-L1 inhibitors (Champiat et al., 2017), various research groups have since examined the phenomenon and proposed distinct criteria for its definition, leading to significant differences in reported HPD rates (Angelicola et al., 2021). To overcome this limitation, Kas and collegues have recently proposed a refined and standardized definition of HPD, building on the criteria previously employed (Kas et al., 2020).

Although the mechanisms of hyperprogression remain unclear (for further details, refer to *Section 7.2.3*), many factors have been associated with this phenomenon. One of the most consistently reported factors is advanced age (≥ 65 years) (Borghaei et al., 2015; Brahmer et al., 2015; Champiat et al., 2017; Motzer et al., 2018). This association may be explained by the natural decline in both innate and adaptive immune responses in older patients–commonly referred to as "immunosenescence"–characterized by impaired T-cell function, increased inflammatory cytokine production, and reduced immune diversity (Solana et al., 2012; Goronzy & Weyand, 2017). Additionally, prior irradiation has also been linked to a higher incidence of HPD (Saâda-Bouzid et al., 2017), likely due to alterations in the TME post-radiotherapy, which promotes the generation of neoantigens that may drive rapid tumor progression in the irradiated areas (Fields et al., 2017). In a retrospective study of NSCLC patients treated with ICIs, HPD was also notably associated with the presence of more than two metastatic sites before treatment initiation (Ferrara, et al., 2018). Genomic alterations also seem to play a critical role, with mouse double minute homolog (*MDM2/MDM4*) amplification and *EGFR* mutations emerging as potential markers for an increased risk of HPD (Kato et al., 2017; Singavi et al., 2017). Furthermore, patients affected with oncogene-driven NSCLC, such as those harboring *ALK*, *EGFR*, or *STK11* mutations, typically do not benefit from ICI therapy (Biton et al., 2018). This is likely due to the "cold" immune microenvironment characteristic of these tumors, which lack significant immune cell infiltration (Lamberti et al., 2020). Finally, elevated serum lactate dehydrogenase (LDH) levels have also been associated with HPD, as high LDH levels are indicative of a hypoxic and acidic microenvironment that impairs the activity of infiltrating T lymphocytes and natural killer (NK) cells (Tunali et al., 2019; Angelicola et al., 2021). In contrast, no significant associations have been reported between HPD and tumor histology, baseline tumor size, or previous lines of therapy (Champiat et al., 2017; Kato et al., 2017; Saâda-Bouzid et al., 2017). The relationship between PD-L1 expression and HPD remains controversial, with studies yielding inconsistent results, even though a significant inverse correlation between PD-L1 tumoral expression and HPD development has been observed in NSCLC patients (Lo Russo et al., 2019).

7. DRUG RESISTANCE IN NSCLC

Resistance to therapy remains a significant challenge in the management of tumors, significantly influencing patient outcomes and the overall efficacy of treatment regimens. Based on the underlying mechanisms by which tumors resist therapies, resistance can be categorized into two main types: primary (or intrinsic) and secondary (or acquired) resistance.

Primary or intrinsic resistance occurs when a tumor intrinsically exhibits a lack of response to therapy from the very onset. This can be attributed to several constitutive factors, including tumor heterogeneity (Lim & Ma, 2019; Zhang et al., 2022), genetic mutations that confer inherent insensitivity to treatment (Lin et al., 2022; Kobayashi, 2023), or the presence of extrinsic tumor factors, such as an unfavorable TME that hinders the effectiveness of immune-based therapies (Son et al., 2017).

In contrast, secondary or acquired, resistance arises after an initial tumoral response to treatment, indicating that the tumor has developed adaptive mechanisms to evade the effects of the therapy over time. This can occur due to various factors, including mutations that render the drug's target undruggable or the activation of compensatory signaling pathways that promote tumor survival despite the therapeutic intervention (Sun et al., 2024).

7.1 Mechanisms of TKI resistance in NSCLC

7.1.1 Primary resistance

The following mechanisms of primary resistance to TKI-based therapy have been reported:

- **Mutations in target genes**. Tumors may harbor mutations that confer inherent resistance to TKIs. For instance, in *EGFR*-mutant NSCLC, mutations such as T790M, C797S, and others can prevent first- and second-generation EGFR-TKIs from effectively binding to their target, leading to primary resistance. Approximately 30% of NSCLC patients with *EGFR*-activating mutations exhibit primary resistance due to these genetic alterations (Lim & Ma, 2019; Koulouris et al., 2022);
- **Lack of sensitizing mutations.** TKIs are specifically designed to target activating mutations that increase the receptor's sensitivity to these drugs. Tumors lacking these mutations do not benefit from TKI therapy. For instance, *EGFR*-mutated tumors without activating mutations in exons 19 or 21, show inherent resistance to EGFR TKIs (Cortot & Jänne, 2014; Stewart et al., 2015);
- **Presence of co-occurring mutations and activation of alternative signaling pathways.** Tumors may rely on compensatory signaling pathways to survive to TKI-mediated inhibition of survival signaling routes. For instance, *MET* amplification has been reported to compensate

for the inhibition of EGFR pathway in NSCLC (Choi et al., 2022; Qin et al., 2023). Similarly, in *ALK*-rearranged NSCLC, the presence of additional mutations involving, for instance, *RET*, *NRG1*, *IDH1* or *NF1*, lead to the activation of alternative signaling pathways which allow the tumor to bypass the antitumor effect of ALK-targeted therapies (McCoach et al., 2018). Moreover, alterations in cell cycle regulators have also been reported to drive primary resistance to osimertinib in *EGFR*-mutated NSCLC (Volta et al., 2023).

- **Tumor heterogeneity**. The presence of different subclonal populations within the tumor may show differential response to treatments, with some cells being inherently resistant due to distinct genetic profiles (Lim & Ma, 2019);
- **Increased drug efflux**. Tumor cells can overexpress efflux pumps such as ATP-binding cassette (ABC) transporters, which actively transport TKIs out of the cells, reducing their intracellular concentration and thereby diminishing their therapeutic effect (Robey et al., 2018; Dinić et al., 2024). In NSCLC, high levels of expression of these pumps have been correlated with increased resistance to EGFR-TKIs (Nishino et al., 2021).

7.1.2 Secondary resistance

The most common adaptive mechanisms of secondary tumor resistance to TKIs are the following and often overlap with those of primary resistance:

- **Mutations in target genes**. During the therapy, tumors can induce mechanisms of selection and adaptation in response to the pressure exerted by drug treatments. In these processes, resistant tumor variants can emerge and be selected to survive and proliferate despite the treatment (Simasi et al., 2014). One of the most well-documented mechanisms of secondary resistance is the emergence of the *EGFR* mutation T790M, which alters the binding site of early-generation TKIs, like gefitinib and erlotinib, leading to reduced drug efficacy. In NSCLC, the T790M mutation occurs in about 50-60% of patients who develop resistance to earlier EGFR-targeted therapies (Ma et al., 2011). Another example is the development of the L1196M mutation in *ALK*-rearranged NSCLCs, which can confer resistance to ALK inhibitors like crizotinib (Zhao et al., 2022);
- **Amplification of the target gene**. Amplification of wild-type *EGFR* (*wtEGFR*) has been reported to significantly contribute to acquired resistance to osimertinib in NSCLC. This resistance mechanism is primarily driven by ligand-induced activation of the EGFR signaling pathway. When *wtEGFR* is amplified, it can lead to increased levels of the receptor, which may activate downstream signaling pathways even in the presence of osimertinib (Ríos-Hoyo et al., 2022);

- **Activation of alternative signaling pathways.** As previously noted, the most frequently activated bypass signaling pathway following TKI treatment is the MET pathway, often driven by gene amplification (Simasi et al., 2014). HER2 activation, driven by gene amplification or overexpression, and ERK pathway activation, stimulated by the development of *BRAF* activating mutations, have also been reported as a secondary resistance mechanism to first- and second-generation EGFR-TKIs (La Monica et al., 2019; Nagasaka et al., 2022);
- **Phenotype transition.** In some cases, NSCLC can undergo a transformation into small cell lung cancer (SCLC) as a mechanism of secondary resistance to TKI-therapies. This histological transformation from NSCLC to SCLC has been reported to occur in 3-15% of patients undergoing treatment with EGFR inhibitors (Oser et al., 2015). Tumor phenotype transition also includes the shift of the tumor cells from an epithelial to a mesenchymal phenotype, through the process known as epithelial-mesenchymal transition (EMT). This transition enhances cell motility, invasiveness and resistance to apoptosis, allowing the tumor to evade the effects of TKIs (Zhu et al., 2019);
- **Crosstalk of target receptors with other RTKs.** When TKIs, such as those targeting EGFR, are administered, they can inadvertently lead to the formation of a heterodimer between EGFR itself and other RTKs in order to preserve tumor survival signaling pathways. A key example is the overexpression of the insulin-like growth factor-1 receptor (IGF1R) during EGFR-directed therapies in NSCLC. Under treatment, EGFR has been reported to interact with IGF1R, resulting in the formation of heterodimers. Heterodimerization activates IGF1R, triggering the downstream PI3K-AKT signaling pathway, resulting in enhanced tumor cell resistance to programmed cell death and reduced sensitivity to TKIs (Liu et al., 2018).

7.2 Mechanisms of ICI resistance in NSCLC

7.2.1 Primary resistance

The subsequent mechanisms have been identified as causes of primary resistance to ICI therapy:

- **Low tumor immunogenicity**. In order to evade immune recognition, tumors may downregulate major histocompatibility complex (MHC) molecules or express insufficient levels of tumor-associated antigens–*e.g.*, due to low intrinsic TMB–leading to inadequate activation and recognition of T cells against the tumor cells (Nagasaki et al., 2022; Zhou et al., 2023);
- **Defects in antigen presentation machinery.** Deficiencies in antigen presentation play a crucial role in primary resistance to immune checkpoint blockade therapies. One significant

mechanism involves the downregulation of MHC class I molecules and the loss of function of β2-microglobulin (B2M), which is essential for proper MHC-I folding and transport to the cell surface. Mutations in the *B2M* gene are indeed among the most common alterations associated with resistance to ICIs (Gettinger et al., 2017; Jenkins et al., 2018). In addition, epigenetic changes affecting TAP (transporter associated with antigen presentation) can also reduce MHC class I expression (Gettinger et al., 2017; Jenkins et al., 2018);

- **Alterations in immune signaling pathways.** Genetic alterations in immune-related signaling pathways, such as the IFN-γ signaling pathway JAK-STAT, can disrupt the ability of tumor cells to respond to ICIs, leading to primary resistance. Normally, reactive T cells recognize neoantigens on tumor cells presented by MHC class I molecules and release IFN-γ in the TME. This triggers the JAK-STAT signaling pathway in tumor cells, leading to increased tumoral PD-L1 expression (Jorgovanovic et al., 2020) (**Figure VII**). Any alteration in the tumor's response to the IFN-γ signaling pathway can inhibit PD-L1 expression induction, rendering anti-PD-(L)1 therapies ineffective. Identified mutations affecting the IFN-γ signaling pathway primarily include deletions in components such as *JAK1*, *JAK2*, *STAT1*, and the IFN-γ receptors genes *IFNGR1* and *IFNGR2* (Zaretsky et al., 2016; Manguso et al., 2017).

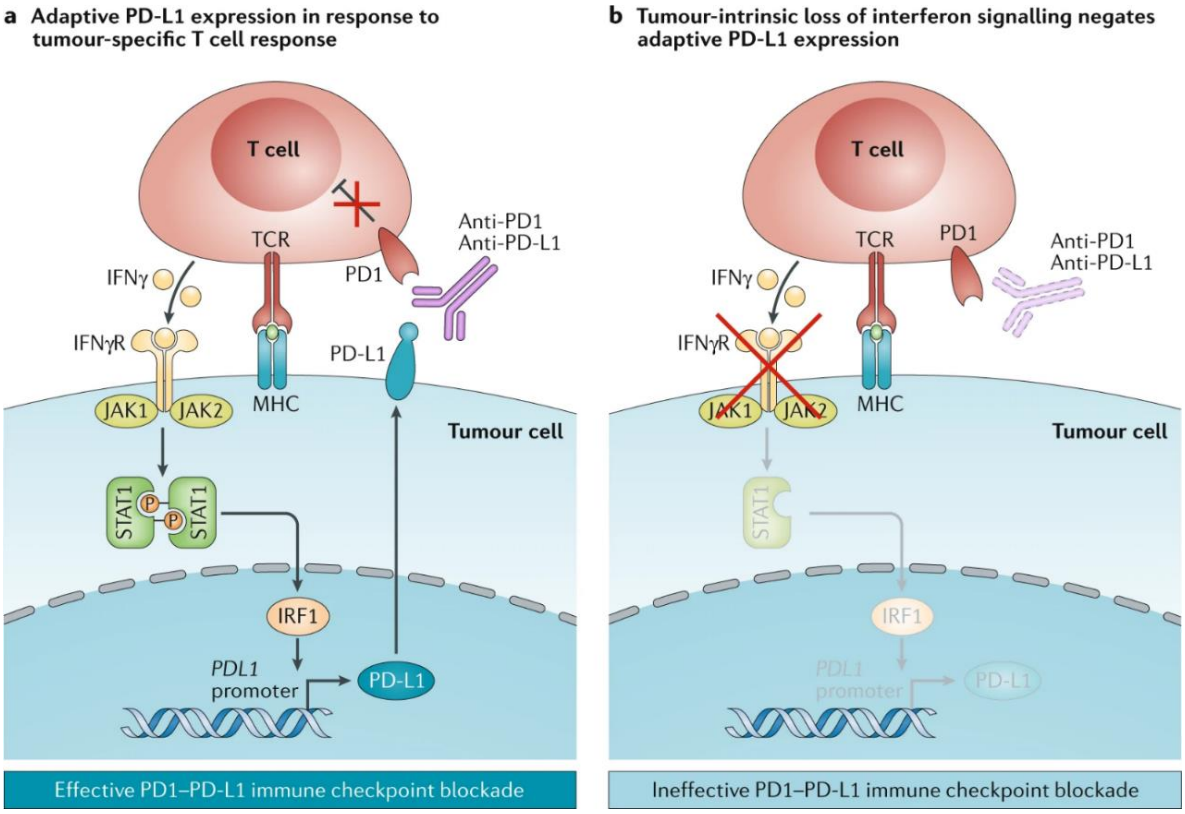

Figure VII. Role of the IFN-γ signaling pathway in the expression of the PD-L1 ligand – from Kalbasi & Ribas, 2020. **(A)** Functional IFN-γ signaling pathway. The recognition of tumor neoantigens presented by the

MHC class I complex by the T-cell receptor (TCR) of the activated T cell stimulates the release of IFN-γ by the T cell itself. The binding of IFN-γ to the IFN-γ receptor (IFNγR) expressed by the tumor cell induces the activation of Janus kinases (JAK) and signal transducer and activator of transcription (STAT). The JAK-STAT signaling pathway activates the transcription of the IFN-γ regulatory factor IRF-1, which in turn activates the transcription of PD-L1. The end result is the adaptive expression of the PD-L1 ligand by the tumor cell, which negatively regulates the anti-tumor lymphocytic response. Treatment with anti-PD-1 or anti-PD-L1 antibodies blocks the inhibition of lymphocyte activity induced by the interaction of PD-L1 with the PD-1 receptor. **(B)** Non-functional IFN-γ signaling pathway. The release of IFN-γ by the activated T cell does not induce the IFN-γ signaling pathway in the tumor cell, where the adaptive expression of PD-L1 is not induced. In the absence of induced PD-L1 expression, treatment with anti-PD-1 or anti-PD-L1 antibodies becomes ineffective. IFNγR: IFN-γ receptor. TCR: T cell receptor.

Moreover, the IFN-γ signaling pathway also induces the expression of the MHC class I complex, which is responsible for antigen presentation on the tumor surface. Tumor cells that are insensitive to the IFN-γ signaling pathway may therefore exhibit reduced expression of the MHC class I complex, allowing for immune evasion (Kalbasi & Ribas, 2020).

For what concerns PD-L1, as previously described, the expression of this checkpoint by tumor cells can contribute to creating an "immune shield" that allows them to evade the antitumor activity of effector T cells. Beyond its role in immune evasion, it has been observed that the expression and stimulation of PD-L1 on the surface of tumor cells is associated with signaling pathways that remain not fully understood, which convey survival signals to the tumor cell itself. It has indeed been demonstrated that PD-L1, when expressed on tumor cells, can mediate intracellular signaling following stimulation by PD-1, inducing anti-apoptotic signals that interfere with the classical apoptotic mechanisms triggered by the Fas ligand, thereby granting tumor cells resistance against the cytotoxic activity of T lymphocytes (Escors et al., 2018). Accordingly, the elimination of the intracellular domain of PD-L1 has been shown to reverse tumor resistance to immune elimination and lead to tumor regression in murine models (Azuma et al., 2008). The cytoplasmic portion of PD-L1 has been indeed found to trigger signals that directly interfere with IFN signaling pathway, reducing tumor cell sensitivity to its cytotoxic effects. This effect is mediated by sequences in PD-L1 cytoplasmic tail, which are capable of inhibiting the STAT3-Caspase7 pathway, activated by IFN, that regulates cell apoptosis (Gato-Cañas et al., 2017). Of note, further studies have revealed that PD-L1 can activate intrinsic signaling pathways even without binding to PD-1, increasing tumor cell proliferation and survival by inhibiting autophagy or through the activation of mTOR, which is involved in promoting tumor glycolytic metabolism (Chang et al., 2015; Clark et al., 2016). Recent evidence suggests that mutations or alterations in PD-L1 expression are closely

associated with primary resistance to ICIs. For instance, amplification of the *PD-L1* gene can lead to overexpression of PD-L1 on tumor cells, which may result in the saturation of the interaction sites for ICIs that target the PD-1/PD-L1 axis (Straub et al., 2016; Yi et al., 2021). Nevertheless, while current evidence suggests that PD-L1 plays a significant role in primary resistance to ICIs, further studies are necessary to fully elucidate these relationships. The literature indeed presents conflicting data regarding the signaling of PD-L1 on tumor cells. While some studies indicate an oncogenic role of PD-L1, as previously described, others also demonstrated a tumor-suppressive role of this modulator, evidencing the complexity of PD-L1's function in cancer biology (Wang et al., 2020).

Differently, the Wnt/β-catenin pathway has demonstrated to be often implicated in primary resistance to ICIs. Activation of this pathway can indeed lead to a tumor-promoting microenvironment that suppresses T-cell infiltration and function, thereby diminishing the effectiveness of ICIs (Nagasaki et al., 2022).

Another critical pathway involved in primary resistance to ICIs is the PTEN-STAT3 signaling pathway. Loss of PTEN function can result in constitutive activation of STAT3, which promotes an immunosuppressive TME characterized by increased expression of immune checkpoint molecules like PD-L1, and increased tumor cell survival (Peng et al., 2012; Cretella et al., 2019).

Finally, genetic mutations in the PI3K-AKT pathway can further contribute to immune evasion. Tumors with such alterations may indeed fail to respond to ICIs due to enhanced survival signaling and diminished responsiveness to immune-mediated cytotoxicity (Collins et al., 2022).

- **Immunosuppressive TME.** Within TME, tumor cells can interact with several stromal and immune cells, creating a context that favors tumor survival and proliferation. Immunosuppressive cells, such as regulatory T cells (Tregs) and myeloid-derived suppressor cells (MDSCs), can inhibit the activity of effector T lymphocytes, hindering their ability to recognize and destroy tumor cells (Schmidt et al., 2012; Yang et al., 2020). Additionally, M2 macrophages, which are often associated with tissue repair and tumor progression, can secrete immunosuppressive factors such as IL-10 and TGF-β, that further inhibit T-cell activation (Boutilier & Elsawa, 2021; Gao et al., 2022). Cancer-associated fibroblasts (CAFs) also contribute to the immunosuppressive microenvironment by secreting cytokines and extracellular matrix components, including IL-6, TGF-β, and CXCL12, that promote tumor growth and inhibit effective immune responses (Glabman et al., 2022; Zhang et al., 2023).

7.2.2 Secondary resistance

Secondary resistance mechanisms to ICIs can overlap with those of primary resistance, but they typically emerge after an initial response to therapy. The main mechanisms are described below:

- **Selection of low immunogenic tumor cell clones.** After an initial response to therapy, tumor heterogeneity becomes a critical factor as more immunogenic cells are targeted and eliminated by the immune system. This selective pressure operated by the treatment and, more broadly, by the immune system–a phenomenon known as "immune editing"–can lead to the outgrowth of low immunogenic tumor clones that express fewer recognizable antigens or that show altered antigen presentation capabilities, as previously described. As these less immunogenic clones proliferate, they escape immune detection, diminishing the overall effectiveness of the treatment (Gejman et al., 2018; Zapata et al., 2023).
- **Adaptive alterations in antigen presentation.** Tumor cells may downregulate or lose the expression of MHC molecules, in order to reduce their recognition by T cells and enabling them to escape immune detection (Cornel et al., 2020);
- **Acquisition of mutations in signaling pathways.** Tumor cells may acquire mutations in pathways like JAK-STAT or PI3K-AKT, which can lead to resistance by bypassing the effects of ICIs or promoting survival signals (for more details refer to *Section 7.2.1*) (Fujiwara et al., 2020; Schoenfeld & Hellmann, 2020);
- **T-cell exhaustion.** Chronic exposure to tumor antigens can lead to T-cell exhaustion, which is a state of dysfunctional T-cell response characterized by upregulation of inhibitory immune checkpoint, such as PD-1 and CTLA-4, with a decline in effector functions and, consequently, reduced effectiveness of ICIs over time (Nagasaki et al., 2022; Wang et al., 2023);
- **Increased expression of alternative immune checkpoints by T cells.** Following initial responses to ICIs, T cells may adapt by upregulating alternative inhibitory receptors, such as TIM-3, LAG-3, TIGIT and VISTA. The co-expression of these alternative checkpoints can lead to a more pronounced state of exhaustion, further dampening T-cell activation and function and diminishing the efficacy of ICI therapy (Wuerdemann et al., 2020; Wang et al., 2023).

7.2.3 Hypothesized mechanisms of hyperprogression

Although the mechanisms underlying hyperprogression during treatment with ICIs are not yet fully understood, it is believed that they may involve processes related to both primary and acquired resistance to ICI therapy, as previously described. Among these mechanisms, increase in Tregs within

the TME, loss of function of effector T cells, modulation of pro-tumorigenic soluble factors, aberrant inflammation, and activation of oncogenic pathways have been proposed (**Figure VIII**).

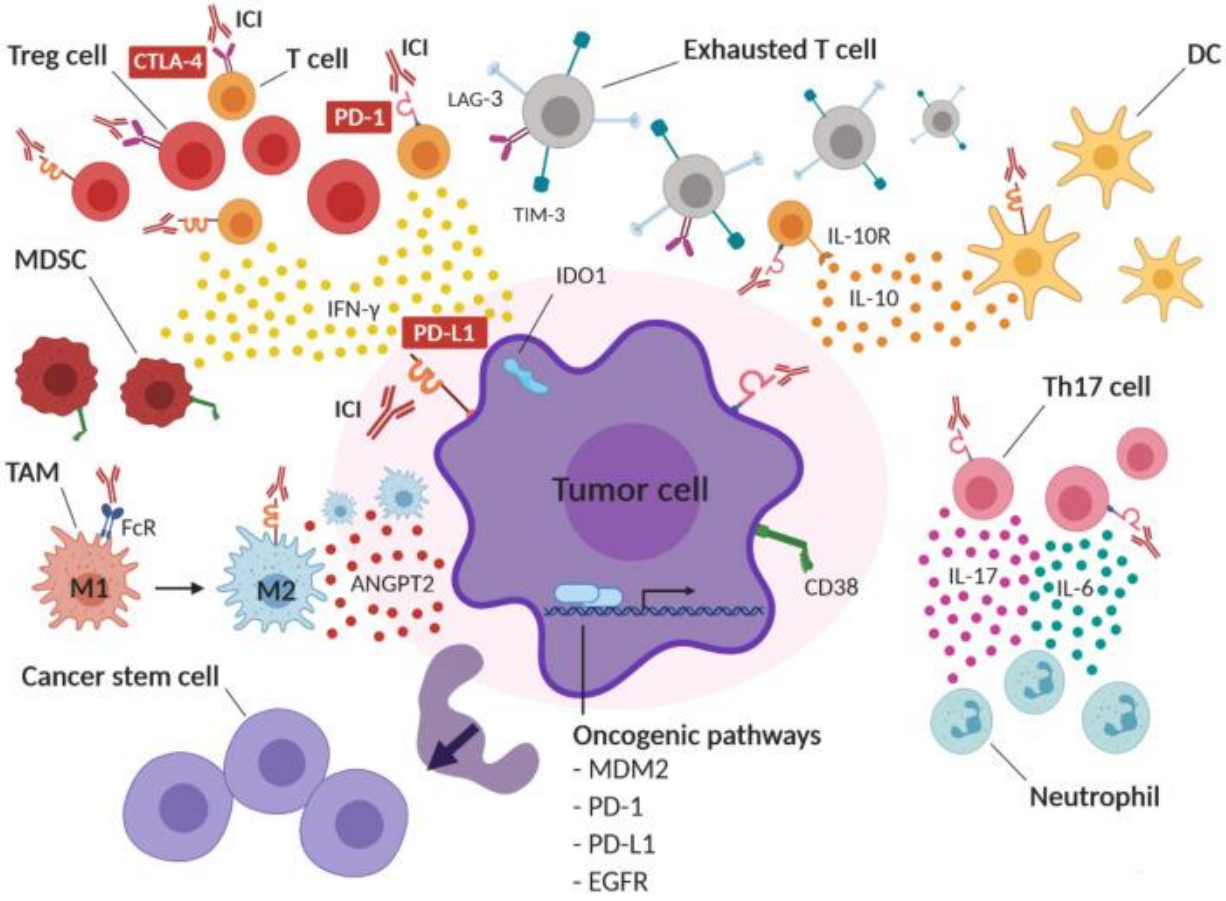

Figure VIII. Hypothesized biological mechanisms underlying hyperprogression induced by treatment with ICIs – from Angelicola et al., 2021. ICI therapy may functionally activate infiltrating regulatory T cells (Tregs), leading to an immunosuppressive tumor microenvironment (TME). At the same time, compensatory upregulation of alternative immune checkpoints, including LAG-3, TIM-3 and CTLA-4, on effector T cells after ICI therapy may induce T-cell exhaustion. Immune checkpoint blockade (ICB) might also induce the expression of CD38 on tumor cells and IFN-γ-dependent recruitment of CD38-expressing myeloid-derived suppressor cells (MDSCs), resulting in immune suppression. Moreover, ICI therapy may induce the upregulation of the immunosuppressive enzyme indoleamine 2,3-dioxygenase 1 (IDO1) and the increased secretion of immunosuppressive cytokines and soluble molecules, including interleukin 10 (IL-10), angiopoietin-2 (ANGPT2) and interferon-gamma (IFN-γ) into the TME. ICB might also functionally boost T helper 1 (not shown) and T helper 17 (Th17) lymphocytes, resulting in neutrophil recruitment and in an inflammatory immunosuppressive TME enriched in interleukin 6 (IL-6) and interleukin 17 (IL-17). In addition, ICIs may bind to Fc receptors (FcR) on tumor-associated macrophages (TAMs), resulting in a shift from M1 to an immunosuppressive M2 phenotype. ICB may also induce an increase in cancer stem cells (CSC) and may activate oncogenic signaling pathways, such as those driven by MDM2, PD-1, PD-L1 and EGFR, thus promoting tumor proliferation. DC: dendritic cell.

- **Expansion of infiltrating Tregs.** It is thought that the immune activation initially stimulated by ICIs may inadvertently lead to a feedback loop that promotes the expansion of Tregs–a phenomenon known as "counter-suppression"–resulting in suppression of T-cell

efficacy and reduced effectiveness of immunotherapy (Barnaba & Schinzari, 2013; Champiat et al., 2018);

- **T-cell exhaustion.** Prolonged exposure to tumor antigens may lead to the exhaustion of T cells and to the compensatory expression of the alternative immune checkpoint TIM-3, LAG-3, TIGIT or VISTA, as previously described. Although ICIs aim to reinvigorate exhausted T cells enhancing their anti-tumor activity, in some cases the persistent stimulation of the immune system can exacerbate exhaustion rather than restore T-cell functionality (Champiat et al., 2018);
- **Release of immunosuppressive mediators in the TME**. It is thought that ICI therapy may induce a compensatory activation of the immune response, characterized by the release of immunosuppressive cytokines and soluble mediators by tumor infiltrating immune cells. For instance, PD-1/PD-L1 blockade has demonstrated to increase IL-10 secretion by dendritic cells (DCs) and to induce the expression of IL-10 receptor (IL-10R) on $CD8^+$ $PD\text{-}1^+$ T cells (Sun et al., 2015; Lamichhane et al., 2017). Similarly, ICI therapy has been associated with increased levels of angiopoietin-2 (ANGPT2), which is an activator of pro-tumor M2 macrophages, and elevated levels of inhibitory molecules such as indoleamine 2,3-dioxygenase (IDO1), which promotes the differentiation of Tregs (Wu et al., 2017; Champiat et al., 2018). Moreover, ICI therapy has also demonstrated to upregulate cluster of differentiation 38 (CD38) on tumor cells−a well-known alternative immune checkpoint−leading to immune suppression and resistance to therapy (Chen et al., 2018).
- **Aberrant inflammation**. Increased secretion of inflammatory cytokines, including IFN-γ, IL-6, and IL-17, released by T helper 1 (Th1) and Th17 cells, has been observed in patients under ICI treatment (Dulos et al., 2012). The cytokine storm derived from aberrant inflammation, can not only promote tumor cell survival, proliferation, and metastasis, but also recruit neutrophils to the tumor site and induce in macrophages the shift from the M1 (pro-inflammatory) phenotype to the M2 (immunosuppressive) phenotype, which further stimulate tumor survival (Champiat et al., 2018). Notably, the interaction between the Fc domain of ICIs and Fc receptors (FcRs) expressed by macrophages has also demonstrated to effectively reprogram macrophages from the M1 to the M2 phenotype in patients experiencing HPD (Lo Russo et al., 2019);
- **Activation of oncologenic pathways**. The activation of oncogenic pathways after ICI therapy is thought to stimulate tumor growth and hyperprogression development. For instance, the amplification of the *MDM2* gene, which is involved in p53 degradation and inhibition, has frequently been reported in HPD patients (Kato et al., 2017). In addition, IFN-γ-induced

interferon regulatory factor 8 (IRF8) can induce MDM2 overexpression by binding to its promoter (Zhou et al., 2009). Moreover, PD-1 signaling pathway has been also implicated into HPD stimulation, as it has been demonstrated that the binding of PD-1 by PD-1−directed ICIs can induce the activation of the oncogenic PI3K-AKT signaling pathway, leading to uncontrolled tumor cell growth (Ludin & Zon, 2017). EGFR activation has also been implicated in HPD development, since it has been reported to drive PD-L1 expression on tumor cells supporting tumor immune exclusion (Akbay et al., 2013; Sun et al., 2018).

In addition to these mechanisms, the paper by Angelicola and colleagues also highlighted additional possible mechanisms of hyperprogression, specifically focusing on the role of IFN-γ of the alternative immune checkpoint known as CD38 (Angelicola et al., 2021).

Regarding the IFN-γ-dependent mechanisms of hyperprogression, this cytokine has been shown to activate the inflammasome pathway in tumor cells by upregulating PD-L1 expression, which subsequently recruits MDSCs into the TME (Theivanthiran et al., 2020). Mutations in the cytoplasmic tail of PD-L1 or in regulatory genes of the inflammasome axis may lead to increased activation of this pathway, contributing to the development of hyperprogression (Angelicola et al., 2021). Additionally, IFN-γ has also been reported to induce IDO1 expression in tumor cells, activating the JNK pathway, which in turn downregulates p53 (Spranger et al., 2013). Based on existing literature, it can be hypothesized that hyperprogressive patients may exhibit constitutive IDO1 expression, hyperactivation of the JNK pathway, and chronic inactivation of p53 (Angelicola et al., 2021). Furthermore, in the context of an hyperactivated immune environment resulting from the concurrent stimulation of tumor-specific $CD8^+$ T cells by ICIs and TCRs by tumor antigens, IFN-γ may trigger a compensatory process known as activation-induced cell death (AICD), which helps prevent uncontrolled immune responses by inducing apoptosis in T cells (Angelicola et al., 2021).

The immune checkpoint CD38 may also contribute to triggering the AICD process (Angelicola et al., 2021). In addition, the upregulation of CD38 after ICI therapy may also lead to the release of adenosine into the TME, triggering the activation of ADORA receptors on tumor cells (Chen et al., 2018). Activation of these receptors has been shown to block the IFN-γ pathway, rendering tumor cells resistant to the cytotoxic effects of IFN-γ, while simultaneously activating oncogenic pathways, such as the JNK signaling axis, leading to p53 downregulation (Milne & Palmer, 2011; Gessi et al., 2017). Furthermore, CD38 has been implicated in activating tumor pathways associated with hypoxia, establishing paracrine and autocrine signaling that promote tumor growth and recruit immunosuppressive cells into the TME. Hyperactivation of these pathways, due to specific mutations or polymorphisms, may contribute to the development of HPD (Angelicola et al., 2021).

8. PRECLINICAL MODELS FOR THE STUDY OF DRUG RESISTANCE IN NSCLC

Preclinical models are essential for understanding the mechanisms of cancer drug resistance and for developing new therapeutic strategies able to overcome this clinical limitation. Resistance to targeted therapies like TKIs and ICIs poses a significant challenge in the treatment of NSCLC, often leading patients to a therapeutic dead-end with few or no effective treatment options remaining. To address this limitation, various preclinical models have been established, ranging from cell lines to genetically engineered mouse models (GEMMs) to patient-derived xenografts (PDXs). These models help simulate the complexity of tumor evolution under drug pressure and provide valuable insights into the molecular mechanisms that drive resistance.

8.1 Cell line models

Cell line models are one of the most widely used and accessible preclinical systems for investigating resistance to targeted therapies in cancer (Mirabelli et al., 2019). These models comprise various established NSCLC cell lines that reflect the genetic and phenotypic diversity observed in tumors (Belloni et al., 2024). Some commonly used NSCLC cell line models are listed below.

- **A549**: a human lung adenocarcinoma cell line often used for sensitivity study of targeted agents such as TKIs (Belloni et al., 2024). It has been largely used for the study of the mechanisms of resistance to EGFR-targeting agents like gefitinib (Rho et al., 2009; Zhao et al., 2016; Liu & Gao, 2019; Tsukumo et al., 2020);
- **H460**: a human large cell lung carcinoma cell line that has been used to study both intrinsic and acquired resistance to different TKIs, helping to elucidate signaling pathways involved in resistance mechanisms (Shi et al., 2012; Patel et al., 2013; Sudo et al., 2013);
- **H1975**: a human lung adenocarcinoma cell line characterized by the presence of the $EGFR^{T790M}$ mutation (Walter et al., 2013). This cell line model has largely been used for the study of resistance to next-generation TKIs like osimertinib (Walter et al., 2013; Tang et al., 2016; Verusingam et al., 2021; Meraz et al., 2023).
- **PC-9**: a human lung adenocarcinoma cell line which harbors the *EGFR* exon 19 deletion, showing sensitivity to EGFR-directed TKIs such as gefitinib and erlotinib (T. K. Hayes et al., 2024). Researchers have developed gefitinib-resistant variants of PC-9, known as PC-9/GR, to investigate the mechanisms underlying acquired resistance to early-generation TKIs (Hamamoto et al., 2017; Song et al., 2019).

In experimental investigations, these cell lines are often chronically exposed to progressive increased concentrations of TKIs over time, in order to obtain resistant sublines characterized by the

presence of genetic alterations and signaling pathway changes associated with resistance, which can be investigated (Koizumi et al., 2005; Lee et al., 2016; Song et al., 2019).

Alternatively, cell line models can also be genetically modified to express specific mutations, enabling the study of intrinsic resistance associated with genetic alterations such as *EGFR* mutations, *KRAS* alterations or *ALK* rearrangements (Park et al., 2017).

The advantages of these models include their ease of manipulation and assessment, experimental reproducibility due to the homogeneity of cell cultures, the possibility of high-throughput drug screening and cost-effectiveness, compared to more complex models (van Staveren et al., 2009). Nevertheless, cell line models also fail to recapitulate the TME and immune interactions present *in vivo*, heavily limiting the complete understanding of drug resistance. In addition, the prolonged expansion of cell cultures *in vitro* may result in genetic drift, resulting in alterations or loss of their original features (Mirabelli et al., 2019).

Given these limitations, primary patient-derived tumor cell cultures (PDC) offer more reliable tumor models, as they better recapitulate the heterogeneity and pathophysiology of the original tumor. These models are obtained by maintaining cancer cells, directly isolated from tumor tissues or patients' body fluids, under 2D tissue culture conditions for a short period of time (Idrisova et al., 2022). Notably, many of the commonly used tumor cell lines mentioned earlier were initially obtained from primary patient-derived tumor cultures. However, continuous passaging and immortalization over time have rendered them less reliable when compared to freshly derived PDCs (Idrisova et al., 2022). Despite their advantages and applications, PDCs also need to be complemented by other preclinical models, as they alone cannot fully capture the complexity of tumor biology.

8.2 Patient-derived Xenografts (PDX)

Patient-derived xenografts (PDXs) consist in the direct implantation of freshly excised patient tumor fragments in immunocompromised mice, allowing for the growth and study of human tumors in a live organism (Jin et al., 2023). These models are highly utilized in cancer research due to their ability to retain the heterogeneity and the biological features of the original tumor. Indeed, PDX models are able to maintain the complexity of the TME, including tumor cell interaction with stromal or immune cells (Liu, Cui, et al., 2023; Fuchs et al., 2024). Moreover, PDX models are also useful tools for the evaluation of personalized therapy strategies, as they allow the testing of therapies on specific tumor characteristics of the individual patients (Hidalgo et al., 2014). PDX models have also demonstrated strong predictive value in identifying biomarkers and testing the efficacy of both molecular compounds and chemotherapy (Garrido-Laguna et al., 2011; Hidalgo et al., 2011; Sartore-Bianchi et al., 2016). In addition, the establishment of PDX-derived cell cultures (PDXC) also represents a useful platform for large-scale screening of drugs (Idrisova et al., 2022).

Nevertheless, PDX models also show limitations. Firstly, the establishment and maintenance of these models can be time-consuming and expensive, as they require high expertise in animal handling (Liu, Wu, et al., 2023). Moreover, the percentage of successful engraftment may significantly vary between different tumor types and samples (Nanni et al., 2019; Okada et al., 2019; Yoshida, 2020; Landuzzi et al., 2021). In addition to this, PDX models frequently exhibit the loss of human tumor stroma, which is replaced by murine stroma components over time, compromising the accuracy of certain studies (Schneeberger et al., 2016). Moreover, the faithful preservation of the original tumor's genomic profile over time in PDX model is questionable, as continuous passaging may result in the development of novel genetic alterations, potentially creating discrepancies between the PDX and the patient's initial tumor (Jin et al., 2023; Sunil & O'Donnell, 2024). Finally, because PDX models are established in immunodeficient mice lacking functional immune systems, they inherently exclude any interaction between the tumor and the human immune system, significantly limiting their use in studying immunotherapies (Choi et al., 2018). However, this limitation has been effectively addressed through the development of humanized PDX models, created by the engraftment of human immune cells or tissues into immunodeficient mice, thereby establishing a more accurate representation of the human immune environment in conjunction with the tumor (Okada et al., 2019). Mice with reconstituted human immune system not only allow for the examination of tumor-immune cell interactions, but also provide a relevant platform for testing various immunotherapies, including ICIs (Choi et al., 2018). Nevertheless, it is important to note that these models only partially mimic the human immune system, failing in representing a complete and functional human immune response (Choi et al., 2018).

Overall, while PDX models offer significant advantages for studying cancer drug resistance, careful consideration of their limitations is necessary for effective application in research and therapy development.

8.3 Syngeneic preclinical models

Syngeneic preclinical models are widely used in preclinical studies of NSCLC, particularly for investigating tumor-immune interactions and responses to immunotherapy. These models involve the transplantation of murine tumor cell lines or tumor fragments derived from spontaneously arising mouse tumors into genetically identical inbred mouse strains (Olson et al., 2018). These strains, such as C57BL/6 or BALB/c, are generated through sibling crosses for at least 20 generations, resulting in a highly homogeneous genetic background (Fontaine & Davis, 2016). The advantage of syngeneic models lies in their use of both the tumor and host from the same species, ensuring that the recipient mice possess an immune system fully compatible with the transplanted tumor, thereby avoiding rejection (Olson et al., 2018). One of the most significant benefits of these models is that they allow

for the study of interactions between tumor cells, the surrounding microenvironment, and the immune system within an immunocompetent host (Saxena & Christofori, 2013; Sanmamed et al., 2016). Moreover, syngeneic models are cost-effective, easy to use, and are backed by extensive genetic information, making them an accessible and robust tool for cancer research (Cheon & Orsulic, 2011).

Two of the most widely used lung syngeneic models include the following:

- **Lewis Lung Carcinoma (LLC) model**. The LLC model was derived from a spontaneous lung tumor developed in a C57BL/6 mouse (Bertram & Janik, 1980). It is one of the most frequently used syngeneic models for lung cancer research, particularly for the study of the immune system's response to therapies. In immunotherapy research, the LLC model has been used to test the effects of anti-PD-(L)1 and anti-CTLA-4 treatments, as well as to evaluate tumor-intrinsic resistance mechanisms and immune evasion strategies (Wu et al., 2020; Olivo Pimentel et al., 2021; Lei et al., 2024);
- **LL/2 model**. Also known as LLC1/LL2 (Lewis Lung Carcinoma 2), this model is a subline of the original LLC model (Duś et al., 1985). Similarly to LLC, the LL/2 model was derived from a spontaneous lung tumor that developed in a C57BL/6 mouse and it is also used for preclinical testing of several therapeutic strategies, including immunotherapy and targeted therapies (Ning et al., 2009; Li et al., 2017).

Despite their several applications, syngeneic models also have notable limitations. One key drawback is the absence of human tumor targets, which means that immune responses may differ from those observed in human-based assays (Jung, 2014). Additionally, the rapid tumor progression seen in syngeneic models does not allow for the development of the chronic inflammation typically observed in human tumors (Gutierrez et al., 2021). The genetic homogeneity of inbred strains further limits their ability to mimic the genetic diversity of human cancers (Zhong et al., 2020). Moreover, many of the tumor cell lines used in syngeneic models are derived from chemically induced tumors, leading to high levels of neoantigens, which might overestimate the efficacy of immunotherapies like ICIs and may be more reflective of "hot" tumors in humans, which are more immunogenic (Chen et al., 2022).

Although syngeneic models provide valuable insights into tumor-immune interactions, their limitations, such as reduced genetic diversity and differences from human tumor microenvironments, should be considered during preclinical investigations.

8.4 Genetically Engineered Mouse Models (GEMMs)

Genetically Engineered Mouse Models (GEMMs) have emerged as a pivotal tool for studying drug resistance in tumors. GEMMs models are engineered to harbor specific genetic aberrations that

mirror those found in human tumors, allowing them to phenocopy the malignancy and faithfully replicate the genetic landscape of the tumor (Kersten et al., 2017; Lampreht Tratar et al., 2018). These models develop spontaneous tumors that arise in their native tissue environment and develop within an immunocompetent host. This allows for the natural interaction between the tumor and the immune system, providing a more accurate representation of the TME, particularly for studies involving immunotherapies. Moreover, GEMMs are well-suited for assessing the efficacy of candidate drugs and studying the effects of specific mutations or pathways in a controlled genetic background (Becher & Holland, 2006). Of note, all the GEMMs can be classified as syngeneic models due to their development from genetically identical inbred mouse strains.

So far, the following GEMMs model have been established for the study of NSCLC drug resistance:

- **GEMMs carrying *EGFR* mutations**. Transgenic mice carrying two of the most common *EGFR* alterations in NSCLC, *i.e.*, L858R missense mutation and in-frame exon 19 deletions, have been successfully established. These mutations are known to sensitize tumors to EGFR-directed TKIs, providing researchers with the opportunity to study tumor evolution over time, after initial treatment with EGFR-TKIs. This model indeed enables the tracking of the emergence of resistance to first-generation EGFR-TKIs (Arteaga, 2006; Politi et al., 2006). GEMMs that also combine different *EGFR* mutations are also available for the study of the complexity of NSCLC resistance to targeted therapies (Kim et al., 2022). Notably, GEMMs models carrying *EGFR* mutations have also been utilized for studies of NSCLC resistance to immunotherapy (Le et al., 2021);
- **GEMMs carrying *ALK* rearrangements.** Transgenic mouse models carrying the *EML4-ALK* fusion have been developed for the study of the response and mechanisms of resistance of *ALK*-rearranged NSCLC to ALK inhibitors such as crizotinib (Pyo et al., 2017);
- **GEMMs carrying *ROS1* rearrangements.** GEMMs harboring *CD74-ROS1* and *SDC4-ROS1* fusions have been developed for the study of the pathogenesis of *ROS1*-rearranged NSCLC and for the investigation of novel therapeutic strategies against this class of tumors (Inoue et al., 2016);
- **GEMMs carrying *KRAS* mutations.** Several transgenic mice harboring *KRAS* mutations, including G12D and G12C mutations, have been developed for the study of the initiation and progression of *KRAS*-mutated lung tumors, for the identification of novel drugs targeting KRAS signaling pathways, and for the study of the mechanisms of resistance to $KRAS^{G12C}$-mutated NSCLC (Jackson et al., 2001; Johnson et al., 2001; Drosten et al., 2018; Lee et al., 2023). Several models of GEMMs carrying co-mutations of *KRAS* and other genes have also

been described. Some examples are the GEMM model characterized by conditional mutations in *KRAS* and *p53* tumor suppressor gene (Jackson et al., 2005; DuPage et al., 2009), or models carrying co-mutations in *KRAS* and *Ink4a/Arf* or *Lkb1* (also known as *STK11*) genes (Ji et al., 2007). All these models showed increased progression of lung tumors and metastatic lesions. Notably, the *p53* and *KRAS* co-mutant GEMM model has been extensively used for studying NSCLC resistance to immunotherapy, as these genes are frequently co-mutated in human NSCLC (Riccardo et al., 2014). Several studies have also demonstrated that lung tumors carrying *KRAS* and *p53* co-mutations are highly immunogenic, but they also develop several mechanisms to suppress the antitumor immune responses, including PD-L1 upregulation and recruitment of immunosuppressive cells (Adeegbe et al., 2018; Boumelha et al., 2022). Finally, the GEMM model harboring $KRAS^{G12D}$ mutation together with *PTEN* knock-out has been used not only for investigations regarding the tumorigenesis of human colorectal cancer (CRC), but also for the study of the interplay between these genes in lung cancer progression and resistance to therapies (de Seranno & Meuwissen, 2010; Davies et al., 2014; Berthelsen et al., 2021).

- **GEMMs with knock-out of immune checkpoint.** Transgenic mice characterized by the loss of PD-L1 expression have been developed to investigate how the loss of tumoral immune checkpoint influence tumor immunity and resistance to ICIs. For instance, a GEMM model of *EGFR*-mutant NSCLC with *PD-L1* knock-out has been used to investigate how IL-6 can influence the TME composition and the response to ICI therapy (Patel et al., 2023).

Despite the advantages provided by the use of these models in cancer research, GEMMs also have several notable drawbacks. One of the main limitations is their relatively low TMB (McFadden et al., 2016; Salehi-Rad et al., 2021). Human NSCLC, especially those driven by mutations in genes like *KRAS*, *TP53*, and *LKB1*, is typically characterized by a high TMB, often resulting in tumors with diverse and complex phenotypes. In contrast, many GEMMs possess only the primary driver mutations and lack the additional protein-altering mutations that contribute to tumor heterogeneity (Salehi-Rad et al., 2021). This limitation makes it difficult for GEMMs to fully recapitulate the mutational complexity of human NSCLC. In addition, GEMMs often suffer from genetic homogeneity due to the use of inbred mouse strains, such as C57Bl/6, where each mouse is genetically identical to the others (Rogers, 2019; Simond & Muller, 2020). This lack of genetic diversity contrasts with the vast heterogeneity found in human cancer, where genetic variability significantly influences tumor behavior and treatment outcomes. Another significant drawback is that many GEMMs fail to develop metastases, a hallmark of advanced NSCLC in humans (Hayes et al., 2014). Since metastasis is a key factor in disease progression and treatment resistance, the lack of this characteristic limits the

utility of GEMMs for studying advanced-stage cancer and therapeutic responses in metastatic settings.

As a result, ongoing research is focused on developing more genetically diverse mouse models to better reflect the complexity of human cancer and enhance the predictive power of preclinical studies (Fitzgerald et al., 2021; Zhu et al., 2023; Abate-Shen & Politi, 2024).

Results

1. DEVELOPMENT OF PATIENT-DERIVED NSCLC PRECLINICAL MODELS

The human NSCLC cell lines most commonly used in lung cancer research and included in commercially available panels were established decades ago (Gazdar, Girard, et al., 2010; Arnal-Estapé et al., 2021). Since exogenous factors (*e.g.*, smoking habits, exposure to particulate matter) can influence cancer cell phenotypes and their heterogeneity, these cell lines often fail to fully replicate the complexity and diversity of treatment responses observed in patients. Further, the continuous propagation of these models over time has likely altered their mutational profile, potentially distancing them from the original tumor characteristics and limiting their relevance in contemporary research (Hynds et al., 2021). In contrast, newly derived primary cell lines established from patients who have developed resistance to immunotherapy or targeted therapies offer the significant advantage of retaining the original tumor heterogeneity, a feature that established cell lines tend to lose over time. This approach not only provides a more accurate representation of the disease but also opens new avenues for personalized medicine, tailored to individual tumor profiles (Miserocchi et al., 2017; Richter et al., 2021).

Moreover, for oncogene-driven NSCLC, commercially available cell lines lack endogenous representation of certain rare mutations, including specific uncommon *EGFR* mutations, *BRAF* mutations, and *ROS1* fusions (S.-Y. Kim et al., 2019). In this regard, the significance of the patient-derived cell cultures established in our laboratory lies in their unique genetic landscape, characterized by rare mutations and distinct resistance profiles. These models offer a critical resource for advancing our understanding of tumor biology and resistance mechanisms, providing novel insights that commercially available lines simply cannot capture.

In the Laboratory of Immunology and Biology of Metastasis directed by Prof. Pier-Luigi Lollini, we established a panel of human NSCLC preclinical models derived from patients exhibiting primary or acquired resistance to the leading approved therapeutic strategies, including tyrosine kinase inhibitors (TKIs) and immunotherapy. In this context, human tumor samples have been collected and used for the establishment of primary cell cultures or patient-derived xenografts (PDXs).

In this study, a cohort of 23 patients was enrolled to investigate resistance mechanisms to TKI-based therapies in advanced NSCLC with rare mutations and/or immunotherapy resistance, yielding a subset of samples that successfully generated primary cell cultures or PDXs.

Table 1 provides a detailed summary of the clinical and molecular characteristics of the patients enrolled in the present study.

Patient case	Tumor mutations	Therapy at the time of sampling	Patient's clinical response
ADK-VR2	SDC4-ROS1 gene fusion	None (baseline)	Progression disease after chemotherapy (first-line) and crizotinib (second-line)
ADK-VR3	$KRAS^{G12D}$	Chemotherapy	Progression disease after chemotherapy
LIBM-ADK-11	$EGFR^{E19delins}$	Osimertinib	Progression disease after osimertinib
ADK-13	$KRAS^{G12C}$	Immunotherapy	Progression disease after chemotherapy (first- and second-line). Slow progression disease after immunotherapy (third-line)
ADK-14	$BRAF^{G466V}$ (class III mutation)	Chemo-immunotherapy	Slow progression disease after chemo-immunotherapy
ADK-15	$EGFR^{L858R}$, DDR2 mutation	Gefitinib	Progression disease after gefitinib
ADK-17	$KRAS^{G12C}$	None (baseline)	Hyperprogressive disease after immunotherapy
ADK-18		Immunotherapy	
ADK-19	$KRAS^{G12C}$	Immunotherapy	Progression disease after chemotherapy (first-line) and hyperprogression disease after immunotherapy (second-line)
ADK-20	KRAS, FGFR3-TACC3 gene fusion $EGFR^{E19del}$	Osimertinib	Progression disease after osimertinib (first-line), and chemo-immunotherapy (second-line)
ADK-21	$KRAS^{G13C}$	Immunotherapy	Progression disease after chemotherapy (first-line) and immunotherapy (second-line)
ADK-25	$KRAS^{G12V}$	Chemo-immunotherapy	Hyperprogressive disease after chemo-immunotherapy
ADK-28	$KRAS^{G12C}$	Immunotherapy	Progression disease after immunotherapy
ADK-30	EGFR, EGFR-RET gene fusion	Osimertinib	Progression disease after osimertinib
ADK-31	EGFR (exon 20 amplification)	Osimertinib	Progression disease after osimertinib

Table 1. List of clinical cases with NSCLC enrolled in the present study (*table continues in the next page*).

Patient case	Tumor mutations	Therapy at the time of sampling	Patient's clinical response
ADK-32	EGFR	Chemo-immunotherapy	Long responder, then progression disease after osimertinib (first-line) and chemo-immunotherapy (second-line)
ADK-34	$KRAS^{G12A}$	Chemo-immunotherapy	Progression disease after chemo-immunotherapy (first-line), stable disease after chemotherapy (second-line)
ADK-35	$KRAS^{G12C}$	Sotorasib	Progression disease after chemo-immunotherapy (first-line), chemotherapy (second-line) and sotorasib (third-line)
ADK-36	$BRAF^{D594G}$ (class III mutation)	Chemo-immunotherapy	Progression disease after chemo-immunotherapy (first-line). Partial response after erlotinib (second-line)
ADK-37	$BRAF^{V600E}$ (class I mutation)	Dabrafenib + Trametinib	Progressive disease after dabrafenib + trametinib
ADK-38	$KRAS^{G12V}$	Chemo-immunotherapy	Progressive disease after chemo-immunotherapy (first-line) and immunotherapy (second-line)
ADK-40	n.d.	Immunotherapy	Rapid progression disease after immunotherapy
ADK-41	BRAF (class III mutation)	Immunotherapy	Progression disease after immunotherapy
ADK-42	n.d.	Chemo-immunotherapy	Mixed response after chemo-immunotherapy

Table 1 (*continued*). List of clinical cases with NSCLC enrolled in the present study.

The establishment of cell lines from fresh tumor tissues achieved a success rate of approximately 50%, whereas PDXs demonstrated a higher success rate of around 73%, with 11 out of 15 PDXs successfully stabilized. Of note, we also effectively established PDX-derived cell cultures (PDXC) from all the stabilized PDXs.

Figure 1 illustrates the growth curves of the efficiently stabilized PDXs, highlighting their growth dynamics and significant differences in tumor growth.

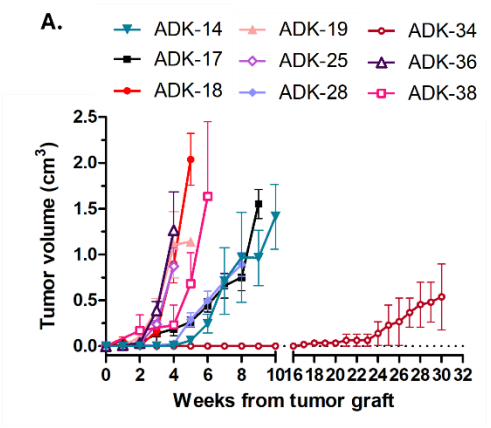

vs	ADK-14	ADK-17	ADK-18	ADK-19	ADK-25	ADK-28	ADK-34	ADK-36	ADK-38
ADK-14		n.s.	***	***	***	n.s.	*	***	***
ADK-17	n.s.		*	***	*	n.s.	n.s.	****	n.s.
ADK-18	***	*		n.s.	n.s.	***	**	n.s.	*
ADK-19	***	***	n.s.		n.s.	****	****	n.s.	***
ADK-25	***	*	n.s.	n.s.		***	***	n.s.	*
ADK-28	n.s.	n.s.	***	****	***		*	****	*
ADK-34	*	n.s.	**	****	***	*		****	***
ADK-36	***	****	n.s.	n.s.	n.s.	****	****		****
ADK-38	***	n.s.	***	***	*	*	***	****	

Minimum significance between group means, starting from 4th week after tumor engraftment, except * = from 5th week and * = from 7th week.

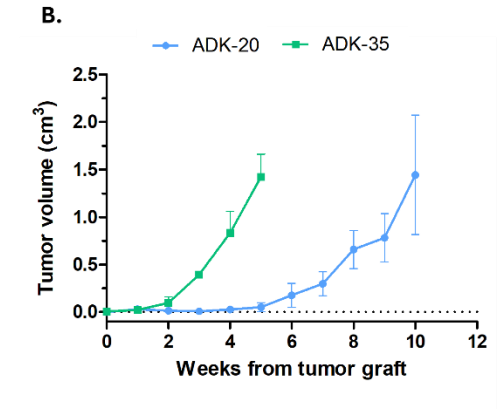

vs	ADK-20	ADK-35
ADK-20		****
ADK-35	****	

Minimum significance between the group means starting from 3rd week after tumor engraftment.

Figure 1. Tumor growth curves of stabilized PDXs established from 11 NSCLC patients. The picture depicts the tumor growth curves of PDXs established from patients who underwent immunotherapy **(A)** or targeted therapy **(B)**, described in **Table 1** (for each curve, n=2-4). Each point represents mean and SEM. Two-way ANOVA was used to compare the groups: **(A)** interaction, $p<0.0001$; volume, $p<0.01$; **(B)** interaction, $p<0.0001$; volume, $p<0.001$. The tables on the right report the minimum level of significance between group means, starting from the 4th **(A)** or 3rd **(B)** week after tumor engraftment (unless otherwise specified), as measured by the Tukey's post-tests. * $p<0.05$, ** $p<0.01$, *** $p<0.001$ and **** $p<0.0001$. n.s.: not significant. SEM: standard error of the mean.

Within the panel of patient-derived preclinical models described above, we focused our investigations on the following patient-derived cell lines:

- LIBM-ADK-11 and ADK-VR2, employed in studies investigating the role played by tumor heterogeneity in the resistance to TKIs;
- ADK-14 and PDX-ADK-36, used to investigate novel therapeutic strategies for oncogene-addicted NSCLC orphan of effective therapies;
- ADK-17, ADK-18, ADK-19 and ADK-25, utilized to define the biological processes responsible for resistance to ICI-based immunotherapy and identify novel therapeutic options to effectively overcome it.

2. THE IMPACT OF TUMOR HETEROGENEITY IN RESISTANCE TO TKI-BASED THERAPIES

Tumor heterogeneity is defined as the coexistence of diverse cell populations within a single tumor, which can vary in genetic, phenotypic, and functional characteristics (El-Sayes et al., 2021). This heterogeneity arises due to microenvironmental and treatment pressures, along with phenotypic shifts driven by genetic and epigenetic alterations (Zhu et al., 2021; A. Zhang et al., 2022; Salemme et al., 2023).

In this context, we present a compelling example of how tumor heterogeneity influences resistance to TKI-based therapies, illustrated by studying two NSCLC cell lines, ADK-VR2 and LIBM-ADK-11 (**Table 1**). Our findings from these models, described below, offer valuable insights into the impact that tumor heterogeneity can affect the response to TKI-targeted therapies.

2.1 ADK-VR2, a preclinical model of NSCLC carrying a *SDC4-ROS1* translocation

ADK-VR2 cell line was established from the pleural effusion of a treatment-naïve NSCLC patient carrying a *SDC4-ROS1* gene fusion, that was primarily resistant to crizotinib.

The low frequency of *ROS1* fusions in NSCLC inevitably limits the availability of preclinical models, significantly hindering the understanding of the mechanisms underlying drug resistance, as well as the development and identification of optimal therapeutic approaches to overcome it.

In the present study, we characterized the ADK-VR2 cell line model and its subpopulations resistant to crizotinib, proving its potential as a new preclinical model for investigating novel therapeutic approaches in *ROS1*-rearranged NSCLC.

The following sections describe the investigations conducted and the results obtained. Part of the data described below were also included in the manuscript Ruzzi, Angelicola et al., *Translational Lung Cancer Research*, 2022 (Ruzzi, Angelicola et al., 2022).

2.1.1 Clinical history and tumor molecular data of the patient

At the moment of diagnosis, the patient, a 46-year-old Asian, non-smoker male, affected with stage IV NSCLC, revealed extensive right pleural effusion and pulmonary spread. According to cytological and molecular analyses on pleural effusion cells, the primary tumor was positive for TTF1 and BerEP4 expression (**Figure 2A,B**), and showed a PD-L1 tumor proportion score (TPS) of 25% (data not shown). In addition, the tumor was negative for *EGFR*, *KRAS* or *ALK* alterations. The only identified alteration, detected through next-generation sequencing (NGS), was *SDC4-ROS1* gene fusion (**Figure 2C**).

As a first-line treatment, the patient received chemotherapy, consisting of cisplatin (75 mg/m^2) and pemetrexed (500 mg/m^2) every 3 weeks, up to four cycles. At the time of the first radiographic

tumor assessment, progressive disease was observed. Therefore, according to tumor *ROS1* status, a second-line treatment with crizotinib 250 mg twice daily was initiated, along with gamma-knife radiotherapy to address three brain lesions. Unfortunately, after two months of TKI-based treatment, the patient experienced once again disease progression, with hepatic and bone metastases, pulmonary lymphangitis, and peritoneal carcinomatosis. Considering the fast disease progression to TKI therapy, a liver biopsy was performed to investigate the molecular profile of the disease. Hematoxylin and eosin (H&E) staining showed the profile of an adenocarcinoma with an acinar structure expressing TTF1 (**Figure 2D,E**), while fluorescence in situ hybridization (FISH) testing confirmed the presence of 5' *ROS1* deletion in 62% of analyzed cells (**Figure 2F**).

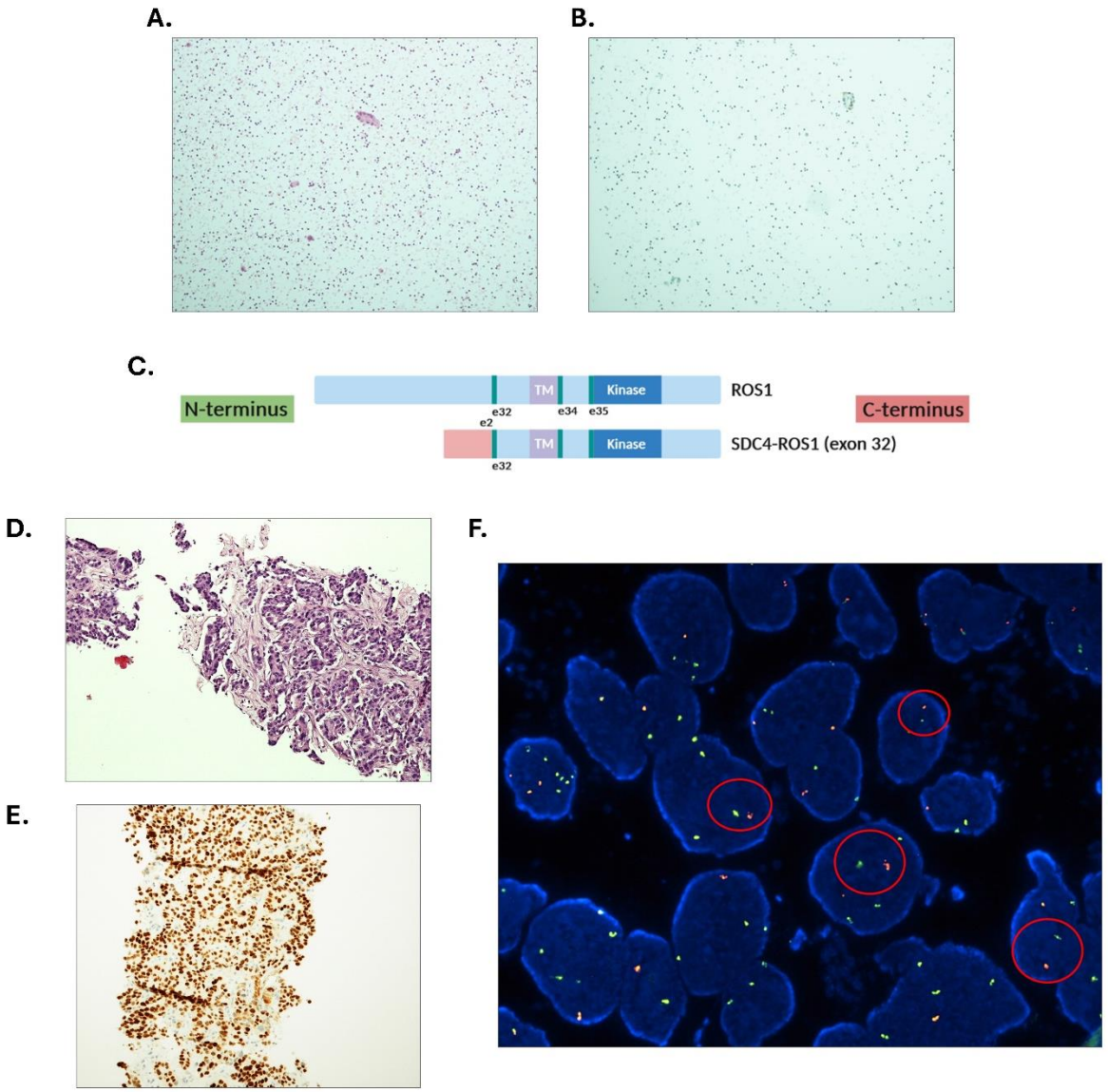

Figure 2. Molecular and morphological characterization of patient's tumor samples. (A,B) Cytological cell blocks from malignant pleural effusion of the patient at the diagnosis. **(A)** H&E staining showing aggregates of neoplastic cells (arrows). ×10 magnification. **(B)** TTF1 staining evidencing a focal positivity (arrows). ×10 magnification. **(C)** Representative illustration of the *SDC4*(exon 2)-*ROS1*(exon 32) rearrangement. **(D,E)** Liver metastasis. **(D)** H&E

staining. **(E)** TTF1 staining. **(F)** FISH image showing the *ROS1* fusion on liver biopsy. Circled areas represent positive cells to 5' *ROS1* fusion (magnification DAPI ×100). H&E: Hematoxylin and eosin; FISH: fluorescence in situ hybridization.

Following palliative radiotherapy, a third-line treatment with lorlatinib was proposed for compassionate use, but was not administered due to rapid disease progression which led to patient's *exitus*.

2.1.2 In vitro sensitivity of the ADK-VR2 cell line to ROS1-directed TKIs and chemotherapeutic agents

Firstly, the sensitivity profile of the ADK-VR2 cell line to multi-TKIs, ALK/ROS1-directed TKIs and pemetrexed was evaluated and compared to the one of the HCC-78 cell line. HCC-78 is a commercial cell line carrying the *SLC34A2-ROS1* fusion, representing the most used preclinical model of *ROS1*-rearranged NSCLC cell line for drug sensitivity tests (Davies et al., 2013; Terrones et al., 2023).

Considering the clinical history of the patient, who showed no response to the first-line chemotherapy and second-line crizotinib treatment, the sensitivity of ADK-VR2 to pemetrexed and crizotinib was tested in 2D culture conditions. ADK-VR2 cell line showed lower sensitivity to pemetrexed compared to HCC-78 cell line (IC_{50}: 0.068±0.013 and 0.0096±0.0009 µM, respectively) (**Figure 3A**). Of note, the sensitivity observed in the HCC-78 cell line was in accordance with previously published data (Davies et al., 2013). As for crizotinib, the 2D-growth of both ADK-VR2 and HCC-78 cell lines was partially inhibited by the drug (IC_{50}: 0.553±0.080 µM and 0.469±0.249 µM, respectively) (**Figure 3B**).

The sensitivity of the cell lines to next-generation ROS1-directed TKIs was then evaluated in both 2D and 3D culture settings. Under adherent culture conditions, the growth of ADK-VR2 was unaffected by lorlatinb, entrectinib or DS-6051b (IC_{50} >1 µM, at least), while HCC-78 showed higher sensitivity to the drugs (lorlatinib, IC_{50} <0.01 µM; entrectinib, IC_{50}: 0.2967±0.1182 µM; DS-6051b, IC_{50}: 0.4309±0.2459 µM) (**Figure 3C**). In contrast, in the 3D culture setting, ADK-VR2 sensitivity to the drugs was enhanced, as not only its colony formation ability showed increased inhibition in presence of crizotinib and entrectinib as compared to HCC-78 cell line, but cell growth was also almost completely inhibited by lorlatinib and DS-6051b, which resulted to be more effective than crizotinib ($p<0.05$ by unpaired *t*-test with Welch's correction) (**Figure 3D**). Lorlatinib was also more effective in reducing ADK-VR2 sphere formation ability (IC_{50}: 0.0003±0.0001 µM), as compared to DS-6051b (IC_{50}: 0.0013±0.0000 µM), crizotinib (IC_{50}: 0.0040±0.0003 µM) and entrectinib (IC_{50}: 0.023±0.005 µM) (IC_{50} comparison by Student's *t*-test: lorlatinib *vs* crizotinib and DS-6051b *vs*

crizotinib, p<0.01; lorlatinib *vs* DS-6051b and entrectinib, p<0.05; DS-6051b *vs* entrectinib, p<0.05). (**Figure 3E**).

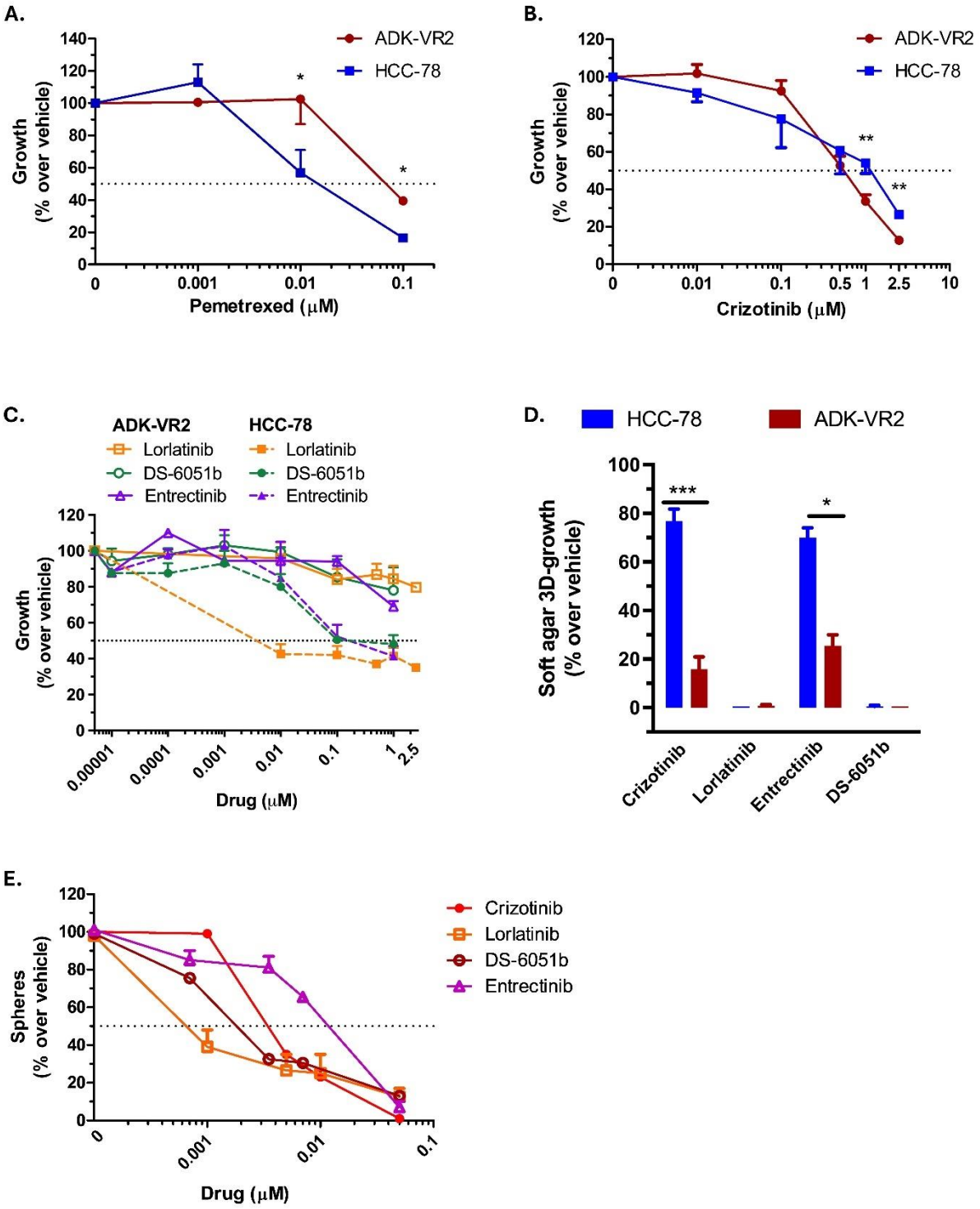

Figure 3. ***In vitro*** **drug sensitivity of ADK-VR2 and HCC-78. (A)** ADK-VR2 and HCC-78 sensitivity to pemetrexed in 2D culture conditions (n=2). *, p<0.05 by Student's *t*-test. Each point represents mean and SEM. **(B)** ADK-VR2 (n=8) and HCC-78 (n=4) sensitivity to crizotinib in 2D culture conditions. **, p<0.01 by Student's *t*-test. Each point represents mean and SEM. **(C)** ADK-VR2 sensitivity to lorlatinib (n=4), DS-6051b (n=3) and entrectinib (n=2) in 2D culture

conditions; HCC-78 sensitivity to lorlatinib (n=2), DS-6051b (n=2) and entrectinib (n=3) in 2D culture conditions. Each point represents mean and SEM. **(D)** Soft agar 3D-growth in the presence of crizotinib 0.01 μM (HCC-78, n=4; ADK-VR2, n=6), lorlatinib 0.01 μM (HCC-78, n=2; ADK-VR2, n=4), entrectinib 0.01 μM (HCC-78, n=2; ADK-VR2, n=2) and DS-6051b 0.01 μM (HCC-78, n=2; ADK-VR2, n=2). *, $p<0.05$ and ***, $p<0.001$ by Student's *t*-test. Each bar represents mean and SEM. **(E)** ADK-VR2 sphere formation ability in presence of crizotinib, lorlatinib, DS-6051b and entrectinib (n=2). Each point represents mean and SEM. SEM: standard error of the mean.

In summary, ADK-VR2 cell line was partially inhibited by crizotinib, but was unaffected by other TKIs such as lorlatinib, entrectinib and DS-6051b, in 2D culture conditions. The activity of these TKIs dramatically changed under 3D culture settings, as in these conditions ADK-VR2 was almost totally inhibited by lorlatinib and DS-6051b.

2.1.3 ADK-VR2 tumorigenic and metastatic ability and in vivo sensitivity to crizotinib

In order to assess the tumorigenic potential of ADK-VR2 *in vivo*, the cell line was subcutaneously (s.c.) injected in immunodeficient mice and the resulting tumors were phenotypically characterized. The mice-derived tumors exhibited features that closely resembled the ones of the primary patient's tumor sample, particularly in terms of H&E staining and TTF1 expression (**Figure 4A,B**).

The metastatic potential of the cell line was also evaluated by intravenous (i.v.) injection into immunodeficient mice. ADK-VR2 cell line demonstrated a high capacity for experimental metastasis, inducing a significant burden of lung metastases (**Figure 4C,D**).

Following the assessment of *in vivo* cell growth, we also tested the sensitivity of ADK-VR2 to crizotinib *in vivo*. Surprisingly, crizotinib significantly inhibited tumor growth as compared to the control group, although it did not completely eradicate the tumor (starting from the 68^{th} day after cell injection, $p<0.01$ at least, by two-way ANOVA test and Bonferroni's post-test) (**Figure 4E**). A slight reduction in spontaneous lung metastatic burden, determined by detecting human cells in the mice's lungs via Real-time PCR (RT-PCR), was also observed in the crizotinib-treated group as compared to the untreated one (**Figure 4F**).

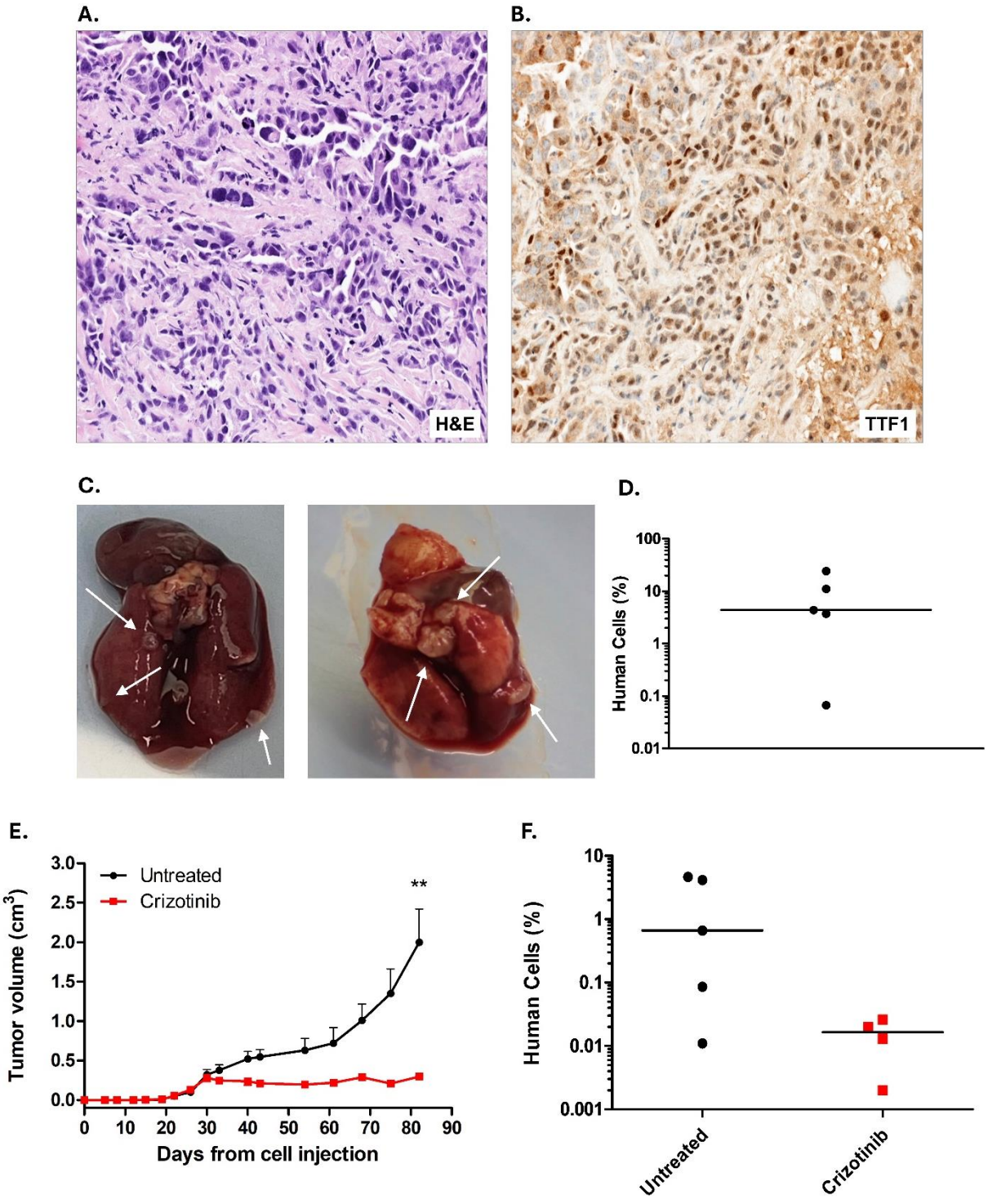

Figure 4. ADK-VR2 *in vivo* growth and sensitivity to crizotinib. (A,B) Phenotypic characterization of a representative tumor induced by subcutaneous (s.c.) injection of ADK-VR2 cells in immunocompromised mice. **(A)** H&E staining. ×20 magnification **(B)** TTF1 staining. ×20 magnification. **(C)** Representative pictures of lung metastases of immunosuppressed mice receiving an intrvenous (i.v.) injection of ADK-VR2 cells. Arrows indicate some metastatic nodules. **(D)** Lung metastatic burden of immunosuppressed mice receiving i.v. injection of ADK-VR2 cells, quantified by RT-PCR. A negative control consisting of only mouse cells was included in each PCR (0% of human cells). Horizontal line represents the median. **(E)** Tumor growth of ADK-VR2 cells s.c. injected in immunosuppressed mice treated with crizotinib (n=4), or not treated (n=5). Two-way ANOVA was used to compare the groups (interaction, $p<0.001$; treatment,

p<0.01). Starting from 68th day after cell injection: **, p<0.01 at least, by Bonferroni's post-test (comparison between group means). Each point represents mean and SEM. **(F)** Lung metastatic load of mice groups described in **(E)**, quantified by RT-PCR. Horizontal line represents the median. H&E: hematoxylin and eosin; RT-PCR: real time-polymerase chain reaction; SEM: standard error of the mean.

In summary, ADK-VR2 cell line demonstrated strong tumorigenic and metastatic capabilities when injected into immunosuppressed mice. Additionally, consistently with *in vitro* findings, the growth of ADK-VR2-derived tumors was heavily inhibited by crizotinib.

2.1.4 In vitro selection of an ADK-VR2 crizotinib-resistant variant

Given the discrepancy between ADK-VR2 response to crizotinib treatment and the clinical response observed in the patient, we isolated a crizotinib-resistant cell line clone from ADK-VR2 cells cultured in the presence of crizotinib under 3D conditions (namely, AG143 clone). Of note, according to the Oncomine panel, ADK-VR2 AG143 did not acquire any additional genetic alterations and retained the same *ROS1* rearrangement observed in the parental cell line. As expected, ADK-VR2 AG143 clone showed a significantly lower sensitivity to crizotinib as compared to the parental cell line in 2D culture setting (IC_{50} >1.5 μM) (**Figure 5A**).

As for next-generation ROS1 inhibitors, ADK-VR2 AG143 did not show any 2D-response to lorlatinib, entrectinib and DS-6051b, similarly to what had been observed in the parental cell line (**Figure 5B**).

Under 3D culture conditions, ADK-VR2 AG143 clone exhibited reduced inhibition of colony formation ability by crizotinib and DS-6051b, while maintaining similar sensitivity to lorlatinib and entrectinib, as compared to ADK-VR2 (**Figure 5C**). Notably, lorlatinib and DS-6051b were more effective than crizotinib in inhibiting the 3D-growth of ADK-VR2 AG143 (**Figure 5C**).

Interestingly, the clone exhibited a reduced capacity for sphere formation under anchorage-independent culture conditions as compared to the parental cell line (ADK-VR2 AG143, number of spheres 95±7, n=4; ADK-VR2, number of spheres 164±7, n=4; p<0.001, by Student's *t*-test). Furthermore, treatment with ROS1-directed TKIs was less effective at inhibiting the sphere formation of the clone compared to ADK-VR2 cell line (**Figure 5D**). Nonetheless, similarly to the previous observations in the parental cell line, lorlatinib (IC_{50}: 0.003±0.001 μM) was more potent than crizotinib (IC_{50}: 0.024±0.010 μM), entrectinib (IC_{50}: 0.059±0.011 μM) and DS-6051b (IC_{50}: 0.106±0.011 μM) in reducing the number of spheres formed by ADK-VR2 AG143 cells (lorlatinib *vs* entrectinib and DS-6051b, and crizotinib *vs* DS-6051b, p<0.05 by Student's *t*-test) (**Figure 5D**).

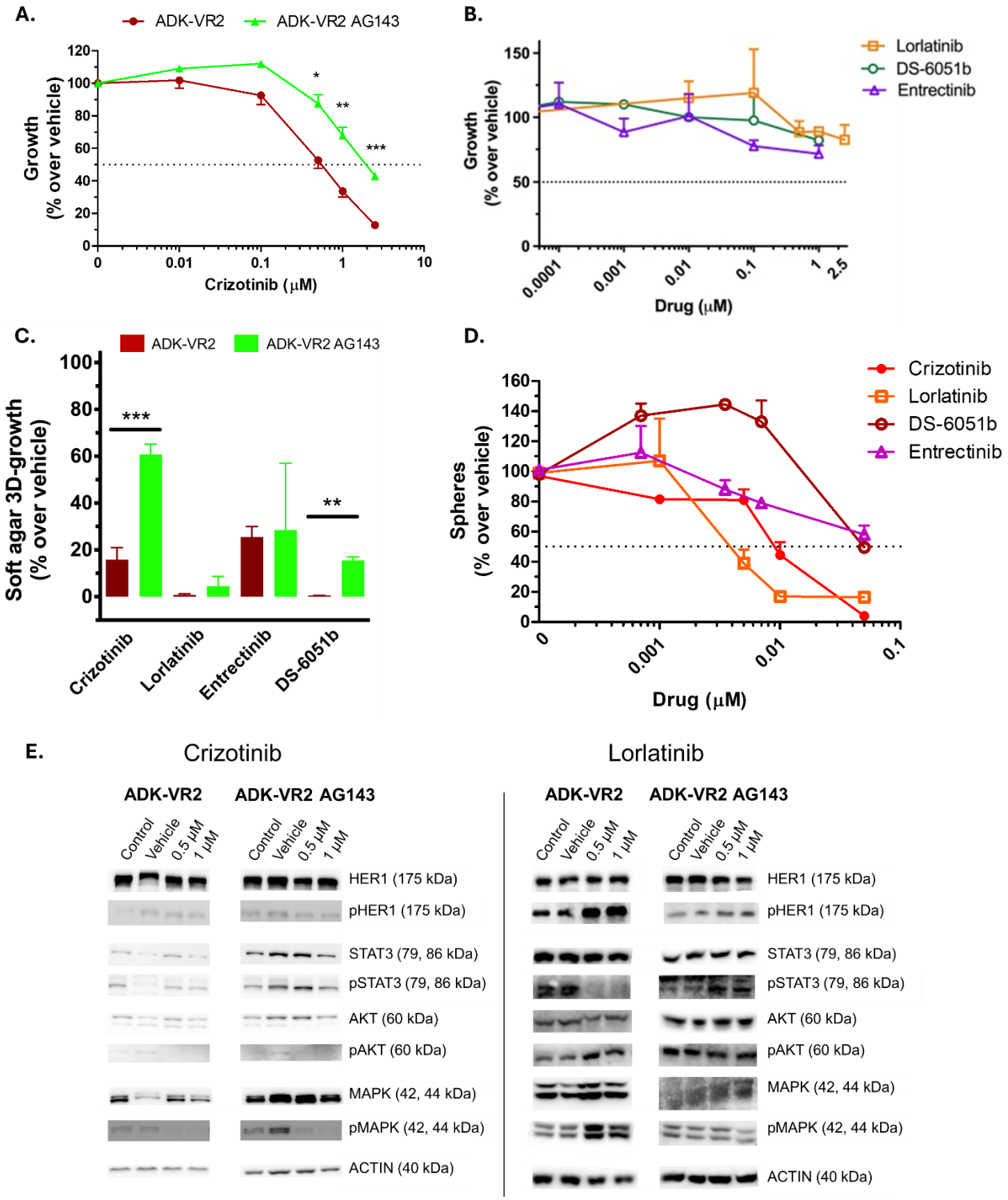

Figure 5. ***In vitro*** **drug response of ADK-VR2 AG143 compared to ADK-VR2. (A)** ADK-VR2 (n=8) and ADK-VR2 AG143 (n=2) sensitivity to crizotinib in 2D culture conditions. *, p<0.05; **, p<0.01 and ***, p<0.001 by Student's *t*-test. Each point represents mean and SEM. **(B)** ADK-VR2 AG143 sensitivity to lorlatinib (n=2), DS-6051b (n=2) and entrectinib (n=2) in 2D culture conditions. Each point represents mean and SEM. **(C)** Soft agar 3D-growth of ADK-VR2 and ADK-VR2 AG143 in the presence of crizotinib 0.01 μM (n=4), lorlatinib 0.01 μM (n=4), entrectinib 0.01 μM (n=2)

and DS-6051b 0.01 μM (n=2). ***, p<0.001 and **, p<0.01 by Student's *t*-test. Each bar represents mean and SEM. **(D)** ADK-VR2 AG143 sphere formation ability in the presence of crizotinib, lorlatinib, DS-6051b and entrectinib (n=2). Each point represents mean and SEM. **(E)** Western blotting analysis on ADK-VR2 and ADK-VR2 AG143 cells treated or not with crizotinib or lorlatinib (0.5 μM or 1 μM). Actin was used as housekeeping protein for protein normalization. SEM: standard error of the mean.

To examine the differentially activated signaling pathways determining the response of ADK-VR2 and ADK-VR2 AG143 to crizotinib and next-generetion ROS1-TKIs and the variations in drug sensitivity observed based on cell culture conditions, Western blot analyses were performed on the cell lines grown in 2D culture conditions in presence of crizotinib or lorlatinib treatments (**Figure 5E**). Crizotinib treatment did not particularly affect HER1 or STAT3 activation in either the ADK-VR2 or the ADK-VR2 AG143 cell line. In contrast, lorlatinib enhanced HER1 activation in ADK-VR2 cell line. As for STAT3, interestingly lorlatinib showed an opposite effect in the two cell lines. Indeed, while the drug markedly inhibited STAT3 activation in the ADK-VR2 cell line, it hyperactivated the protein in the ADK-VR2 AG143 clone. Similarly, the activation of MAPK and AKT resulted to be enhanced by lorlatinib in the parental cell line, but it was slightly inhibited or unaffected in the clone. Differently, crizotinib strongly reduced MAPK activation in both the cell lines (**Figure 5E**).

To conclude ADK-VR2 AG143 cell line characterization, we tested its tumorigenicity *in vivo* through s.c. injection in immunosuppressed mice. The *in vivo* growth of the clone resulted to be slower as compared to the one of the parental cell line (starting from 2nd week after cell injection, p<0.001 at least, by two-way ANOVA test and Bonferroni's post-test) (**Figure 6A**). Notably, the ADK-VR2 AG143-derived tumors retained the histological and phenotypical features of the patient's tumor sample (**Figure 6B**).

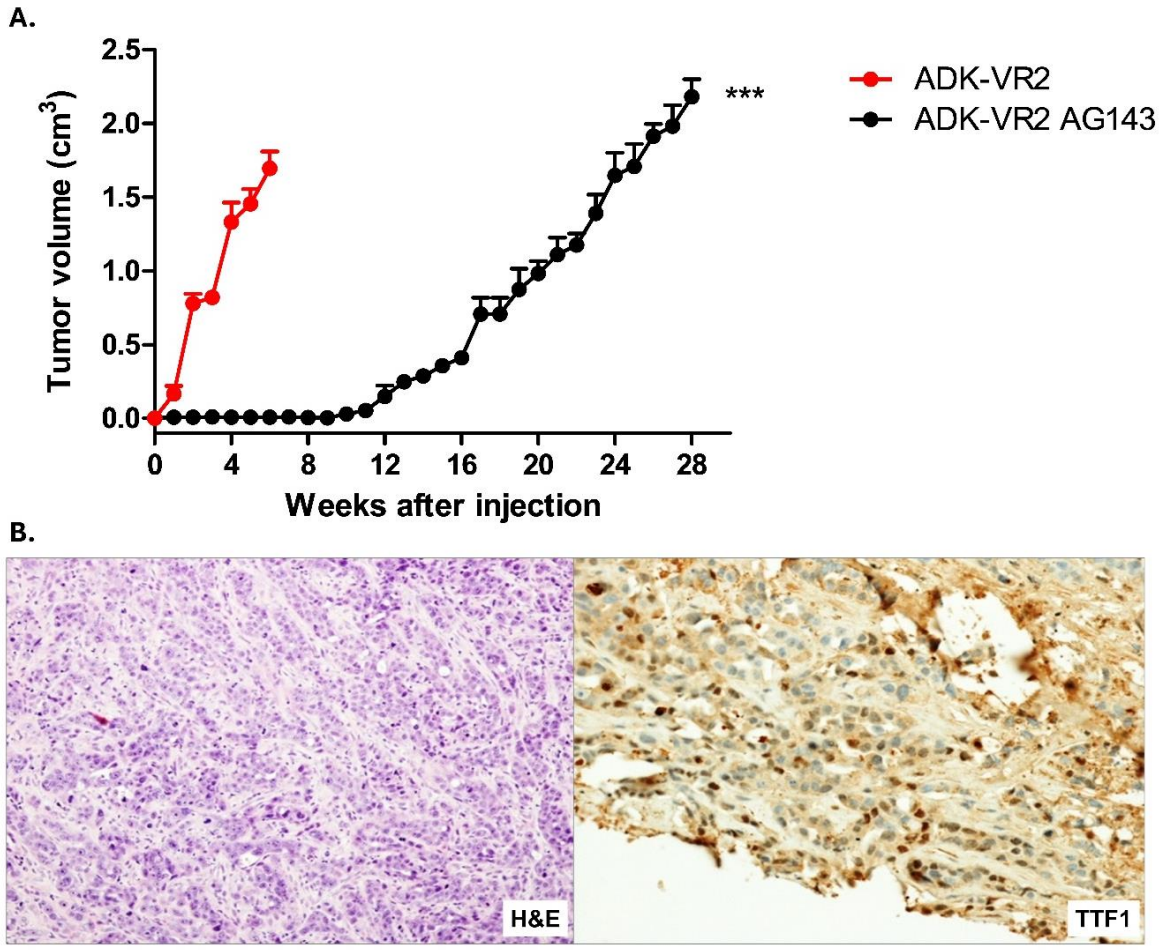

Figure 6. ADK-VR2 AG143 *in vivo* growth. (A) Comparison of tumor growth of ADK-VR2 and ADK-VR2 AG143 cells subcutaneously (s.c.) injected in immunosuppressed mice (n=3 for each group). Two-way ANOVA was used to compare the groups (interaction, $p<0.001$; volume: $p<0.001$). Starting from the 2nd week after cell injection: ***, $p<0.001$ by Bonferroni's post-test (comparison between group means). Each point represents mean and SEM. **(B)** Phenotypic characterization of a representative tumor induced by s.c. injection of ADK-VR2 AG143 cells in immunosuppressed mice. Left, H&E staining. ×20 magnification. Right, TTF-1 staining. ×20 magnification. H&E: hematoxylin and eosin; SEM: standard error of the mean.

In summary, the crizotinib-resistant ADK-VR2 AG143 clone showed no response to next-generation ROS1-TKIs under 2D culture conditions, but demonstrated marked sensitivity to lorlatinib in a 3D culture setting. Notably, ADK-VR AG143 clone also exhibited a reduced ability to form spheres and slower *in vivo* growth as compared to the parental cell line ADK-VR2.

2.2 LIBM-ADK-11, a cell line derived from an osimertinib-resistant NSCLC patient carrying an uncommon *EGFR* mutation

2.2.1 LIBM-ADK-11 phenotypical characterization and in vitro drug sensitivity

The LIBM-ADK-11 cell line was derived from the pleural effusion of a NSCLC patient carrying a rare *EGFR* mutation (exon 19, p.Leu747_Pro753delinsSer), who progressed following osimertinib-based treatment.

The phenotypic characterization of the cell line revealed some notable variations in its protein expression profile across successive *in vitro* cell passages. The cytofluorimetric analysis indeed initially highlighted the presence of a subpopulation of cells highly expressing the CD44 marker, which was, however, progressively lost over *in vitro* passages (percentage of $CD44^{+}$ cells, 14^{th} *in vitro* passage: 31%; 43^{rd} *in vitro* passage: 0%) (**Figure 7A**). Similarly, an $HER3^{negative}$ cell subpopulation was also lost across *in vitro* passages (**Figure 7B**). While HER1 expression showed no noticeable variations (**Figure 7C**), HER2, in contrast, exhibited a broad expression profile in the FACS histogram of low-passage cells, which subsequently narrowed in successive cell passages, indicating a shift towards a more defined HER2 expression pattern (**Figure 7D**).

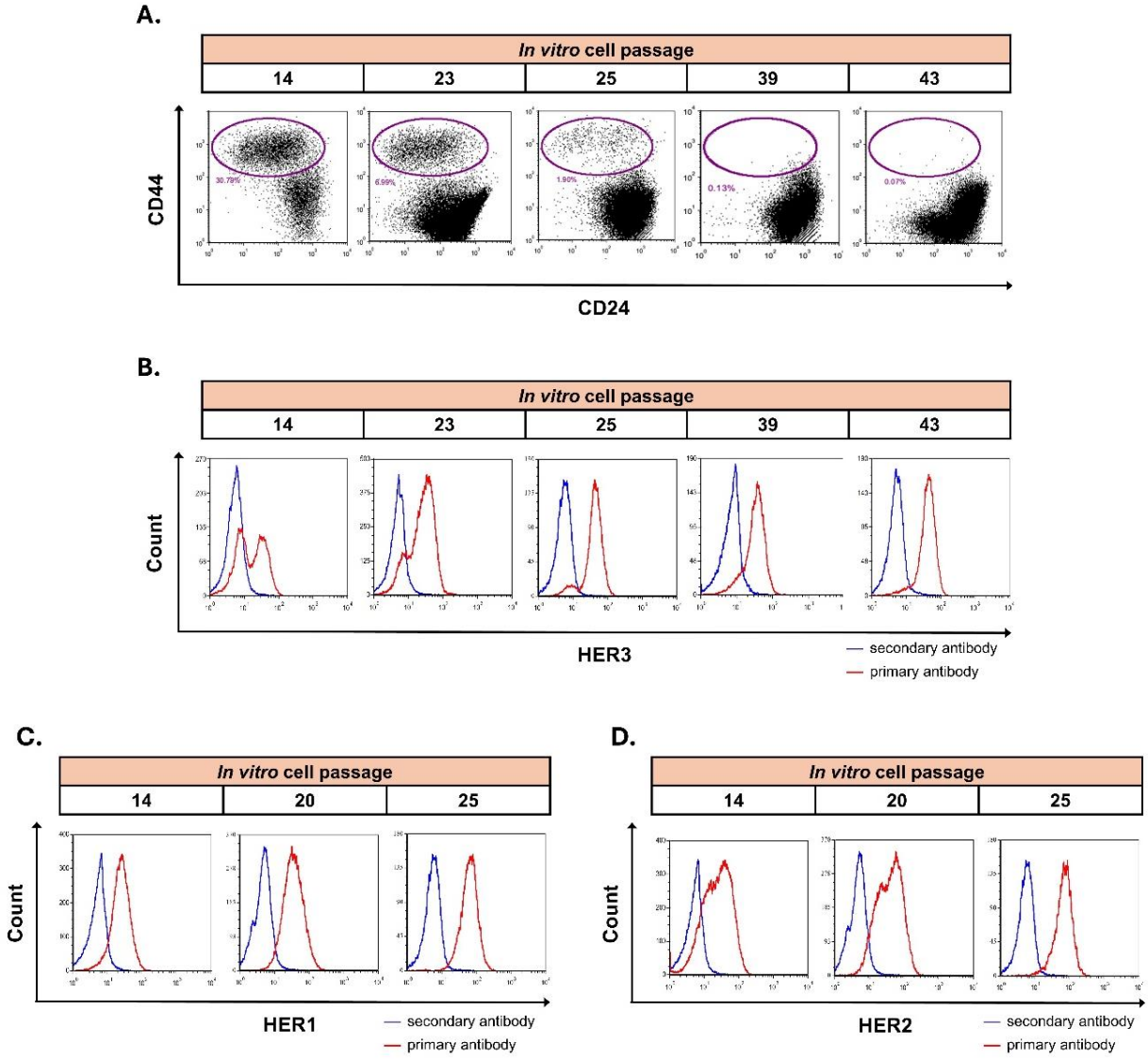

Figure 7. LIBM-ADK-11 phenotypical characterization over *in vitro* cell passages. (A) CD24 and CD44 expression on different LIBM-ADK-11 *in vitro* cell passages. **(B)** HER3 expression on different LIBM-ADK-11 *in vitro* cell passages. Median Fluorescence Intensity (MFI), 14th passage: 15; 23rd passage: 22; 25th passage: 37; 39th passage: 35; 43rd passage: 43. **(C)** HER1 expression on different LIBM-ADK-11 *in vitro* cell passages. MFI, 14th passage: 49; 20th passage: 30; 25th passage: 58. **(D)** HER2 expression on different LIBM-ADK-11 *in vitro* cell passages. MFI, 14th passage: 31; 20th passage: 35; 25th passage: 64.

Considering these variations in the phenotypic profile of LIBM-ADK-11 during cell culture propagation, the sensitivity of LIBM-ADK-11 cell line to multiple EGFR inhibitors was evaluated in 2D culture conditions, on both low and high-passage cells. Interestingly, the *in vitro* response of the cell line to EGFR-targeted TKIs appeared to be influenced by its passage number. Indeed, while low-passage LIBM-ADK-11 cells (LP-LIBM-ADK-11, 12th and 15th passages) were resistant to osimertinib treatment in 2D-culture conditions (IC_{50}: 7.11±0.59 μM), high-passage LIBM-ADK-11

cells (HP-LIBM-ADK-11, 36th and 42nd passages) reacquired the sensitivity to the drug (IC_{50}: 0.09±0.04 μM) (**Figure 8A**).

A similar difference in cell sensitivity to other EGFR-TKIs, *i.e.* erlotinib and afatinib, was observed between low and high-passage cells (erlotinib, LP-LIBM-ADK-11 IC_{50}: 16.27±4.22 μM, HP-LIBM-ADK-11 IC_{50}: 0.15±0.07 μM; afatinib, LP-LIBM-ADK-11 IC_{50}: 6.35±2.49 μM, HP-LIBM-ADK-11 IC_{50}: 0.01±0.00 μM) (**Figure 8B,C**).

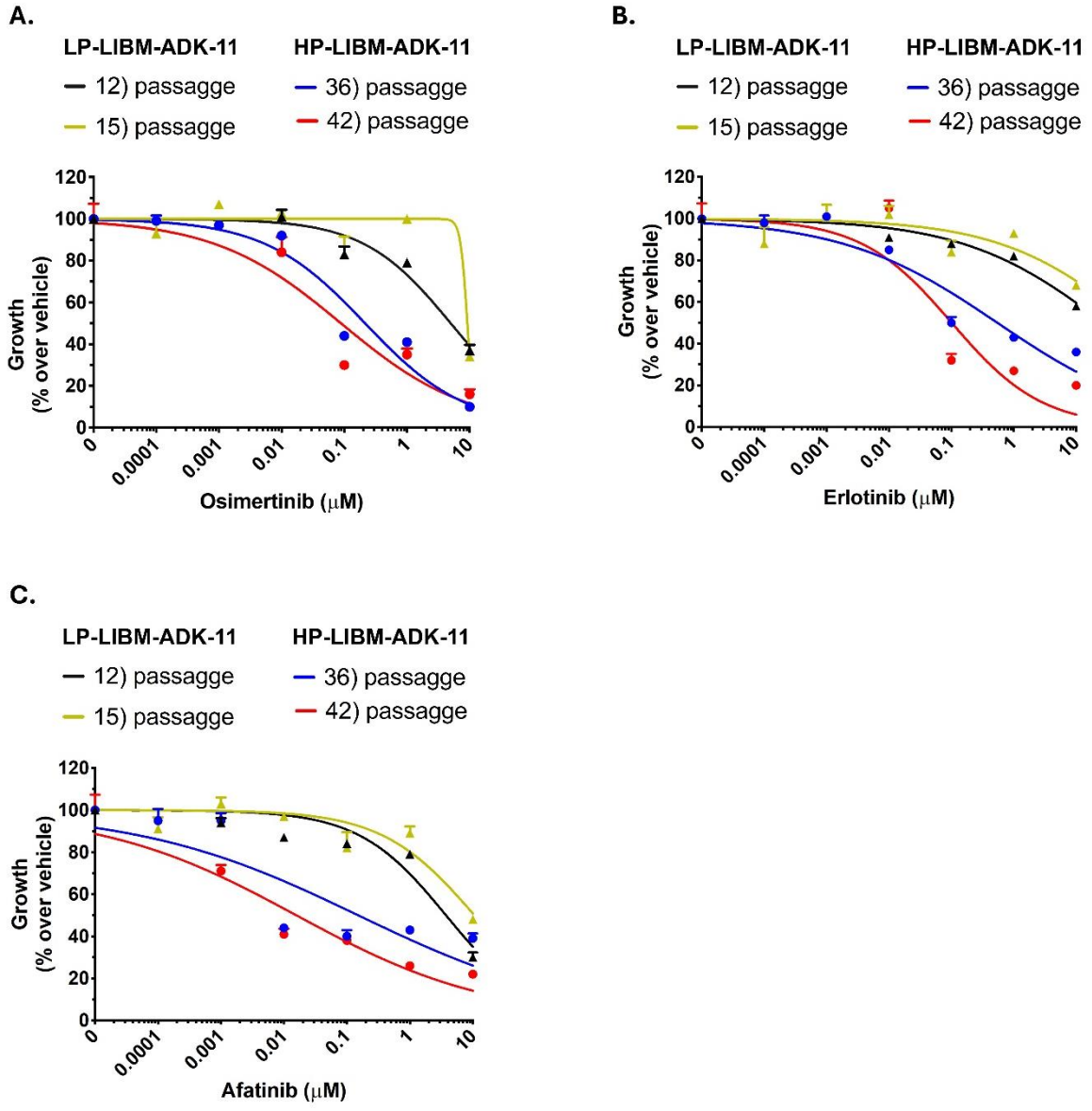

Figure 8. LIBM-ADK-11 2D-sensitivity to EGFR-directed TKIs over *in vitro* cell passages. Low-passage (LP) and high-passage (HP) LIBM-ADK-11 sensitivity to osimertinib **(A)**, erlotinib **(B)** and afatinib **(C)** (n=1, each one with 3 technical replicates). Each bar represents mean and SEM. SEM: standard error of the mean.

In summary, phenotypical and functional features of the LIBM-ADK-11 cell line, including protein expression profiles and *in vitro* response to EGFR-directed TKIs, were markedly influenced

by *in vitro* cell passage. LP-LIBM-ADK-11 cells, which showed the presence of CD44^{high} and HER3^{negative} cell subpopulations, were resistant to EGFR-TKIs *in vitro*. In contrast, HP-LIBM-ADK-11 cells, which lost the CD44^{high} and the HER3^{negative} cell subpopulations, regained *in vitro* sensitivity to EGFR-TKIs.

2.2.2 Investigation of the role of the CD44^{high} LIBM-ADK-11 cell subpopulation in osimertinib resistance

To verify if the CD44^{high} cell subpopulation identified in the LP-LIBM-ADK-11 cell line was involved in its resistance to EGFR inhibition *in vitro*, LP-LIBM-ADK-11 cells were sorted to isolate the two CD44^{high} and CD44^{low} cell subpopulations.

As previously shown, the phenotypic characterization of LP-LIBM-ADK-11 cell line had evidenced the presence of cell subpopulations with differential CD44 expression (**Figure 7A**). Specifically, the cell line comprised two distinct cell subpopulations, exhibiting different levels of CD44 expression: P2 (CD44^{high}) and P4 (CD44^{low}) (**Figure 9A**).

P2-CD44^{high} and P4-CD44^{low} were isolated from the LP-LIBM-ADK-11 cell line using sorting and their CD44 expression profile was assessed and compared to the one of the pre-sorted parental cell line (**Figure 9B**).

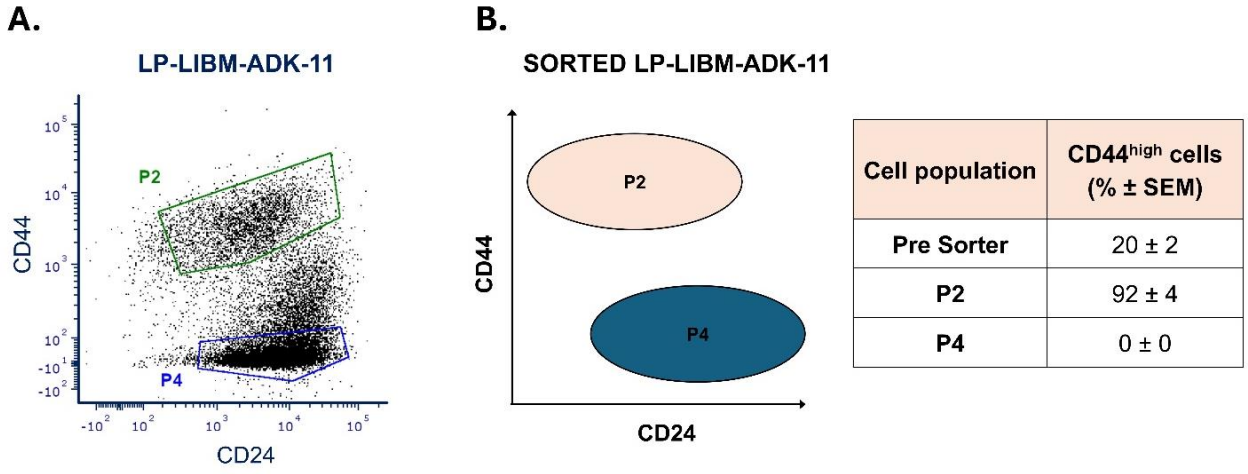

Cell population	CD44^{high} cells (% ± SEM)
Pre Sorter	20 ± 2
P2	92 ± 4
P4	0 ± 0

Figure 9. Isolation of P2-CD44^{high} and P4-CD44^{low} cell subpopulations from the LP-LIBM-ADK-11 cell line through cell sorting. (A) Dot plot of LP-LIBM-ADK-11 cells stained for CD44 and CD24 markers showing the gates P2 and P4 used to sort the correspondent cell subpopulations. **(B)** Schematic representation of LP-LIBM-ADK-11 cell sorting (left) and percentages of CD44-expressing cells in each cell population before (pre-sorter) and after (P2 and P4) the sorter (right, n=2). SEM: standard error of the mean.

To determine whether the presence of the CD44^{high} subpopulation was responsible for the differential sensitivity to EGFR-TKIs in LP-LIBM-ADK-11 and HP-LIBM-ADK-11 cell lines, the individual sensitivity of the P2-CD44^{high} and P4-CD44^{low} cells to osimertinib was tested *in vitro*.

As expected, P2-CD44^{high} cells were resistant to osimertinib in 2D-culture conditions (IC_{50}: 8.413±0.412 µM) (**Figure 10A**), similarly to what had been previously observed for LP-LIBM-ADK-11 (**Figure 8A**). On the contrary, P4-CD44^{low} cells resulted to be as sensitive to osimertinib as HP-LIBM-ADK-11 cells (IC_{50}: 0.058±0.001 µM) (**Figure 8A** and **Figure 10A**).

In order to explore the molecular mechanisms determining the differential *in vitro* response of the two sorted cell lines to osimertinib, the state of EGFR phosphorylation of P2 and P4 cells was evaluated in presence or not of the treatment. Despite the insensitivity of the P2-CD44^{high} sorted cell line to osimertinib *in vitro*, the EGFR-TKI significantly inhibited EGFR phosphorylation in both sorted P2-CD44^{high} and P4-CD44^{low} cells as compared to vehicle ($p<0.05$ by One Sample t test) (**Figure 10B**), suggesting a mechanism of resistance to osimertinib in the P2-CD44^{high} cell line not affecting the inhibition of EGFR phosphorylation.

To confirm the role played by CD44^{high} population in osimertinib resistance, we treated LP-LIBM-ADK-11 cells with osimertinib *in vitro* for 3 to 6 days and monitored changes in the CD44 expression profile over time. The results showed that osimertinib induced a progressive increase in CD44 expression on treated cells, with a notable rise observed as early as 72 hours after treatment (osimertinib *vs* vehicle, percentage of CD44^{high} cells: 43% *vs* 16%) (**Figure 10C**). After 6 days of treatment, this effect resulted in a 4-fold increase in the percentage of the CD44^{high} cells as compared to the vehicle (osimertinib *vs* vehicle, percentage of CD44^{high} cells: 38% *vs* 9%) (**Figure 10C**). Notably, osimertinib treatment also resulted in a simultaneous, progressive reduction in the CD44^{low} cells fraction (osimertinib *vs* vehicle, percentage of CD44^{low} cells after 6 days: 58% *vs* 89%) (**Figure 10C**).

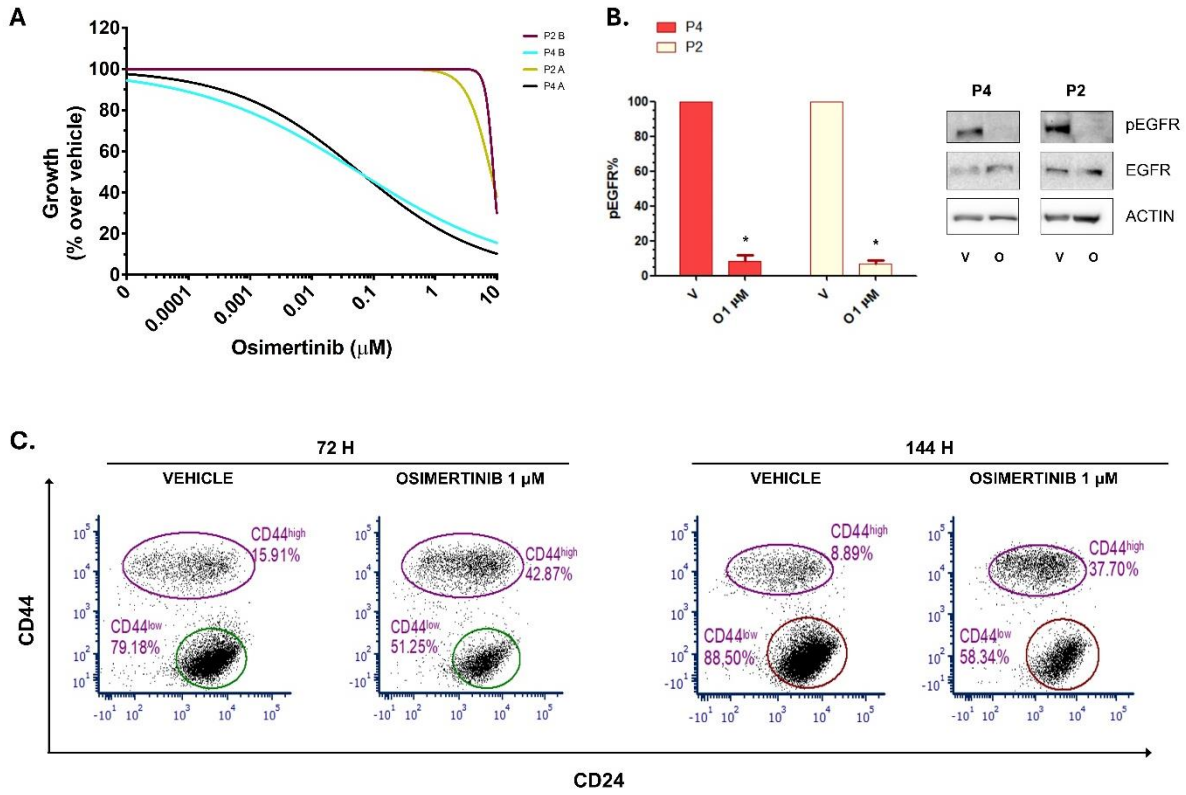

Figure 10. ***In vitro*** **response of P2-CD44^{high} and P4-CD44^{low} sorted cell lines to osimertinib and osimertinib influence on CD44 expression. (A)** P2-CD44^{high} and P4-CD44^{low} sensitivity to osimertinib in 2D-culture conditions (n=2 biological replicates–A and B–for each cell line). **(B)** Effect of osimertinib treatment (O) on EGFR phosphorylation in P2-CD44^{high} and P4-CD44^{low} sorted cells as compared to the vehiche (V) ($p<0.05$ by One Sample t test, n=2). **(C)** CD44 and CD24 expression profiles of LP-LIBM-ADK-11 after 72 or 144 hours of treatment with osimertinib 1 uM or vehicle, assessed by cytofluorimetric analysis.

To sum up, isolation of P2-CD44^{high} and P4-CD44^{low} cell subsets from LP-LIBM-ADK-11 through cell sorting, followed by their sensitivity testing to osimertinib, confirmed that the CD44^{high} cell subpopulation was indeed the source of osimertinib resistance in LP-LIBM-ADK-11. Furthermore, osimertinib treatment of LP-LIBM-ADK-11 cells led to a reversal of the ratio between CD44^{high} and CD44^{low} cells over time.

2.2.3 Comparison of the transcriptomic profile of sorted P2 and P4 cells

To identify molecular biomarkers or genetic pathways associated with resistance to osimertinib, the transcriptome of P2 and P4 cell lines was investigated for comparison. The results identified 3517 differentially expressed genes between the cell lines (p-adj <0.01 and Log2FC >1 or <-1), of which 1983 up-regulated and 1534 down-regulated in the P2 cell line compared to P4 (**Figure 11A**). Analyses conducted through the Enrichr platform allowed us to identify the biological processes in which the differentially expressed genes were involved (**Figure 11B**).

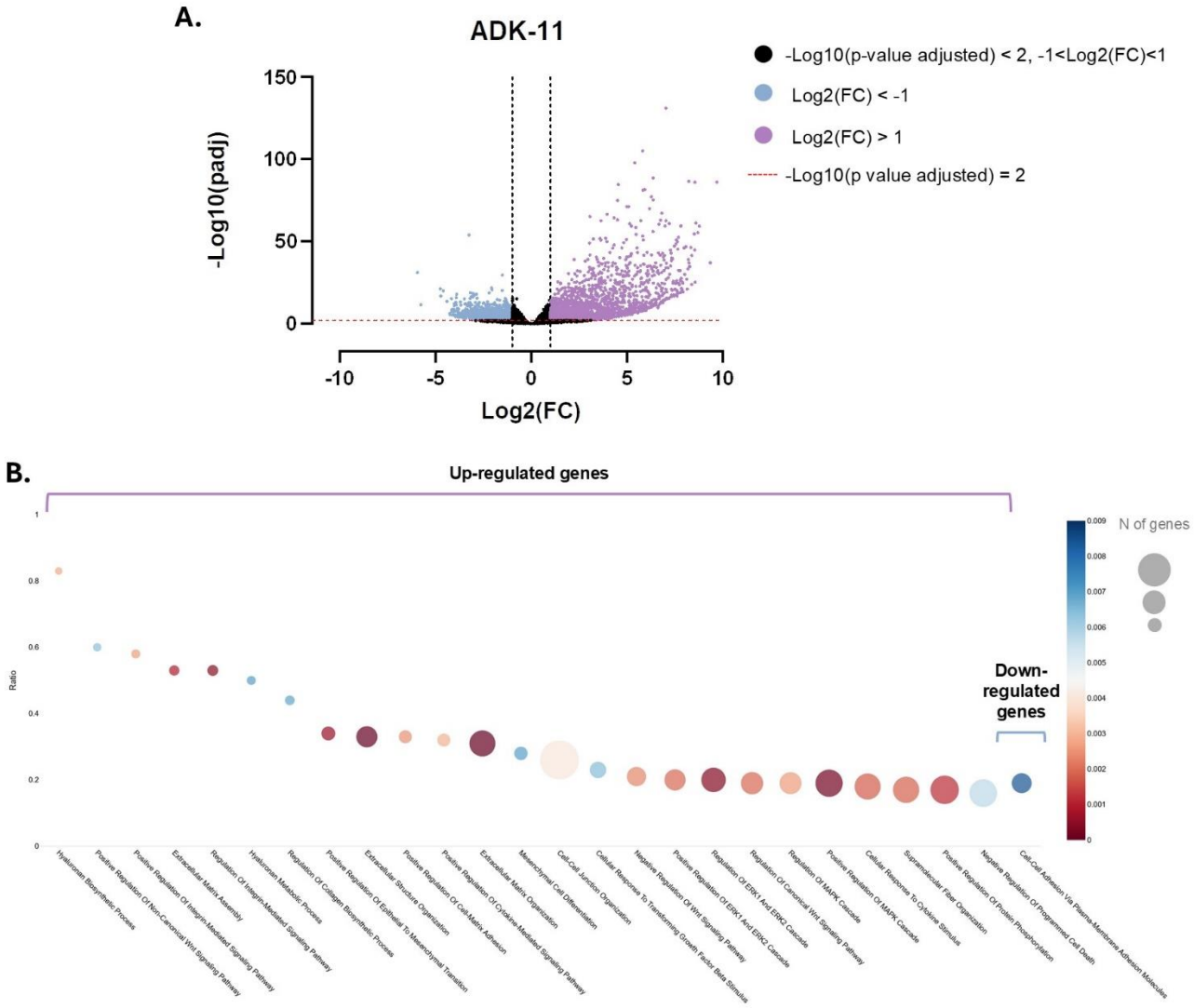

Figure 11. Transcriptome analysis of sorted P2 and P4 cell lines. (A) Heatmap showing the -Log10 adjusted p-value of differentially expressed genes (p-adj <0.01 and -1<Log2FC<1) in P2 and P4 cells. **(B)** Bubble plot showing the main biological processes enriched in up-regulated and down-regulated genes, identified by over representation analysis of differentially expressed genes. The size of the dots represents the absolute number of differentially expressed genes.

According to over representation analysis, up-regulated genes in the P2 cell line were involved in several biological processes, including extracellular matrix assembly and remodeling (*MFAP4*, *EFEMP2*, *HAS1*, *PXDN*, *HAS2*, *HAS3*, *EMILIN1*, *GAS6*, *FBLN5*, *LAMA2*, *LRP1*, *LAMB2*, *PRDM5*, *ZNF469*, *NID1*, *AGT*, *DDR2*), hyaluronan biosynthetic process (*CEMIP*, *HAS1*, *HAS2*, *HAS3*, *IL1B*), activation of MAPK signaling pathway (among the up-regulated genes: *CD40*, *FGF1*, *FGF2 ROBO1*, *TNFAIP8L3*, *CCN2*, *PDGFRA*, *PDGFRB*, *IL11*, *MAP2K1*, *NRG1*, *MTURN*, *IL1B*, *ROR2*, *GAS6*, *CD44*, *NOTCH2*) and regulation of Wnt signaling circuit (among the up-regulated genes: *GLI3*, *SOX7*, *SOX9*, *IGFBP1*, *IGFBP4*, *IGFBP6*, *CAV1*, *WNT5A*, *COL1A1*, *ZEB2*, *BMP2*, *SNAI2*, *FGF10*).

Notably, several genes involved in epithelial-mesenchymal transition (EMT) and cell plasticity were also found to be upregulated in the P2 cell line as compared to the P4 one (*i.e.*, *SNAI1*,

SNAI2, SOX9, FGFR1, SMAD3, TWIST1, IL1B, COL1A1). In contrast, genes involved in cell-cell adhesion resulted to be down-regulated in P2 cells as compared to P4 (**Figure 11B**).

Additionally, transcriptomic analysis also highlighted a significantly increased expression of the *ERBB3* gene in the P4 cell line as compared to the P2 one (Log2FC: -2.931, p-adj: 1.46E-08). These data suggest that the $CD44^{high}$ population observed in the low-passage LIBM-ADK-11 cell line, which is lost over *in vitro* passages, may indeed be an $HER3^{low}$ cell subpopulation, explaining the changes in HER3 expression observed in high-passage LIBM-ADK-11 cells (**Figure 7A,B**).

Taken together, these findings suggest a distinct difference in key molecular pathways between P2 and P4 cell lines, particularly those involved in cell plasticity, extracellular matrix remodeling, and growth factor signaling, which may underlie the phenotypic and functional changes observed between early and late-passage LIBM-ADK-11 cells.

3. EXPLORING NOVEL THERAPEUTIC STRATEGIES FOR DRUG-ORPHAN NSCLC MUTATIONS

Despite significant advancements in targeted therapies for NSCLC, a substantial number of driver mutations remain orphaned, lacking effective treatment options (Fois et al., 2021; Friedlaender et al., 2024). Among these orphan mutations, *BRAF* class III mutations are particularly notable, as they display impaired or reduced kinase activity and their unique mechanisms of action complicate the development of effective targeted therapies (Bracht et al., 2019). Furthermore, the rarity of these mutations poses an additional challenge in the pursuit of targeted inhibitors, as limited patient populations hinder comprehensive research and clinical trials. The lack of effective therapies for these orphan mutations highlights a pressing unmet clinical need in NSCLC treatment, driving continued exploration into novel druggable targets.

In this regard, investigations conducted on the two *BRAF* class III-mutated NSCLC cell lines ADK-14 and PDX-ADK-36, have provided compelling insights, revealing an intriguing sensitivity to a drug commonly employed in the clinical management of NSCLC. This finding suggests promising avenues for further therapeutic development and underscores the potential for novel treatment options targeting these elusive mutations.

3.1 ADK-14 and PDX-ADK-36: two NSCLC cell lines carrying *BRAF* class III mutations

ADK-14 cell line was established from a biopsy of a lymph node metastasis of a patient with stage IV NSCLC harboring the *BRAF* class III mutation G466V, at progression after first-line treatment with pembrolizumab.

PDX-ADK-36 cell line was derived from the tumor mass of a PDX established from the lymph node metastasis of a stage IVB NSCLC carrying the *BRAF* class III mutation D594G, at progression after chemo-immunotherapy. The patient was treated with erlotinib as a second-line treatment after the establishment of both the PDX and PDX-ADK-36 cell line, showing a partial response.

The investigations described in the following sections, whose results have been in part included in the manuscript Di Federico, Angelicola et al., *JCO Precision Oncology* 2024, were inspired by clinical observations suggesting a potential and promising effect of erlotinib treatment in NSCLC patients carrying *BRAF* class III mutations, as described below (Di Federico, Angelicola et al., 2024).

3.1.1 Clinical activity of the EGFR-TKI erlotinib in two patients with BRAF class III-mutated NSCLC

Two patients with stage IV NSCLC harboring a *BRAF* class III mutation without other genomic driver alterations under care at the Medical Oncology Unit of the S. Orsola-Malpighi Hospital, received erlotinib after conventional treatments.

The first patient, a 60-year-old male, former smoker, carrying the $BRAF^{D594N}$ mutation, received 4 cycles of chemotherapy as first-line treatment (carboplatin AUC5 day 1 plus gemcitabine 1000 mg/m^2 days 1,8) together with stereotactic radiation therapy for the treatment of a single brain metastasis. Given the intrathoracic nodal progression at the first radiographic tumor reassessment following chemotherapy initiation, docetaxel (75 mg/m^2) was administered as a second-line treatment for 10 cycles, resulting in stable disease. Nevertheless, subsequent disease progression was detected in a mediastinal lymph node, prompting the initiation of third-line treatment with erlotinib (150 mg daily) in July 2011, which led to a complete response (**Figure 12A**).

NGS performed on tumor biopsy collected before the initiation of erlotinib treatment identified a *BRAF* class III mutation (D594N) and a *CTNNB1* mutation (S37C), but no *EGFR* alterations. The patient is still on erlotinib treatment after 12 years, maintaining a sustained complete response throughout.

The second patient, a 60-year-old female, heavy smoker, carrying the $BRAF^{D594G}$ mutation, is the patient from which the PDX-ADK-36 cell line was derived. She received as a first-line treatment 3 cycles of chemo-immunotherapy (carboplatin AUC5, pemetrexed 500 mg/m^2 and pembrolizumab 200 mg every 3 weeks). Based on clinical and radiographic evidence of disease progression following the initial treatment, and the favorable response observed in the first patient, a second-line therapy with erlotinib (150 mg daily) was started. After one month, the patient demonstrated an objective partial response, with a reduction of 40% or more in measurable tumor lesions (**Figure 12B**). Unfortunately, the patient passed away a few days after the tumor reassessment

at home, likely due to cardiovascular complications, although the exact cause of death could not be determined.

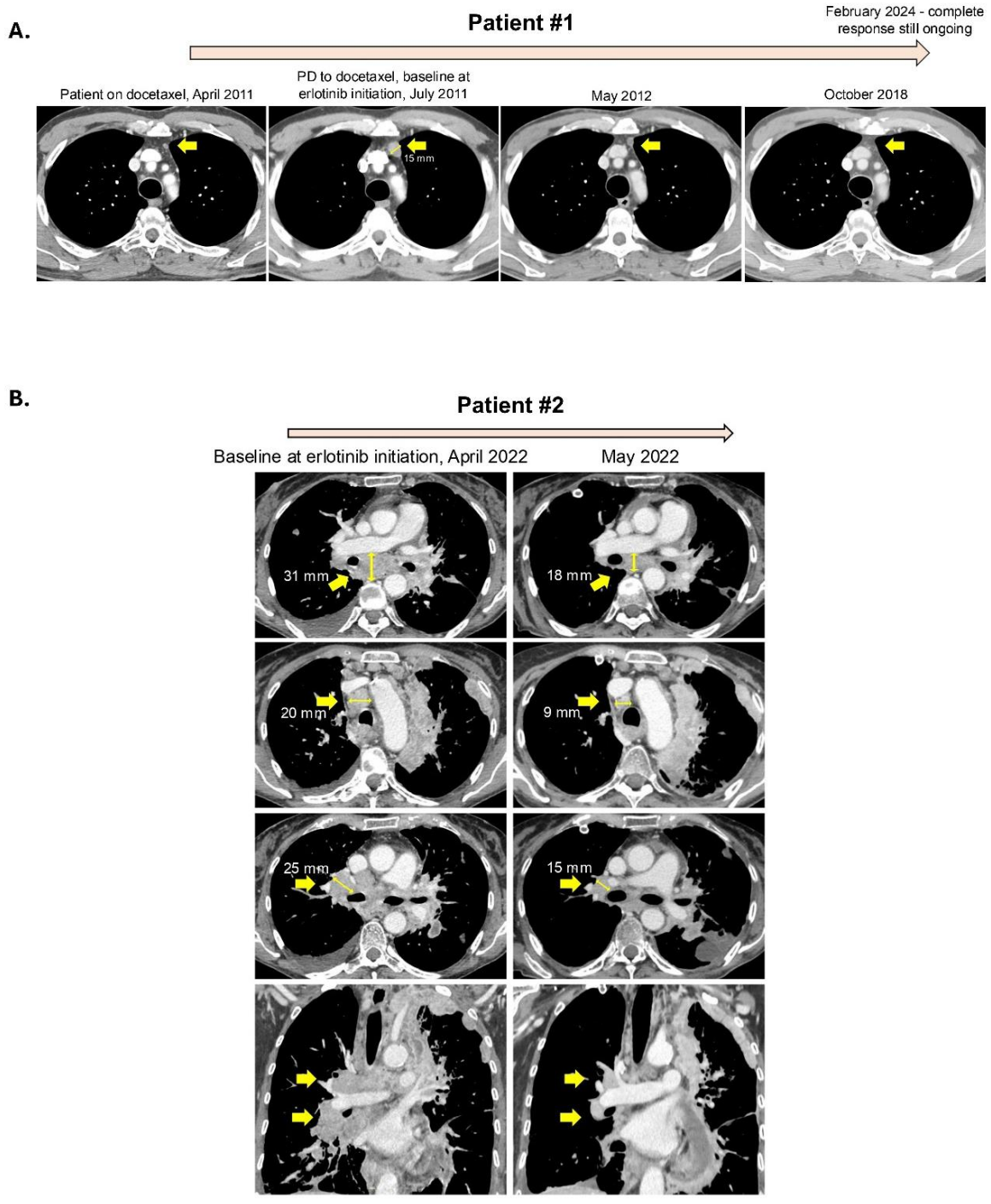

Figure 12. Radiographic evaluation of erlotinib efficacy in two patients with *BRAF*-class III mutated-NSCLC. (A) Computed tomography scans showing the tumor response to erlotinib in the first patient after progressive disease (PD) to docetaxel, with documented gradual shrinkage of a prevascular lymph node metastasis over time. **(B)** Computed tomography scans showing tumor response to erlotinib in the second patient, with documented shrinkage of measurable disease in right hilar, subcarinal, and right upper paratracheal lymph node metastases.

3.1.2 Activity of erlotinib in BRAF class III-mutated NSCLC cell lines

To validate the above-described clinical findings regarding the efficacy of erlotinib in *BRAF* class III-mutated NSCLC, the *in vitro* sensitivity of ADK-14 and PDX-ADK-36 to erlotinib was tested in both 2D and 3D culture conditions, and it was compared with the drug sensitivity of two *EGFR*-mutated cell lines (HCC827 and PC-9, both carrying the $EGFR^{G746\_A750del}$ mutation), used as positive controls. Erlotinib sensitivity was also assessed in a *BRAF* class I-mutated cell line (HCC364, carrying a $BRAF^{V600E}$ mutation), a *BRAF* class II-mutated cell line (NCI-H1395, carrying a $BRAF^{G469A}$) and a *KRAS*-mutated cell line (ADK-17, carrying a $KRAS^{G12V}$ mutation), which were meant to act as negative controls.

In 2D culture conditions, erlotinib partially inhibited the growth of both *BRAF* class III-mutated cell lines (ADK-14, IC_{50}: 7.11±0.73 μM; PDX-ADK-36, IC_{50}: 6.33±2.13 μM) (**Figure 13A**).

As expected, erlotinib efficiently inhibited the growth of the two *EGFR*-mutated cell lines at lower doses (HCC827, IC_{50}: 0.06±0.005 μM; PC-9, IC_{50}: 0.04±0.004 μM), while no effect on the growth of the *BRAF* class I- and *KRAS*-mutated cell lines was observed (HCC364 and ADK-17, IC_{50} >25 μM) (**Figure 13A**). As for the *BRAF* class II-mutated cell line, erlotinib inhibited its growth at doses similar to those inhibiting *BRAF* class III-mutated cell lines (NCI-H1395, IC_{50}: 5.51±1.60 μM) (**Figure 13A**).

The efficacy of erlotinib was then tested under 3D culture conditions. Consistently with the results observed in the 2D culture setting, erlotinib partially or completely reduced the colony formation ability of the two *BRAF* class III-mutated cell lines ADK-14 (IC_{50}: 1.14±0.26 μM) and PDX-ADK-36 (IC_{50}: 0.23±0.04 μM), the two *EGFR*-mutated cell lines (HCC827, IC_{50} <0.01 μM; PC-9, IC_{50}: 0.03±0.02 μM) and the *BRAF* class II-mutated cell line (NCI-H1395, IC_{50}: 0.05±0.02 μM) in 3D-soft agar assay (**Figure 13B**). In contrast, erlotinib efficacy was markedly reduced in the *BRAF* class I- and *KRAS*-mutated cell lines (HCC364, IC_{50}: 5.81±0.12 μM; ADK-17, IC_{50} >10 μM) (**Figure 13B**).

Erlotinib exerted a similar efficacy in sphere formation assays. The strongest effect in inhibiting cells' sphere formation ability was observed in *EGFR*-mutated cells (HCC827, IC_{50}: <0.01 μM; PC-9, IC_{50}: 0.05±0.01 μM) (**Figure 13C**). A certain inhibitory ability was also observed in *BRAF* class III-mutated cells (ADK-14, IC_{50}: 0.34±0.04 μM; PDX-ADK-36, IC_{50}: 0.11±0.02 μM) and *BRAF* class II-mutated cells (NCI-H1395, IC_{50}: 4.75±1.63 μM), while a notably weaker effect was observed in *BRAF* class I- and *KRAS*-mutated cell lines (HCC364, IC_{50}: 12.67±0.86 μM; ADK-17, IC_{50}: 9.34±0.46 μM) (**Figure 13C**).

In order to explain the sensitivity of *BRAF* class III-mutated cell lines to EGFR inhibition, EGFR activation state was assessed through Western blot analyses in all seven cell lines, before and

after erlotinib treatment. In basal conditions, 30 hours after cell seeding, a strong activation of EGFR was detected in the *BRAF* class III-mutated cell lines (ADK-14 and PDX-ADK-36) and in the *EGFR*-mutated ones (HCC827 and PC-9), but not in *BRAF* class I- (HCC364), *BRAF* class II- (NCI-H1395) and *KRAS*-mutated (ADK-17) cell lines (**Figure 13D**). After erlotinib treatment, the ratio between the phosphorylated form of EGFR and total EGFR (pEGFR/EGFR ratio) resulted to be significantly reduced in the *BRAF* class III-mutated cells (ADK-14 and PDX-ADK-36) and in the *EGFR*-mutated cell lines (HCC827 and PC-9) as compared to the vehicle ($p<0.05$, by Student's *t*-test) (**Figure 13E**). No changes in EGFR activation state were observed in the remaining cell lines (ADK-17, HCC364 and NCI-H1395) following erlotinib treatment (**Figure 13E**).

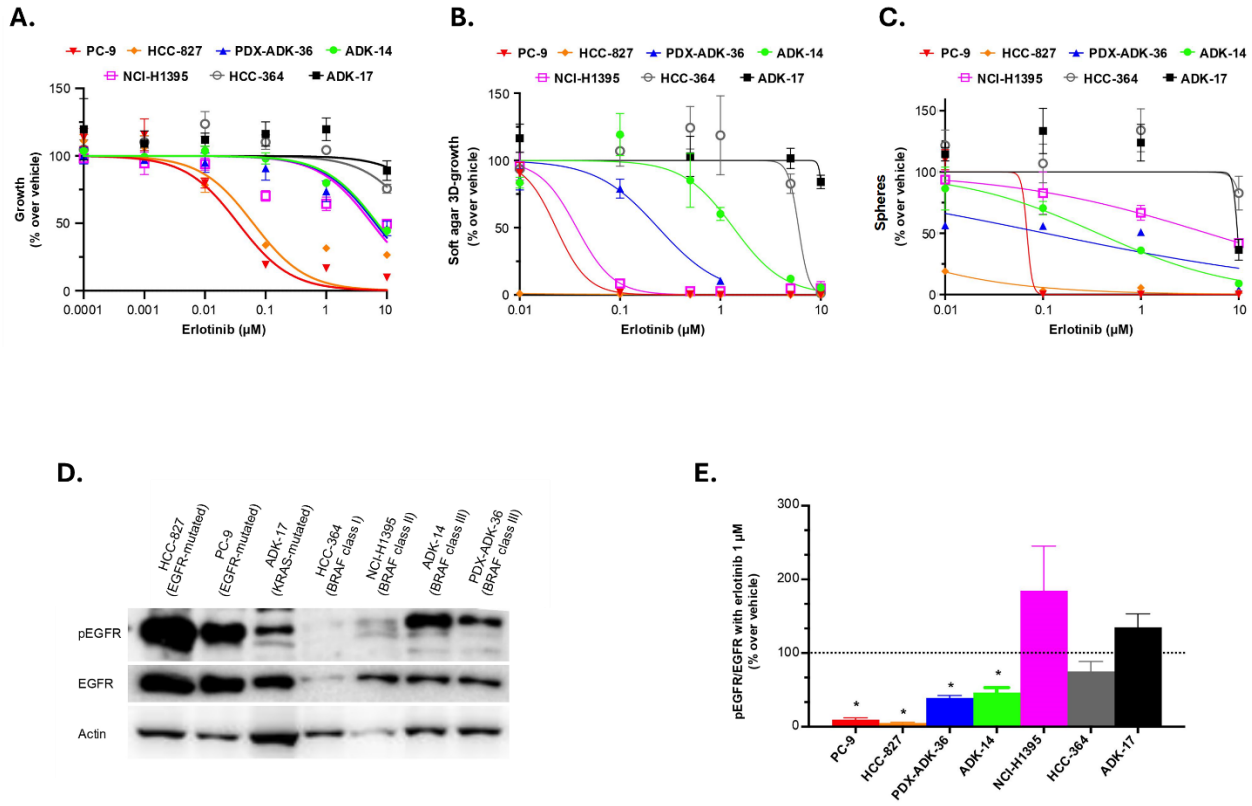

Figure 13. Comparative *in vitro* response of *BRAF*-, *EGFR*- and *KRAS*- mutated cell lines to erlotinib and their baseline EGFR activation. (A) Effect of different doses of erlotinib on cell 2D-growth (n=2-5 experiments, each one with three replicates). Each bar represents mean and SEM. **(B)** Effect of different doses of erlotinib on cell colony formation ability in 3D-soft agar assay (n=2-4 replicates). Each bar represents mean and SEM. **(C)** Effect of different doses of erlotinib on sphere formation ability (n=2-4 replicates). Each bar represents mean and SEM. **(D)** Western blots showing baseline EGFR activation, evaluated 30 hours after cell seeding (n=2 replicates for each cell line). **(E)** Effect of erlotinib administration on EGFR phosphorylation, measured as pEGFR/EGFR ratio. *, $p<0.05$ *vs* vehicle, by Student's *t*-test (n=2-4 replicates). SEM: standard error of the mean.

In summary, we can state that the previously described clinical efficacy of erlotinib on *BRAF* class III-mutated NSCLC was corroborated by *in vitro* results, as the EGFR-TKI effectively inhibited the growth of the *BRAF* class III-mutated ADK-14 and PDX-ADK-36 cell lines, in both 2D and 3D

cell culture settings. Notably, the *BRAF* class II-mutated NCI-H1395 cell line also exhibited a certain sensitivity to the drug, despite its low basal activation of EGFR and the absence of variations in the pEGFR/EGFR ratio following erlotinib treatment, which, on the contrary, was observed in *EGFR*- and *BRAF* class III-mutated cell lines.

3.1.3 Activity of other EGFR and non-EGFR−directed inhibitors in BRAF class III-mutated NSCLC cell lines

Given the demonstrated efficacy of erlotinib on *BRAF* class III-mutated cell lines, we explored whether the sensitivity of these cells could be also extended to next-generation TKIs or to other EGFR-targeting drugs. To this end, we evaluated the effectiveness of second-generation EGFR TKIs (afatinib and dacomitinib), the third-generation EGFR TKI osimertinib, and the EGFR-directed monoclonal antibody cetuximab, within a 2D culture setting.

Similarly to the previously observed erlotinib-related results, afatinib and dacomitinib partially inhibited the 2D-growth of the *BRAF* class III-mutated cell lines, showing a stronger effect on the PDX-ADK-36 cell line (afatinib, ADK-14, IC_{50}: 8.242±1.151 µM; PDX-ADK-36, IC_{50}: 1.439±0.227 µM; dacomitinib, ADK-14, IC_{50}: 12.92±0.43 µM; PDX-ADK-36, IC_{50}: 2.013±0.244 µM) (**Figure 14A,B**). As expected, the drugs exerted no effect on the growth of the *KRAS*-mutated cell line (ADK.17, afatinib, IC_{50} >100 µM; dacomitinib, IC_{50} >30 µM) (**Figure 14A,B**). Of note, afatinib also partially inhibited the 2D-growth of the *BRAF* class I-mutated cell line (HCC364, IC_{50}: 7.705±1.646 µM), while strongly inhibiting the growth of the *EGFR*-mutated ones, as expected (PC-9 and HCC827, IC_{50}: <0.008 µM) (**Figure 14A**).

The sensitivity of the *BRAF* class III-mutated cell lines to osimertinib, which is the current standard of care for NSCLC patients with EGFR mutations, and cetuximab was also assessed and compared to that of cell lines harboring other classes of *BRAF* mutations, as well as those with *EGFR* or *KRAS* mutations, which served as positive and negative controls, respectively.

Osimertinib inhibited the growth of *BRAF* class III- (ADK-14, IC_{50}: 7.17±2.20 µM; PDX-ADK-36, IC_{50}: 1.61±0.32 µM) and *BRAF* class II- (NCI-H1395, IC_{50}: 1.63±0.58 µM) mutated cell lines, in line with previous data, as well as *EGFR*-mutated cells (HCC827, IC_{50} <0.01 µM; PC-9, IC_{50}: 0.04±0.02 µM) (**Figure 14C**). Again, no effect was observed on the *BRAF* class I-mutated cell line (HCC364, IC_{50} >18 µM) and on the *KRAS*-mutated one (ADK-17: IC_{50} >100 µM) (**Figure 14C**). As for the EGFR-directed monoclonal antibody cetuximab, it did not have a significant effect on any of the cell lines, except for the *EGFR*-mutated HCC827 line (HCC827, IC_{50}: 0.252±0.023 µM; other cell lines, IC_{50} >100 µM) (**Figure 14D**).

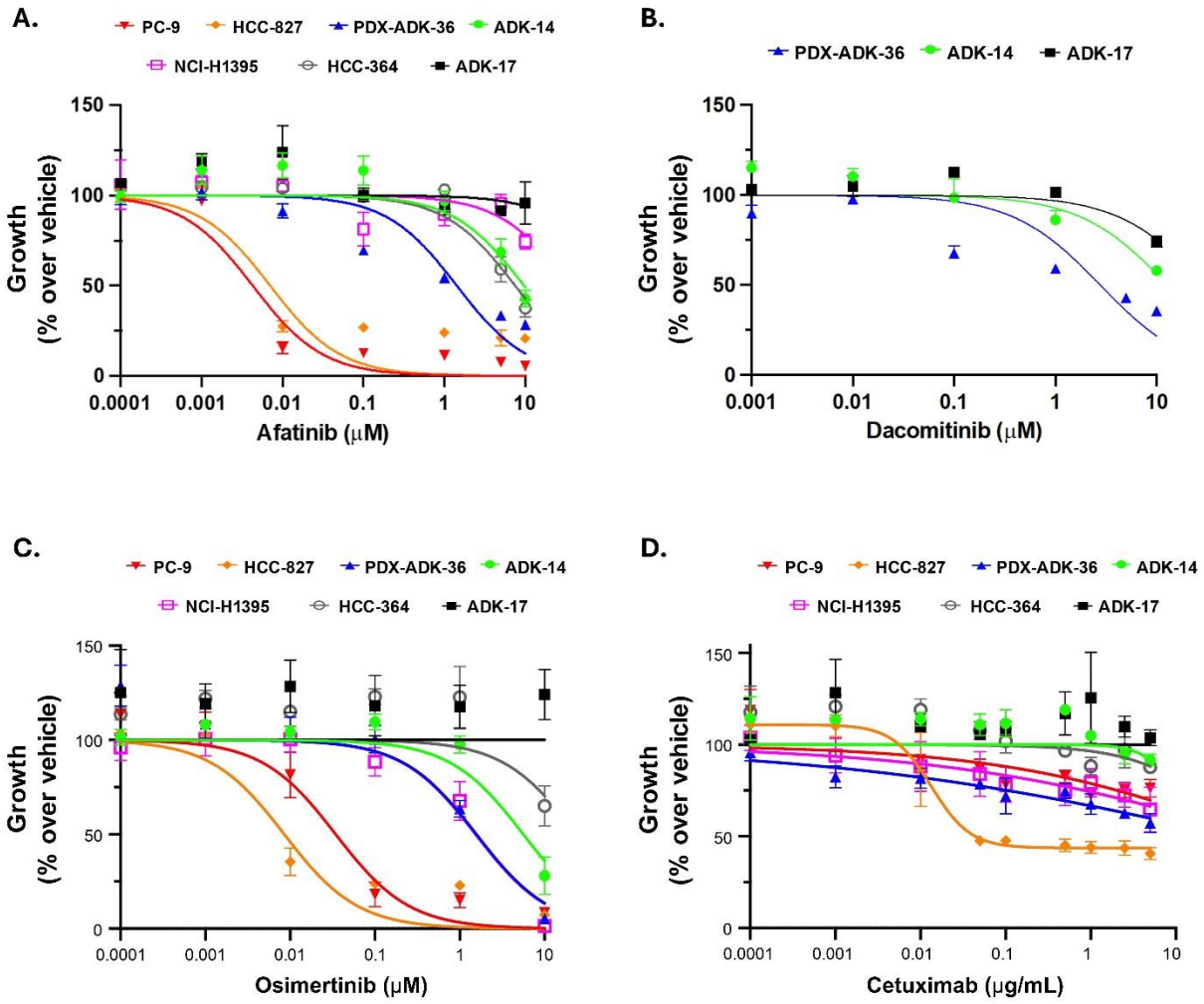

Figure 14. Comparative *in vitro* response of *BRAF*-, *EGFR*- or *KRAS*- mutated cell lines to EGFR-directed agents in 2D culture conditions. (A) Cell sensitivity to afatinib (n=2, each one with 3 technical replicates). Each point represents mean and SEM. **(B)** Cell sensitivity to dacomitinib (n=2 experiments, each one with three replicates). Each point represents mean and SEM. **(C)** Cell sensitivity to osimertinib (n=2-6 experiments, each one with three replicates). Each point represents mean and SEM. **(D)** Cell sensitivity to cetuximab (n=2-3 experiments, each one with three replicates). Each point represents mean and SEM. SEM: standard error of the mean.

To confirm the data regarding the sensitivity of the *BRAF* class III-mutated cell lines to EGFR inhibition, we also tested the sensitivity of ADK-14 and PDX-ADK-36 to an intermediate-generation EGFR inhibitor (*i.e.*, dacomitinib) in 3D culture conditions. In 3D soft-agar assay, dacomitinib efficiently inhibited PDX-ADK-36 colony formation, in accordance with the results obtained in 2D culture setting (IC_{50}: 0.05±0.028 μM) (**Figure 15A**). The drug also showed a partial inhibitory effect on ADK-14 and ADK-17 cell lines (ADK-14, IC_{50}: 1.838±0.079 μM; ADK-17, IC_{50}: 1.205±0.315 μM) (**Figure 15A**).

Differently, in sphere formation assay, dacomitinib significantly inhibited the sphere formation ability of both ADK-14 and PDX-ADK-36, while showing no effect on ADK-17 cells (**Figure 15B**).

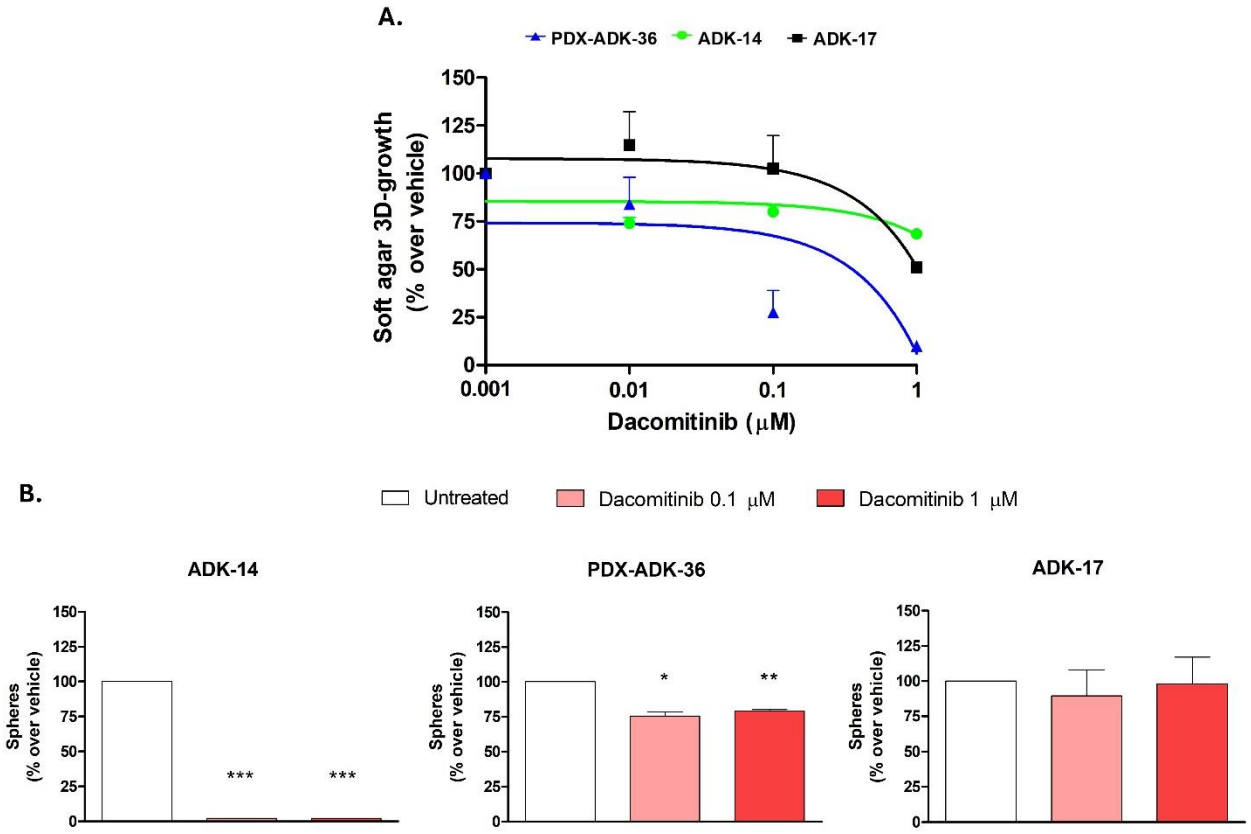

Figure 15. Comparative response of ADK-14, PDX-ADK-36, and ADK-17 cell lines to dacomitinib in 3D culture conditions. (A) Soft agar 3D-growth in the presence of dacomitinib 0.01, 0.1 or 1 µM (n=1-3 experiments, each one with two replicates). Each point represents mean and SEM. **(B)** Sphere formation ability in presence of dacomitinib 0.1 or 1 µM (n=1-3 experiments, each one with two replicates). *, $p<0.05$; **, $p<0.01$ and ***, $p<0.001$ by One sample t test (each group *vs* theoretical mean of 100). Each bar represents mean and SEM. SEM: standard error of the mean.

Considering the favorable response of the *BRAF* class III-mutated cell lines to EGFR targeting, we investigated whether simultaneous targeting of both EGFR and MEK, through the combination of erlotinib and trametinib, could confer a therapeutic advantage over the individual treatments. Trametinib has been reported to be particularly effective in *BRAF* class I-mutated NSCLC in combination with BRAF inhibitors, but not on *BRAF* class III-mutated tumors (Nebhan et al., 2021). Accordingly, the drug did not exert any strong effect on the 2D-growth of both the *BRAF* class III-mutated cell lines (ADK-14, IC_{50}: 10.984±1.851 µM; PDX-ADK-36, IC_{50}: 3.807±1.673 µM), nor on ADK-17 cell growth (IC_{50} >70µM) (**Figure 16A**).

Interestingly, the 2D-growth inhibition of *BRAF* class III-mutated cells was significantly enhanced by combining erlotinib with trametinib, compared to their use as single agents ($p<0.05$ at

least, by Student's *t*-test) (**Figure 16B**). This synergic activity was not observed in the *KRAS*-mutated cell line (**Figure 16B**).

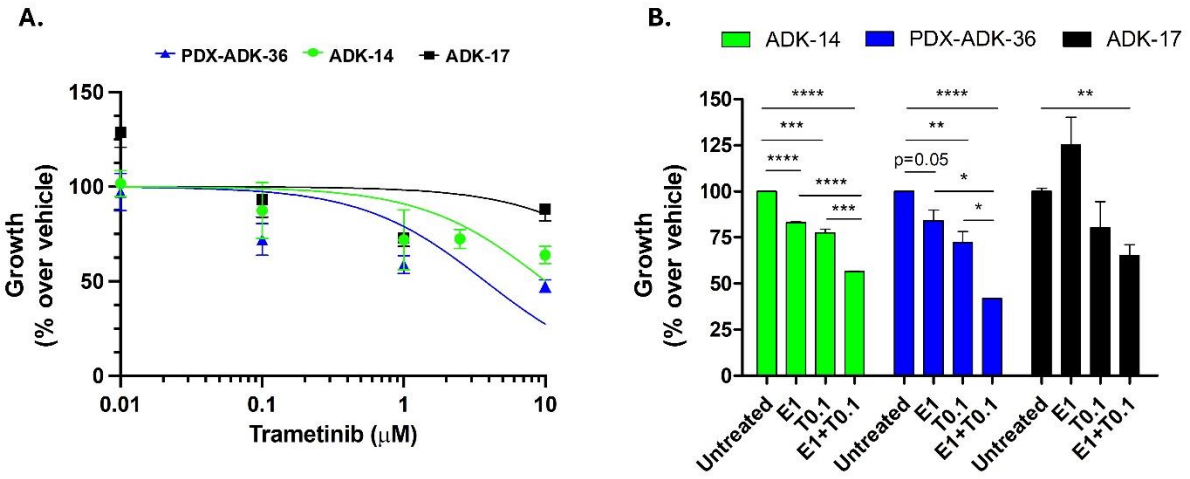

Figure 16. Comparative *in vitro* response of ADK-14, PDX-ADK-36, and ADK-17 cell lines to trametinib alone or in combination with erlotinib. (A) Cell sensitivity to trametinib in 2D culture conditions (n=2-6 experiments, each one with three replicates). Each point represents mean and SEM. **(B)** Cell sensitivity to single or combined treatment with trametinib and/or erlotinib 0.1 or 1 μM in 2D culture conditions (n=2-3). *, p<0.05; **, p<0.01; ***, p<0.001; **** p<0.0001, by unpaired t test. Each bar represents mean and SEM. E1: erlotinib 1 μM; T0.1: trametinib 0.1 μM. SEM: standard error of the mean.

To sum up, the sensitivity of *BRAF* class III-mutated cell lines to EGFR inhibition was further confirmed through drug sensitivity assays involving second- and third-generation EGFR-TKIs, *i.e.* afatinib, dacomitinib and osimertinib. ADK-14 and PDX-ADK-36 cell growth was efficiently inhibited by these EGFR-targeting agents in either 2D or 3D cell culture conditions. In contrast, the *KRAS*-mutated ADK-17 cell line showed no response to the drugs. Interestingly, the *BRAF* class II-mutated cell line, NCI-H1395, also exhibited sensitivity to osimertinib *in vitro*. Notably, the 2D growth of *BRAF* class III-mutated cell lines was not particularly inhibited by the MEK-TKI trametinib, but this effect was significantly enhanced when combined with erlotinib, resulting in a greater inhibition of cell growth compared to either treatment alone.

In closing, to further validate our findings regarding the sensitivity of *BRAF* class III-mutated NSCLC to EGFR-TKIs, we consulted the Cancer Cell Line Encyclopedia (Broad, 2019) via cBioPortal (www.cbioportal.org) for NSCLC cell lines harboring *BRAF* class III mutations (Cerami et al., 2012; J. Gao et al., 2013; Ghandi et al., 2019). The database provided information and treatment data about two *BRAF* class III-mutated NSCLC cell lines, carrying the same mutation identified in the ADK-14 cell line (G466V), without additional oncogenic alterations. These data were compared to the ones regarding NSCLC cell lines carrying other driver mutations classified as "oncogenic" or "likely oncogenic" by OncoKB (https://www.oncokb.org), including *BRAF* class II (n=5), *EGFR*

(n=5) and *KRAS* (n=36) alterations. Of note, cell lines carrying a $EGFR^{T790M}$ co-mutation were excluded, given their well-known lack of sensitivity to EGFR-TKIs and, among *EGFR* mutations, only exon 19 deletions or L858R alterations were included in the research. We queried data regarding the *in vitro* sensitivity of the selected cell lines to several drugs, including EGFR-TKIs of first- (gefitinib) and second- (afatinib) generation, a MEK-TKI (trametinib), a BRAF inhibitor (dabrafenib), a multi-TKI (cabozantinib) and a chemotherapy drug (doxorubicin) (**Figure 17**).

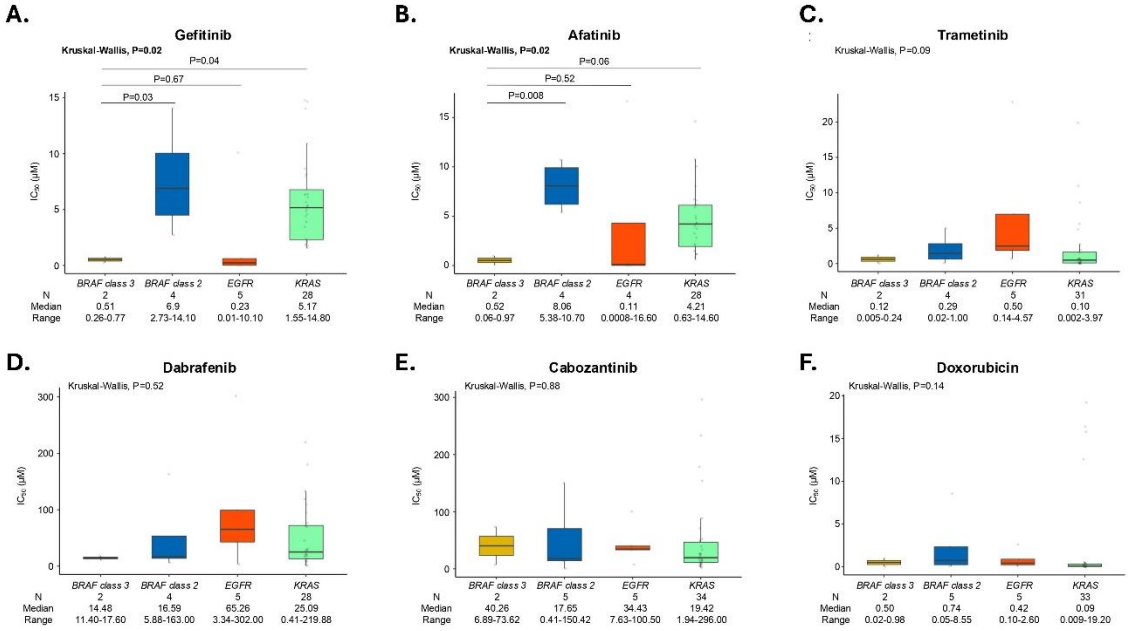

Figure 17. Activity of multiple therapeutic agents on NSCLC cell lines carrying *BRAF* class III, *BRAF* class II, *EGFR*, or *KRAS* driver mutations, as reported by the data collected in the Cell Line Encyclopedia. (A) Activity, expressed as median IC_{50}, of the EGFR inhibitors gefitinib **(A)** and afatinib **(B)**, the MEK inhibitor trametinib **(C)**, the BRAF inhibitor dabrafenib **(D)**, the multi-TKI cabozantinib **(E)** and doxorubicin **(F)**.

Of note, the four groups of oncogene-addicted cell lines showed statistically significant differences in drug sensitivity only when treated with the EGFR-TKIs gefitinib (p=0.02) and afatinib (p=0.02), which resulted to be more effective in *BRAF* class III and *EGFR*-mutated cell lines as compared to *BRAF* class II and *KRAS*-mutated cells (**Figure 17A,B**). Specifically, the group of *BRAF* class III-mutated cell lines showed a median IC_{50} of 0.51 µM (range: 0.26-0.77) and 0.52 µM (range: 0.06-0.97) when treated with gefitinib and afatinib, respectively. These values were significantly lower than the median IC_{50} of the *BRAF* class II-mutated group (gefitinib: 6.9 µM, p=0.03; afatinib: 8.06 µM, p=0.008) and the *KRAS*-mutated one (gefitinib: 5.17 µM, p=0.04; afatinib: 4.21 µM, p=0.06), but comparable to the median IC_{50} of the *EGFR*-mutated group (gefitinib: 0.23 µM, p=0.67; afatinib: 0.11 µM, p=0.52) (**Figure 17A,B**). Treatment with other agents did not show any significant difference in cell sensitivity across the oncogene-addicted groups (**Figure 17C-F**).

Overall, the data provided by Cancer Cell Line Encyclopedia aligned with our findings, confirming the increased sensitivity of *BRAF* class III-mutated NSCLC cell lines to EGFR-targeting TKIs.

4. INVESTIGATING THE MECHANISMS UNDERLYING RESISTANCE TO ICIs IN NSCLC THROUGH PRECLINICAL MODELS OF IMMUNOTHERAPY RESISTANCE

Despite the significant breakthroughs that immunotherapy has brought to the treatment of NSCLC, a subset of patients continues to experience paradoxical and detrimental responses to these therapies (Okwundu et al., 2021). Currently, the lack of reliable predictive biomarkers hampers the early identification of these patients, presenting a substantial challenge in clinical practice (Bai et al., 2020). Moreover, the underlying mechanisms driving these paradoxical responses remain largely unexplored and poorly understood. Gaining insights into these mechanisms is essential for refining patient selection and optimizing the efficacy of immunotherapy in NSCLC.

In this context, the availability of two cell line models, ADK-17 and ADK-18, established from tumor samples of the same patient, one prior to the initiation of treatment and the other following the development of hyperprogression after ICI therapy, provides a valuable platform for investigating tumor behavior and resistance mechanisms. To further support this investigation, the establishment of a preclinical *in vivo* model of resistance to ICIs in syngeneic immunocompetent mice complemented the cellular line models, providing a more comprehensive framework for understanding resistance mechanisms to immunotherapy.

These models, along with the results obtained, are presented in the following sections. Some of the data described below were also included in the manuscript Angelicola et al., *Journal of Translational Medicine*, 2025 (Angelicola et al., 2025).

4.1 ADK-17 and ADK-18, two cell lines derived from samples of an immunotherapy-resistant patient at baseline and after hyperprogression development

4.1.1 Clinical history and molecular data of the patient

The patient from which the cell lines were established was a 64-year-old woman, former light smoker (10 pack-year) diagnosed with stage IVA NSCLC (time of diagnosis: Tdx). As first-line treatment, the patient received 5 cycles of pembrolizumab (**Figure 18A**). However, at the first radiological assessment via computed tomography, signs of hyperprogressive disease (HPD) were observed, with metastatic spread to soft tissues, thoracic wall, as well as abdominal and thoracic lymph nodes (time of hyperprogression: Thy) (**Figure 18B**). Second-line treatment with

pembrolizumab, carboplatin, and pemetrexed was administered, but no clinical improvement was observed. A third-line therapy with docetaxel was initiated, also without clinical benefit, and the patient ultimately died from further progression of the tumor (**Figure 18A**).

Tumor cells derived from pleural effusion at the time of diagnosis (Tdx) were positive for PD-L1 (TPS: 70%) and CD44 (31% of tumor cells were 2+ positive) (**Figure 18C**). A $KRAS^{G12V}$ mutation was detected in the tumor sample obtained at Tdx through NGS analysis. A second sample, collected before treatment (time of baseline: Tb), from pleural effusion and parietal pleura, was also analyzed. In this second sample CD44 expression was absent in tumor cells and found only in stromal components, while PD-L1 TPS remained at 70% (**Figure 18C**). Additionally, tumor cells at both Tdx and Tb points were positive for TTF-1 and Ber-EP4 (data not shown). At the time of hyperprogression evidence (Thy), tumor cells collected from a subcutaneous biopsy showed positivity for the expression of TTF-1 and Ber-EP4 (data not shown), PD-L1 (TPS: 65%) and CD44 (58% of tumor cells were 2+ positive) (**Figure 18C**).

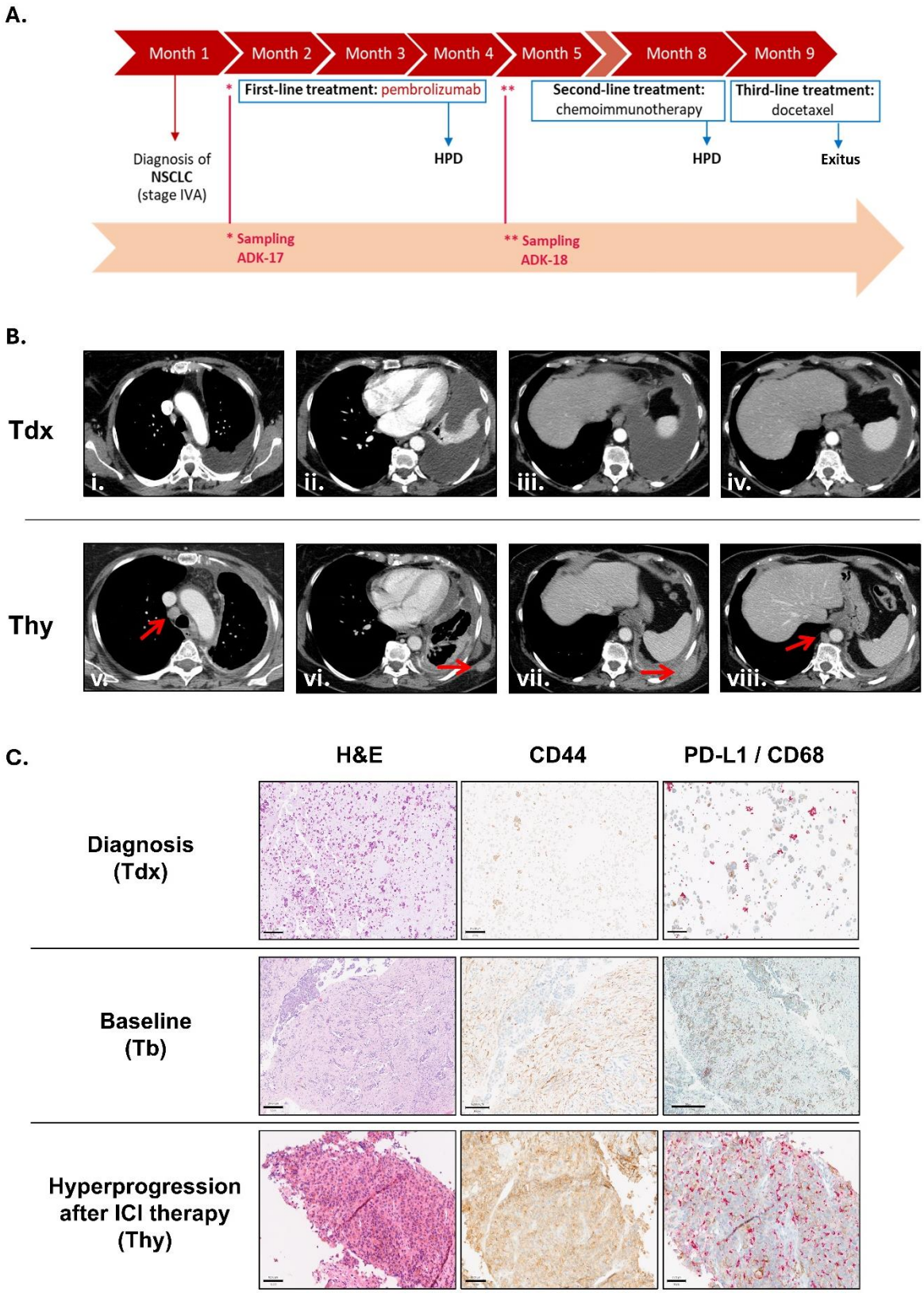

Figure 18. Patient's clinical history and tumor features before and after ICI treatment. Time points, Tdx: time of the diagnosis; Tb: time of baseline; Thy: time of hyperprogression. **(A)** Timeline of patient's clinical history and therapeutic schedule. **(B)** Imaging findings at the time of diagnosis (Tdx) **(i.–iv.)** and of progression to immunotherapy

(Thy) **(v.−viii.)**. Small right paratracheal lymph node **(i.)** progressed on immunotherapy (**v.**, red arrow). Left pleural effusion (**ii.**) and left pleurodesis signs associated with the appearance of subcutaneous metastatic site (**vi.**, red arrow). Left pleural effusion (**iii.**) and left pleurodesis signs associated with the appearance of a metastatic site at the left thoracic wall (**vii.**, red arrow). Small right paraortic lymph node (**iv.**) progressed on immunotherapy (**viii.**, red arrow). **(C)** Hematoxylin and eosin staining (H&E) and CD44 and PD-L1 immunohistochemical staining of tumor samples. Tdx: pleural effusion; Tb: pleural biopsy; Thy: subcutaneous lesion. **Left:** H&E, black line from top to bottom: 313.30 µm, 204.97 µm and 92.60 µm; **middle:** membrane CD44 expression on neoplastic cells, black line from top to bottom: 313.30 µm, 120.01 µm, 80.01 µm; **right:** PD-L1 expression on tumor cells by double stain for PD-L1 and CD68 (PD-L1: brown, CD68: red), black line from top to bottom: 139.24 µm, 300 µm and 61.73 µm. HPD: hyperprogressive disease.

4.1.2 Establishment and characterization of ADK-17 and ADK-18 cell lines

ADK-17 and ADK-18 cell lines were established from tumor samples collected at two time points: prior to the initiation of ICI therapy (Tb) and at the time of radiological evidence of HPD during ICI treatment (Thy), respectively. The $KRAS^{G12V}$ mutation, previously detected in the tumor at the Tdx point, was also confirmed in both cell lines through Real-Time PCR and Whole Transcriptome Sequencing (data not shown).

Under adherent culture conditions, the cell lines exhibited distinct morphology and behavior: while ADK-17 formed a compact, homogeneous monolayer of polygonal cells, ADK-18 displayed a less organized, stratified cell layer (**Figure 19A**). Additionally, ADK-18 cells demonstrated the ability to form organoids, a capability that, on the contrary, was not observed in the ADK-17 cell line (**Figure 19B**). Notably, the organoids exhibited positive expressions of CD44 and Ki-67 (**Figure 19C**).

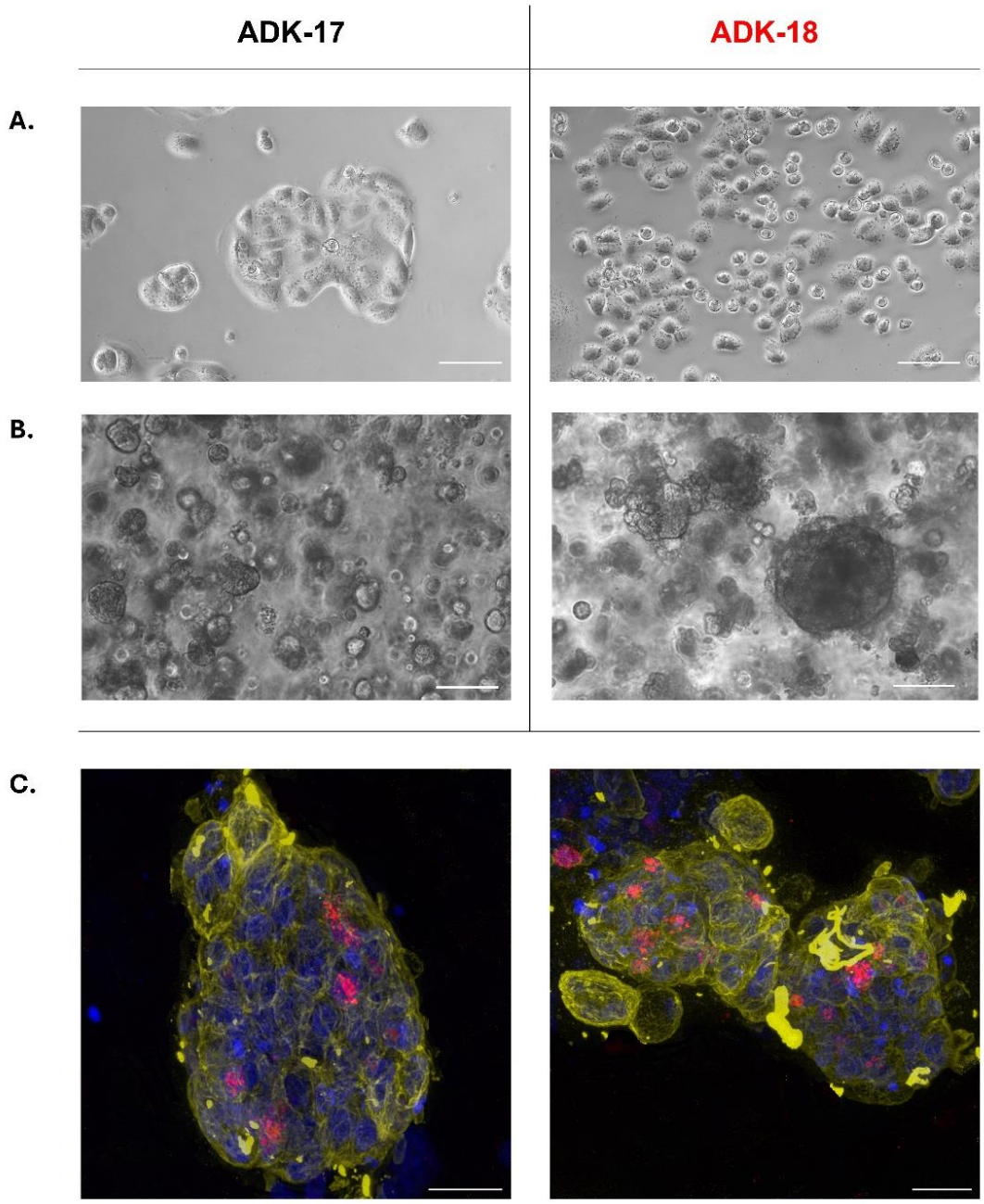

Figure 19. Morphological, phenotypical and functional characterization of ADK-17 and ADK-18 cell lines. (A) Morphology of ADK-17 and ADK-18 cells cultured under 2D conditions, observed through an inverted microscope. White line corresponds to 100 µm. **(B)** Structures observed two weeks after the seeding of ADK-17 and ADK-18 cells in Matrigel with appropriate organoid medium. White line corresponds to 100 µm. **(C)** Immunostaining of an organoid derived from ADK-18 cell line performed using Hoechst 33342 (blue) together with anti-Ki-67 (red) and anti-CD44 (yellow) antibodies. White line corresponds to 20 µm. Leica TCS SP8 Microscope, HC PL APO CS2 40x/1.30 OIL optical zoom 2.5x (left) or 2x (right).

Based on these observations, the growth capacity of the cell lines was assessed for comparison, both *in vitro* and *in vivo*. Overall, the ADK-18 cell line exhibited enhanced growth capacity under all evaluated conditions, showing a significantly higher 2D and 3D-soft-agar

clonogenicity, sphere-forming ability and 2D-growth capacity compared to ADK-17 cells (**Table 2**). In accordance, ADK-18 also showed a significant decrease of cells in the G1 phase of the cell cycle compared to ADK-17. Additionally, the PDX established from the tumor biopsy at the Thy point (ADK-18 tumor) demonstrated significant faster growth compared to the PDX derived from the tumor sample at the Tb point (ADK-17 tumor) (**Figure 1** and **Table 2**).

	ADK-17	**ADK-18**	**p-value**
2D-growth (cell population doublings−168 hours)	2.92±0.04	4.01±0.16	< 0.01
2D-clonogenicity (%)	1±1%	29±1%	< 0.001
3D-soft-agar clonogenicity (%)	0.15±0.05%	18.15±0.50%	< 0.001
Sphere formation ability (number of spheres)	51±2	82±5	< 0.05
Cells in the G1 phase of the cell cycle (%)	63±3%	47±2%	< 0.01
PDX tumor growth rate (doubling time–weeks)	1.430±0.154	0.562±0.104	< 0.05

Table 2. Growth-related features of ADK-17 and ADK-18 cell lines or tumors. Statistical analysis: Student's *t*-test (n=2-3).

In parallel, a transcriptomic analysis on the cell lines was performed to identify key gene expression differences between the cell models. Notably, the analysis revealed significant differences between ADK-17 and ADK-18 cells (PC1: 96% variance), evidencing 3525 genes differentially expressed between the two cell lines (p-adj <0.01 and Log2FC >1 or <-1), of which 1732 up-regulated and 1793 down-regulated in the ADK-18 cell line as compared to ADK-17 (**Figure 20A**).

Over-representation analysis indicated that up-regulated genes were associated with a wide range of biological processes (GO terms BP). Notably, the top 20 GO terms BP revealed enrichment in pathways related to various cell types and tissues, including neural, epithelial, bone, muscle, and connective tissues, suggesting a less differentiated phenotype in the ADK-18 cell line as compared to ADK-17 (**Figure 20B-i.**). Conversely, down-regulated genes in the ADK-18 cell line were linked to the differentiation status of epithelial cells, supporting evidence of a partial EMT in these cells

(**Figure 20B-ii.**). Up-regulated genes were enriched in molecular functions (GO terms MF), including channel activity, ion transport, insulin-like growth factor binding, growth factor activity, and binding to carbohydrates and glycosaminoglycan (**Figure 20B-iii.**), while down-regulated genes were enriched in molecular functions associated with cell-cell interactions and cytoskeletal binding, including actin filaments, laminin binding and DNA binding (**Figure 20B-iv.**). Interestingly, GSEA analysis identified clusters of genes associated with plasticity, the WNT pathway, and the cell cycle, which were predominantly upregulated in the ADK-18 cell line (**Figure 20C**).

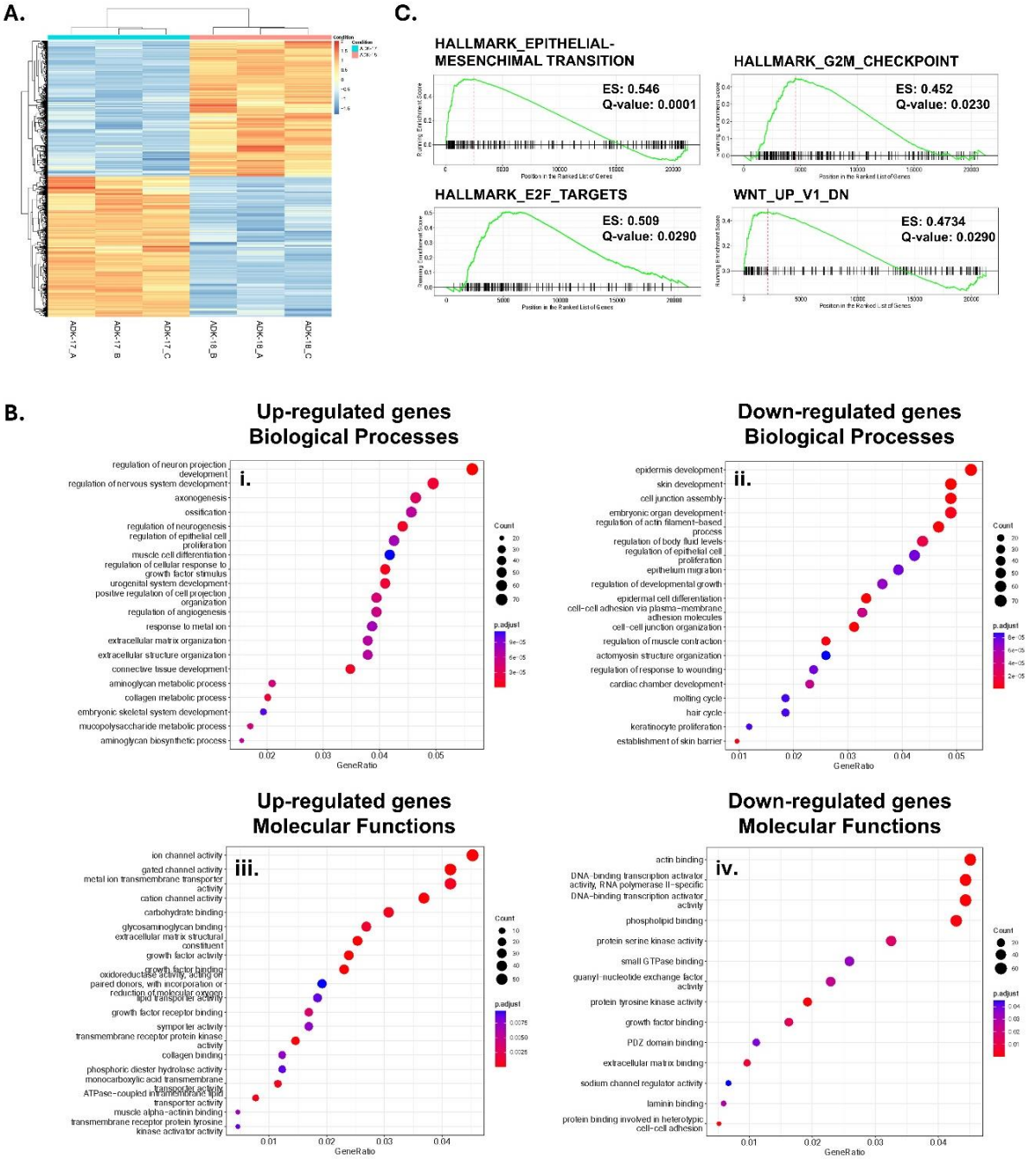

Figure 20. Transcriptome analysis of ADK-18 *vs* ADK-17 cell lines. (A) Heatmap showing the z-score of normalized expression values (RLOG) of differentially expressed genes (DEG, p-adj <0.01 and Log2FC >1 or <-1) in ADK-18 *vs*

ADK-17 cells. **(B) i. – ii.:** top-20 GO term Biological Processes enriched in up-regulated **(i.)** and down-regulated **(ii.)** genes, identified by over representation analysis of DEG; **iii. – iv.:** top-20 GO term Molecular Functions enriched in up-regulated **(iii.)** and down-regulated **(iv.)** genes, identified by over representation analysis of DEG. **(C)** GSEA enrichment plots of curated lists related to plasticity, WNT pathway, cell cycle and invasiveness.

In summary, the phenotypic and functional characterization of our cell lines revealed more aggressive traits in the ADK-18 model as compared to ADK-17. Transcriptome analysis further demonstrated a distinct gene expression profile between the two cell lines, highlighting the hypothesis of modulation of genes that promote plasticity traits in the ADK-18 cell line.

4.1.3 Expression of CD44 transcript isoforms in ADK-17 and ADK-18 cell lines

CD44 is a transmembrane glycoprotein involved in various cellular processes, including cell adhesion, migration, and signaling (Jordan et al., 2015). Interestingly, its expression has also been associated with cancer progression, invasiveness and plasticity (Chen et al. 2018). Even though CD44 primarily binds to hyaluronic acid, it can also interact with other ligands, including osteopontin, collagen, and matrix metalloproteinases (Senbanjo & Chellaiah, 2017). CD44 exists in multiple isoforms generated through alternative splicing of the *CD44* gene, which gives rise to the standard form of the protein (CD44 standard, CD44s) and a variety of CD44 variant isoforms (CD44 variants, CD44v), which differ in their extracellular domain and that participate in distinct biological processes (Chen et al. 2018).

In our cell line models, CD44 showed different profiles of expression, resulting highly expressed by the ADK-18 cell line as compared to ADK-17 (Log2FC: 2.882, p-adj: 6.20E-49) (**Figure 21A,B**).

Given that in cancer biology, specific CD44 isoforms have been implicated in tumor progression, metastasis, and therapy resistance (Ponta et al., 2003), we specifically investigated the transcriptional profile of both the cell lines for CD44 variants, evidencing differential abundance in ADK-18 *vs* ADK-17 cell line (**Figure 21C**).

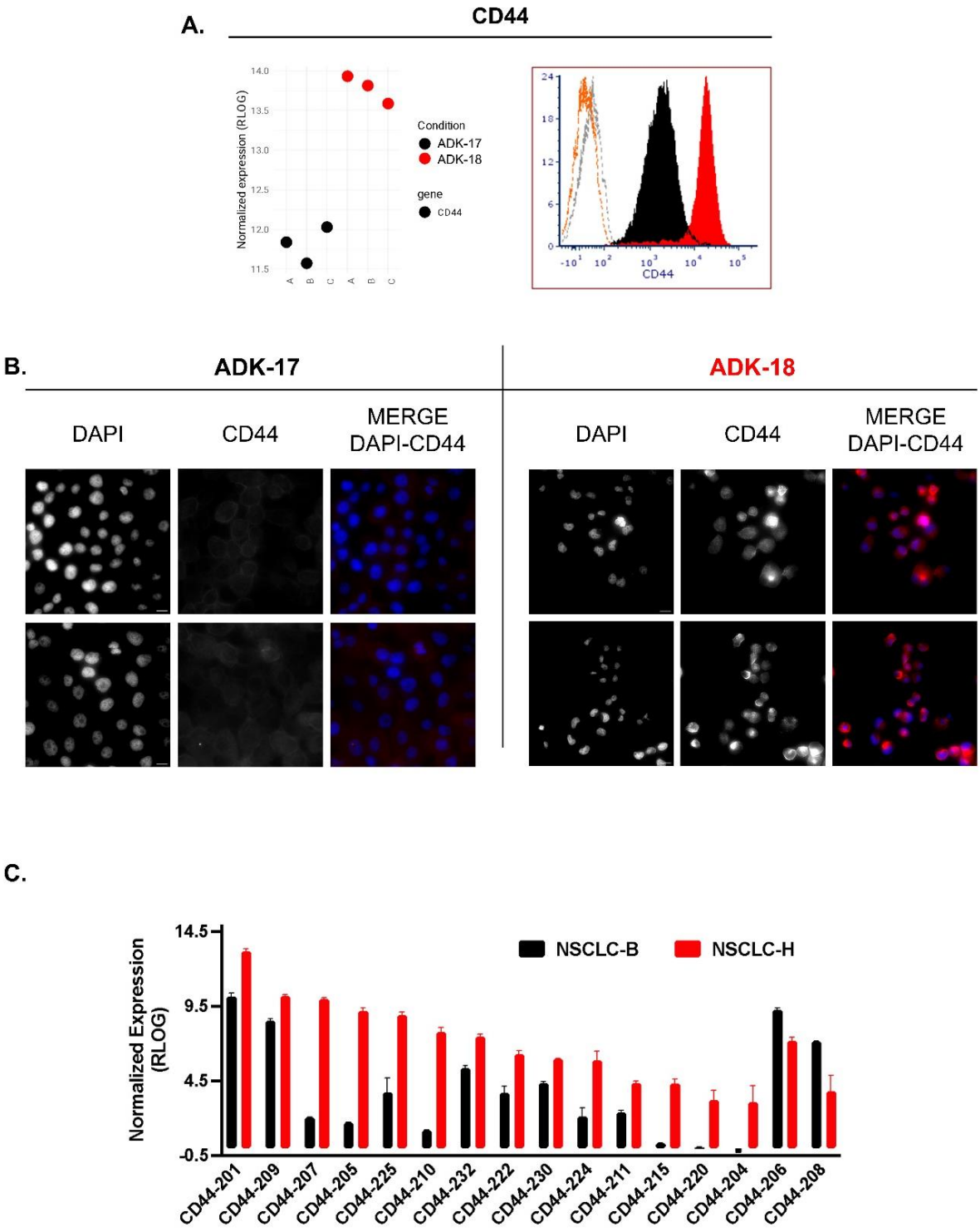

Figure 21. CD44 expression in ADK-17 and ADK-18 cell lines. (A) Left: normalized expression (RLOG) of the *CD44* gene, as identified by RNAseq analysis; **right:** CD44 protein expression quantified by flow-cytometry (ADK-17, grey: unstained control, black: stained sample; ADK-18, orange: unstained control, red: stained sample). **(B)** Immunostaining of ADK-17 and ADK-18 adherent cells. CD44 (red) and DAPI (blue) staining. White line corresponds to 20 µm. Leica widefield system, equipped with an inverted Leica DMi8 microscope, a Leica DFC9000GT cMOS camera and driven by Leica Application Suite X, working with a 40x dry objective (Leica HC PL FLUORTAR L40x/0.6). **(C)** Normalized

expression (RLOG) of CD44 transcript isoforms, as identified by RNAseq analysis. Log2FC and p-adj of each transcript isoform in ADK-18 *vs* ADK-17 are reported in Table 3.

The levels of expression of CD44 transcript isoforms ranged from low (Transcripts Per Kilobase Million, TPM <3) to high (TPM >10) levels between the cell lines (**Table 3**).

Transcript	Short name	UNIPROT ID	Description	ADK17 (TPM)	ADK18 (TPM)	baseMean	Log2FC	p-adj
ENST00000263398	CD44-201	P16070-12	Merged Havana/Ensembl protein coding	3.233	62.422	6657.373	3.841	6.07E-42
ENST00000425428	CD44-207	Q86UZ1	Merged Havana/Ensembl non-sense-mediated decay	0	24.163	925.628	14.718	1.25E-26
ENST00000433892	CD44-209	P16070-10	Merged Havana/Ensembl protein coding	2.345	13.648	854.948	2.100	5.02E-18
ENST00000352818	CD44-205	P16070-18	Merged Havana/Ensembl protein coding	0	26.391	532.705	13.805	2.91E-22
ENST00000415148	CD44-206	P16070-4	Merged Havana/Ensembl protein coding	5.471	1.146	442.793	-2.577	1.69E-12
ENST00000527326	CD44-225	--	processed transcript retained intron	0.442	30.109	388.920	4.658	0.00324
ENST00000434472	CD44-210	P16070-11	Merged Havana/Ensembl protein coding	0	5.702	200.444	12.229	2.21E-16
ENST00000531118	CD44-232	--	processed transcript retained intron	0.739	6.729	128.240	2.674	7.40E-10
ENST00000428726	CD44-208	P16070-1	Merged Havana/Ensembl protein coding	0.586	0.074	108.956	-2.241	0.03343
ENST00000526025	CD44-222	E9PKC6	Ensembl protein coding	0.197	2.674	59.353	3.126	0.0000163
ENST00000526669	CD44-224	H0YD13	Ensembl protein coding	0.064	3.416	56.917	4.827	0.0000372
ENST00000528922	CD44-230	--	protein coding CDS not defined	0.228	1.415	47.053	2.086	0.00000336

Table 3. *CD44* (ENSG00000026508) gene isoform analysis. Detected isoforms, ADK-18 *vs* ADK-17. TPM: Transcripts Per Kilobase Million (*table continues in the next page*).

Transcript	Short name	UNIPROT ID	Description	ADK17 (TPM)	ADK18 (TPM)	baseMean	Log2FC	p-adj
ENST00000525241	CD44-215	--	processed transcript retained intron	0	3.014	18.227	7.949	0.0000251
ENST00000279452	CD44-204	H0Y2P0	Ensembl protein coding	0	0.985	16.381	0.456	0.006981
ENST00000442151	CD44-211	H0Y5E4	Merged Havana/Ensembl protein coding	0.030	0.362	15.988	2.702	0.001073
ENST00000525688	CD44-220	H0YF08	Ensembl protein coding	0	1.183	10.533	6.326	0.005413

Table 3 (*continued*). *CD44* (ENSG00000026508) gene isoform analysis. Detected isoforms, ADK-18 *vs* ADK-17. TPM: Transcripts Per Kilobase Million.

ADK-18 cell line mainly showed increased levels of the short transcript isoforms CD44-201 (CD44s), CD44-205, CD44-209, CD44-222 and CD44-230 (**Figure 21C**). Other transcript isoforms more expressed in ADK-18 cells compared to ADK-17 cells included CD44-204, CD44-211, CD44-220 and CD44-224. In addition, ADK-18 cell line also showed increased levels of two transcripts with a premature translation termination codon (CD44-207 and CD44-210) and three transcripts unable to be translated due to intron retaining (CD44-215, CD44-225 and CD44-232), compared to ADK-17 (**Figure 21C**). Interestingly, although total CD44 transmembrane protein was more highly expressed in ADK-18 cells compared to ADK-17 cells, longer transcripts of the protein, such as CD44-206 (CD44v6) and CD44-208 (CD44v2-v10), were more abundant in the ADK-17 cell line than ADK-18 (**Figure 21C**).

Overall, transcriptomic data revealed distinct expression patterns of CD44 transcripts between the ADK-17 and ADK-18 cell lines, highlighting an association between shorter CD44 isoforms and resistance to immunotherapy.

4.1.4 Expression of immune-related proteins in ADK-17 and ADK-18 cell lines

Considering the several phenotypical differences identified between the two cell lines, we also examined the expression profiles of proteins involved in tumor's response to immunotherapy in our models. PD-L1 is an immune checkpoint glycoprotein that can inhibit the immune system's ability to attack cancer cells by binding to the PD-1 receptor expressed by T cells (Zhang et al., 2021). Tumors with high PD-L1 expression often evade immune detection and are associated with resistance to immune responses (Cha et al., 2019). For this reason, PD-L1 represents one of the most common targets for immune checkpoint blocker (De Giglio et al., 2021). In addition, PD-L1 expression is also considered a key biomarker for predicting the efficacy of ICIs targeting the PD-1/PD-L1 axis, as

tumors expressing high levels of PD-L1 are more likely to respond to these therapies (Grossman et al., 2021). Interestingly, PD-L1 resulted to be overexpressed in the ADK-17 cell line as compared to ADK-18 (**Figure 22A,B**).

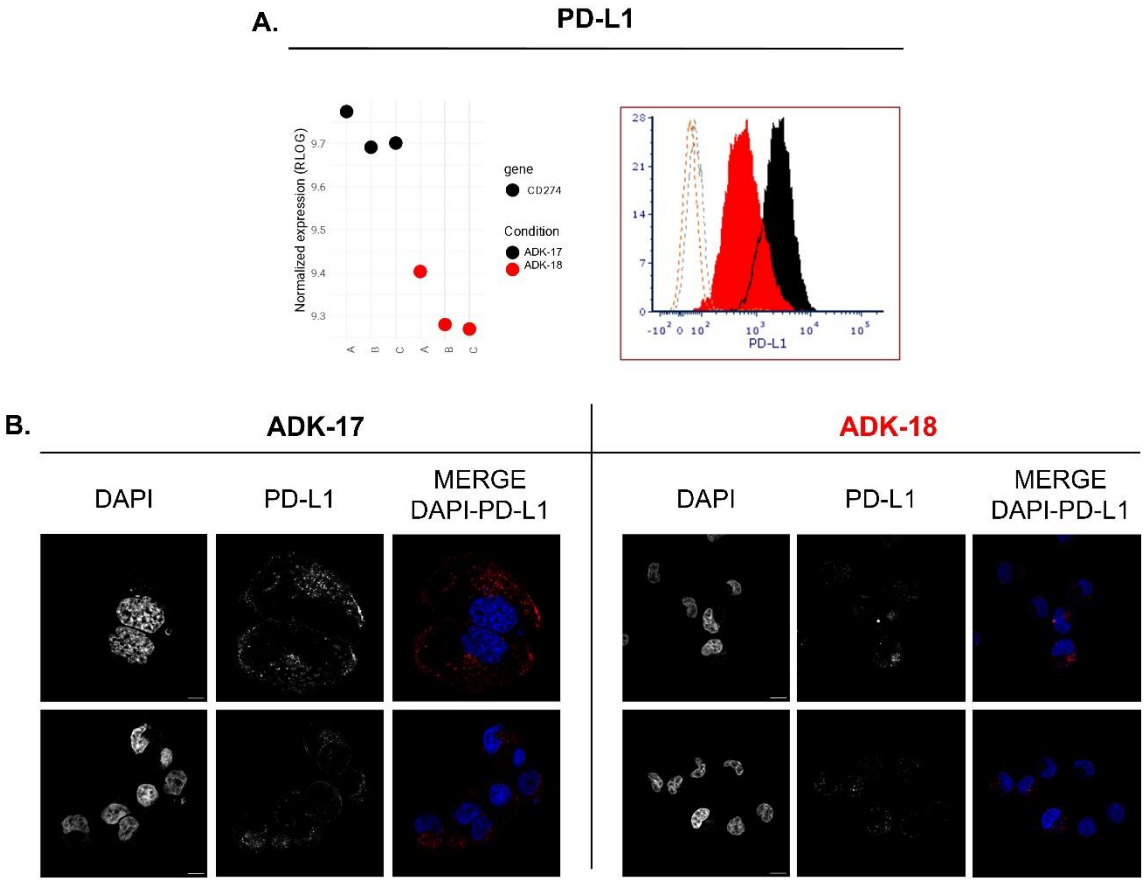

Figure 22. Expression of PD-L1 in ADK-17 and ADK-18 cell lines. (A) Normalized expression (RLOG) of *PD-L1* (CD274) gene, as identified by RNAseq analysis (Log2FC: -0.589, p-adj: 0.0003), and validation by flow cytometry (ADK-17, grey: unstained control, black: stained sample; ADK-18, orange: unstained control, red: stained sample). **(B)** PD-L1 (red) and DAPI (blue) staining. White line corresponds to 10 µm. Leica TCS SP8 confocal microscope equipped with a Leica DMi8 inverted microscope, a tunable excitation laser source (White Light Laser) and driven by Leica Application Suite X, working with a 63x oil immersion objective (Leica HC PL APO CS2 63x/1.40).

Together with these investigations, genes and proteins associated with the activation of signaling pathways related to inflammation and tumor aggressiveness were also evaluated in the two cell lines. Interestingly, a subgroup of enriched score genes associated to GSEA analysis and related to the cellular response to IFN-gamma (IFN-γ) and IFN-alpha (IFN-α) was down-regulated in ADK-18 cells compared to ADK-17 cells, while, on the contrary, genes associated with IFN-beta (IFN-β) cellular responses and IL6/JAK/STAT3 signaling were up-regulated in ADK-18 cells (**Figure 23A**).

Interestingly, GSEA analysis also showed an up-regulation of the "inflammatory response" Hallmark gene in the ADK-18 cell model as compared to the ADK-17 one (**Figure 23B**).

Additionally, the evaluation of the activation status of signaling pathways related to inflammation and cell aggressiveness revealed increased activation of IFNGR1, STAT1, JAK2, IRF3 and MAPK in ADK-18 compared to ADK-17, but reduced activation of STAT3 (**Figure 23C**).

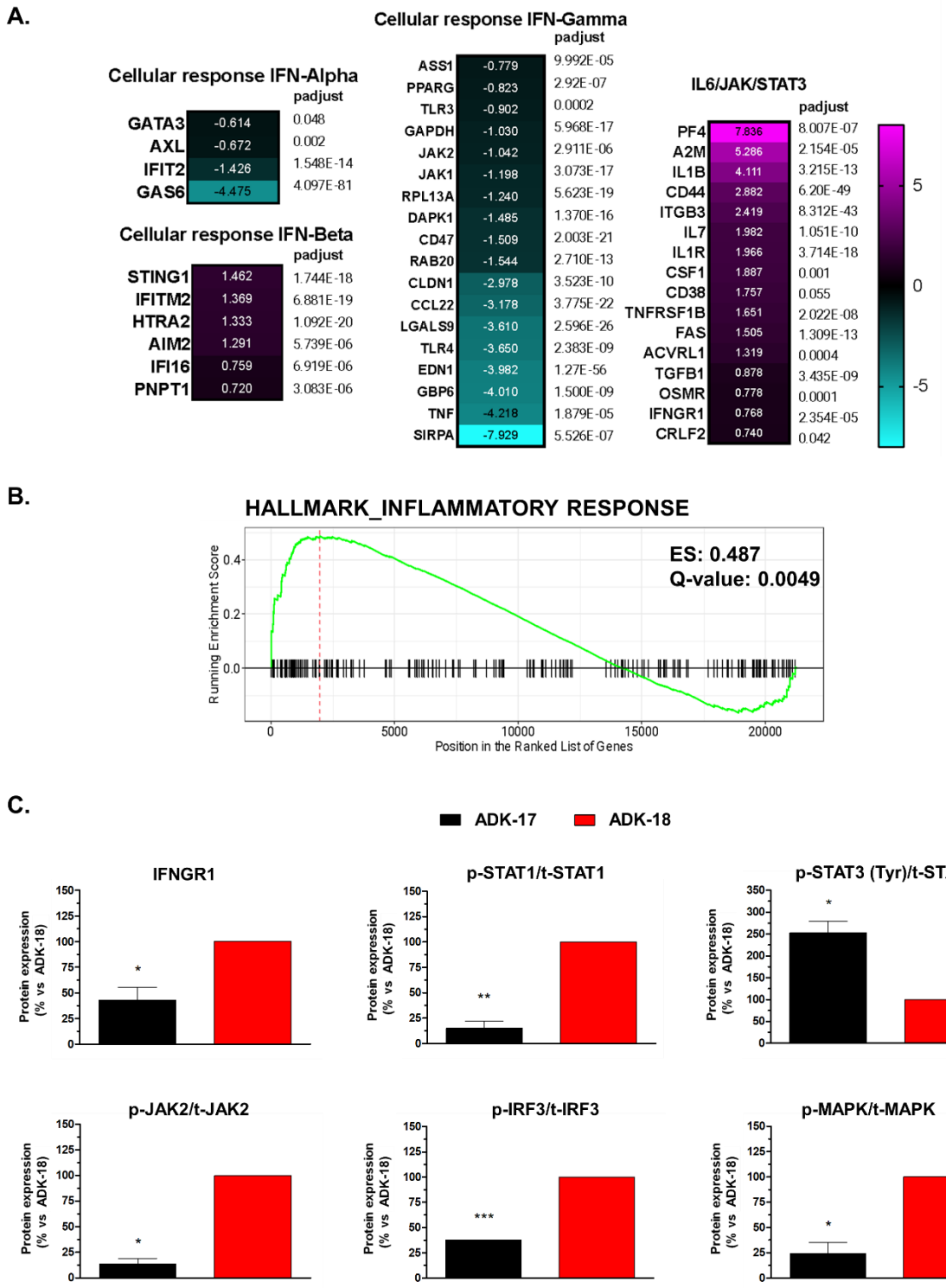

Figure 23. Expression of genes and proteins associated with inflammation and tumor aggressiveness in ADK-17 and ADK-18 cell lines. (A) Heatmap showing the Log2FC of a subgroup of enriched score genes associated to GSEA analysis, which are involved in immune-related cellular responses and inflammation. Log2FC of differentially expressed genes in ADK-18 compared to ADK-17 is reported in the box and p-adj is reported on the right. **(B)** GSEA analysis of

curated list related to inflammatory response. **(C)** Western blot analysis for proteins involved in response to inflammatory stimuli and cell proliferation (n=3, except for p-JAK2/t-JAK2 and p-IRF3/t-IRF3, in which n=2). *, p<0.05, **, p<0.01 and ***, p<0.001 by One Sample t test (each group *vs* theoretical mean of 100). Each bar represents mean with SEM. SEM: standard error of the mean.

To sum up, the ADK-18 cell line exhibited increased expression of genes involved in inflammation pathways, such as IFN-β signaling, and in tumor aggressiveness, *i.e.*, IL6/JAK/STAT3, together with increased activation of mediators of the IFN-γ signaling pathway, compared to ADK-17 cells. Conversely, PD-L1 expression was found to be reduced in the ADK-18 model compared to ADK-17.

4.1.5 In vitro response of ADK-17 and ADK-18 cell lines to IFN-γ

The mechanism of action of ICIs involves enhancing T-cell activation and reversing T-cell exhaustion by targeting immune checkpoints. IFN-γ, known for its antiproliferative, cytostatic, pro-apoptotic, and immunogenic effects on tumor cells, is believed to mediate the antitumor response of cytotoxic T-cell populations restored through ICI therapy (Jorgovanovic et al., 2020). Therefore, we assessed the effect of IFN-γ on ADK-17 and ADK-18 cells *in vitro*, simulating the interaction between tumor cells and the antitumor cytokine released by reactivated cytotoxic T cells under ICI treatment.

Under adherent culture conditions, both ADK-17 and ADK-18 exhibited a weak response to IFN-γ, as indicated by limited inhibition of cell proliferation and minimal induction of immunological markers, such as PD-L1 and major histocompatibility complex (MHC) class I (**Figure 24A**).

Interestingly, under low-dose cell seeding conditions the cell lines exhibited completely different responses to the cytokine. Indeed, while ADK-17 maintained its resistance to the antiproliferative effect of IFN-γ (**Figure 24B**), ADK-18 showed a significant reduction in its 2D-clonal efficiency compared to control (**Figure 24C**).

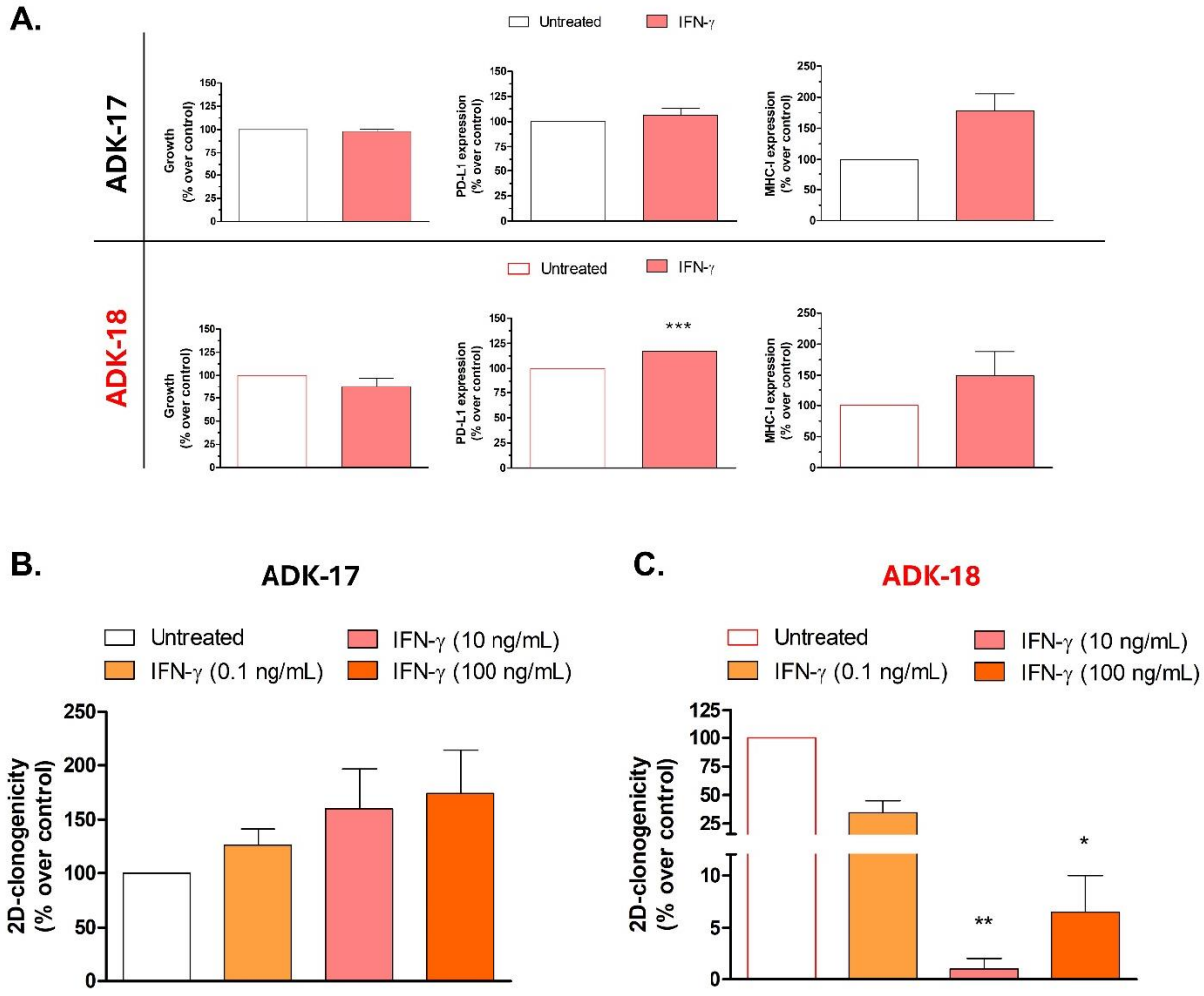

Figure 24. Response of ADK-17 and ADK-18 cell lines to IFN-γ treatment in 2D culture conditions. (A) Sensitivity of ADK-17 and ADK-18 cell lines to the antiproliferative effect of IFN-γ (7 ng/mL) (left, n=2) and percentage of induction of PD-L1 expression (middle, n=2) and MHC class I complex (right, n=2) in the presence of IFN-γ. ***, p<0.001 by One Sample t test (group *vs* theoretical mean of 100). Bar represents mean and SEM. **(B,C)** 2D-clonal efficiency of ADK-17 **(B)** and ADK-18 **(C)** cell lines in the presence of different doses of IFN-γ (n=6 and n=2, respectively). *, p<0.05 and **, p<0.01 by One sample t test (each group *vs* theoretical mean of 100). Each bar represents mean and SEM. SEM: standard error of the mean.

To better understand this discrepancy in treatment response between the two cell lines, the activation of key mediators involved in IFN pathways and cell growth signaling was assessed in both ADK-17 and ADK-18 cells in presence of low (0.1 ng/mL) or high (100 ng/mL) doses of IFN-γ. Interestingly, in the ADK-17 model, IFN-γ treatment stimulated not only the activation of canonical mediators of the IFN-γ signaling pathway, such as STAT1, JAK1 and JAK2, but it also triggered the activation of STAT2 and IRF9, which are typical mediators of type I-IFN signaling pathway (Vella et al., 2022). Notably, IFN-γ also mildly stimulated MAPK activation (**Figure 25A**). In contrast, in the ADK-18 model, IFN-γ treatment unexpectedly failed to strongly activate the IFN-γ pathway

mediators STAT1 and JAK2, but enhanced MAPK activation (**Figure 25B**). Additionally, low-dose IFN-γ appeared to slightly increase IRF9 protein expression, similarly to what was observed in the ADK-17 cell line (**Figure 25B**).

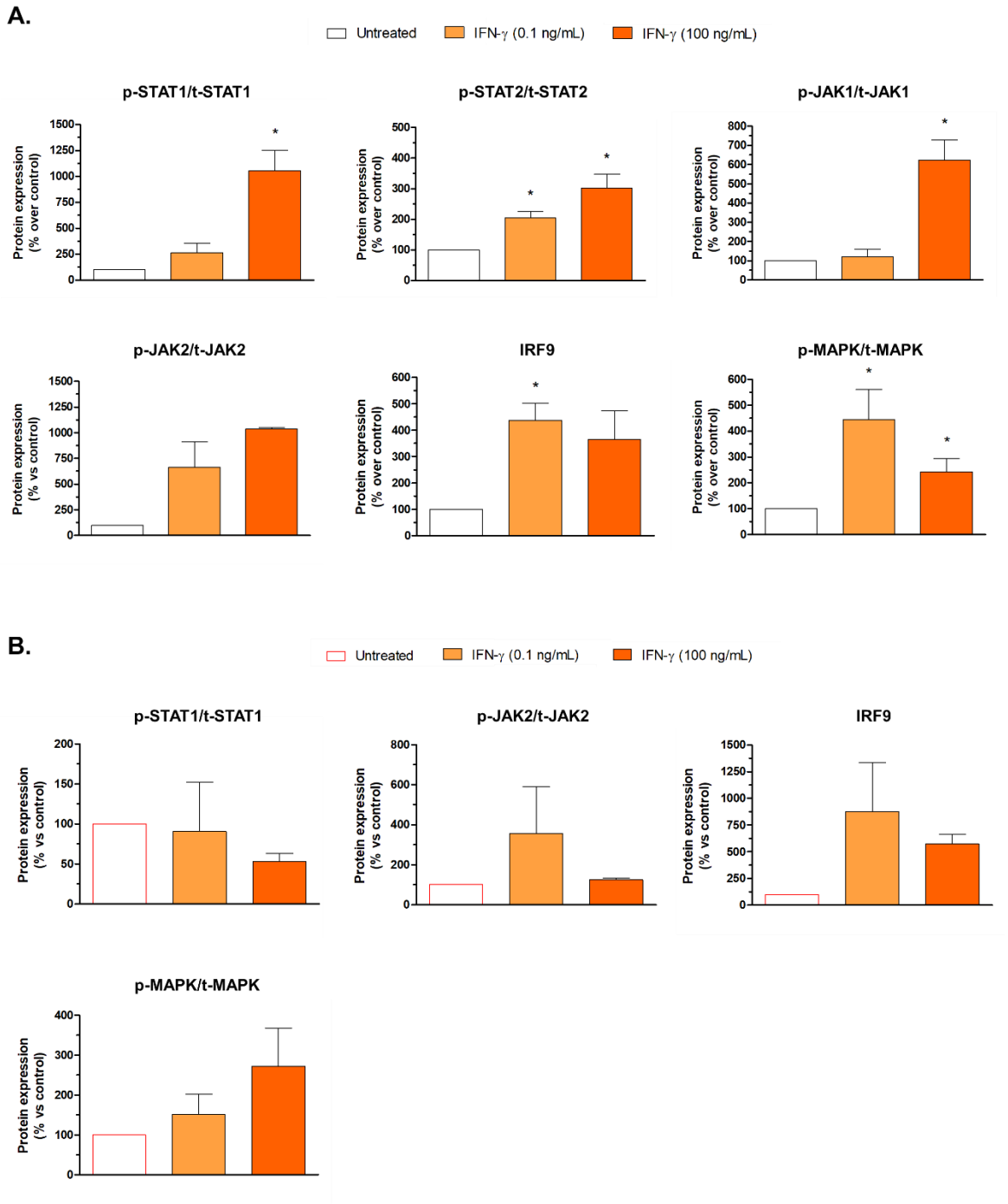

Figure 25. Activation levels of proteins involved in IFN signaling and in cell growth on ADK-17 and ADK-18 cells treated with IFN-γ under 2D culture conditions. (A) Western blot analyses on ADK-17 cells treated with low (0.1 ng/mL) or high (100 ng/mL) doses of IFN-γ (n=2, at least). *, $p<0.05$ by One Sample t test (each group *vs* theoretical mean of 100). Each bar represents mean and SEM. **(B)** Western blot analyses on ADK-18 cells treated with low (0.1 ng/mL) or high (100 ng/mL) doses of IFN-γ (n=2, at least). Each bar represents mean and SEM. SEM: standard error of the mean.

Surprisingly, in 3D culture conditions IFN-γ exhibited a growth-stimulating effect on ADK-17 cells, leading to a significant increase in the number of soft-agar colonies (**Figure 26A**). Moreover, low-dose IFN-γ treatment induced a significant increase in ADK-17 sphere production as compared to control and to high-dose IFN-γ treatment (**Figure 26B**).

Unlike the ADK-17 cell line, ADK-18 retained its sensitivity to IFN-γ under 3D culture conditions, as the cytokine significantly inhibited its ability to form colonies in soft agar (**Figure 26C**) and its sphere formation capacity (**Figure 26D**).

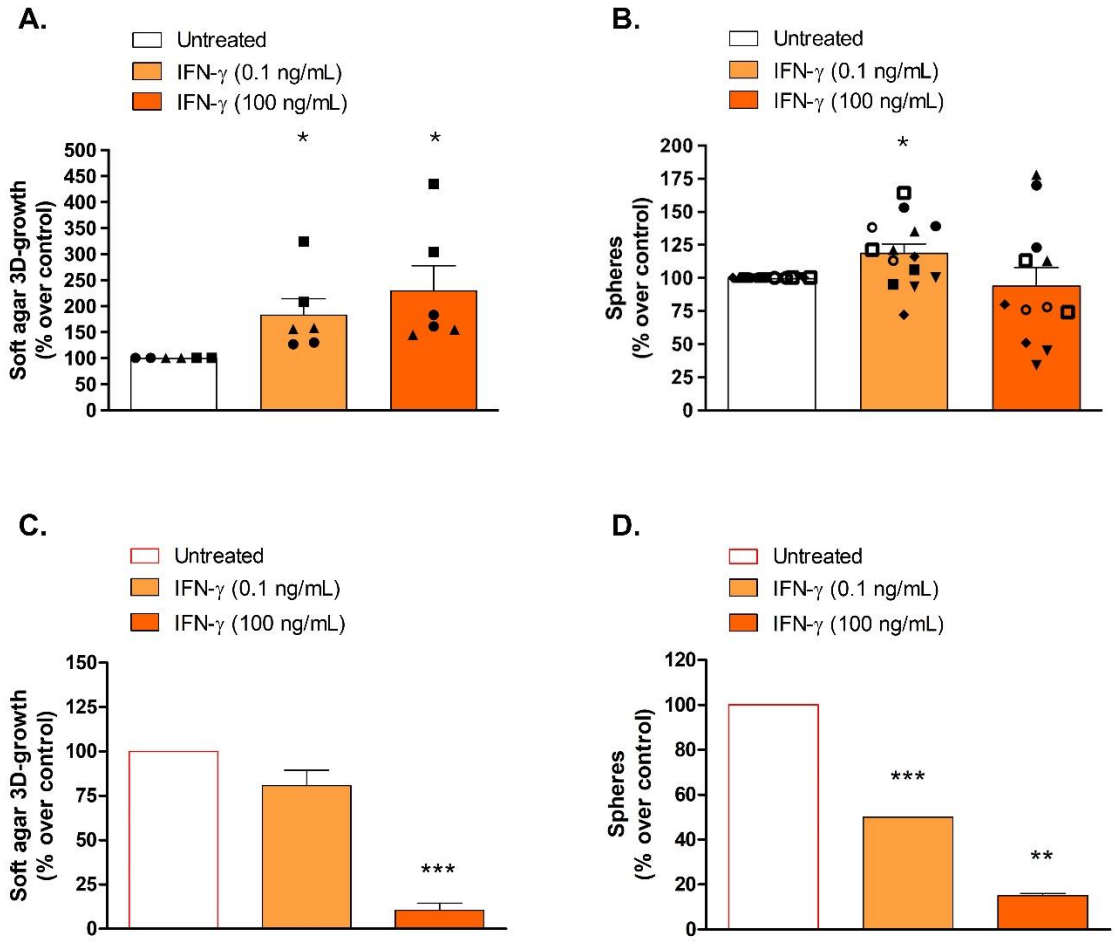

Figure 26. Response of ADK-17 and ADK-18 cell lines to different doses of IFN-γ in 3D culture conditions. (A) ADK-17 soft-agar colony formation in the presence of low (0.1 ng/mL) and high (100 ng/mL) doses of IFN-γ (n=6, three experiments−circle, triangle, square−each one with two technical replicates). *, $p<0.05$ by One sample t test (each group *vs* theoretical mean of 100). Each bar represents mean and SEM. Each dot represents a replicate. **(B)** ADK-17 sphere formation in the presence of low (0.1 ng/mL) and high (100 ng/mL) doses of IFN-γ (untreated and IFN-γ 0.1 ng/mL: n=14, seven experiments−different symbols−, each one with two technical replicates; IFN-γ 100 ng/mL: n=12, six experiments, each one with two technical replicates). *, $p<0.05$ by One sample t test (each group *vs* theoretical mean of 100). Each bar represents mean and SEM. Each dot represents a replicate. **(C)** ADK-18 soft-agar colony formation in the presence of low (0.1 ng/mL) and high (100 ng/mL) doses of IFN-γ (n=3, two experiments, each one with two technical replicates). ***, $p<0.001$ by One sample t test (each group *vs* theoretical mean of 100). Each bar represents mean and

SEM. **(D)** ADK-18 sphere formation in the presence of low (0.1 ng/mL) and high (100 ng/mL) doses of IFN-γ (n=2, one experiment with two technical replicates). **, p<0.01 and ***, p<0.001 by One sample t test (each group *vs* theoretical mean of 100). Each bar represents mean and SEM. SEM: standard error of the mean.

To assess whether ICI resistance is linked to tumor cell sensitivity to IFN-γ, as suggested by the behavior of ADK-18 cell model, we also evaluated the *in vitro* response to IFN-γ of two additional patient-derived cell lines, *i.e.*, ADK-19 and ADK-25. As previously mentioned, these cell lines were established in our laboratory from biopsies of two NSCLC patients at the moment of HPD development following ICI-based treatment (**Table 1**) and, similarly to the ADK-18 cell model, exhibited elevated levels of CD44 expression (**Figure 27A**).

In accordance with previous findings regarding ADK-18 cells, ADK-19 and ADK-25 cell lines also showed a striking sensitivity to IFN-γ, as the cytokine significantly inhibited the colony formation capacity of both the cell models in 3D soft agar assay (**Figure 27B,C**).

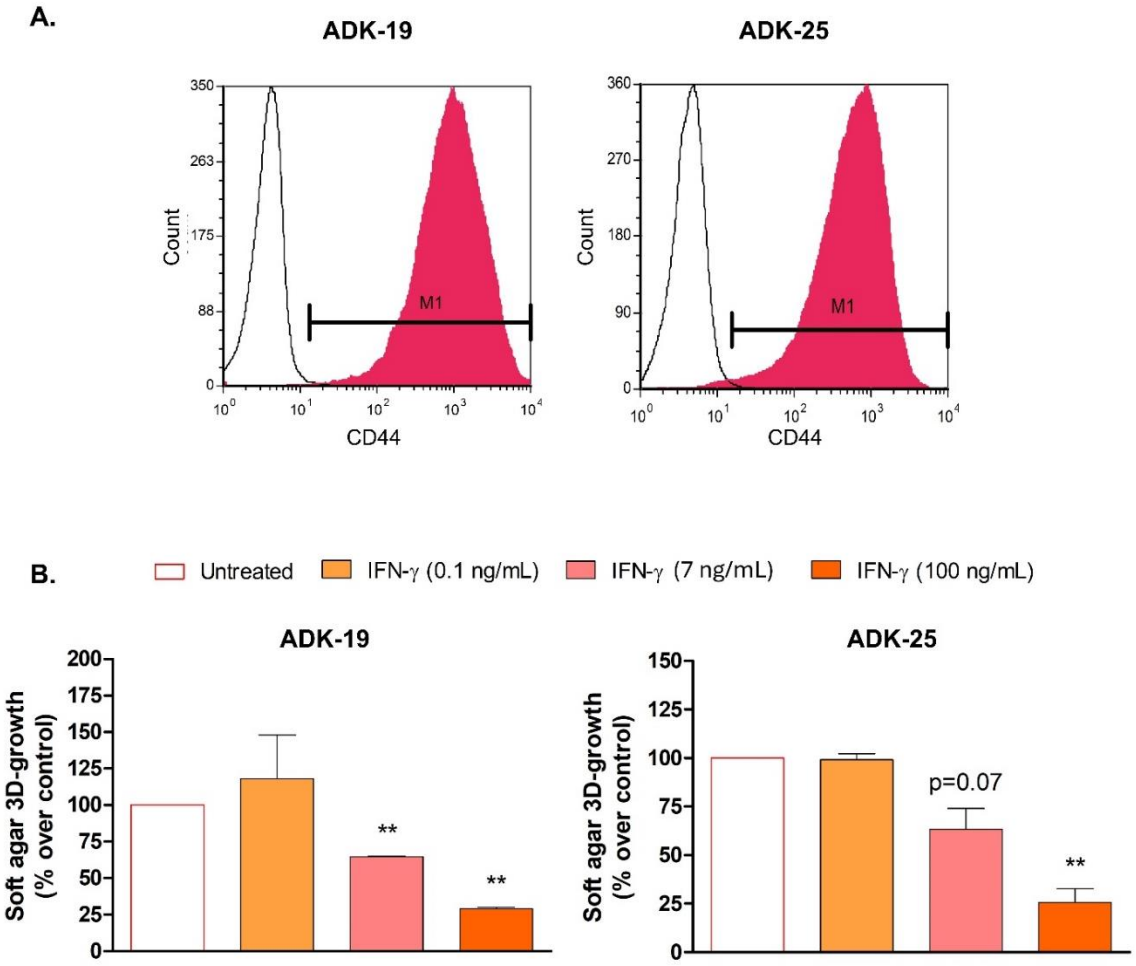

Figure 27. Phenotypical and functional characterization of ADK-19 and ADK-25 cell lines. (A) Representative histograms depicting the expression of CD44, quantified by flow-cytometry. Empty histograms: unstained controls. CD44 Mean Fluorescence Intensity (MFI), ADK-19: 904±399 (n=2); ADK-25: 762±6 (n=2). M1: marker. **(B)** ADK-19 and

ADK-25 soft-agar colony formation in the presence of different doses of IFN-γ (n=2-3). **, p<0.01 by One sample t test (each group *vs* theoretical mean of 100). Each bar represents mean and SEM. SEM: standard error of the mean.

Subsequently, to investigate the atypical response to IFN-γ observed in the ADK-17 cell line, "bulk agar" cell lines were established from 2D-subcultered ADK-17 soft-agar colonies grown in presence of IFN-γ treatments (namely, ADK-17 BA clones) (**Figure 28**).

Interestingly, despite both high and low doses of IFN-γ promoted 3D-cell growth (**Figure 26A**), only "bulk agar" cells derived from colonies grown in the presence of low-dose IFN-γ (namely, ADK-17 BA.γ0.1 cells) showed a partial change in cell morphology and increased CD44 expression compared to control (**Figure 28**).

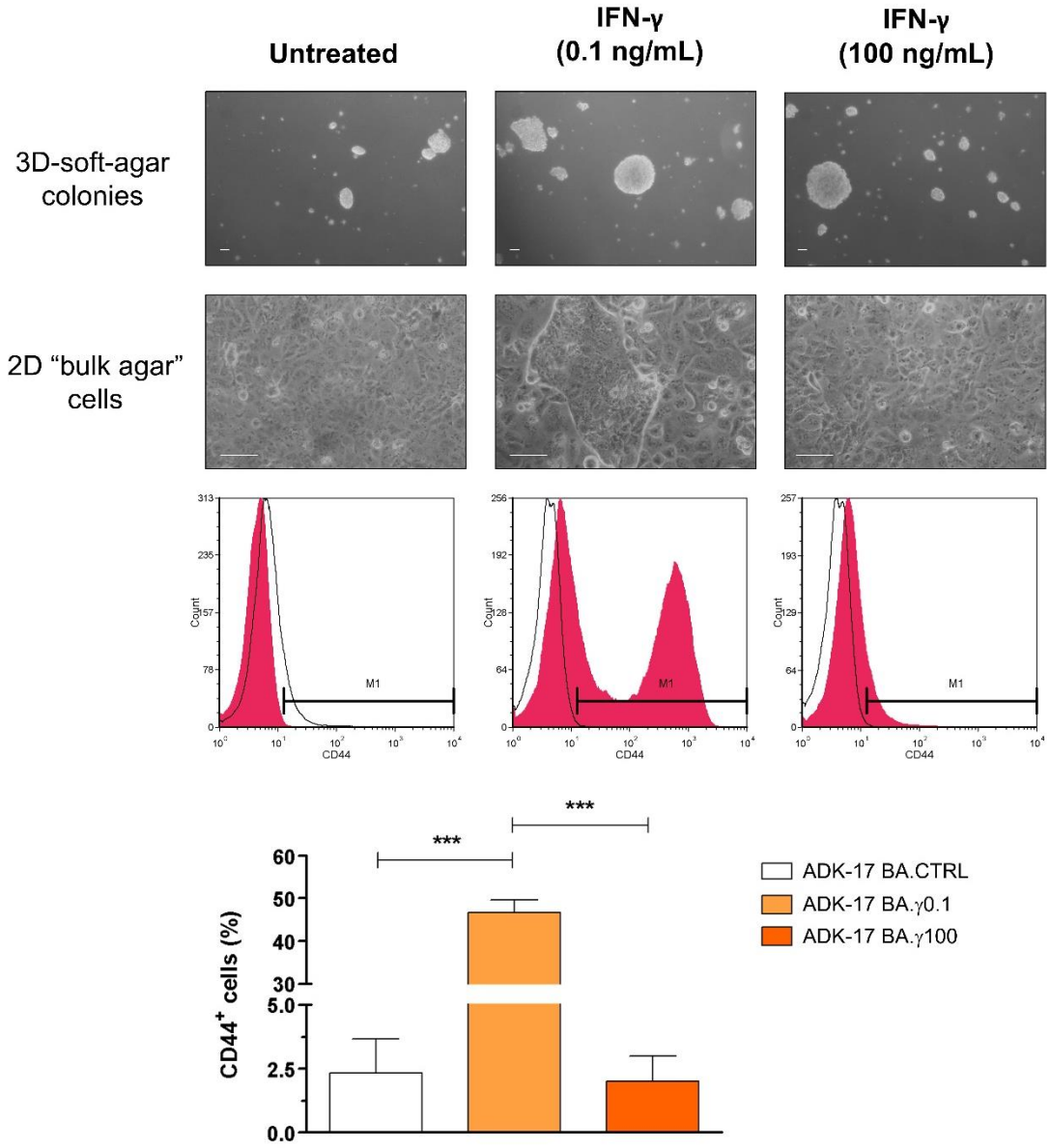

Figure 28. Phenotypical characterization of ADK-17 BA clones. Morphological and phenotypical characterization of ADK-17 BA clones obtained from 2D-subcultered agar colonies grown in the presence of IFN-γ. **First line:** representative pictures of ADK-17 soft-agar colonies grown without any treatment or in the presence of IFN-γ, observed through an

inverted microscope in dark-field; **second line:** morphologies of ADK-17 "bulk agar" cell lines cultured under 2D-adherent conditions, observed through an inverted microscope. White line corresponds to 100 µm; expression of CD44 (**third line**) and percentage of $CD44^+$ cells (**bottom**) on ADK-17 BA clones cultured under 2D-adherent conditions, measured by cytofluorimetric analysis. CD44 Mean Fluorescence Intensity (MFI), ADK-17 BA.CTRL: 8.33±3.84; ADK-17 BA.γ0.1: 265.00±22.65; ADK-17 BA.γ100: 11.67±5.17 (M1: marker) (n=3). ***, $p<0.001$ by Student's *t*-test. Each bar represents mean and SEM. SEM: standard error of the mean.

Taken together, these data suggest impaired canonical IFN-γ signaling in both ADK-17 and ADK-18 cell lines, as evidenced by the absence of an IFN-γ-dependent antiproliferative effect and the failure of the cytokine in effectively inducing PD-L1 and MHC class I expression in 2D culture conditions. However, under conditions of low cell seeding density or 3D culture conditions, the antiproliferative effect of the cytokine became apparent in the ADK-18 cell line, but not in the ADK-17 one. Rather, *in vitro* evidence points to a pro-growth effect of IFN-γ on 3D-cultured ADK-17 cells, along with a direct IFN-γ–mediated regulation of CD44 expression, observed only at low cytokine doses. Moreover, similarly to ADK-18 cell model, the two patient-derived cell lines ADK-19 and ADK-25, established from tumors of hyperprogressive patients, also demonstrated pronounced sensitivity to IFN-γ treatment in the 3D soft-agar assay. These data further support the association between ICI resistance, elevated CD44 expression, and a paradoxical responsiveness of cell lines derived from ICI-resistant tumors to IFN-γ *in vitro*.

4.1.6 PD-L1 modulation on the ADK-17 cell line

PD-L1 is known to exhibit pro-tumor functions that are not solely dependent on its interaction with the PD-1 receptor (Escors et al., 2018). Several studies have indeed demonstrated the presence of PD-L1–mediated intracellular signaling in tumor cells, independent of PD-1 (Hudson et al., 2020; Yadollahi et al. 2021; Alkaabi et al., 2023; Nieto et al., 2023; Cavazzoni et al., 2024) . Thus, we evaluated the effect of PD-L1 modulation on the ADK-17 cell line. First, PD-L1 was targeted with the monoclonal antibody (mAb) atezolizumab under 3D culture conditions. Despite the blockade of PD-L1 did not affect ADK-17 growth in 3D soft-agar assay (**Figure 29A**), the ADK-17 BA clone derived from the soft-agar colonies grown in presence of atezolizumab treatment (*i.e.*, ADK-17 BA.Atezo) showed a striking increase in CD44 expression, together with a partial change in cell morphology (**Figure 29B**). Accordingly, atezolizumab treatment also significantly increased ADK-17 capacity of forming spheres (**Figure 29C**). The evaluation of the intracellular pathways influenced by PD-L1 blockade in ADK-17 cells also evidenced increased activation of MAPK in the presence of atezolizumab treatment (**Figure 29D**).

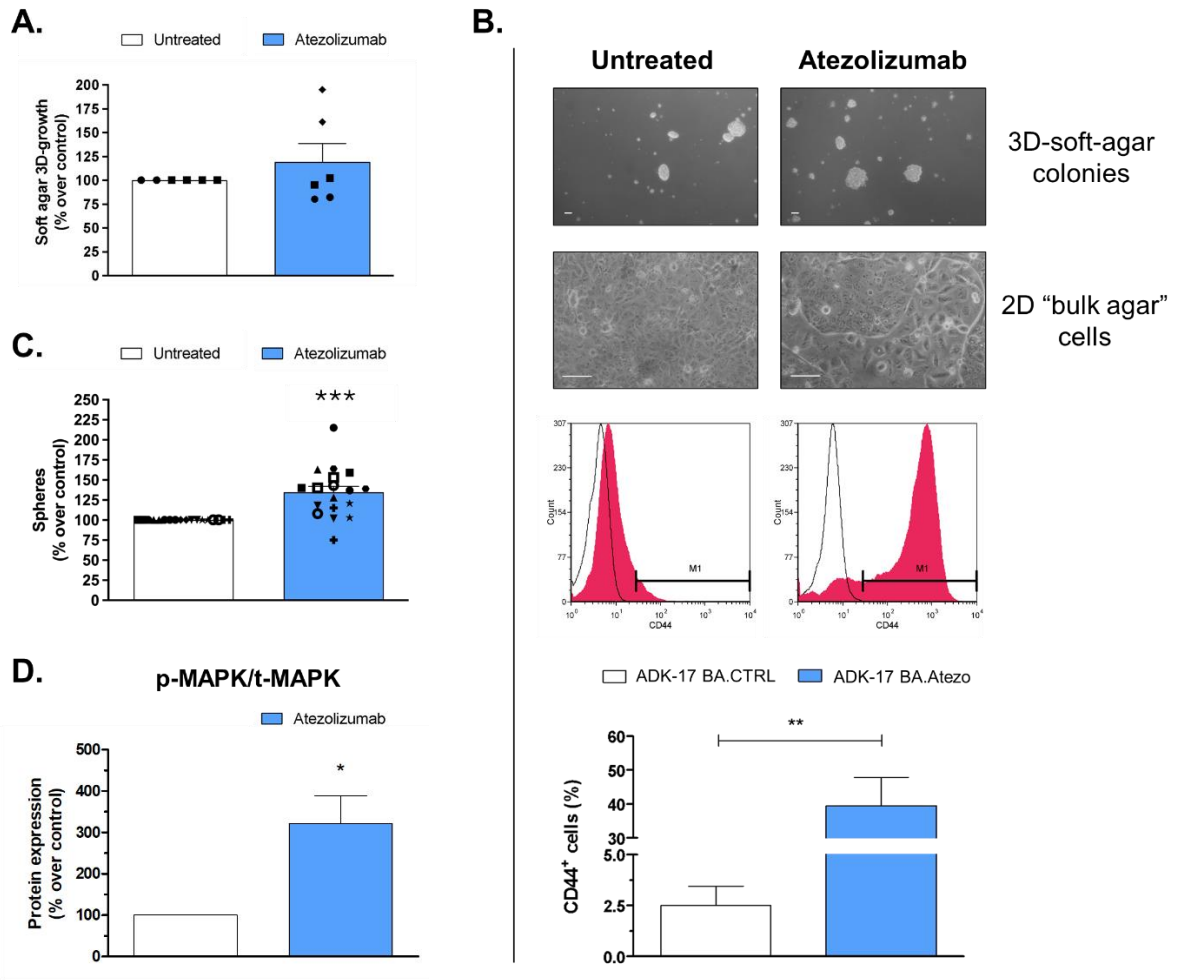

Figure 29. Response of the ADK-17 cell line to PD-L1 modulation in 2D and 3D culture conditions. (A) ADK-17 soft-agar colony formation in the presence of atezolizumab 10 µg/mL (n=6, three experiments−circle, triangle, square−, each one with two technical replicates). Each bar represents mean and SEM. Each dot represents a replicate. **(B)** Morphological and phenotypical characterization of ADK-17 BA clones obtained from 2D-subcultered agar colonies grown in the presence of atezolizumab 10 µg/mL. **First line:** representative pictures of ADK-17 soft-agar colonies grown without any treatment or in the presence of atezolizumab, observed through an inverted microscope in dark-field; **second line:** morphologies of ADK-17 "bulk agar" cell lines cultured under 2D-adherent conditions, observed through an inverted microscope. White line corresponds to 100 µm; expression of CD44 (**third line**) and percentage of $CD44^+$ cells (**bottom**) on ADK-17 BA clones cultured under 2D-adherent conditions, measured by cytofluorimetric analysis. CD44 Mean Fluorescence Intensity (MFI), ADK-17 BA.CTRL: 8.00±2.74; ADK-17 BA.Atezo: 353.00±120.99 (M1: marker) (n=4). **, p<0.01 by Student's *t*-test. Each bar represents mean with SEM. **(C)** ADK-17 sphere formation in the presence of atezolizumab 10 µg/mL (n=18, nine experiments−different symbols−, each one with two technical replicates). ***, p<0.001 by One sample t test (group *vs* theoretical mean of 100). Each bar represents mean and SEM. Each dot represents a replicate. **(D)** Western blot analysis for MAPK activation in ADK-17 cells treated with atezolizumab 5 µg/mL in 2D-adherent culture conditions (n=4). *, p<0.05 by One sample t test (group *vs* theoretical mean of 100). Each bar represents mean with SEM. SEM: standard error of the mean.

To further validate the effect of PD-L1 modulation on cell behavior, we transfected the ADK-17 cell line with a CRISPR/Cas9 guide targeting the PD-L1 encoding gene, deriving two cell clones

(ADK-17 CL1 and ADK-17 CL2) characterized by a partial ablation of PD-L1 expression (**Figure 30A**). Interestingly, the two ADK-17 clones not only showed a partial change in cell morphology, exhibiting a phenotype that was similar to the one of the ADK-18 cell line (**Figure 30B**), but they also showed increased expression of CD44 (**Figure 30C**). Additionally, compared to the parental cell line, ADK-17 CL1 and CL2 cells also displayed a marked increase in *in vitro* growth rate, which was comparable, or even exceeded, to that of ADK-18 cells (**Figure 30D,E**).

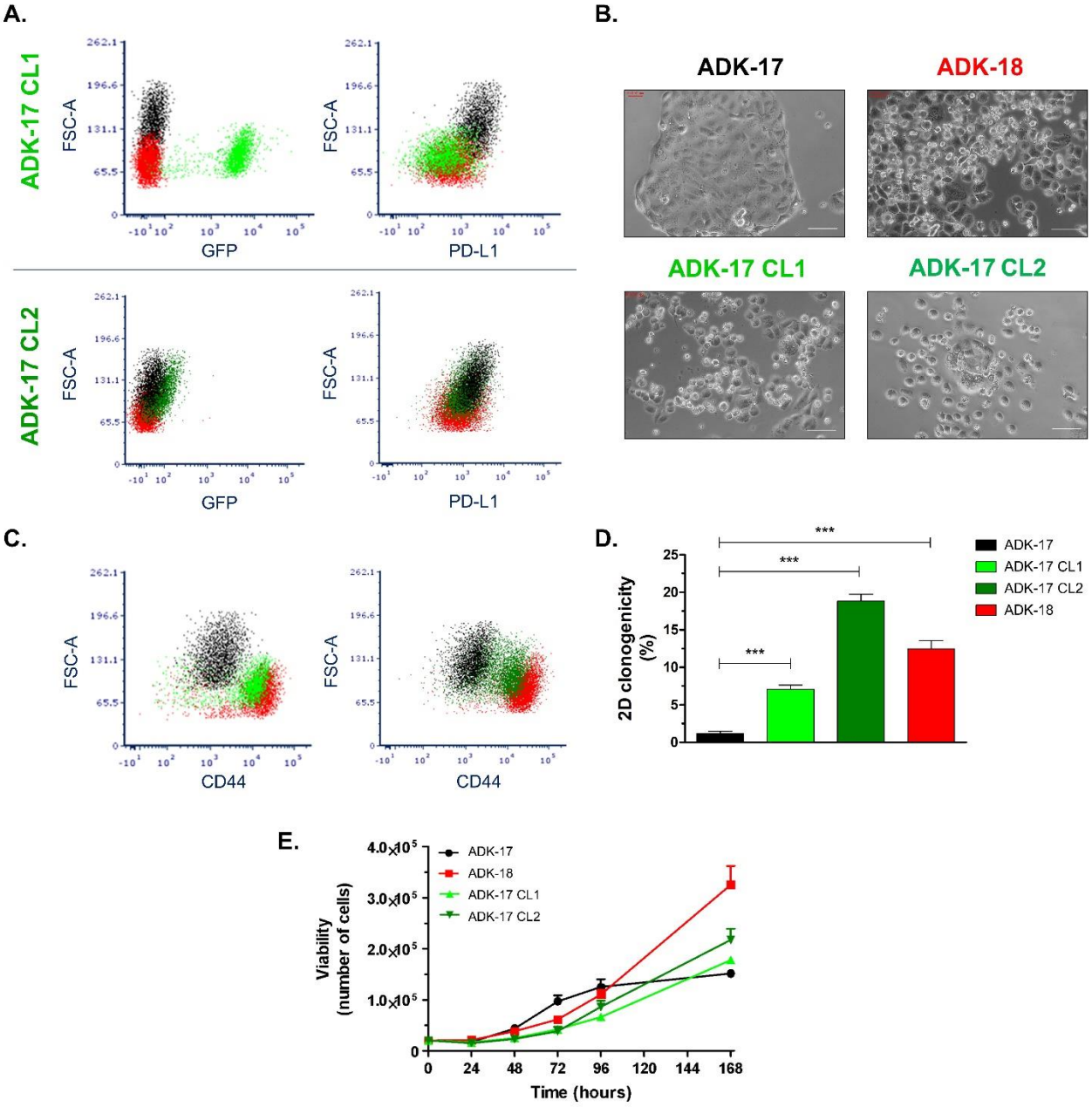

	ADK-17	ADK-17 CL1	ADK-17 CL2	ADK-18	p-value
Cell population doublings	2.92±0.04	3.16±0.05	3.44±0.15	4.01±0.16	17 *vs* 18 ** 17 *vs* 17 CL1 * 17 CL1 *vs* 18 * 17 *vs* 17 CL2 * 17 CL2 *vs* 18 n.s.

Student's *t*-test

Figure 30. Comparison of cell phenotype and cell behavior between ADK-17, ADK-17 CL1, ADK-17 CL2 ad ADK-18 cell lines in 2D culture conditions. (A) Expression of GFP and PD-L1 on ADK-17 (black), ADK-17 CL1 (green), ADK-17 CL2 (dark green) and ADK-18 (red) cell lines, measured by cytofluorimetric analysis. **Up**, PD-L1 Mean Fluorescence Intensity (MFI): ADK-17, 2210; ADK-17 CL1, 361; ADK-18, 501; **bottom**, PD-L1 MFI: ADK-17, 1600; ADK-17 CL2, 990; ADK-18, 657. **(B)** Representative photos of ADK-17, ADK-17 CL1, ADK-17 CL2 and ADK-18 cell lines, observed through an inverted microscope in dark-field. White line corresponds to 100 µm. **(C)** Expression of CD44 on ADK-17 (black), ADK-17 CL1 (green), ADK-17 CL2 (dark green) and ADK-18 (red) cell lines cultured under 2D-adherent conditions, measured by cytofluorimetric analysis. **(D)** Comparison of 2D-clonal efficiency between ADK-17, ADK-17 CL1, ADK-17 CL2 and ADK-18 cell lines (n=6). ***, $p<0.001$ by Student's *t*-test. Each bar represents mean and SEM. **(E)** Comparison of cell growth curves (ADK-17 and ADK-18: n=3, ADK-17 CL1 and CL2: n=2). Bars represent mean and SEM. Cell population doublings during 168 hours of culture in 2D-growth adherent conditions are reported in the table in the bottom. *, $p<0.05$ and **, $p<0.01$ by Student's *t*-test. SEM: standard error of the mean.

Collectively, these findings suggest that the PD-L1 expressed on ADK-17 cells directly regulates CD44 expression, and that its inhibition promotes increased tumor cell growth in both 2D and 3D anchorage-independent cell culture assays, highlighting a significant role for PD-L1 in modulating cancer cell stemness and tumor growth.

4.1.7 Evaluation of in vitro behavior of the ADK-17 BA clones and their response to IFN-γ

To determine whether CD44 expression conferred an ADK-18–like phenotype to the AD-17 BA clones, we evaluated the *in vitro* aggressiveness of the cells under various culture conditions. Despite the evaluation of the growth curves of ADK-17 BA clones in adherent culture conditions did not evidence any growth difference (**Figure 31A**), the clonogenic assay performed at low cell seeding densities revealed a striking enhancement in the clonal colony-forming efficiency of ADK-17 BA.Atezo and ADK-17 BA.γ0.1 cell lines (**Figure 31B**), which, as previously described, were characterized by elevated CD44 expression (**Figure 28** and **Figure 29B**).

Curiously, under anchorage-independent 3D culture conditions, the $CD44^{high}$ ADK-17 BA cell lines showed decreased capacity of forming spheres as compared to ADK-17 BA.CTRL cells (**Figure 31C**). In contrast, the 3D soft-agar assay confirmed the previously observed increased growth capacity of the $CD44^{high}$ ADK-17 BA.Atezo and ADK-17 BA.γ0.1 cell lines, as compared to the $CD44^{low}$ ones, *i.e.*, ADK-17 BA.CTRL and ADK-17 BA.γ100 (**Figure 31D**).

The sensitivity of ADK-17 BA clones to atezolizumab and IFN-γ was then tested *in vitro* to assess the potential presence of atypical cellular responses to these treatments, as previously observed in the parental cell line. Surprisingly, only the $CD44^{high}$ ADK-17 BA.Atezo and ADK-17 BA.γ0.1 cell lines exhibited a significant sensitivity to high doses of IFN-γ as compared to controls in 3D soft-agar assay (**Figure 31E**). In contrast, ADK-17 BA.CTRL and ADK-17 BA.γ100 cell lines showed

no response to IFN-γ treatment. None of ADK-17 BA clones responded to the treatment with atezolizumab (**Figure 31E**).

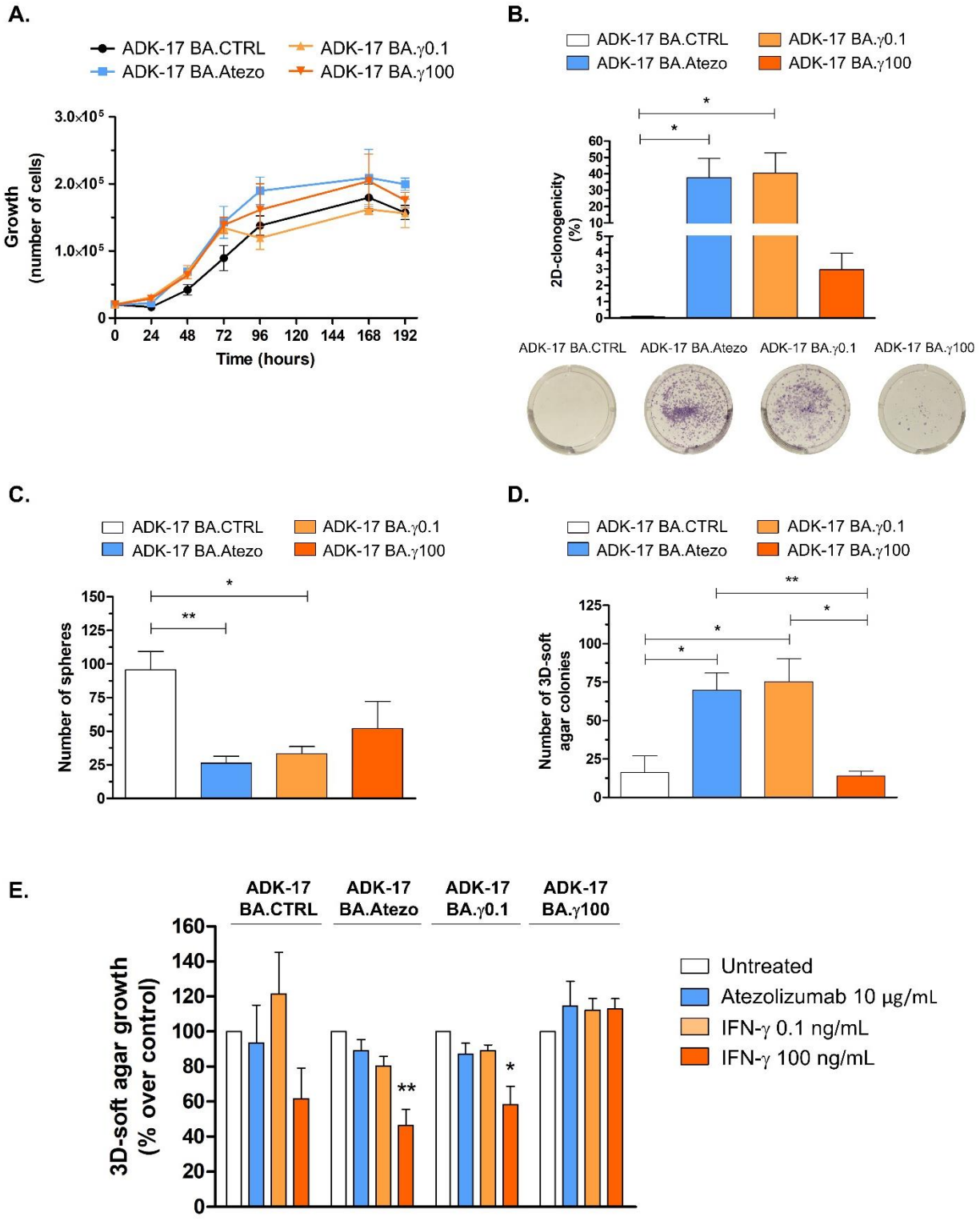

Figure 31. Comparison of *in vitro* cell growth capacity and sensitivity to treatments between ADK-17 BA clones. **(A)** Cell growth curves of ADK-17 BA clones (n=2). Bars represent mean and SEM. **(B)** 2D-clonal efficiency of ADK-17 BA clones (n=3). *, p<0.05 by Student's *t*-test. Each bar represents mean and SEM. **(C)** Sphere forming ability of

ADK-17 BA clones (ADK-17 BA.CTRL, ADK-17 BA.Atezo and ADK-17 BA.γ0.1: n=3; ADK-17 BA.γ100: n=2). *, p<0.05 and **, p<0.01 by Student's *t*-test. Each bar represents mean and SEM. **(D)** 3D soft-agar colony formation ability of ADK-17 BA clones (n=3). *, p<0.05 and **, p<0.01 by Student's *t*-test. Each bar represents mean with SEM. **(E)** Soft-agar colony formation ability of ADK-17 BA clones in the presence of atezolizumab (10 μg/ml) or low (0.1 ng/mL) or high (100 ng/mL) doses of IFN-γ (n=6, three experiments, each one with two technical replicates). *, p<0.05 and **, p<0.01 by One sample t test (group *vs* theoretical mean of 100). Each bar represents mean and SEM. SEM: standard error of the mean.

In summary, the evaluation of the proliferative capacity of ADK-17 BA clones *in vitro* revealed enhanced proliferation ability in the $CD44^{high}$ ADK-17 BA.Atezo and ADK-17 BA.γ0.1 cell lines as compared to the $CD44^{low}$ ones, *i.e.*, ADK-17 BA.CTRL and ADK-17 BA.γ100 cells, in both 2D clonogenic assay and 3D soft agar growth. In addition, $CD44^{high}$ ADK-17 BA clones also showed a re-sensitization to the antiproliferative effect of IFN-γ in 3D soft-agar assay, as compared to the $CD44^{low}$ cells, further supporting the previously described results regarding ADK-17 and ADK-18 cell line behavior.

4.2 BoLC.8M3, a preclinical *in vivo* model of resistance to ICI-based immunotherapy

The BoLC.8M3 cell line is a murine adenocarcinoma cell line obtained in the Laboratory of Biology and Immunology of Metastasis directed by Prof. Lollini from a lung tumor developed in a transgenic BALB/c mouse harboring the human $KRAS^{G12D}$ mutation and that was knock-out for both p53 alleles.

Considering the critical role of $KRAS^{G12D}$ mutations and p53 knockout in the context of ICI resistance (Y. Tang et al., 2024), our cell model, harboring these specific mutations, provides an exceptional platform for investigating the underlying mechanisms of ICI resistance.

4.2.1 BoLC.8M3 in vivo response to anti-PD-L1 treatment

Primarily, we tested the response of the tumors derived from the BoLC.8M3 cell line to the anti-PD-L1 monoclonal antibody atezolizumab in an immunocompetent, syngeneic BALB/c mouse model.

Treatment with atezolizumab not only failed to reduce tumor growth compared to the control, but also appeared to have a detrimental effect, partially accelerating tumor progression (**Figure 32A**). Conversely, the treatment did not exert any significant effect on lung metastatic load (median, untreated: 14±5 metastases; treated, 18±8 metastases) (**Figure 32B**).

Although tumor growth did not differ significantly between the treated and untreated groups across all time points, the results were close to statistical significance (p=0.07 by two-way ANOVA test). Further post-hoc statistical analysis revealed a significant difference in the means between the

two groups at the final time point ($p<0.01$ by Bonferroni's post-test), implying that the treatment's effect may take time to manifest (**Figure 32A,C,D**).

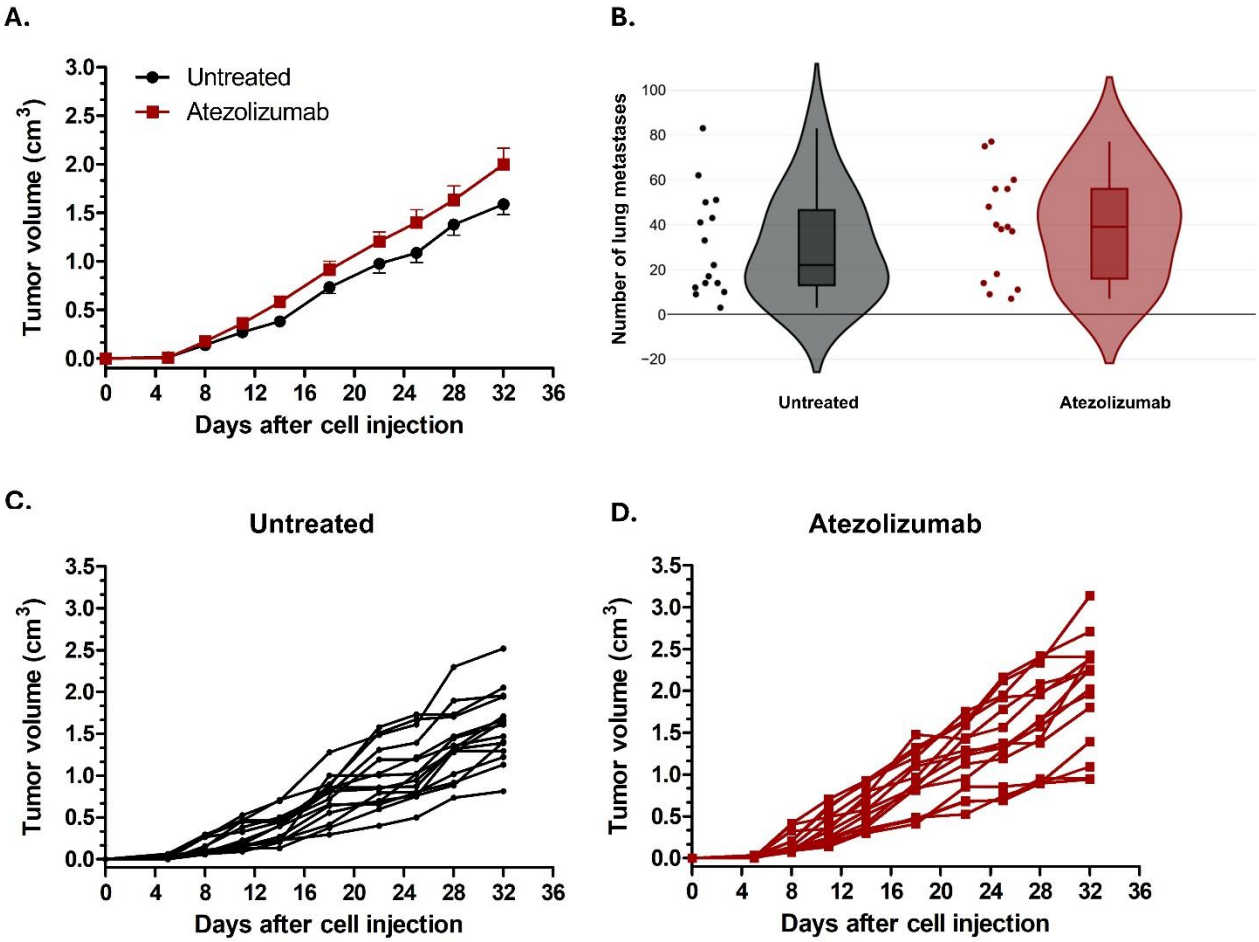

Figure 32. Response of BALB/c mice bearing BoLC.8M3 tumors to atezolizumab treatment. (A) Tumor growth of subcutaneously (s.c.) injected BoLC.8M3 cells in BALB/c mice treated with atezolizumab 10 mg/Kg, starting 1 day after cell injection, or in untreated mice (n=15 for each group). Two-way ANOVA was used to compare the groups (interaction, $p<0.01$; treatment, $p=0.07$). Day 32nd after cell injection: **, $p<0.01$ by Bonferroni's post-test (comparison between group means). Each point represents mean and SEM. **(B)** Violin plots overlaid with box plots showing the lung metastatic load in mice described in **(A)**, counted under a dissection microscope (n=15 for each group). Boxes indicate the interquartile range of the data; vertical lines represent the range of values, including the minimum and maximum data points; horizontal lines represent the medians. SEM: standard error of the mean.

To explore the potential role of immune cell populations in treatment resistance, we assessed the immune infiltrate in the TME of the untreated and treated groups. Notably, the analysis revealed a significant increase in the expression of the *Ncr1* gene, which encodes a specific marker for NK cell populations, in the tumors of the atezolizumab-receiving group compared to the untreated one ($p<0.05$ by Student's *t*-test), together with nearly significant increased expression of the *Pdcd1* gene, encoding the PD-1 immune checkpoint (**Figure 33A,B**).

Interestingly, Western blot analysis of protein expression in BoLC.8M3 tumors demonstrated a significant increase in β-catenin levels in mice treated with atezolizumab compared to untreated mice ($p<0.05$ by One Sample t test) (**Figure 33C**). Additionally, the tumors of mice receiving atezolizumab administration also exhibited significantly increased activation of AKT protein as compared to the tumors of untreated mice ($p<0.05$ by One Sample t test) (**Figure 33D**).

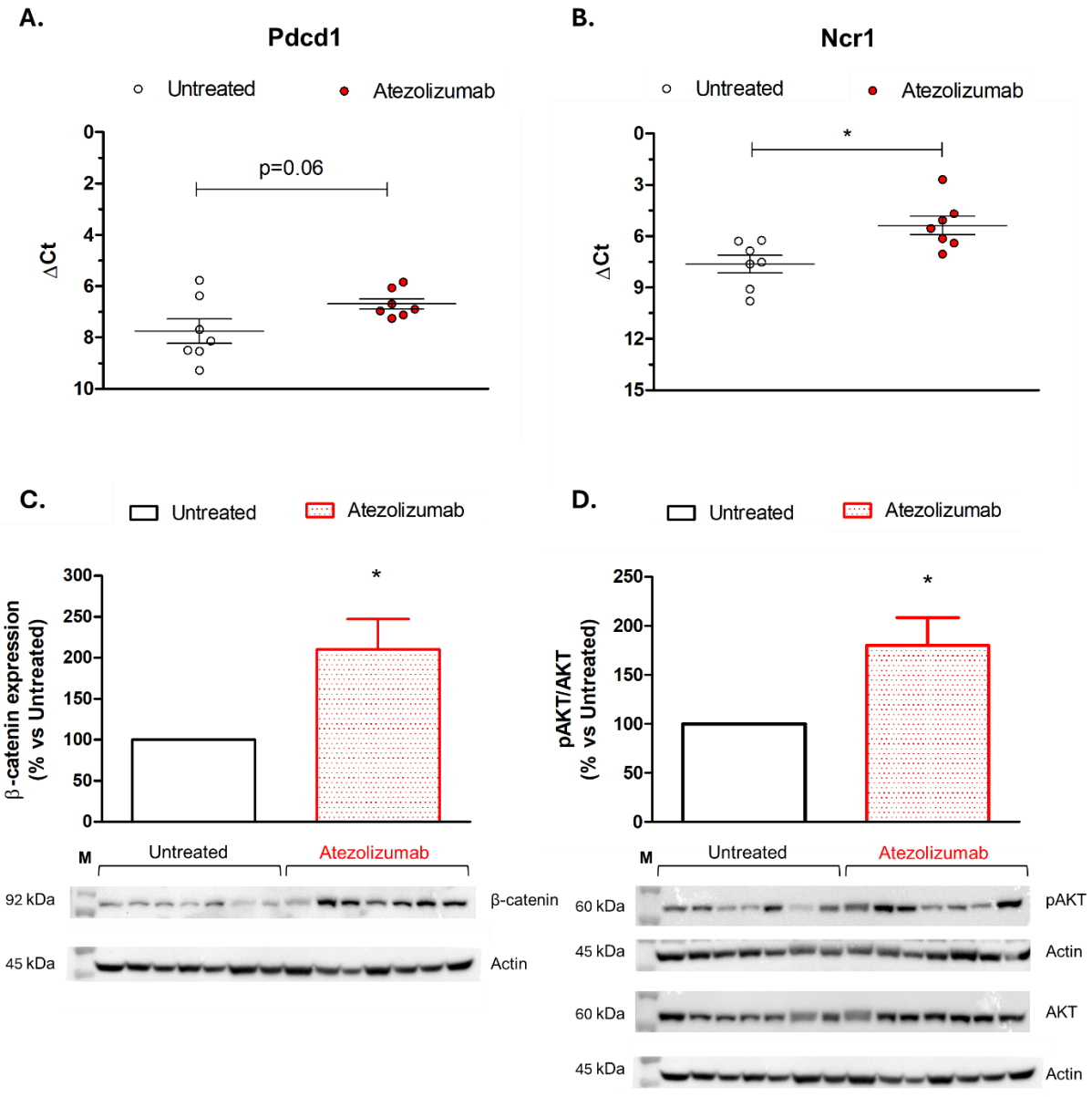

Figure 33. Evaluation of the tumor microenvironment (TME) and protein expression in BoLC.8M3 tumors from untreated mice and mice treated with atezolizumab. (A,B) Expression of the *Pdcd1* gene **(A)** or *Ncr1* gene **(B)** in representative BoLC.8M3 tumors from untreated mice or those treated with atezolizumab, measured by RT-PCR. Expression was normalized over *Tbp* (Total Binding Protein) gene expression ($\Delta Ct = Ct_{gene} - Ct_{Tbp}$). Horizontal lines represent mean and SEM. *, $p<0.05$ by Student's *t*-test (n=7 for each group). **(C)** Levels of β-catenin expression measured by Western blot analysis (for each group, n=2 at least). Actin was used as housekeeping protein for protein normalization. *, $p<0.05$ by One Sample t test (group *vs* theoretical mean of 100). Bar represents mean and SEM. **(D)** Activation levels

of AKT protein measured by Western blot analysis (for each group, n=2 at least). Actin was used as housekeeping protein for protein normalization. *, p<0.05 by One Sample t test (group *vs* theoretical mean of 100). Bar represents mean and SEM. M: marker. RT-PCR: Real-Time PCR; SEM: standard error of the mean.

Based on these findings, we conclude that the BoLC.8M3 cell model treated *in vivo* with atezolizumab effectively replicates the resistance to ICI therapy observed in clinical settings. Tumors that progressed during treatment exhibited increased NK cell infiltration, elevated β-catenin expression, and heightened activation of AKT signaling, suggesting that these immune populations and pathways may play a critical role in driving resistance to ICIs.

4.2.2 In vitro response of the BoLC.8M3 cell line to IFN-γ

Considering the previous findings from the ADK-17 and ADK-18 human models, we evaluated the response of the BoLC.8M3 cell line to IFN-γ treatment *in vitro.*

Under adherent culture conditions, murine IFN-γ significantly inhibited the growth of the BoLC.8M3 cell line, albeit modestly (**Figure 34A**) and efficiently induced the expression of PD-L1 (median fluorescence, untreated: 1 fluorescence unit; IFN-γ: 37 fluorescence units) and H-2 proteins of the mouse major histocompatibility complex (H-2, median fluorescence, untreated: 2 fluorescence units; IFN-γ: 170 fluorescence units) (**Figure 34B**). Notably, the cells also exhibited high expression of CD44 at the basal level (**Figure 34C**).

Unexpectedly, treatment of the BoLC.8M3 cell line with intermediate or high doses of IFN-γ in 3D culture conditions led to a pronounced and significant increase in the growth of soft-agar colonies compared to the control (**Figure 34D**).

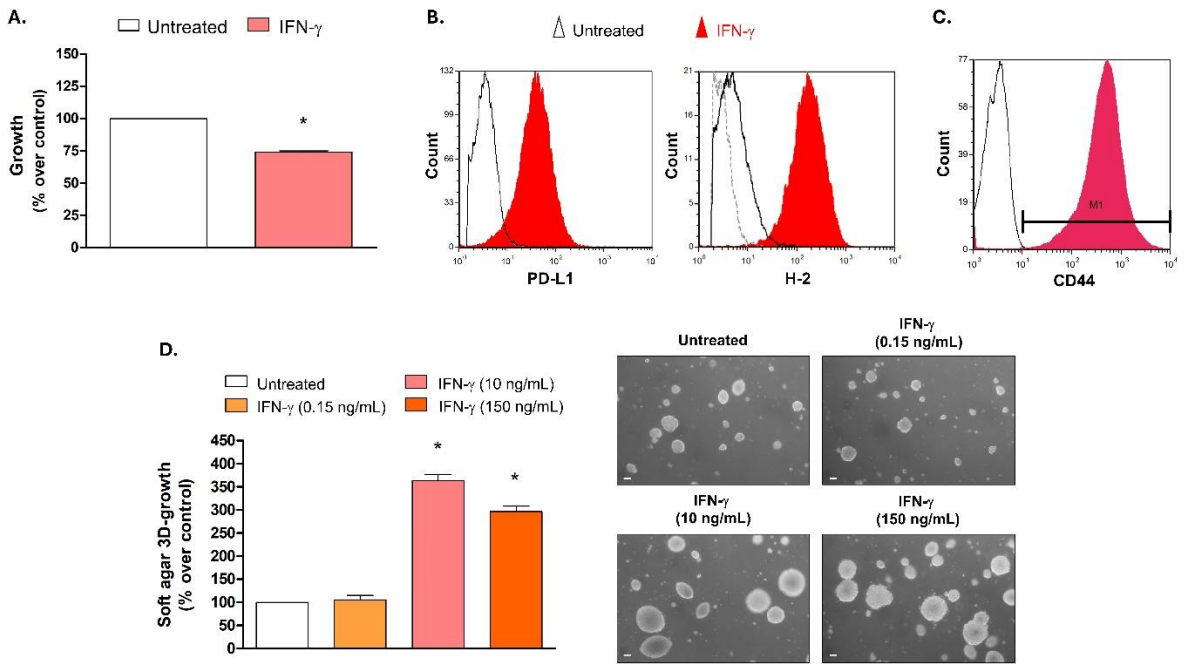

Figure 34. BoLC.8M3 characterization and response to different doses of IFN-γ *in vitro*. (A) Sensitivity of the BoLC.8M3 cell line to the antiproliferative effect of IFN-γ (10 ng/mL) in 2D culture conditions (n=2). *, p<0.05 by One Sample t test (each group *vs* theoretical mean of 100). Each bar represents mean and SEM. **(B)** Representative histograms depicting the expression levels of PD-L1 and H-2 in untreated BoLC.8M3 cells (empty histograms) compared to BoLC.8M3 cells treated with IFN-γ (10 ng/mL) (filled red histograms). Dashed line: baseline level of the fluorophore-labeled antibody. **(C)** Representative histogram depicting the expression of CD44, quantified by flow-cytometry. Empty histogram: unstained control. CD44 Mean Fluorescence Intensity (MFI): 602. M1: marker. **(D)** BoLC.8M3 soft-agar colony formation in the presence of different doses of IFN-γ (n=2). *, p<0.05 by One sample t test (each group *vs* theoretical mean of 100). Each bar represents mean and SEM. Right: representative pictures of BoLC.8M3 soft-agar colonies grown without any treatment or in the presence of IFN-γ, observed through an inverted microscope in dark-field. White line corresponds to 100 µm. SEM: standard error of the mean.

To sum up, the behavior and phenotype of the BoLC.8M3 did not completely reflect the features observed in the ADK-17 cell model in 2D culture conditions, as BoLC.8M3 cells exhibited high basal expression of CD44 and efficient induction of PD-L1 by IFN-γ. Nevertheless, the cell line also showed an atypical *in vitro* response to IFN-γ in 3D culture conditions, which partially resembled the one observed in the ADK-17 cell line model (**Figure 26A**).

Discussion

1. DEVELOPMENT OF PATIENT-DERIVED NSCLC PRECLINICAL MODELS

The investigation of drug resistance mechanisms in non-small cell lung cancer (NSCLC) is crucial for developing effective novel therapeutic strategies, particularly in light of the significant limitations of current treatment options (Rivera-Concepcion et al., 2022; Meyer et al., 2024). Despite the numerous established cell lines provide a foundation for preclinical research, these models often fail to accurately reflect the complexity of tumor heterogeneity and biological mechanisms orchestrating drug resistance in patients (Gazdar, Gao, et al., 2010; Hynds et al., 2021). For this reason, there is a pressing need to develop novel patient-derived preclinical models able to bridge the gap between preclinical research and clinical reality.

The panel of patient-derived NSCLC preclinical models established in our laboratory was derived from a cohort of patients which was extremely heterogeneous in terms of mutational profiles and therapeutic histories.

Overall, we successfully established 12 patient-derived cell lines from 24 tumor samples collected from 23 patients with advanced NSCLC, resulting in an establishment success rate of 50%. Furthermore, from 15 engrafted tumor samples, we generated a total of 11 patient-derived xenografts (PDXs), achieving an impressive overall engraftment rate of 73%. These outcomes not only surpass the success rates reported by other research groups but also highlight our proficiency in generating stabilized patient-derived preclinical models (Zheng et al., 2011; Chen et al., 2019; S.-Y. Kim et al., 2019). In most published studies, the number of preclinical models, including PDX and primary cell lines, derived from patients with advanced stage IV NSCLC is significantly lower compared to those from early-stage tumors (Zheng et al., 2011; Chen et al., 2019; Mirhadi et al., 2022). Of note, the number of models sourced from patients who have previously undergone therapy or progressed to treatments is also notably limited (Zheng et al., 2011; Chen et al., 2019; S.-Y. Kim et al., 2019). Conversely, all of our models were derived from advanced stages of NSCLC tumors, most of which had undergone one or more cycles of therapy, leading to resistance and thereby enhancing the significance of our research. Establishing preclinical models of NSCLC from patients with advanced-stage disease is indeed challenging, not only due to complications related to sample collection stemming from disease progression and the deterioration of patients' clinical profiles, but also because of the effects that prior treatments can have on tumor biology and on their capacity for *in vitro* and *in vivo* engraftment (X. Chen et al., 2021; Fuchs et al., 2024; Sunil & O'Donnell, 2024).

Regarding the higher establishment success rate observed in our PDX models compared to our primary cell lines, this may be attributed to the preservation of tumor microenvironment components that support tumor growth, including stromal elements, as well as a more effective maintenance of tumor heterogeneity compared to primary cell cultures, as documented in the literature (Jiang et al., 2018; Mirhadi et al., 2022; Sunil & O'Donnell, 2024).

Overall, the diversity of the cohort of patients from which these models were derived allowed us to obtain a useful platform for comprehensively investigations of the various mechanisms of resistance to both tyrosine kinase inhibitors (TKIs) and immunotherapy, as well as for exploring novel therapeutic options for NSCLC patients.

2. THE IMPACT OF TUMOR HETEROGENEITY IN RESISTANCE TO TKI-BASED THERAPIES

Tumor heterogeneity represents a critical survival and adaptive mechanism for cancer, manifesting in the existence of distinct tumor subpopulations that vary in genetic, epigenetic, and phenotypic traits (El-Sayes et al., 2021). This diversity not only enables tumors to endure therapeutic pressures but also promotes their evolution in response to environmental challenges. As a result, tumor cells can rapidly adapt to external stimuli, leading to a selection process that favors the survival and proliferation of populations best suited to their microenvironment. This dynamic nature of tumors presents significant challenges for cancer therapy, as it facilitates the persistence of resistant cell populations and undermines therapeutic efficacy (Zhu et al., 2021).

This selection process was clearly exemplified in the ADK-VR2 and LIBM-ADK-11 cancer models, in which tumor heterogeneity played a critical role in driving resistance and adaptation.

2.1 ADK-VR2, a preclinical model of NSCLC carrying a *SDC4-ROS1* translocation

The ADK-VR2 clinical case refers to a treatment-naïve patient affected with advanced NSCLC harboring *SDC4-ROS1* fusion, who exhibited primary resistance to the ROS1-directed TKI crizotinib following the failure of chemotherapy. The corresponding patient-derived cell line was established from the patient's pleural effusion prior to the initiation of targeted therapy. Notably, ADK-VR2 represents the first ever-established cell model carrying a *SDC4-ROS1* fusion directly derived from a patient naïve for any ROS1-directed TKI, highlighting its critical importance as a unique resource for the study of the biology of *ROS1*-driven NSCLC in a context that reflects the disease prior to any targeted therapeutic intervention (Ruzzi, Angelicola et al., 2022).

This cell model partially reflected the clinical response of the primary tumor, demonstrating reduced *in vitro* sensitivity to pemetrexed as compared to HCC-78 cell line, an established cell model

of NSCLC expressing a *ROS1* fusion gene (*SCL34A2-ROS1*), which has been reported to be sensitive to the drug, as most *ROS1*-mutated NSCLC cell lines (Davies et al., 2013). However, it quickly became evident that the cell line exhibited a divergent response to crizotinib compared to the primary tumor. The ADK-VR2 cell line indeed showed a certain sensitivity to crizotinib *in vitro*, which was comparable or even higher as compared to HCC-78, which is known for its sensitivity to the multi-target TKI (Davies et al., 2012; Yasuda, de Figueiredo-Pontes, et al., 2012). Furthermore, a pronounced sensitivity of the ADK-VR2 cell model to crizotinib was also confirmed *in vivo*. Nevertheless, it is important to note that the sensitivity observed has consistently been partial rather than complete.

In light of these discrepancies between the behavior of the cell line and the original tumor's response to therapy, we isolated a crizotinib-resistant clone from the cell line, designated ADK-VR2 AG143. The obtainment of this clone aimed to characterize the features of crizotinib resistance inherent to the original tumor, with a particular focus on identifying resistant subpopulations within the ADK-VR2 cell line. Comparative sensitivity tests to early- and next-generation ROS1-directed TKIs were conducted between the parental cell line and its crizotinib-resistant clone. Investigations conducted under three-dimensional (3D) anchorage-dependent culture conditions evidenced a strong sensitivity of both the cell lines to next-generation ROS1-TKIs (DS-6051b, entrectinib and loraltinib). Only in sphere forming assay, the AG143 showed a marked resistance to DS-6051b and entrectinib compared to the parental cell line. Obviously, the AG143 clone showed no sensitivity to crizotinib in all the analyzed conditions, unlike the parental cell line. Interestingly, there was an evident discrepancy in cell sensitivity results among 2D and 3D assays, as in adherent conditions both ADK-VR2 and AG143 clone showed high resistance to all the next-generation TKIs. The differences in tumor sensitivity to TKIs in 2D versus 3D cell cultures are well documented. Generally, TKIs show enhanced sensitivity in 2D cultures due to simplified cellular interactions, which, however, do not fully replicate the complexities of tumor architecture and resistance circuits present *in vivo* (Rodríguez-Hernández et al., 2020; Heid et al., 2022). However, in the case of ROS1-directed TKIs, the situation appears to be reversed, as reported by recent literature which describes increased efficacy of these inhibitors under 3D culture conditions (Terrones et al., 2024). This phenomenon could be associated with the specific mechanisms of resistance of ROS1-mutated tumors. Gong and colleagues indeed demonstrated that the re-sensitization of crizotinib-resistant HCC-78 cells to the drug under 3D conditions is mediated by the suppression of EGFR activation, which is a common compensatory pathway activated in case of resistance to ROS1 inhibitors, and, consequently, to the restoration of tumor cells' dependence on the *ROS1* oncogene (Gong et al., 2018). Translating these findings to our cell models, we observed that the response of our cell lines to crizotinib remained consistent across

both 2D and 3D culture conditions, possibly indicating that EGFR compensatory pathway activation is unlikely to play a role in the resistance mechanisms of ADK-VR2 and its cell subpopulations to crizotinib. Moreover, the possibility of resistance due to secondary mutations in the target gene can be ruled out, as next-generation sequencing (NGS) analysis of the AG143 clone confirmed the absence of any additional known pathogenic mutations beyond the *ROS1* fusion.

In contrast, considering lorlatinib as representative of next-generation ROS1-directed TKIs, we observed a re-sensitization of both the cell models to the TKI under 3D culture conditions. Nevertheless, the drug seemed to induce different molecular responses in the cell lines. In the ADK-VR2 cell line, lorlatinib treatment seemed to stimulate EGFR activation and EGFR downstream signaling mediators such as MAPK and AKT. Conversely, in the ADK-VR2 AG143 clone this kind of stimulation was not detected. Rather, lorlatinib strongly activated STAT3 in the AG143 clone.

These observations support the hypothesis that ADK-VR2 cell model may be prone to developing resistance to next-generation ROS1-TKIs through the activation of collateral pathways, such as the EGFR one (Katayama et al., 2023). For what concerns the AG143 clone, the strong activation of STAT3 observed in the AG143 clone could suggest that this pathway is being co-opted as a compensatory survival mechanism in response to lorlatinib, allowing the crizotinib-resistant cells to bypass the effects of ROS1 inhibition. Aberrant STAT3 activation has indeed been reported as an established mechanism of adaptive resistance to lorlatinib in *ALK*-rearranged lung cancer (Yanagimura et al., 2022).

These observations suggest that the two cell lines employ different strategies to resist the effects of next-generation ROS1-TKIs. Further molecular investigations are needed to elucidate the differential resistance mechanisms between ADK-VR2 and its crizotinib-resistant clone.

Surprisingly, the AG143 clone exhibited reduced sphere forming capacity and *in vivo* growth as compared to ADK-VR2. These findings may appear counterintuitive, given the common assumption that treatment-resistant cell lines are inherently more stem-like and aggressive in nature (Del Re et al., 2018). The explanations for the unexpected behavior observed in AG143 may be as follows. Firstly, ADK-VR2 AG143 may be undergoing what is referred to as “oncogene shock”, a phenomenon characterized by a transient imbalance in pro-survival and pro-apoptotic signals, along with alterations in cellular metabolism that occur in cancer cells that are highly dependent on oncogenes when the oncogenic signal is disrupted−such as through TKI-mediated inhibition (Sharma & Settleman, 2010; Pagliarini et al., 2015). Secondly, it can be supposed that AG143 clone may exhibit impairment of specific noncoding RNAs (ncRNAs), which have been reported to be implicated in the maintenance of stemness features in EML-ALK^{+} NSCLC cell lines and whose transcription has demonstrated to be inhibited by crizotinib treatment (Yang et al., 2018).

Looking ahead, single-cell RNA sequencing may enable us to better identify and characterize the distinct subpopulations within the ADK-VR2 cell model. Furthermore, whole exome sequencing of the AG143 clone, in comparison to the parental cell line, could offer new insights into the mechanisms underlying crizotinib resistance and the role of tumor heterogeneity in this context.

2.2 LIBM-ADK-11, a cell line derived from an osimertinib-resistant NSCLC patient carrying an uncommon *EGFR* mutation

The LIBM-ADK-11 cell model was established in our laboratory from the pleural effusion of a patient affected with advanced NSCLC, carrying an uncommon *EGFR* mutation in exon 19 (p.Leu747_Pro753delinsSer), who experienced disease progression after first-line treatment with osimertinib. Notably, the aforementioned mutation has been associated with reduced sensitivity to osimertinib and shorter progression-free survival (PFS) compared to patients carrying more prevalent *EGFR* variants (Grant et al., 2023).

As we delved into our investigations with the cell line, we noticed intriguing shifts in both functional and phenotypic cell characteristics that unfolded over the course of progressive cell culture, which raised questions about the underlying biological significance of these changes. The phenotypical characterization of the cell line indeed highlighted the presence of a distinct cell subpopulation highly expressing the CD44 marker in low-passage cells (LP-LIBM-ADK-11). CD44 is a cell surface glycoprotein that plays a crucial role in cell-cell interactions, cell adhesion, and migration (Senbanjo & Chellaiah, 2017). Additionally, this protein is involved in various biological processes, including immune response, wound healing, and tissue remodeling (Jordan et al., 2015). In the context of cancer, CD44 has often been associated with tumor progression and metastasis, acting as a marker for cancer stem cells (CSCs) (Orian-Rousseau, 2015). In NSCLC, elevated levels of CD44 have been indeed associated with stemness properties, epithelial-to-mesenchymal transition (EMT), tumor initiation, therapy resistance and recurrence (Luo et al., 2014). Interestingly, we observed that the expression of this marker was progressively lost over sequential *in vitro* passages, resulting in high-passage cells (HP-LIBM-ADK-11) which ultimately displayed a complete loss of the cell subpopulation highly expressing CD44. In parallel, it was evident that a cell subpopulation showing low expression of HER3 was also lost over *in vitro* passages.

These phenotypic shifts were accompanied by functional differences between low- and high-passage cells, particularly regarding their sensitivity to EGFR inhibitors. Indeed, while LP-LIBM-ADK-11 cells displayed consistent resistance to second- and third-generation EGFR TKIs, including afatinib, erlotinib, and osimertinib−mirroring the clinical response of the original tumor−HP-LIBM-ADK-11 cells demonstrated a re-sensitization to these agents. The sorting of the LP-LIBM-ADK-11 cell line for CD44 expression allowed us to isolate two distinct subpopulations from the primary

heterogenous cell line, *i.e.*, $CD44^{high}$ (P2) and $CD44^{low}$ (P4) cell lines, and to test their sensitivity to osimertinib *in vitro*. Our results identified the source of osimertinib resistance in the $CD44^{high}$-P2 cell line within the LP-LIBM-ADK-11 model. Indeed, P2 cells showed no sensitivity to osimertinib treatment *in vitro* compared to $CD44^{low}$-P4 cell line, which, on the contrary, showed a marked sensitivity to the EGFR-TKI. Additionally, we also demonstrated that the increase of CD44 expression in LP-LIBM-ADK-11 cells could be directly induced by osimertinib treatment, confirming that *EGFR*-mutated tumor cells modulate CD44 expression in response to exposure to EGFR-TKIs, likely as a mechanism of adaptive resistance. Importantly, while CD44 expression has been reported in various TME components involved in tumor resistance and stemness, including cancer-associated fibroblasts (CAFs), we confirmed that the CD44-expressing cells were indeed tumor cells rather than fibroblasts, as evidenced by the presence of the EGFR p.L747_P753>S mutation within the CD44-positive population (Kinugasa et al., 2014).

At this point, it became evident that CD44 played a crucial role in mediating resistance to osimertinib in our model. In the context of *EGFR*-mutated NSCLC previous studies have also suggested an association between tumor expression of CD44 and resistance to EGFR-directed TKIs. For instance, Suda and colleagues demonstrated a direct regulation of EMT and mesenchymal phenotype by CD44 in *EGFR*-mutated NSCLC cells that had been chronically treated with EGFR-TKIs and developed resistance to these agents. Notably, EMT-like changes have been recognized as a well-established mechanism of acquired resistance to EGFR-TKIs in *EGFR*-mutated tumor cells (Suda et al., 2012; La Monica et al., 2013). The association between CD44 expression and the acquisition of the EMT phenotype was also confirmed in tumor specimens from patients with EGFR-TKI refractory tumors (Suda et al., 2018). However, in this study, the authors were unable to reverse the resistance of these cell lines to osimertinib through CD44 knock-down, though they did manage to prevent their mesenchymal phenotype shift. Another research group also reported a correlation between osimertinib resistance development and CD44 expression, by demonstrating the role of miR-204 in overcoming osimertinib resistance by reducing cancer stemness and EMT through the inhibition of CD44 signaling pathway (Wu et al., 2024). Notably, in this case the authors also obtained a restored sensitivity to osimertinib in resistant lung cancer cells by inhibiting CD44 (Wu et al., 2024).

Interestingly, the comparative transcriptomic analysis of LIBM-ADK-11 P2 and P4 cell lines evidenced increased expression of several genes involved in EMT and tumor plasticity in the P2 cell line as compared to the P4 one, in accordance with the previously described published data. Genes such as *SNAI1, SNAI2, SOX9* and *TWIST1*, which were overexpressed in P2 cells, are indeed well-established regulators of the EMT process (Carrasco-Garcia et al., 2022; den Hollander et al., 2024). *FGFR1* gene also resulted to be up-regulated in the P2 cell line and, interestingly, amplification or

hyperactivation of this gene has been reported as an EGFR-independent mechanism of resistance to osimertinib in NSCLC (Minari et al., 2016; Lu et al., 2020). Of particular interest is the *SMAD3* gene, which was also found to be upregulated in the P2 cell line. This gene is indeed a downstream central mediator of the TGF-β signaling pathway, which plays a crucial role in EMT, migration and tumor progression (Liu et al., 2021). Of note, CD44 has been reported to directly interact with TGF-β receptors, including TGF-βRI, enhancing TGF-β signaling pathways and leading to phosphorylation of SMAD2/SMAD3 complexes. This interaction further supports the relevance of CD44 in molecular mechanisms of resistance to osimertinib through the stimulation of a mesenchymal phenotype in *EGFR*-mutated tumor cells. Interestingly, up-regulation of genes associated with increased hyaluronan biosynthetic process and Wnt signaling activation was also observed in the P2 cell line compared to the P4 one. Hyaluronic acid is the primary ligand for CD44, triggering the activation of its downstream signaling pathway (Ponta et al., 2003). Additionally, CD44 has been demonstrated to acts as a positive feedback regulator of the Wnt/β-catenin signaling pathway by activating the lipoprotein receptor-related protein 6 (LRP6) (Schmitt et al., 2015).

Despite all the functional and transcriptomic evidence supporting a central role of CD44 in the underlying mechanisms of resistance to EGFR-directed TKIs in our cell line model, the precise molecular mechanism through which CD44 influences this resistance remains unknown. We confirmed that these mechanisms do not affect the inhibition of EGFR in presence of osimertinib in the P2 cell line, as demonstrated by Western blot analyses. These observations suggest that osimertinib resistance in LP-LIBM-ADK-11 cell line may be driven by EGFR-independent mechanisms, potentially involving alternative signaling pathways such as *MET* amplification or activation of the PI3K-AKT or MAPK pathways, as reported in literature (La Monica et al., 2019; Leonetti et al., 2019; Volta et al., 2023). In this context, it is important to mention that CD44 not only acts as a receptor for hyaluronic acid and other ligands, but it also functions as a critical co-receptor for many RTKs, amplifying their signaling capacity in cancer cells (Orian-Rousseau, 2015). Of note, CD44 has been reported to also act as a co-receptor for HER3, whose expression was also found to be dynamic between low- and high-passage LIBM-ADK-11 (Ponta et al., 2003). Despite HER3 increased expression has been associated with osimertinib resistance (Bronte et al., 2023; Q. Chen et al., 2023), in our studies it appeared to be linked with cell re-sensitization to EGFR inhibition, as demonstrated by phenotypic characterization of the LIBM-ADK-11 cell model and transcriptomic analyses on P2 and P4 cell populations. Increased expression of HER3 in osimertinib-sensitive subpopulations in LIBM-ADK-11 may be a mechanism of adaptation of the cells in response to drug-induced stress (Vicencio et al., 2022). Nevertheless, there is limited data available to elucidate the role of this RTK in our cell model, aside from the certainty that its bypass activation or overexpression

is not the mechanism by which LP-LIBM-ADK-11 cells resist the effects of osimertinib. Considering the function of CD44 as a coreceptor, we can hypothesize that EGFR-independent mechanisms of resistance to EGFR-TKIs in our cell line model and, more broadly, in *EGFR*-mutated NSCLC may involve the activation of collateral signaling pathways, facilitated by CD44 action. Alternatively, CD44 expression in osimertinib-resistant cells might be circumstantial, reflecting unknown mechanisms that also lead to its increased expression. In either case, the relevance of CD44 may lie in its potential as a predictive biomarker of EMT or other plastic features associated with the acquisition of resistance to EGFR-TKIs. Further investigations will be crucial to fully elucidate these mechanisms and to clarify the role of CD44 in resistance dynamics.

3. EXPLORING NOVEL THERAPEUTIC STRATEGIES FOR DRUG-ORPHAN NSCLC MUTATIONS

The highly heterogeneous genomic landscape of NSCLC has spurred the development of targeted therapies, revolutionizing the treatment of this disease. However, a subset of oncogenic driver mutations, referred to as “drug-orphan” mutations, continues to lack effective targeted therapies due to the distinct molecular properties these alterations confer on the corresponding proteins. Tumors with these alterations are indeed still treated as non-oncogene-addicted malignancies, relying instead on immunotherapy and chemotherapy, which often demonstrate suboptimal efficacy (Gibson et al., 2023). Therefore, identifying novel therapeutic strategies for managing these mutations remains a pressing unmet clinical need (Abuali et al., 2022).

A prominent example of drug-orphan mutations in NSCLC is represented by *BRAF* class II and *BRAF* class III mutations. Unlike *BRAF* class I mutations, which can be targeted by BRAF inhibitors, class II and class III mutations are characterized by a reduced kinase activity and may activate downstream signaling pathways through various mechanisms, including RAS activation (Y. Chen et al., 2023). This complex mechanism of action makes it difficult to develop inhibitors that effectively target these mutated forms of the BRAF protein and, as a result, therapeutic strategies for these classes of tumors remain severely limited.

3.1 ADK-14 and PDX-ADK-36: two NSCLC cell lines carrying *BRAF* class III mutations

The ADK-14 and PDX-ADK-36 cell models–a patient-derived cell line and a PDX-derived cell culture (PDXC), respectively–were both originally derived from patients with advanced NSCLC harboring two distinct *BRAF* class III mutations at progression after immunotherapy alone or in combination with chemotherapy. The rationale for the experiments conducted on these cell models was grounded in clinical retrospective observation highlighting the significant efficacy of the EGFR-

TKI erlotinib in two patients with *EGFR* wild-type and *BRAF* class III-mutated NSCLC under the care of the Medical Oncology Unit of the S. Orsola-Malpighi Hospital. One of these cases was represented by the ADK-36 clinical case, which was sampled before the administration of the EGFR-TKI.

In vitro sensitivity tests confirmed the efficacy of second- and third-generation EGFR-TKIs, including erlotinib, afatinib dacomitinib and osimertinib, in inhibiting the growth of these *BRAF* class III-mutated cell models. Of note, these results were further validated using a publicly available dataset (Cancer Cell Line Encyclopedia, Broad 2019). Interestingly, *BRAF* class II-mutated cell lines carrying the $BRAF^{G469A}$ mutation, initially used as controls, exhibited a sensitivity to these EGFR-TKIs comparable to that observed in the ADK-14 and PDX-ADK-36 models. In contrast, the growth of the *BRAF* class I-mutated cell line HCC-364 and the *KRAS*-mutated cell line ADK-17 resulted to be unaffected by EGFR inhibition, as expected (Massarelli et al., 2007; L. Zhang et al., 2022).

In order to unravel the mechanisms behind the observed patterns of cell responses to EGFR-directed TKIs, variations in the state of EGFR activation after erlotinib treatment were evaluated in the investigated cell lines. In parallel, the basal activation of EGFR was also assessed. Interestingly, enhanced basal activation of EGFR was detected only in ADK-14 and PDX-ADK-36 cell lines, as well as in *EGFR*-mutated positive controls, but not in the other cell models. These observations confirmed the hypothesis that *BRAF* class III-mutated cell lines may rely on this receptor and its signaling for their growth and survival, thereby explaining the inhibitory effects observed in these cell models in presence of EGFR-TKIs. In support of this, we observed that the activation of EGFR was also significantly inhibited in ADK-14 and PDX-ADK-36 after erlotinib treatment. In contrast, the *BRAF* class II-mutated cell line did not exhibit basal EGFR activation, nor did it show inhibition of EGFR signaling following erlotinib treatment. This observation aligns with findings from a recent study in which the authors demonstrated that *BRAF* class II-mutated NSCLC may respond to next-generation EGFR-TKIs due to off-target direct binding of the drugs to the mutated BRAF protein (Huo et al., 2022). Considering the intermediate kinase activity that characterizes *BRAF* class II mutations, it is reasonable that a direct inhibition of the protein may result in an interruption of pro-growth and survival tumor signaling (Sahin & Klostergaard, 2021). Conversely, this mechanism does not seem plausible for *BRAF* class III mutations, in which the kinase activity of the protein is heavily impaired or absent (Sahin & Klostergaard, 2021). Rather, we hypothesize that in *BRAF* class III-mutated NSCLC the mutant form of BRAF might amplify a RAS signal, which is already stimulated upstream by the hyperactivated EGFR. We propose that while wild-type EGFR hyperactivation contributes to tumor growth, it may not be sufficient on its own to drive proliferation without the presence of the concurrent *BRAF* mutation. In accordance with our data and hypotheses, evidence of

increased sensitivity of *BRAF* class III-mutated tumors to EGFR inhibition has been reported in the literature, together with increased activation of RAS mediators in a variety of tumors harboring *BRAF* class III mutations (Özgü et al., 2024). Additionally, EGFR inhibitors, including erlotinib and cetuximab, were also effective in NSCLC and colorectal cancer (CRC) harboring *BRAF* class III mutations (Yao et al., 2017). Notably, anti-EGFR antibodies have demonstrated high activity in *BRAF* class III-mutated CRC, but not in *BRAF* class II-mutated colon tumors (Yaeger et al., 2019). These results are in accordance with the different hypothesized mechanisms of sensitivity to EGFR inhibition between *BRAF* class II and class III mutations, as described previously. In this context, we hypothesize that BRAF proteins carrying class III mutations may amplify not only EGFR signaling, but also the pathways of other RTKs. Increased activation of MET and HER2 receptors has indeed been reported in tumors carrying *BRAF* class III mutations (Bracht et al., 2019; Yan et al., 2022; Puri et al., 2023). Based on our findings and literature evidence, in tumors lacking specific therapeutic targets, it may be beneficial to evaluate the activation levels of various RTKs to identify potential new therapeutic targets. This approach could enhance treatment strategies by uncovering alternative pathways that drive tumor growth and resistance, ultimately leading to more effective and personalized therapeutic options for patients.

Interestingly, the *in vitro* activity of erlotinib on ADK-14 and PDX-ADK-36 was significantly enhanced in presence of trametinib, compared to each treatment administered individually. Despite low BRAF kinase activity, tumors carrying *BRAF* class III mutations manage to still activate the MAPK pathway through RAS-dependent mechanisms or by transactivating CRAF through dimerization, suggesting that these tumors rely on MAPK signaling for their progression and survival (Dankner et al. 2018). Based on these data we suppose that the combination therapy of EGFR-TKIs and MEK inhibitors may offer significant benefits to NSCLC patients harboring *BRAF* class III mutations, potentially enhancing treatment efficacy and improving clinical outcomes for this class of tumors. Obviously, it would be essential to develop strategies to mitigate the inherent toxicity associated with trametinib, as this toxicity may be exacerbated by its combination with erlotinib or other EGFR-TKIs (Hoffner & Benchich, 2018; Chalmers et al., 2019).

4. INVESTIGATING THE MECHANISMS UNDERLYING RESISTANCE TO ICIs IN NSCLC THROUGH PRECLINICAL MODELS OF IMMUNOTHERAPY RESISTANCE

While immunotherapy has significantly advanced the treatment of NSCLC, a notable group of patients still faces paradoxical and adverse reactions to these therapies (Okwundu et al., 2021).

Indeed, it is estimated that only a subset of NSCLC patients (10-20%) derives durable clinical benefit after immune checkpoint inhibitors (ICIs)-based treatment (Yuan et al., 2019).

Among the reactions that hinder the efficacy of immunotherapy, hyperprogressive disease (HPD), consisting in a paradoxical acceleration of tumor growth under the treatment, represents one of the most detrimental responses to therapy (Camelliti et al., 2020).

The absence of reliable predictive biomarkers complicates the timely identification of individuals that will experience harmful responses to ICIs, posing a considerable challenge in clinical settings (Bai et al., 2020). This limitation in early detection restricts clinicians' ability to customize treatment strategies, which may result in patients receiving therapies that are either ineffective or even harmful. Furthermore, the mechanisms that contribute to these paradoxical responses or to treatment resistance are largely uncharted and not well understood, resulting in unresponsive patients facing an inevitable therapeutic dead end. In this respect, understanding these mechanisms represents a crucial clinical need for improving patient selection and enhancing the effectiveness of immunotherapy in NSCLC.

4.1 ADK-17 and ADK-18, two cell lines derived from samples of an immunotherapy-resistant patient at baseline and after hyperprogression development

ADK-17 and ADK-18 cell models were established in our laboratory from tumor specimens obtained in two distinct clinical timepoints from a single patient who progressed after immunotherapy. While the ADK-17 cell line was established from the pleural effusion of the patient prior to the initiation of any treatment, ADK-18 was derived from a metastatic biopsy collected when clinical evidence of HPD was observed.

The establishment of both ADK-17 and ADK-18 cell models from a single patient is a fortunate and unique opportunity, particularly given the challenges associated with obtaining patient-derived models exhibiting hyperprogression, which is a phenomenon that generally occurs at a low frequency (Angelicola et al., 2021). This pair of models not only allows for direct comparative studies of tumor behavior pre- and post-immunotherapy, facilitating a deeper understanding of the molecular changes associated with treatment response and resistance to ICIs, but also minimizes intertumoral variability, thereby enhancing the reliability of the findings.

The first observations that emerged from our investigations were the striking phenotypical and functional differences between the two cell models. The ADK-18 cell culture indeed exhibited increased stem-like and plastic features as compared to the ADK-17 one, demonstrated by its culture morphology, its transcriptomic profile and its ability to generate organoids. Additionally, the ADK-18 model also demonstrated increased aggressive traits as compared to ADK-17, as evidenced by its

increased *in vitro* growth in both adherent and three-dimensional culture conditions and increased *in vivo* growth rate of its corresponding PDX compared to the ADK-17 model.

The assessment of the transcriptomic profile of the cell lines also yielded valuable useful insights. Transcriptomic analysis identified over three thousand differentially expressed genes between the two cell lines, indicating a significant shift in the transcriptome that may have contributed to the patient's clinical outcome. Specifically, the ADK-18 cell model exhibited increased representation of genes involved in the differentiation of various tissue and cell types (*e.g.*, neural, epithelial, bone, muscle and connective tissues), compared to ADK-17, together with increased expression of genes involved in EMT and in the IL6/JAK/STAT3 pathway, possibly indicating a highly plastic phenotype of the cell line (Johnson et al., 2018).

An aspect that captured our attention was the markedly increased expression of the CD44 marker in the ADK-18 cell model compared to the ADK-17. This was particularly noteworthy since elevated expression of this protein had also been previously observed on two additional patient-derived cell lines (ADK-19 and ADK-25), both established from tumor samples of two distinct patients at progression after ICI-therapy, who also developed hyperprogression. Accordingly, in their enlightening work, Li and colleagues also reported increased expression of CD44 in the ICI-treated tumors of their syngeneic murine model of HPD (Li et al. 2023). As previously mentioned, CD44 is a well-established marker of stemness in several malignancies, including NSCLC (Thapa & Wilson, 2016). Considering that, in addition to the standard isoform of the protein (standard CD44, CD44s), multiple CD44 isoforms have also been identified in both normal and malignant cells (Ponta et al., 2003), we specifically investigated the transcriptional profile of both the cell lines for CD44 variants. Interestingly, the analysis evidenced opposite patterns of expression of CD44 transcript isoforms between the cell line models. Indeed, while the ADK-18 cell line showed an enrichment of short transcripts lacking several exons of the variable region of the protein, including CD44s (CD44-201), ADK-17 cell line, in contrast, exhibited increased presence of long CD44 isoforms, including the well-characterized CD44v6 variant (CD44-206) (Ni et al., 2014; Ma et al., 2019). Unfortunately, the role and impact of these distinct CD44 isoforms on tumor progression and therapeutic response are not well defined and hugely vary between different tumor types (Chen et al. 2018). Therefore, the differing expression patterns of CD44 transcript isoforms between the two cell lines will warrant further investigation.

Another noteworthy observation was the stark contrast in the responses of ADK-17 and ADK-18 cell models to IFN-γ treatment *in vitro*. Although both cell lines demonstrated a suboptimal response to the cytokine under 2D culture conditions, exhibiting limited inhibition of cell proliferation and reduced induction of immunological mediators such as PD-L1 and major histocompatibility

complex I (MHC-I), ADK-18 displayed an unexpected and pronounced sensitivity to the antiproliferative effects of IFN-γ in conditions of low cell seeding density and 3D culture settings. In contrast, the ADK-17 cell line exhibited a highly atypical response to IFN-γ, characterized by the cross-activation of mediators in the type-I IFN pathways−including STAT2 and IRF9−and increased cell proliferation, especially in 3D culture settings (Platanias, 2005).

The disruption of the IFN-γ signaling pathway in tumor cells has been increasingly recognized as a significant mechanism contributing to resistance to ICIs. A deficient tumor response to IFN-γ stimulation indeed leads to reduced induction of PD-L1 expression, limiting the efficacy of ICI therapy, and in absent induction of MHC-I, decreasing tumor immunogenicity (Kalbasi & Ribas, 2020). Interestingly, evidence of an involvement of type I-IFN signaling in tumor resistance to immunotherapy has also been reported (Benci et al., 2016; Memon et al., 2024). Alterations of both type I and type II-IFN signaling pathways have been indeed identified in a few cases of NSCLC patients who developed ICI resistance (Hiltbrunner et al., 2023). While there is a notable interplay between the IFN-γ signaling pathway and type I-IFN pathways, due to the sharing of common mediators including STAT1 and JAK2, each pathway is characterized by its own distinct mediators and functions, contributing to the complex regulation of immune responses (Platanias, 2005). The atypical activation of type I-IFN pathway mediators by IFN-γ in the ADK-17 model may suggest an unexplored crosstalk between these pathways, a phenomenon not previously documented in the literature. Rather, existing reports have only highlighted the ability of IFN-γ to induce non-canonical transcriptional complexes that resemble the ones of type I-IFN pathways (Ivashkiv, 2018).

Turning back to the pro-growth effect of IFN-γ, it is important to mention that especially low-doses of the cytokine stimulated the colony and sphere formation ability of the ADK-17 model. These data are in accordance with the findings of Song and colleagues, who demonstrated that low doses of IFN-γ trigger the activation of an alternative signaling pathway mediated by ICAM1 in NSCLC cell lines, subsequently leading to increased cancer stemness (M. Song et al., 2019). Consistent with these reports, in our study low doses of IFN-γ also seemed to induce the expression of CD44 in ADK-17 cells, as demonstrated by the protein expression profile of ADK-17 BA clones, *i.e.*, the clones derived from ADK-17 soft-agar colonies grown in presence of IFN-γ. The observation that PD-L1 modulation could elicit similar effects in ADK-17 cells, both in terms of cell growth stimulation and CD44 increased expression, is particularly intriguing, as it suggests the existence of a molecular circuit between IFN-γ and PD-L1 that converges on the modulation of CD44 expression and tumor stemness. In this regard, the involvement of PD-L1 in plasticity modulation of both cancer cells and macrophages has also been documented, even though the literature presents conflicting data (L. Gao et al., 2019; Mansour et al., 2020; Cao et al., 2024).

Let us now turn our attention to the paradoxical observations presented in our study: assuming that low doses of IFN-γ and PD-L1 can influence cancer stemness, thereby enhancing tumor cell aggressiveness and survival−as demonstrated by the increased aggressive traits of ADK-18 and CD44^{high} ADK-17 BA clones−why would it result in the tumor re-sensitizing to the antiproliferative effect of IFN-γ? Not only ADK-18, but also ADK-19, ADK-25, ADK-17 BA.γ0.1 and ADK-17 BA.Atezo showed a certain sensitivity to the cytokine *in vitro*. Additionally, ADK-18 also exhibited increased basal activation of mediators of the IFN-γ pathway, including IFNGR1, STAT1 and JAK2, compared to ADK-17. Even though the reactivation of tumor sensitivity to IFN-γ may seem counterintuitive, we can hypothesize different explanations. Firstly, reactivated IFN-γ signaling may modulate the tumor microenvironment (TME), enabling the survival of more aggressive cell populations through the process of immunoediting (Vesely & Schreiber, 2013). Additionally, the activation of the canonical JAK-STAT cascade, activated by IFN-γ, has also been associated with increased tumor cell survival (Zhao et al., 2024). Alternatively, IFN-γ has been reported to sometimes suppress immune responses in a manner that benefits tumor progression (Angelicola et al., 2021). By promoting immunosuppression, the reactivation of IFN-γ signaling may enable tumor cells to create a more favorable environment for proliferation, inhibiting immune-mediated tumor cell killing (Mazet et al., 2023). Another hypothesis regards the capacity of IFN-γ of activating collateral signaling pathways associated with tumor stemness and progression in hyperprogressive tumors, including the Wnt/β-catenin signaling, as comprehensively demonstrated by Li and colleagues (Li et al. 2023).

The range of hypotheses and underlying mechanisms related to our observations is extensive, emphasizing the need for further investigation. Ultimately, these findings carry significant implications for the appropriate use of ICIs, underscoring the critical need to develop strategies for the early identification of patients who are likely to experience poor or detrimental responses to therapy, thereby enabling more personalized and effective treatment approaches to optimize therapeutic outcomes.

4.2 BoLC.8M3, a preclinical *in vivo* model of resistance to ICI-based immunotherapy

The BoLC.8M3 cell line is a murine adenocarcinoma cell line developed in our laboratory, derived from a lung tumor grown in a transgenic BALB/c mouse that carried the human KRAS^{G12D} mutation and had undergone knock-out of *p53*.

The presence of co-mutations of KRAS^{G12D} and p53 knock-out has been largely implicated in resistance to immunotherapy, particularly in NSCLC (Adeegbe et al., 2018; Tang et al., 2024). The KRAS^{G12D} mutation has indeed been reported to contribute to an immunosuppressive TME, impairing

$CD8^+$ T cell infiltration and resulting in ICI therapy failure (Liu et al. 2022; Qiao et al. 2024). Additionally, the loss of the tumor suppressor p53 has been reported to further promote tumor survival by inhibiting apoptosis and enabling tumor cells to evade immune surveillance (Chen 2016; Wang et al. 2024). Together, these mutations create a more pronounced immune exclusion effect and contribute to a more aggressive tumor phenotype, further complicating treatment outcomes. Considering this evidence, BoLC.8M3 appeared to be a promising model to deepen our investigations regarding ICI resistance, allowing us to study these mechanisms in a syngeneic and immunocompetent context.

The evaluation of BoLC.8M3 cell responses to the anti-PD-L1 monoclonal antibody atezolizumab in an immunocompetent, syngeneic mouse model revealed not only a marked resistance of the BoLC.8M3-derived tumors to treatment but also a partially accelerated tumor progression, resembling the hyperprogressive disease (HPD) phenomenon observed in clinical settings. Of note, the detrimental effect of the treatment became more pronounced in the later stages of the experiments, indicating the importance of considering the timing of treatment when analyzing its effects in order to refine our model.

The assessment of immune infiltration within the TME of tumors treated with atezolizumab compared to untreated tumors revealed a significant increase in $PD\text{-}1^+$ cells and natural killer (NK) lymphocytes in the treated group. Typically, in patients who develop resistance to ICIs, a rise in PD-1-expressing T cells is indicative of T-cell exhaustion and, consequently, of a highly immunosuppressive TME (Parvez et al., 2023). Conversely, increased infiltration of NK cells in the tumors that progressed after atezolizumab treatment might appear paradoxical, since this cell population is renowned for its anticancer properties (Wolf et al., 2023). However, studies have shown that infiltrating NK cells in patients who develop resistance to ICIs might exhibit impaired effector functions, mirroring the exhaustion phenomenon commonly observed in T cells (Cao et al. 2020; Dean et al. 2024). In addition, several groups have also demonstrated a capacity of the TME in shaping NK cells functions, converting their anti-tumoral phenotype in a pro-tumoral, pro-inflammatory and pro-angiogenic one (Gemelli et al., 2022). Moreover, an interesting work by Lo Russo and colleagues proposed a novel possible mechanism underlying hyperprogression in NSCLC, involving the interaction between ICIs and Fc receptors (FcR) expressed on macrophages. According to these findings, this interaction induced a pro-tumoral phenotype in these immune cells, stimulating tumor progression (Lo Russo et al., 2019). Since NK cells also express FcR receptors and can also exhibit a pro-tumor phenotype, it can be hypothesized that ICIs might also interact with these immune cells, inducing changes in their tumor-related activities (Pinto et al., 2022).

Interestingly, we also detected increased expression of β-catenin and enhanced activation of AKT in atezolizumab-treated tumors as compared to the untreated ones. Notably, the activation of the Wnt/β-catenin signaling pathway has been reported to play a crucial role in tumor immune escape and resistance to ICIs (Muto et al., 2023). For instance, the enlightening work by Li and colleagues also demonstrated that the IFN-γ–mediated activation of the β-catenin signaling pathway is a mechanism of tumor progression in HPD patients and preclinical models (Li et al. 2023). For what concerns AKT activation, despite the wide range of processes in which this mediator is involved, it has been specifically demonstrated that its activation by IFN-γ can modulate PD-L1 expression on tumor cells, contributing to tumor immune escape (Y. Gao et al., 2018).

These findings once again suggested a central role of IFN-γ in the molecular and immune mechanisms driving tumor progression after ICI treatment. Building on this rationale, and in line with investigations conducted in the ADK-17 and ADK-18 cell models, we proceeded to evaluate the response of the BoLC.8M3 cell line to IFN-γ treatment *in vitro*. While the cell line exhibited partial sensitivity to the cytokine under 2D culture conditions and an optimal IFN-γ–dependent induction of PD-L1 and H-2 immune modulators, we also observed once again a paradoxical increase in BoLC.8M3 growth in 3D culture settings in presence of IFN-γ. Notably, the cell line also exhibited high expression of the CD44 marker, in accordance with our previous findings and with published studies.

The parallels between the results observed in this cell model and those from the ADK-17 and ADK-18 cell lines are evident, despite some minor discrepancies. For instance, while the 3D-growth of the ADK-17 cell line was stimulated by both low and high doses of IFN-γ, in this case intermediate to high doses of the cytokine enhanced cell proliferation. Additionally, whereas ADK-17 exhibited relatively low expression of CD44, which progressively increased in presence of IFN-γ or PD-L1 modulation, BoLC.8M3 showed a high basal level of CD44 expression.

These differences can be attributed to the distinct nature of the two models, with ADK-17 being a human-derived cell line and BoLC.8M3 originating from a murine model. Species-specific variations in cellular pathways and responses to cytokines, such as IFN-γ, likely contribute to the observed discrepancies. For instance, the higher basal CD44 expression in BoLC.8M3 may reflect inherent differences in its genetic background, such as the *p53* knock-out (Cao et al., 2022), and the differential regulation of immune modulators between human and murine cells. Alternatively, it may be hypothesized that the BoLC.8M3 model might be characterized by a tumor phenotype that lies between those of the ADK-17 and the ADK-18 models, representing an intermediate stage of phenotypic transformation associated with tumor resistance.

In any case, the primary roles of IFN-γ and tumor responses to this cytokine in the development of detrimental effects to ICI therapy are evident. Further studies are needed to deepen the understanding of the mechanisms underlying these tumor responses to IFN-γ, in order to identify predictive biomarkers for hyperprogression and enhance patient stratification in cancer treatment.

Conclusions

Non-Small Cell Lung Cancer (NSCLC) is not a single entity, but it is rather a complex mosaic constituted of several pieces representing a multitude of genetic and phenotypic variations, shaped by the environmental exposures, the individual biological responses and unique genetic landscape of each patient. In this sea of multiplicity, one unwavering truth stands out as constant and unique, which is the heterogenous nature of this malignancy. This heterogeneity can manifest in various ways: some tumors may harbor specific mutations or exhibit the activation of collateral pathways that confer resistance to targeted therapies, while others may adopt adaptive strategies to evade the immune system surveillance.

The results of this thesis vividly illustrate the profound heterogeneity inherent in NSCLC, efficiently represented, in the first place, by the panel of patient-derived preclinical models obtained in our laboratory, which provided a vital platform to study the multifaceted mechanisms of resistance to tyrosine kinase inhibitors (TKIs) and immunotherapy, and to investigate novel, promising therapeutic strategies.

Among the models of this panel, ADK-VR2 and LIBM-ADK-11 have offered a clear demonstration of how tumor resistance to TKIs can be driven by the presence of distinct tumor subclones, each exhibiting uniquely specific phenotypic and functional characteristics, including differential response to the drugs themselves–such as crizotinib and lorlatinib, for the ADK-VR2 AG143 clone, or osimertinib, for LIBM-ADK-11 P2 cells–or differential expression of tumor markers–such as CD44, highly expressed by the osimertinib-resistant LIBM-ADK-11 P2 cell subpopulation. The identification of the survival mechanisms of these TKI-resistant subclones could enable their specific targeting and their elimination, thereby overcoming or preventing drug resistance.

Other models, such as ADK-14 and PDX-ADK-36, have provided a valuable platform for the identification of a novel potential therapeutic strategy consisting in EGFR inhibition for the treatment of tumors harboring the well-characterized *BRAF* class III orphan mutations, possibly offering new avenues for treatment where current options are limited.

Finally, ADK-17 and ADK-18 models represent a valuable resource for tracking the evolution of immune checkpoint inhibitors (ICI) resistance within a single patient, offering a unique opportunity to observe how therapeutic resistance develops and unfolds over time and to identify the mechanisms underlying the phenomenon of hyperprogression. Through these models, we identified a regulatory circuit involving IFN-γ, PD-L1, and CD44 that governs tumor stemness and aggressiveness, potentially driving tumor progression during ICI treatment. The central role of IFN-γ in promoting tumor progression during immunotherapy was confirmed in the transgenic BoLC.8M3 cell model, in which, similarly to the ADK-17 cell line, IFN-γ exerted an atypical pro-growth effect *in vitro* and

plausibly mediated the activation of oncogenic signaling pathways, including β-catenin and AKT circuits, resulting in increased BoLC.8M3 tumor growth in presence of ICI treatment *in vivo*.

These findings prompt a re-evaluation of current therapeutic paradigms and call for integrated strategies that consider both the immune landscape and tumor biology in patients. Future research should focus on elucidating the molecular mechanisms underlying ICI resistance, particularly the role of IFN-γ in promoting tumor progression, together with the identification of predictive biomarkers to better stratify patients who may be at risk of hyperprogression during ICI therapy.

Materials and Methods

1. DEVELOPMENT OF PATIENT-DERIVED NSCLC PRECLINICAL MODELS

A panel of human tumor cell lines and patient-derived xenografts (PDXs) derived from non-small cell lung cancer (NSCLC) patients, was developed in the Laboratory of Immunology and Biology of Metastasis directed by Prof. Pier-Luigi Lollini. This panel included preclinical models derived from tumors exhibiting primary or acquired resistance to the leading approved therapeutic strategies, including tyrosine kinase inhibitors (TKIs)-based targeted therapies and immunotherapy.

Thanks to the collaboration with Dr. Francesco Gelsomino, belonging to the Medical Oncology Unit of the S. Orsola-Malpighi Hospital, directed by Prof. Andrea Ardizzoni, human tumor samples derived from patients with disease progression following TKIs-based treatment or immune checkpoint inhibitors (ICIs) therapy have been collected and used for the establishment of patient-derived preclinical models, including primary cell cultures and patient-derived xenografts (PDXs).

The studies were conducted in accordance with the Declaration of Helsinki (as revised in 2013). Human samples were collected after patients gave their informed consent. The protocol was approved by the Ethics Committee Center Emilia-Romagna Region, Italy (protocol 130/2016/U/Tess or GR-2018-12368031). Human samples and metadata including relevant clinical data were de-identified before being shared between laboratories involved in these studies.

1.1 Primary patient-derived cell cultures

The patient samples from which the panel of NSCLC patient-derived cell cultures were derived included both tumor biopsies and metastatic tissues, as well as patients' pleural effusions.

The cell lines derived from pleural effusions (*i.e.*, ADK-VR2, ADK-VR3, LIBM-ADK-11, ADK-15, ADK-17, ADK-31, ADK-32, ADK-37 and ADK-40), were established after centrifugation of the pleural effusions, as previously described (Ruzzi, Angelicola et al., 2022). Specifically, pleural effusions were centrifugated at 250 *g* for 5 minutes and the resulting cell sediments were subsequently seeded in 25 cm^2 PRIMARIA tissue culture flasks (Corning).

For the cell lines obtained from tumor fragments (*i.e.*, ADK-13, ADK-14, ADK-18, ADK-19, ADK-20, ADK-21, ADK-25, ADK-28, ADK-30, ADK-34, ADK-35, ADK-36, ADK-38, ADK-41 and ADK-42) the following protocol was employed: tumor biopsies were dissected with sterile surgical scalpels and the resulting fragments were placed into 25 cm^2 PRIMARIA tissue culture flasks.

The primary cell cultures were established and cultured in RPMI medium (Thermo Fisher Scientific) supplemented with 10% fetal bovine serum (FBS, Thermo Fisher Scientific), 100 U/mL

penicillin and 10 µg/mL streptomycin (Thermo Fisher Scientific), or in MammoCult medium (STEMCELL Technologies) supplemented with 1% FBS, 100 U/mL penicillin and 10 µg/mL streptomycin. The cell lines were grown at 37°C in a humidified atmosphere at 5% CO_2.

1.2 Patient-derived xenograft models (PDXs)

8-30–week-old BALB/c Rag2 −/−; Il2rg −/− (BRG) immunodeficient mice (breeders kindly provided by Drs T. Nomura and M. Ito, Central Institute for Experimental Animals, CIEA, Kawasaki, Japan) (Nomura et al., 2008) were bred under sterile conditions in our animal facilities and were used for PDX establishment. The starting material for PDX establishment consisted of fresh tumor tissues or patients' lung fluids, as previously described for the establishment of the primary cell cultures.

To generate PDXs from pleural effusions, the fluids were centrifuged at 250 *g* for 5 minutes to obtain cell sediment. BRG mice received subcutaneous (s.c.) injection of 10^7 (ADK-17) or 3×10^6 (ADK-40) cells, in the right hind leg.

To establish PDXs from tumor fragments, slices of tumor biopsies with a diameter of around 3-4 mm or tumor cell suspensions were implanted in the left flank (ADK-14, ADK-18, ADK-19, ADK-20, ADK-21 and ADK-22) or into the interscapular fat pad (ADK-25, ADK-28, ADK-34, ADK-35, ADK-36, ADK-38, ADK-39, ADK-41 and ADK-42) of anesthetized BRG mouse. PDX tumors were subsequently propagated until the third *in vivo* passage by s.c. implantation of tumor fragments in anesthetized BRG mice, as previously described for other PDX cancer models (Landuzzi et al., 2021). Tumor diameter was measured weekly with sterile calipers and volume was calculated using the formula $\pi[\sqrt{(a\times b)3}]/6$, where a = maximal tumor diameter and b= major tumor diameter perpendicular to a. When tumors reached a volume of about 1.5-2 cm^3, animals were euthanized and an accurate necropsy was performed.

All animal procedures were performed in accordance with European directive 2010/63/UE and Italian Law (No. DL26/2014). Experimental protocols were reviewed and approved by the institutional animal care and use committee of the University of Bologna and by the Italian Ministry of Health with letter 32/2020-PR.

2. THE IMPACT OF TUMOR HETEROGENEITY IN RESISTANCE TO TKI-BASED THERAPIES

Part of these Materials and Methods has been described in the paper by Ruzzi, Angelicola and colleagues (Ruzzi, Angelicola et al., 2022).

2.1 Cell lines

ADK-VR2 cell line was established in our laboratory, as previously described (*Materials and Methods – Section 1.1*), from the pleural effusion of a treatment-naïve patient with *SDC4-ROS1*–positive NSCLC, who was primarily resistant to crizotinib (Xalkori, Pfizer). The cell line was routinely cultured in MammoCult medium supplemented with 1% FBS, 100 U/mL penicillin and 10 µg/mL streptomycin.

ADK-VR2 AG143 is a clone of the ADK-VR2 cell line isolated from a 3D culture in the presence of crizotinib 0.02 µM (Merck Life Science), three weeks after cell seeding. The clone was cultured and grown under the same conditions described above.

HCC-78 cell line was kindly provided by Prof. Manuela Iezzi (G. D'Annunzio University, Chieti, Italy). Cells were cultured in RPMI medium supplemented with 10% FBS, 100 U/mL penicillin and 10 µg/mL streptomycin.

LIBM-ADK-11 cell line was established in our laboratory, as previously described (*Materials and Methods – Section 1.1*), from the pleural effusion of a NSCLC patient carrying a rare *EGFR* mutation in exon 19 (p.Leu747_Pro753delinsSer), who progressed after receiving osimertinib (Tagrisso, AstraZeneca Pharmaceuticals). The cell line was cultured in RPMI medium supplemented with 10% FBS, 100 U/mL penicillin and 10 µg/mL streptomycin.

LIBM-ADK-11 P2 and P4 are two LIBM-ADK-11 cell subpopulations sorted by CD44 expression from the low-passage LIBM-ADK-11 cell line. The cells were cultured and grown under the same conditions described above.

Cells were cultured at 37°C in a humidified 5% CO_2 atmosphere and were split once or twice a week according to density using 0.05% trypsin-EDTA (Thermo Fisher Scientific).

2.2 Mice

NOD-SCID-Il2rg−/− (NSG) immunodeficient mice (breeders received from Charles River Laboratories) and BRG mice were bred under sterile conditions in our animal facilities.

NSG mice were used to assess the *in vivo* sensitivity of the ADK-VR2 cell line to crizotinib. BRG mice were utilized for the evaluation of ADK-VR2 and ADK-VR2 AG143 tumorigenicity and metastatic ability.

All animal procedures were performed in accordance with European directive 2010/63/UE and Italian Law (No. DL26/2014); experimental protocols were reviewed and approved by the institutional animal care and use committee of the University of Bologna and by the Italian Ministry of Health with letter 32/2020-PR.

2.3 Molecular analyses

Total RNA was extracted from cell pellets using TRIzol Reagent (Total RNA Isolation Reagent, Thermo Fisher Scientific) or GenUP Total RNA Kit (Biotechrabbit), following the manufacturer's recommendations. DNA was extracted using a PureLink Genomic DNA Mini kit (Thermo Fisher Scientific), according to the manufacturer's instructions.

The detection of *EGFR* and *KRAS* mutations was performed on ADK-VR2 cell blocks obtained from pleural effusion by Real-Time Polymerase Chain Reaction (RT-PCR) (TheraScreen-Qiagen).

The *EGFR* p.L747_P753>S mutation in exon 19 was detected in the LIBM-ADK-11 cell line by using the Oncomine Focus Assay (Thermo Fisher Scientific). The frequency of the *EGFR* p.L747_P753>S mutation in the LIBM-ADK-11 P2 and P4 sorted cell lines was assessed through pyrosequencing.

Immunohistochemistry was performed on the formalin-fixed, paraffin-embedded sections of liver biopsies using the following pre-diluited antibodies: PDL1 (clone SP263 Ventana, Roche), ALK (clone D5F3, Ventana), and TTF1 (Clone 8G7G3/1, Ventana), Ep-CAM/Epithelial Specific Antigen (clone BerEP4, Ventana), calretinin (clone SP85, Ventana). Hematoxylin and eosin (H&E) staining was also performed on the same specimens. The presence of gene rearrangements was evaluated by fluorescence in situ hybridization (FISH), performed using the Zytolight SPEC ROS1 Dual Color Break Apart Probe (ZytoVision).

For whole transcriptome sequencing (WTS) on ADK-VR2 cells, cDNA libraries were synthesized from 500 ng total RNA using the TruSeq Stranded mRNA kit (Illumina), following manufacturer's protocol. For whole exome sequencing (WES), libraries were synthesized with Nextera Rapid Capture Exome Kit (Illumina) from the cell line and patients' peripheral blood following the manufacturer's instructions.

The WTS on LIBM-ADK-11 cells was performed by Eurofin Genomics according to the protocol for the INVIEW Transcriptome Discovery service (https://eurofinsgenomics.eu/en/next-generation-sequencing/ngs-built-for-you/inview-transcriptome/inview-transcriptome-discover/).

Gene Ontology (GO) enrichment analysis of differentially expressed genes (DEGs) with p-adj <0.01 and Log2 fold change (Log2FC) >1 and <-1 has been performed using the online source Enrichr (https://maayanlab.cloud/Enrichr/), on the 26th of July 2024.

2.4 Direct and indirect immunofluorescence and flow cytometry

Harvested cells were analyzed by immunofluorescence and cytofluorometric analysis (CyFlow Space, Sysmex Partec). Cell suspensions obtained from cell lines were filtered using 100 µm pore filters (Partec). For each sample, 0.5×10^6 cells were collected and centrifuged at 12,000 rpm

for 30 seconds. After removing the supernatant, cell pellets were directly resuspended in 50 µl of the following primary or conjugated antibodies: anti-human CD24AF488 (clone ML5, BioLegend), anti-human CD44PE (clone IM7, BioLegend), anti-human HER1 (clone 528, Calbiochem), anti-human HER2 (clone MGR2, kindly provided by Dr. E. Tagliabue, Istituto Nazionale dei Tumori, Milan), anti-human HER3 (clone Sgp1, Bio-Optica). Control samples were resuspended in an equivalent volume of RPMI + 5% FBS.

After a 30-minute incubation on ice with the primary antibodies, the samples were washed with RPMI + 5% FBS and then centrifuged at the previously mentioned speed. Pellets from the direct immunofluorescence samples were resuspended in 1 mL of PBS (Phosphate Buffer Saline, Thermo Fisher Scientific).

For indirect immunofluorescence, an anti-mouse IgG labeled with Alexa Fluor 488 (Thermo Fisher Scientific) was used as secondary antibody. Cell pellets were resuspended in 50 µl of secondary antibody and incubated on ice for 30 minutes. Following incubation, the samples were washed with RPMI + 5% FBS, centrifuged at the previously specified speed, and resuspended in an ethidium bromide solution in PBS at a final concentration of 1 µg/mL (SIGMA). Ethidium bromide is a DNA intercalating agent that selectively penetrates dead cells, allowing them to be distinguished and excluded during flow cytometry analysis.

Cytofluorimetric analysis was performed using CyFlow Space (Sysmex Partec) and data were analyzed with FCS Express 5 (De Novo Software).

2.5 Cell sorting by Flow Cytometry (FACS) procedure

Low-passage LIBM-ADK-11 cells were stained with anti-human CD44PE (clone IM7) and anti-human CD24AF488 (clone ML5).

Cell sorting was performed according to the purity mask using Cell Sorter FACS ARIA III (Becton Dickinson). Only single cells were selected for sorting through gating and were then seeded in culture medium.

2.6 Drug sensitivity in 2D culture condition

ADK-VR2, HCC-78 and ADK-VR2 AG143 cell lines were seeded at 0.05×10^6 cells (or 0.1×10^6 cells for experiments testing cell sensitivity to pemetrexed) per well into 24-well plates (Corning) in MammoCult + 1% FBS (for ADK-VR2 and ADK-VR2 AG143) or RPMI + 10% FBS (for HCC-78).

Low-passage (12^{th}-15^{th} *in vitro* cell passages) and high-passage (36^{th}-42^{nd} *in vitro* cell passages) LIBM-ADK-11 cells were plated at 0.1×10^5 cells/well in 96-well plates in RPMI + 10% FBS (Corning).

LIBM-ADK-11 P2 and P4 cells were seeded at 0.5×10^6 cells/25 cm^2 cell culture flasks (Falcon) in RPMI + 10% FBS.

After 24 hours from seeding, cells were treated by adding 555 µL (for cell culture flasks), 100 µL (for 24-well plates) or 10 µL (for 96-well plates) of a 10× solution of each drug, *i.e.*, pemetrexed, crizotinib, lorlatinib, entrectinib, DS-6051b, osimertinib, erlotinib and afatinib (Merck Life Science and Selleck Chemicals), vehicle (DMSO, Merck Life Science) or fresh medium in each well.

Drug final concentrations are reported in the figures or in figure legends.

Cell growth was assessed 72 hours after treatment by vital counting on Neubauer's hemocytometer using vital colorant erythrosine (Sigma) or using the WST-1 reagent (Merck Life Science), according to the manufacturer's instructions.

2.7 Drug sensitivity in 3D soft-agar assay

ADK-VR2, ADK-VR2 AG143 and HCC-78 cells were seeded at 500 cells/well in 24-well plates in semisolid medium–MammoCult + 1% FBS + 0.33% agar (Sea-Plaque Agarose, Lonza), containing crizotinib, lorlatinib, entrectinib or DS-6051b 0.01 µM, with a 0.5% agarose underlay. Colonies (diameter >90 µm) were counted 2-4 weeks later under an inverted microscope in dark-field, as previously described (Palladini et al., 2018).

2.8 Drug sensitivity in sphere formation assay

Cells were seeded at 4,000 cells in 4 mL complete MammoCult medium without serum in 6-well Ultra-Low attachment plates (Corning), according to the MammoCult Human Medium Kit protocol. Drugs and vehicle were added to the medium at different doses, reported in figures or in figure legends. Cells were incubated at 37°C in a humidified 5% CO_2 atmosphere for a week. Spheres, *i.e.*, multi-cell structures with a diameter larger than 90 µm, were counted about 7 days after cell seeding (Giusti et al. 2021).

2.9 Tumorigenicity and metastatic cell capacity

The tumorigenicity of ADK-VR2 cell line and ADK-VR2 AG143 clone was evaluated in 13–25-week-old male BRG mice. Mice received s.c. injection of 9×10^6 cells, in a hind leg (n=3). Tumor diameter was measured weekly with sterile calipers and volume was calculated using the formula $\pi[\sqrt{(a\times b)3}]/6$, where a = maximal tumor diameter and b = major tumor diameter perpendicular to a. Before tumors reached the volume of 2.5 cm^3, mice were euthanized by CO_2 inhalation and cervical dislocation. An accurate necropsy was performed, and lungs were collected for the evaluation of metastatic dissemination.

The metastatic capacity of ADK-VR2 cell line was assessed by the intravenous (i.v.) injection of 0.5×10^6 cells into a caudal vein of 19–23-week-old male BRG mice (n=5). Animals were inspected

weekly and euthanized as described above at any initial sign of metastatic growth or, alternatively, 18 weeks after cell injection. At necropsy, lungs were dissected to investigate metastatic dissemination.

2.10 *In vivo* treatment with crizotinib

Crizotinib was formulated in 5% DMSO, 30% PEG300 (Merck Life Science) and 65% double distilled water. ADK-VR2 cell line was s.c. injected at the dose of 10^6 cells in 37-week-old NSG female mice. The animals were randomized into a control and a treated group. Five mice were enrolled in each test group in order to have an 80% chance of showing, with a 5% significance, a 65% of success in the experimental group. Starting from the 12^{th} day after cell injection, treated mice received crizotinib 50 mg/kg daily *per os* by gavage (5 mice were enrolled but a censored mouse at 6 week from cell injection was not included in tumor growth analysis: n=4), while the control group was not treated (n=5). Animals were checked weekly, and tumors were measured with sterile calipers. Tumor volume was calculated as described previously and mice were sacrificed as described in the previous sections.

2.11 Quantification of lung metastases

Lungs were minced with scissors and passed through 70 μm cell strainers (Becton Dickinson) to obtain homogeneous cell suspensions. Genomic DNA was extracted from cell suspensions and molecular quantification of lung metastatic load was performed by RT-PCR with human-specific primers, as previously described (Nanni et al., 2012). Specifically, genomic DNA was extracted with 10 mM Tris-HCl buffer pH 8.3 containing 50 mM KCl, 2.5 mM $MgCl_2$, 0.01% gelatin, 0.45% Igepal, 0.45% Tween 20 and 120 mg/mL proteinase K (all reagents from Merck Life Science) by overnight incubation at 56 °C followed by 30 min incubation at 95°C to inactivate the proteinase K. A sequence of the α-satellite region of human chromosome 17 was amplified. RT-PCR was performed using a Thermal Cycler CFX96 real time system C1000 (Bio-Rad Laboratories). To quantify human cells, a standard curve was constructed by adding scalar amounts of MDA-MB-453 human cells to a constant number of mouse cells. Ct (threshold cycle) values obtained from the experimental samples were interpolated in the standard curve run in each PCR (Bio-Rad CFX Manager). A negative control consisting of only mouse cells was included in each PCR. Ct values higher than Ct of the lowest standard curve point or the negative control were considered as negative (0% of human cells).

2.12 Western Blotting

The effect of crizotinib, lorlatinib or osimertinib (0.5 μM or 1 μM) was evaluated on ADK-VR2, ADK-VR2 AG143 or LIBM-ADK-11 cell lines after exposing cells to the treatments for 6 hours. An untreated sample and a sample treated with vehicle ran in parallel as controls.

Protein extraction and Western blotting were performed as reported previously (De Giovanni et al., 2014). Briefly, protein extraction was performed in the lysis buffer PhosphoSafe Extraction Reagent (Novagen) supplemented with protease inhibitors (Protease Inhibitor Cocktail, Sigma 100×). After 10 min incubation, suspensions were centrifuged (12,800 *g*, 15 min, 4°C) and proteins harvested at -80°C for further analysis.

Protein concentration was quantified using DC™ Protein Assay (Bio-Rad Laboratories). Proteins were then separated on an 8% polyacrylamide gel and then transferred to polyvinylidene difluoride membranes (Bio-Rad Laboratories). After blocking in TBST + 5% Milk (Bio-Rad Laboratories), membranes were incubated overnight at 4°C with the following primary antibodies: anti-HER1 (clone D38B1, diluted 1:1000, Cell Signaling), anti-pHER1 (Tyr1068) (clone D7A5, diluted 1:1000, Cell Signaling), anti-Stat3 (clone 124H6, diluted 1:1000, Cell Signaling), anti-pStat3 (clone D3A7, diluted 1:2000, Cell Signaling), anti-Akt (diluted 1:1000, Cell Signaling), anti-pAkt (clone D9E, diluted 1:1000, Cell Signaling), anti-p44/42 MAPK (clone 137F5, diluted 1:1000, Cell Signaling) and anti phospho-p44/42 MAPK (clone E10, diluted 1:1000, Cell Signaling). Anti-Actin antibody (diluted 1:1000, Merck Life Science) was used to detect reference proteins. After 3 washes in TBST, membranes were incubated with either polyclonal horse-radish-peroxidase (HRP) conjugated anti-rat IgG antibody (diluted 1:3000, Bio-Rad Laboratories), or anti-mouse IgG antibody (diluted 1:1000, Santa Cruz Biotechnology).

Proteins were detected by chemiluminescent reaction visualized using a digital imaging system (Bio-Rad Laboratories, Azure Biosystems) and band densitometry was performed to quantify the protein abundance.

3. EXPLORING NOVEL THERAPEUTIC STRATEGIES FOR DRUG-ORPHAN NSCLC MUTATIONS

Part of these Materials and Methods has been described in the paper by Di Federico, Angelicola and colleagues (Di Federico, Angelicola et al., 2024).

3.1 Patient selection

For the conducted studies, patients with advanced NSCLC harboring *BRAF* class III mutations without other concurring driver alterations detected by NGS panel (Oncomine Focus Assay – ThermoFisher Scientific, Kit RUO), were selected. Specifically, we searched for patients who received EGFR-TKI–based treatment in the Medical Oncology Unit of the S. Orsola-Malpighi

Hospital. Two patients treated with erlotinib (Tarceva, Roche) 150 mg daily after failure of standard treatments were identified.

3.2 Cell lines

ADK-14 cell line was established in our laboratory, as previously described (*Materials and Methods – Section 1.1*), from a biopsy of a lymph node metastasis of a patient with stage IV NSCLC harboring the *BRAF* class III mutation G466V, who progressed after first-line treatment with pembrolizumab (Keytruda, Merck Life Science). The cell line was established and cultured in MammoCult + 1% FBS.

PDX-ADK-36 cell line is a PDX-derived cell cultures (PDXC) established from the tumor mass of the 2nd passage PDX of the ADK-36 patient case (**Table 1**), who harbored the *BRAF* class III mutation D594G. The PDX was established as previously described (*Materials and Methods – Section 1.2*), prior to the patient's initiation of erlotinib treatment. PDX-ADK-36 was derived as follows: after the sacrifice of the BRG mouse used to obtain the PDX, the tumor mass was excised and collected in cold PBS. The tumor mass was then dissected with a sterile surgical scalpel and the resulting fragments were placed into 25 cm^2 PRIMARIA tissue culture flasks. The cell line was established and cultured in RPMI + 10% FBS.

ADK-17 was established as previously described (*Materials and Methods – Section 1.1*) and cultured in RPMI + 10% FBS. Further details will be provided in the subsequent sections.

PC-9 and HCC827 are pre-established NSCLC cell lines harboring the $EGFR^{G746\_A750del}$ mutation, both cultured in RPMI + 10% FBS.

HCC364 and NCI-H1395 are pre-established NSCLC cell lines harboring a *BRAF* class I (V600E) and a *BRAF* class II (G469A) mutation, respectively. Both the cell lines were cultured in DMEM medium (Dulbecco's Modified Eagle's medium, Thermo Fisher Scientific) supplemented with 10% FBS.

Cells were cultured at 37 °C in a humidified 5% CO_2 atmosphere and were split once or twice a week according to density using 0.05% trypsin-EDTA.

3.3 Drug sensitivity in 2D culture conditions

Cells were seeded at 5,000 cells/well into 96-well plate in MammoCult + 1% FBS (ADK-14), RPMI + 10% FBS (HCC827, PDX-ADK-36 and ADK-17) or DMEM + 10% FBS (HCC364 and NCI-H1395). PC-9 cells were seeded at 1,000 cells/well into 96-well-plate in RPMI + 10%FBS. After 24 hours from seeding, cells were treated with drugs (erlotinib, afatinib, dacomitinib, osimertinib and trametinib–all by Selleck Chemicals–or cetuximab, by Merck Life Science) by adding 10 µL of a 10× solution of each drug or vehicle (DMSO) in each well. Drug concentrations are reported in the figures

or in figure legends. Cell growth was assessed 72 hours later by WST-1 cell proliferation assay, according to the manufacturer instructions.

3.4 Drug sensitivity in 3D soft-agar assay

ADK-14 and PDX-ADK-36 cells were seeded at 500 cells/well in 24-well plate in semisolid medium–MammoCult + 1% FBS + 0.33% agar, containing drugs, with a 0.5% agarose underlay. HCC364 and NCI-H1395 were seeded at 4,000 cells/well in 24-well plate in semisolid medium–DMEM + 10% FBS + 0.33% agar, containing drugs, with a 0.5% agarose underlay. HCC827 and ADK-17 cells were seeded at 2,000 cells/well and PC-9 at 500 cells/well in 24-well plate in semisolid medium–RPMI + 10% FBS + 0.33% agar, containing drugs, with a 0.5% agarose underlay. Colonies with a diameter larger than 90 µm were counted 2-4 weeks later under an inverted microscope in dark-field, as previously described (Ruzzi, Angelicola et al., 2022).

3.5 Drug sensitivity in sphere formation assay

Cells were seeded at 5,000 cells (for NCI-H1395 cells) or 10,000 cells in 4 mL complete MammoCult medium without serum in 6-well Ultra-Low adherence plates, according to the MammoCult Human Medium Kit protocol. Drugs and vehicle were added to the medium at different doses, reported in figures or in figure legends. Cells were incubated at 37°C in a humidified 5% CO_2 atmosphere for a week. Spheres, *i.e.*, multi-cell structures with a diameter larger than 90 µm, were counted about 7 days after cell seeding (Ruzzi, Angelicola et al., 2022).

3.6 Western Blotting

The effect of erlotinib 1 µM on all the cell lines was evaluated after exposing cells to the treatment for 6 hours. An untreated sample and a sample treated with the vehicle (DMSO) ran in parallel as controls.

Western blotting was performed as previously described (*Materials and Methods – Section 2.12*). The following primary antibodies were used: anti-HER1 (clone D38B1, diluted 1:1000, Cell Signaling) and anti-pHER1 (Tyr1068) (clone D7A5, diluted 1:1000, Cell Signaling). Mouse monoclonal anti-Actin antibody (clone 8H10D10, 1:3000, Cell Signaling) or anti-vinculin antibody (clone V284, 1:2000, Merck Life Science) were used to detect reference proteins. Membranes were incubated with polyclonal horse-radish-peroxidase (HRP) conjugated anti-rabbit and anti-mouse IgG antibodies (Bio-Rad Laboratories). Re-Blot Plus Strong Solution (Merck Life Science) was used if needed.

4. INVESTIGATING THE MECHANISMS UNDERLYING RESISTANCE TO ICIs IN NSCLC THROUGH PRECLINICAL MODELS OF IMMUNOTHERAPY RESISTANCE

Part of these Materials and Methods has been described in the paper by Angelicola and colleagues (Angelicola et al., 2025).

4.1 Clinical history of the patient and cell lines

A 64-year-old, former light smoker (10 pack-year) woman was diagnosed with stage IVA NSCLC. At the time of hyperprogression under pembrolizumab treatment, the tumor was classified as a poorly differentiated, stage IVB NSCLC. Tumor samples were collected before and after treatment initiation, at three different time points. Two samples were obtained before treatment: one sample at the diagnosis (time of diagnosis, Tdx) and the other one a month after the diagnosis (time of baseline, Tb). The third sample was obtained three months after treatment initiation, at the time of radiological evidence of hyperprogression disease (HPD) (time of hyperprogression, Thy).

ADK-17 cell line was derived from the pleural effusion of the treatment-naïve patient at the Tb point, while ADK-18 was established from a subcutaneous thoracic tumor biopsy collected at the Thy point.

ADK-17 "bulk agar" cell lines (ADK-17 BA clones) are four clones of ADK-17 cell line derived by picking-up and then 2D-subculturing ADK-17 soft-agar colonies grown in the presence of the only medium (ADK-17 BA.CTRL), IFN-γ 0.1 ng/mL (ADK-17 BA.γ0.1), IFN-γ 100 ng/mL (ADK-17 BA.γ100) or atezolizumab 10 μg/mL (ADK-17 BA.Atezo), four weeks after cell seeding. The clones were cultured and grown under the same conditions of the parental cell line.

ADK-17 CRISPR/Cas9 clones (ADK-17 CL1 and ADK-17 CL2), are two clones of ADK-17 obtained by genetically editing the ADK-17 cell line through the CRISPR/Cas9 system, specifically modified to silence PD-L1 expression. The clones were cultured and grown under the same conditions of the parental cell line, in the presence of puromycin (1 μg/mL) (Thermo Fisher Scientific).

ADK-19 cell line was derived from a biopsy of a lymph node metastasis of a patient with stage IV NSCLC, who developed HPD after receiving atezolizumab (Tecentriq, Genectech) as a second-line therapy, following chemotherapy (**Table 1**).

ADK-25 cell line was established from a tumor biopsy of a patient with stage IV NSCLC, who developed hyperprogression after receiving chemo-immunotherapy (**Table 1**).

The methodology for deriving the patient-derived cell lines is detailed in *Section 1.1* of *Materials and Methods*.

The BoLC.8M3 lung adenocarcinoma cell line was derived from the spontaneous lung tumor of a BALB/c transgenic mouse model generated in the Laboratory of Immunology and Metastasis Biology, directed by Prof. Pier-Luigi Lollini. This transgenic model harbored the oncogenic $KRAS^{G12D}$ mutation and a heterozygous knockout of the *p53* gene.

The cell lines were established and cultured in RPMI + 10% FBS (ADK-17, ADK-18, ADK-19 and ADK-25 cell lines) or in DMEM + 20% FBS (BoLC.8M3 cell line), and grown at 37°C in a humidified atmosphere at 5% CO_2 and were split once or twice a week according to density using 0.05% trypsin-EDTA.

4.2 Mice

BRG mice were bred under sterile conditions in our animal facilities and were used for *in vivo* evaluation of the sensitivity of the BoLC.8M3 cell line to the mAb atezolizumab.

All animal procedures were performed in accordance with European directive 2010/63/UE and Italian Law (No. DL26/2014); experimental protocols were reviewed and approved by the institutional animal care and use committee of the University of Bologna and by the Italian Ministry of Health with letter 32/2020-PR.

4.3 Molecular analyses

From formalin-fixed paraffin-embedded (FFPE) tumor blocks collected at different time points (Tdx, Tb and Thy), 3 μm-thick sections were cut. Hematoxylin and eosin (H&E) staining was performed on the FFPE sections and the immunohistochemistry studies were conducted with the automatic immunohistochemistry stainer of the instrument, Benchmark Ultra (Ventana/Roche Group). The following pre-diluted antibodies were used: PD-L1 TPS (clone SP263, Ventana/Roche), TTF-1 (clone 8G7G3/1, Ventana/Roche) and Ber-EP4 (clone BER-EP4, Ventana/Roche). Immunostaining for CD44 was performed by using a polyclonal antibody (ab157107, Abcam) at dilution 1:1200 and was conducted with antigen retrieval Cell Conditioning 1 for 40 min at 99°C. The revelation system used was OptiView DAB (12 minutes linker and 12 minutes HRP multimer) (Ventana/Roche).

The mutational profile of the sample obtained at the Tdx point was investigated by using the Oncomine Focus Assay (Thermo Fisher Scientific), able to identify 35 hotspot genes, including *KRAS*. Sequencing was performed by using the Ion GeneStudio S5 (Thermo Fisher Scientific).

The $KRAS^{G12V}$ mutation. identified in the tumor at the Tdx point, was also detetcted in both ADK-17 and DK-18 cell lines by RT-PCR and Whole Transcriptome Sequencing (WTS).

4.4 Whole Transcriptome Sequencing (WTS)

Total RNA was extracted from three different *in vitro* passages (between 16th and 31st) of ADK-17 and ADK-18 2D-cultured cells using the GenUP Total RNA Kit (Biotechrabbit GmbH), according to the manufacturer's instructions. RNA integrity was assessed by electrophoretic analysis on a 2100 Bioanalyzer (Agilent Technologies) loaded with an RNA 6000 Nano Chip. All samples showed a RNA integrity number (RIN) > 8. RNA concentration was measured by a Qubit 4 fluorometer with a Qubit RNA BR Assay and RNA purity was assessed with a NanoDrop 8000 Spectrometer (Thermo Fisher Scientific). Total RNA libraries were prepared by IIGM - Italian Institute for Genomic Medicine (Turin, Italy) with the Illumina Stranded Total RNA Prep with Ribo-Zero Plus kit (Illumina Inc.), according to manufacturer's instructions without protocol modifications.

Quality of reads was assessed using the FastQC software. STAR aligner (v2.7.9a) was used to identify differentially expressed isoforms, while gene and isoform expression quantification has been performed using RSEM (v1.3.1) and Salmon (v0.13.1), respectively, based on the *Homo sapiens* Ensembl v.110 annotation. Gene Ontology (GO) enrichment analysis of differentially expressed genes (DEGs) with p-adj <0.01 and Log2 fold change (Log2FC) >1 and <-1 has been performed using ClusterProfiler (v4.6.2).

For single nucleotide variants (SNV) calling, filtered reads were aligned to the *Homo sapiens* reference genome (GENCODE release 36) using STAR v2.7.8a in two-pass mode.

4.5 Organoids establishment

Approximately 0.3×10^5 cells were resuspended in Geltrex LDEV-Free Reduced Growth Factor (RGF) Basement Membrane Extract (BME) (Thermo Fisher Scientific), seeded in low adhesion 48-well plates (Greiner Bio-One), and, after domes polymerization, an expansion medium was added. The organoid expansion medium was composed of Advanced DMEM/F-12 (Thermo Fisher Scientific) with 1% penicillin/streptomycin, 1% Glutamax (Thermo Fisher Scientific), 10 mM HEPES (Thermo Fisher Scientific) with the addition of 25 ng/mL fibroblast growth factor 7 (FGF7) (Proteintech), 100 ng/mL FGF10 (QKine), 100 ng/mL Noggin (Proteintech), 500 nM A83-01 (Tocris), 10 µM ROCK inhibitor (Y-27632) (Tocris), 0.5 µM SB202190 (Merck Life Science), 1.25 mM N-acetyl-L-cysteine (Merck Life Science), 10 mM nicotinamide (Merck Life Science), 10% R-Spondin1 conditioned medium (Merck Life Science), 50 ng/mL epidermal growth factor (EGF) (Proteintech) and B-27 (1:50) (Thermo Fisher Scientific). Organoids were disaggregated by gentle pipetting and incubation in cold PBS for 1 hour on ice, every 14 days.

4.6 Immunofluorescence assay

ADK-17 and ADK-18 adherent cultures were stained for CD44 or PD-L1. For CD44 staining, cells were fixed with 4% paraformaldehyde (PFA) (Merck Life Science) for 10 minutes at 4°C. After

washing with PBS, cells were permeabilized with PBS containing 0.1% Triton X-100 (Sigma-Aldrich) and then the blocking was performed with 1% bovine serum albumin (BSA) (Pan Biotech) + 0.1% Triton X-100 diluted in PBS. The primary antibody CD44 (clone IM7, 1:600, BioLegend) and the secondary antibody goat anti-rat IgGAF555 (1:500, Thermo Fisher Scientific) were used for staining. DAPI (BioLegend), which was incubated for 30 minutes at room temperature, was used to counterstain nuclei. Images were captured on a Leica widefield system, equipped with an inverted Leica DMi8 microscope (Leica Microsystem). PD-L1 evaluation was performed on live cells stained with anti-human PD-L1 (5 μg/mL, atezolizumab, Selleck Chemicals) and with goat anti-human IgG AF674 (1:1000, Thermo Fisher Scientific). Nuclei counterstaining was performed by incubating cells for 10 minutes with DAPI. Images were captured on Leica TCS SP8 confocal microscope equipped with a Leica DMi8 inverted microscope (Leica Microsystem).

ADK-18 organoids were stained for Ki-67 and CD44. The organoids were gently removed from their matrix by incubation in cold PBS for 1 hour and then fixed in cold 4% paraformaldehyde for 40 minutes at 4°C. Subsequently, cell structures were resuspended in PBS containing 0.1% Tween20 (Applichem, Darmstadt) for 10 minutes at 4°C and blocked for 1 hour at room temperature in PBS containing 0.1% Triton X-100 and 2% bovine serum albumin (BSA) solution to minimize background non-specific staining. Then, the primary antibodies CD44 (clone IM7, 1:250) and Ki-67 (clone SP6, 1:250, Thermo Fisher Scientific) diluted in PBS containing 0.1% Triton X-100 and 0.5% BSA were incubated overnight at 4°C on a shaker. After washing, 1 hour incubation with the secondary antibodies (1:500, Thermo Fisher Scientific) goat anti-rat IgGAF555 (for CD44 staining) and goat anti-rabbit AF647 (for Ki-67 staining) was performed. Hoechst 33342 (1:8000, Thermo Fisher Scientific) was incubated for 20 minutes at room temperature in a dark room to counterstain nuclei. Confocal images were captured on a Leica SP8 inverted confocal microscope.

4.7 Direct and indirect immunofluorescence and flow cytometry

Harvested cells were analyzed by immunofluorescence and cytofluorimetric analysis, as previously described (*Materials and Methods – Section 2.4*). The following antibodies were used for direct and indirect immunofluorescence: anti-human PD-L1 (5 μg/mL, atezolizumab, Tecentriq, Roche or Selleck Chemicals), anti-human MHC class I (clone W6/32, 1:80, Sera-Lab), anti-mouse CD44PE or BV711 (clone IM7, 1:10, BioLegend), anti-mouse PD-L1–PE (clone MIH5, diluted 1:100, eBioscience), mouse IgG1-PE (isotype control, clone G235-2356, diluted 1:40, BD Biosciences), anti-mouse H-2K^{d}D^{d} (clone CL9010-A, diluted 1:100, Cedarlane), anti-mouse CD44PE (clone IM7, 1:10, BioLegend). For indirect immunofluorescence goat anti-human IgG secondary antibody FITC or AF674 (1:20, Thermo Fisher Scientific) and anti-mouse IgGAF488 (1:100, Thermo Fisher Scientific) were used as secondary antibodies.

Cell cycle analysis was performed by using the Phase-FlowT Alexa Fluor 647 BrdU Kit (BioLegend), according to the manufacturer's instructions, only performing the staining with 7-Aminoactinomycin D.

Data were acquired by using CyFlow Space (Sysmex Partec) and BD FACS Lyric cytometer and analyzed by using FCS Express (De Novo Software).

4.8 CRISPR/Cas9 genome editing

The silencing of PD-L1 in ADK-17 cells was performed by using PD-L1 (CD274) Human Gene non-homology mediated CRISPR knock-out kit (KN413071, Origene), according to the manufacturer's instructions. The kit contained two RNA guides and a linear donor DNA including genes for puromycin resistance and green fluorescence protein (GFP). TransIT-X2® Dynamic Delivery System MIR 6004 (Mirus Bio) was used for transfection. Cells were selected and maintained in 1 μg/mL puromycin, obtaining the two cell line clones ADK-17 CL1 and ADK-17 CL2, derived from ADK-17 cells transfected with guide 1 and guide 2, respectively. The expression levels of PD-L1 and CD44 on the clones were measured by flow cytometry.

4.9 2D-growth and clonogenic assay

Cells were seeded in a 24-well plate at 0.2×10^5 cells/well in RPMI + 10% FBS (for ADK-17 and ADK-18 cells and for ADK-17 BA clones) or RPMI + 10% FBS + 1 μg/mL puromycin (for ADK-17 CL1 and ADK-17 CL2 cells) for cell growth evaluation. The clonogenic assay was performed by seeding 400, 800 or 1,600 cells/well in 6-well plates. After 7 days, cultures were fixed in 96% ethanol and stained with 0.05% crystal violet. Colonies, *i.e.*, groups with more than 10 cells, were counted under an inverted microscope or by using ImageJ software.

To assess cell sensitivity to IFN-γ or PD-L1 inhibition, cells were seeded at 0.5×10^6 cells/25 cm^2 cell culture flasks in RPMI + 10% FBS (ADK-17, ADK-18, ADK-19 and ADK-25 cells) or at 1×10^6 cells/25 cm^2 cell culture flasks in DMEM + 20% FBS (BoLC.8M3 cells).

After 24 hours, cells were treated with recombinant human IFN-γ (kindly provided by G. Garotta, F. Hoffmann-La Roche & Co.) or with recombinant mouse IFN-γ (kindly provided by Dr. G.R. Adolf, Ernst-Boehringer Institute, Vienna, Austria) by adding 555 μL of a 10× solution of the cytokine (final concentrations are reported in figures or in figure legends).

Cell growth and immunological modulation of MHC class I complex, H-2, PD-L1 and CD44 were assessed 72 hours later by vital counting on Neubauer's hemocytometer using vital colorant erythrosine and cytofluorimetric analysis.

4.10 3D soft-agar colony formation assay

For 3D soft-agar clonogenicity evaluation, ADK-17 and ADK-18 cells were seeded at 200 cells/well in 24-well plates in semisolid medium consisting of RPMI + 10% FBS + 0.33% agar, with a 0.5% agarose underlay.

For the assessment of cell line sensitivity to IFN-γ treatment or PD-L1 modulation in 3D culture conditions, cells were seeded at 500 (for ADK-18 cell line), 1,000 (for ADK-17 BA clones and for ADK-19 and ADK-25 cell lines), 2,000 (for ADK-17 cell line) or 10,000 (for BoLC.8M3 cell line) cells/well in 24-well plate in semisolid medium consisting of RPMI + 10% FBS or DMEM + 20% FBS + 0.33% agar, containing recombinant human/mouse IFN-γ, atezolizumab (Tecentriq, Genetech) or only medium, with a 0.5% agarose underlay. Colonies (diameter >90 μm) were counted 2-3 weeks later under an inverted microscope in dark-field, as previously described (Palladini et al., 2017). Photos were taken with a Canon EOS 600D.

4.11 Sphere-formation assay

For the assessment of sphere formation ability, cells were seeded at 500 (for ADK-17 BA clones) or at 0.1×10^5 (for ADK-17 and ADK-18 cell lines) cells in 4 mL of complete MammoCult medium without serum in 6-well Ultra-Low adherence plates, according to the MammoCult Human Medium Kit protocol. For the assessment of cell line sensitivity to IFN-γ treatment or PD-L1 modulation in sphere-formation assay, ADK-17 cells were seeded at 500, 5,000 or 10,000 cells and ADK-18 was seeded at 10,000 cells in 4 mL complete MammoCult medium. Recombinant human IFN-γ or atezolizumab were added to the medium at the concentrations reported in figures or in figure legends. Cells were incubated at 37°C in a humidified 5% CO_2 atmosphere for a week. Spheres, *i.e.*, multi-cell structures with a diameter larger than 90 μm, were counted one week after seeding under an inverted microscope in dark field (Ruzzi, Angelicola et al., 2022).

4.12 *In vivo* treatment with anti–PD-L1 monoclonal antibody

The experiments were conducted in immunocompetent, 7−8-week-old male syngeneic BALB/c mice. The mice were randomized into an untreated group and a group treated with anti–PD-L1 antibody atezolizumab (Tecentriq, Genentech). BoLC.8M3 cells were s.c. injected at the dose of 10^5 cells in a hind leg (n=15 for each group). Starting from one day after cell injection, treated mice received intraperitoneal (i.p.) administrations of atezolizumab 10 mg/kg bi-weekly, every 3 or 4 days, for the entire duration of the experiment. The control group received no treatment. Animals were checked weekly, and tumors were measured with sterile calipers. Tumor volume was calculated as described previously and mice were sacrificed as described in the previous sections. An accurate necropsy was performed, and lungs were collected to evaluate metastatic dissemination through metastasis counting using a dissection microscope.

4.13 Real-Time PCR

Total RNA was extracted from frozen tumor samples, which were mechanically dissociated by gentleMACS Octo Dissociator (Milteny Biotech GmbH). Extraction was performed according to the TRIzol protocol. RNA was quantified by Qubit Assay Kit (Thermo Fisher Scientific). 1 µg of RNA was reverse transcribed with iScript cDNA Synthesis Kit (Bio-Rad Laboratories). 10 ng of cDNA were analyzed for each sample. cDNA was amplified using Sso Advanced SyBR Green Supermix reagent (Bio-Rad Laboratories). Reactions were performed by Thermal Cycler CFX96 (Bio-Rad Laboratories). Analysis was performed using Bio-Rad CFX Manager 3.1 Software and relative quantification was calculated as $\Delta_{Ct}= Ct_{gene}-Ct_{housekeeping}$. TATA Box Binding Protein (TBP) was used as housekeeping gene. The following Bio-Rad assays were used: Pdcd1 (qMmuCID0011570) and Ncr1 (qMmuCID0015089).

4.14 Western Blotting

Protein extraction was performed as reported previously. For frozen tumor samples, proteins were extracted by mechanically dissociating the samples by gentleMACS Octo Dissociator. Protein quantification was performed as previously described (*Materials and Methods – Section 2.12*).

The effect of IFN-γ 0.1 and 100 ng/mL (Proteintech) or anti-PD-L1 mAb atezolizumab 5 µg/ml (Selleck Chemicals) on ADK-17 and ADK-18 cell lines was evaluated after exposing cells to the immune modulators for 6 hours. An untreated sample ran in parallel as controls.

Basal levels of proteins expression were also evaluated in ADK-17 and ADK-18 cells.

Western blotting was performed as previously described (*Materials and Methods – Section 2.12*).

The list of primary antibodies used for Western blot analyses is reported in **Table 4**.

Membranes were incubated with either polyclonal horse-radish-peroxidase (HRP) conjugated anti-rabbit IgG antibody (diluted 1:500/1:1000, Bio-Rad Laboratories), or anti-mouse IgG antibody (diluted 1:1000, Bio-Rad Laboratories).

Proteins were detected by chemiluminescent reaction visualized using a digital imaging system (Bio-Rad Laboratories, Azure Biosystems) and band densitometry was performed to quantify the protein abundance.

Antibody (target)	Clone	Molecular Weight (KDa)	Dilution
IFNGR1	E444	45-90	1:1000
JAK1	6G4	130	1:1000
phospho-JAK1 (Tyr 1034/1035)	D7N4Z	130	1:1000
JAK2	D2E12	125	1:1000
phospho-JAK2 (Tyr 1007/1008)	C80C3	125	1:1000
STAT1	D1K9Y	84, 91	1:1000
phospho-STAT1 (Tyr 701)	D4A7	84, 91	1:1000
STAT2	D9J7L	97, 113	1:1000
phospho-STAT2 (Tyr 690)	D3P2P	97, 113	1:500
STAT3	D1B2J	79, 86	1:1000
phospho-STAT3 (Tyr 705)	D3A7	79, 86	1:1000
IRF9	D2T8M	48	1:1000
IRF3	D6I4C	50-55	1:1000
phospo-IRF3 (Ser 386)	E7J8G	50-55	1:1000
pMAPK42/44 (Erk1/2)	137F5	42-44	1:1000
phospho-pMAPK 42/44 (Erk1/2) (Thr202/Tyr204)	D13.14.4E	42-44	1:500
NDRG1	D8G9	46	1:1000
Actin	8H10D10	45	1:3000
Actin	AC-40	45	1:3000
GAPDH	D16H11	37	1:1000
β-catenin	D10A8	92	1.1000
AKT	-	60	1:1000
pAKT	D9E	60	1:1000

Table 4. List of antibodies used for Western blot analyses. All the antibodies by Cell Signaling Technology, except anti-actin AC-40, by Merck Life Science.

5. STATISTICAL ANALYSIS

Experimental *in vitro* conditions analyzed with statistical measures were repeated two times, at least (the number of replicates is reported in figure legends). Statistical tests were performed according to assumptions of the tests and to the variance between the compared groups.

The significance of differences in cell growth rates and sensitivity to drugs was assessed through the two-tailed unpaired Student's *t*-test, t-test with Welch's correction, One sample t test, Mann-Whitney U test or the Kruskal-Wallis test, as appropriate. The test used is reported in each figure legend. All p-values are two-sided and confidence intervals are at the 95% level, with significance pre-defined to be at $p<0.05$. For One sample t test, the mean of each analyzed group was compared to the hypothetical mean of 100. Calculations of the IC_{50} (half maximal inhibitory concentration) of each used drug were based on the interpolation of the growth percentages with a sigmoid dose-response curve by Prism GraphPad version 5 (GraphPad software, La Jolla) and IC_{50} Calculator | AAT Bioquest (IC50 Calculator | AAT Bioquest). The significance of differences in IC_{50} between cell lines and drugs was evaluated by calculating the IC_{50} for each replicate and comparing group values using Student's *t*-test.

The significance of differences between *in vivo* growth curves was assessed by using the analysis of variance (ANOVA) and the post-hoc Bonferroni's or Tukey's multiple comparison tests for three groups or more, according to assumptions of the tests and the variance between the compared groups.

Statistical analyses were performed through Prism GraphPad version 5 and 10.

References

Abate-Shen, C., & Politi, K. (2024). The Evolution of Mouse Models of Cancer: Past, Present, and Future. *Cold Spring Harbor Perspectives in Medicine*, a041736. https://doi.org/10.1101/cshperspect.a041736

Aberle, D. R., Adams, A. M., Berg, C. D., Black, W. C., Clapp, J. D., Fagerstrom, R. M., Gareen, I. F., Gatsonis, C., Marcus, P. M., & Sicks, J. D. (2011). Reduced Lung-Cancer Mortality with Low-Dose Computed Tomographic Screening. *New England Journal of Medicine*, *365*(5), 395–409. https://doi.org/10.1056/NEJMoa1102873

Abuali, I., Lee, C.-S., & Seetharamu, N. (2022). A narrative review of the management of BRAF non-V600E mutated metastatic non-small cell lung cancer. *Precision Cancer Medicine*, *5*, 13–13. https://doi.org/10.21037/pcm-21-49

Adashek, J. J., Kato, S., Ferrara, R., Lo Russo, G., & Kurzrock, R. (2020). Hyperprogression and Immune Checkpoint Inhibitors: Hype or Progress? *The Oncologist*, *25*(2), 94–98. https://doi.org/10.1634/theoncologist.2019-0636

Addeo, A., Banna, G. L., & Friedlaender, A. (2021). KRAS G12C Mutations in NSCLC: From Target to Resistance. *Cancers*, *13*(11), 2541. https://doi.org/10.3390/cancers13112541

Adeegbe, D. O., Liu, S., Hattersley, M. M., Bowden, M., Zhou, C. W., Li, S., Vlahos, R., Grondine, M., Dolgalev, I., Ivanova, E. V., Quinn, M. M., Gao, P., Hammerman, P. S., Bradner, J. E., Diehl, J. A., Rustgi, A. K., Bass, A. J., Tsirigos, A., Freeman, G. J., Che, H., & Wong, K.-K. (2018). BET Bromodomain Inhibition Cooperates with PD-1 Blockade to Facilitate Antitumor Response in Kras-Mutant Non–Small Cell Lung Cancer. *Cancer Immunology Research*, *6*(10), 1234–1245. https://doi.org/10.1158/2326-6066.CIR-18-0077

Aguado, C., Chara, L., Antoñanzas, M., Matilla Gonzalez, J. M., Jiménez, U., Hernanz, R., Mielgo-Rubio, X., Trujillo-Reyes, J. C., & Couñago, F. (2022). Neoadjuvant treatment in non-small cell lung cancer: New perspectives with the incorporation of immunotherapy. *World Journal of Clinical Oncology*, *13*(5), 314–322. https://doi.org/10.5306/wjco.v13.i5.314

Ahmed, S. R., Petersen, E., Patel, R., & Migden, M. R. (2019). Cemiplimab-rwlc as first and only treatment for advanced cutaneous squamous cell carcinoma. *Expert Review of Clinical Pharmacology*, *12*(10), 947–951. https://doi.org/10.1080/17512433.2019.1665026

Ahn, B. C., Kim, Y. J., Kim, D.-W., Lee, K. H., Lee, Y., & Han, J.-Y. (2024). Lorlatinib in TKI naïve, advanced ROS1-positive non-small-cell lung cancer: A multicenter, open-label, single-arm, phase 2 trial. *Journal of Clinical Oncology*, *42*(16_suppl), 8519–8519. https://doi.org/10.1200/JCO.2024.42.16_suppl.8519

Ahn, J., & Nagasaka, M. (2023). Spotlight on Cemiplimab-rwlc in the Treatment of Non-Small Cell Lung Cancer (NSCLC): Focus on Patient Selection and Considerations. *Cancer Management and Research*, *Volume 15*, 627–634. https://doi.org/10.2147/CMAR.S325856

Akbay, E. A., Koyama, S., Carretero, J., Altabef, A., Tchaicha, J. H., Christensen, C. L., Mikse, O. R., Cherniack, A. D., Beauchamp, E. M., Pugh, T. J., Wilkerson, M. D., Fecci, P. E., Butaney, M., Reibel, J. B., Soucheray, M., Cohoon, T. J., Janne, P. A., Meyerson, M., Hayes, D. N., Shapiro, G. I., Shimamura, T., Sholl, L. M., Rodig, S. J., Freeman, G. J., Hammerman, P. S., Dranoff, G. & Wong, K.-K. (2013). Activation of the PD-1 Pathway Contributes to Immune Escape in EGFR-Driven Lung Tumors. *Cancer Discovery*, *3*(12), 1355–1363. https://doi.org/10.1158/2159-8290.CD-13-0310

Alkaabi, D., Arafat, K., Sulaiman, S., Al-Azawi, A. M., & Attoub, S. (2023). PD-1 Independent Role of PD-L1 in Triple-Negative Breast Cancer Progression. *International Journal of Molecular Sciences*, *24*(7). https://doi.org/10.3390/ijms24076420

Allen, T. C., Xiao, Y., Yang, B., Croix, D., Abraham, A., Redpath, S., Engstrom-Melynk, J., Shah, R., Madala, J., & Bernicker, E. H. (2021). Anaplastic lymphoma kinase rearrangement prevalence in patients with advanced non-small cell lung cancer in the United States - retrospective real world data. *Oncotarget*, *12*(23), 2308–2315. https://doi.org/10.18632/oncotarget.28114

Almquist, D., & Ernani, V. (2021). The Road Less Traveled: A Guide to Metastatic ROS1-Rearranged Non–Small-Cell Lung Cancer. *JCO Oncology Practice*, *17*(1), 7–14. https://doi.org/10.1200/OP.20.00819

Alvarado, A., & Arce, I. (2016). Metabolic Functions of the Lung, Disorders and Associated Pathologies. *Journal of Clinical Medicine Research*, *8*(10), 689–700. https://doi.org/10.14740/jocmr2668w

Amatu, A., Sartore-Bianchi, A., Bencardino, K., Pizzutilo, E. G., Tosi, F., & Siena, S. (2019). Tropomyosin receptor kinase (TRK) biology and the role of NTRK gene fusions in cancer. *Annals of Oncology*, *30*, viii5–viii15. https://doi.org/10.1093/annonc/mdz383

American Lung Association. (2022). *New Report: Critically Low Lung Cancer Screening Rates Reveal Opportunity to Save More Lives*. https://www.lung.org/media/press-releases/state-of-lung-cancer-2022

Amicizia, D., Piazza, M. F., Marchini, F., Astengo, M., Grammatico, F., Battaglini, A., Schenone, I., Sticchi, C., Lavieri, R., Di Silverio, B., Andreoli, G. B., & Ansaldi, F. (2023). Systematic Review of Lung Cancer Screening: Advancements and Strategies for Implementation. *Healthcare*, *11*(14), 2085. https://doi.org/10.3390/healthcare11142085

Andrini, E., Mosca, M., Galvani, L., Sperandi, F., Ricciuti, B., Metro, G., & Lamberti, G. (2022). Non-small-cell lung cancer: how to manage RET-positive disease. *Drugs in Context*, *11*, 1–12. https://doi.org/10.7573/dic.2022-1-5

Angelicola, S., Ruzzi, F., Landuzzi, L., Scalambra, L., Gelsomino, F., Ardizzoni, A., Nanni, P., Lollini, P. L., & Palladini, A. (2021). IFN-γ and CD38 in hyperprogressive cancer development. *Cancers*, *13*(2), 1–25. https://doi.org/10.3390/cancers13020309

Angelicola, S., Giunchi, F., Ruzzi, F., Frascino M., Pitzalis, M., Scalambra, L., Semprini M. S., Pittino O. M., Cappello, C., Siracusa, I., Chillico, I. C., Di Noia, M., Turato, C., De Siervi, S., Lescai, F., Ciavattini, T., Lopatriello, G., Bertoli, L., De Jonge, H., Iamele, L., Altimari, A., Gruppioni, E., Ardizzoni, A., Rossato, M., Gelsomino, F., Lollini, P. L. & Palladini, A. (2025). PD-L1 and IFN-γ modulate Non-Small Cell Lung Cancer (NSCLC) cell plasticity associated to immune checkpoint inhibitor (ICI)-mediated hyperprogressive disease (HPD). *Journal of Translational Medicine*, *23*(2), 1–25. https://doi.org/10.1186/s12967-024-06023-8

Anguera, G., & Majem, M. (2018). BRAF inhibitors in metastatic non-small cell lung cancer. *Journal of Thoracic Disease*, *10*(2), 589–592. https://doi.org/10.21037/jtd.2018.01.129

Araghi, M., Mannani, R., Heidarnejad maleki, A., Hamidi, A., Rostami, S., Safa, S. H., Faramarzi, F., Khorasani, S., Alimohammadi, M., Tahmasebi, S., & Akhavan-Sigari, R. (2023). Recent advances in non-small cell lung cancer targeted therapy; an update review. *Cancer Cell International*, *23*(1), 162. https://doi.org/10.1186/s12935-023-02990-y

Arcila, M. E., Chaft, J. E., Nafa, K., Roy-Chowdhuri, S., Lau, C., Zaidinski, M., Paik, P. K., Zakowski, M. F., Kris, M. G., & Ladanyi, M. (2012). Prevalence, Clinicopathologic Associations, and Molecular Spectrum of ERBB2 (HER2) Tyrosine Kinase Mutations in Lung Adenocarcinomas. *Clinical Cancer Research*, *18*(18), 4910–4918. https://doi.org/10.1158/1078-0432.CCR-12-0912

Armstrong, K., Kim, J. J., Halm, E. A., Ballard, R. M., & Schnall, M. D. (2016). Using lessons from breast, cervical, and colorectal cancer screening to inform the development of lung cancer screening programs. *Cancer*, *122*(9), 1338–1342. https://doi.org/10.1002/cncr.29937

Arnal-Estapé, A., Foggetti, G., Starrett, J. H., Nguyen, D. X., & Politi, K. (2021). Preclinical Models for the Study of Lung Cancer Pathogenesis and Therapy Development. *Cold Spring Harbor Perspectives in Medicine*, *11*(12). https://doi.org/10.1101/cshperspect.a037820

Arriagada, R., Bergman, B., Dunant, A., Le Chevalier, T., Pignon, J.-P., & Vansteenkiste, J. (2004). Cisplatin-Based Adjuvant Chemotherapy in Patients with Completely Resected Non–Small-Cell Lung Cancer. *New England Journal of Medicine*, *350*(4), 351–360. https://doi.org/10.1056/NEJMoa031644

Arteaga, C. L. (2006). EGF receptor mutations in lung cancer: From humans to mice and maybe back to humans. *Cancer Cell*, *9*(6), 421–423. https://doi.org/10.1016/j.ccr.2006.05.014

Attili, I., Corvaja, C., Spitaleri, G., Del Signore, E., Trillo Aliaga, P., Passaro, A., & de Marinis, F. (2023). New Generations of Tyrosine Kinase Inhibitors in Treating NSCLC with Oncogene Addiction: Strengths and Limitations. *Cancers*, *15*(20), 5079. https://doi.org/10.3390/cancers15205079

Awad, M. M., Oxnard, G. R., Jackman, D. M., Savukoski, D. O., Hall, D., Shivdasani, P., Heng, J. C., Dahlberg, S. E., Jänne, P. A., Verma, S., Christensen, J., Hammerman, P. S., & Sholl, L. M. (2016). MET Exon 14 Mutations in Non–Small-Cell Lung Cancer Are Associated With Advanced Age and Stage-Dependent MET Genomic Amplification and c-Met Overexpression. *Journal of Clinical Oncology*, *34*(7), 721–730. https://doi.org/10.1200/JCO.2015.63.4600

Azuma, T., Yao, S., Zhu, G., Flies, A. S., Flies, S. J., & Chen, L. (2008). B7-H1 is a ubiquitous antiapoptotic receptor on cancer cells. *Blood*, *111*(7), 3635–3643. https://doi.org/10.1182/blood-2007-11-123141

Bai, R., Lv, Z., Xu, D., & Cui, J. (2020). Predictive biomarkers for cancer immunotherapy with immune checkpoint inhibitors. *Biomarker Research*, *8*(1), 34. https://doi.org/10.1186/s40364-020-00209-0

Bandi, P., Star, J., Ashad-Bishop, K., Kratzer, T., Smith, R., & Jemal, A. (2024). Lung Cancer Screening in the US, 2022. *JAMA Internal Medicine*, *184*(8), 882. https://doi.org/10.1001/jamainternmed.2024.1655

Bar, J., Peled, N., Schokrpur, S., Wolner, M., Rotem, O., Girard, N., Aboubakar Nana, F., Derijcke, S., Kian, W., Patel, S., Gantz-Sorotsky, H., Zer, A., Moskovitz, M., Metro, G., Rottenberg, Y., Calles, A., Hochmair, M., Cuppens, K., Decoster, L., Reck, M., Limon, D., Rodriguez, E., Astaras, C., Bettini, A., Häfliger, S., & Addeo, A. (2023). UNcommon EGFR Mutations: International Case Series on Efficacy of Osimertinib in Real-Life Practice in First-LiNe Setting (UNICORN). *Journal of Thoracic Oncology*, *18*(2), 169–180. https://doi.org/10.1016/j.jtho.2022.10.004

Barnaba, V., & Schinzari, V. (2013). Induction, control, and plasticity of Treg cells: The immune regulatory network revised? *European Journal of Immunology*, *43*(2), 318–322. https://doi.org/10.1002/eji.201243265

Bartlett, E. C., Kemp, S. V., Ridge, C. A., Desai, S. R., Mirsadraee, S., Morjaria, J. B., Shah, P. L., Popat, S., Nicholson, A. G., Rice, A. J., Jordan, S., Begum, S., Mani, A., Derbyshire, J., Morris, K., Chen, M., Peacock, C., Addis, J., Martins, M., Kaye, S. B., Padley, S., Devaraj, A., McDonald, F., Robertus, J. L., Lim, E., Barnett, J., Finch, J., Dalal, P., Yousaf, N., Jamali, A., Ivashniova, N., Phillips, C., Newsom-Davies, T., Lee, R., Vaghani, P., Whiteside, S., & Vaughan-Smith, S. (2020). Baseline Results of the West London lung cancer screening pilot study – Impact of mobile scanners and dual risk model utilisation. *Lung Cancer*, *148*, 12–19. https://doi.org/10.1016/j.lungcan.2020.07.027

Becher, O. J., & Holland, E. C. (2006). Genetically Engineered Models Have Advantages over Xenografts for Preclinical Studies. *Cancer Research*, *66*(7), 3355–3359. https://doi.org/10.1158/0008-5472.CAN-05-3827

Belloni, A., Pugnaloni, A., Rippo, M. R., Di Valerio, S., Giordani, C., Procopio, A. D., & Bronte, G. (2024). The cell line models to study tyrosine kinase inhibitors in non-small cell lung cancer with mutations in the epidermal growth factor receptor: A scoping review. *Critical Reviews in Oncology/Hematology*, *194*, 104246. https://doi.org/10.1016/j.critrevonc.2023.104246

Benci, J. L., Xu, B., Qiu, Y., Wu, T. J., Dada, H., Twyman-Saint Victor, C., Cucolo, L., Lee, D. S. M., Pauken, K. E., Huang, A. C., Gangadhar, T. C., Amaravadi, R. K., Schuchter, L. M., Feldman, M. D., Ishwaran, H., Vonderheide, R. H., Maity, A., Wherry, E. J., & Minn, A. J. (2016). Tumor Interferon Signaling Regulates a Multigenic Resistance Program to Immune Checkpoint Blockade. *Cell*, *167*(6), 1540-1554.e12. https://doi.org/10.1016/j.cell.2016.11.022

Berthelsen, M. F., Leknes, S. L., Riedel, M., Pedersen, M. A., Joseph, J. V., Hager, H., Vendelbo, M. H., & Thomsen, M. K. (2021). Comparative Analysis of Stk11/Lkb1 versus Pten Deficiency in Lung Adenocarcinoma Induced by CRISPR/Cas9. *Cancers*, *13*(5), 974. https://doi.org/10.3390/cancers13050974

Bertram, J. S., & Janik, P. (1980). Establishment of a cloned line of Lewis lung carcinoma cells adapted to cell culture. *Cancer Letters*, *11*(1), 63–73. https://doi.org/10.1016/0304-3835(80)90130-5

Biton, J., Mansuet-Lupo, A., Pécuchet, N., Alifano, M., Ouakrim, H., Arrondeau, J., Boudou-Rouquette, P., Goldwasser, F., Leroy, K., Goc, J., Wislez, M., Germain, C., Laurent-Puig, P., Dieu-Nosjean, M.-C., Cremer, I., Herbst, R., Blons, H., & Damotte, D. (2018). TP53, STK11, and EGFR Mutations Predict Tumor Immune Profile and the Response to Anti–PD-1 in Lung Adenocarcinoma. *Clinical Cancer Research*, *24*(22), 5710–5723. https://doi.org/10.1158/1078-0432.CCR-18-0163

Borcoman, E., Kanjanapan, Y., Champiat, S., Kato, S., Servois, V., Kurzrock, R., Goel, S., Bedard, P., & Le Tourneau, C. (2019). Novel patterns of response under immunotherapy. In *Annals of Oncology* (Vol. 30, Issue 3, pp. 385–396). Oxford University Press. https://doi.org/10.1093/annonc/mdz003

Borgeaud, M., Parikh, K., Banna, G. L., Kim, F., Olivier, T., Le, X., & Addeo, A. (2024). Unveiling the Landscape of Uncommon EGFR Mutations in NSCLC-A Systematic Review. *Journal of Thoracic Oncology*, *19*(7), 973–983. https://doi.org/10.1016/j.jtho.2024.03.016

Borghaei, H., Paz-Ares, L., Horn, L., Spigel, D. R., Steins, M., Ready, N. E., Chow, L. Q., Vokes, E. E., Felip, E., Holgado, E., Barlesi, F., Kohlhufl, M., Arrieta, O., Burgio, M. A., Fayette, J., Lena, H., Poddubskaya, E., Gerber, D. E., Gettinger, S. N., Rudin, C. M., Rizvi, N., Crina, L., Blumenschein, G. R., Antonia, S. J., Dorange, C., Harbison, C. T., Graf Finckenstein, F., & Brahmer, J. R. (2015). Nivolumab versus docetaxel in advanced nonsquamous non-small-cell lung cancer. *New England Journal of Medicine*, *373*(17), 1627–1639. https://doi.org/10.1056/NEJMoa1507643

Boulanger, M. C., Schneider, J. L., & Lin, J. J. (2024). Advances and future directions in ROS1 fusion-positive lung cancer. *The Oncologist*. https://doi.org/10.1093/oncolo/oyae205

Boumelha, J., de Carné Trécesson, S., Law, E. K., Romero-Clavijo, P., Coelho, M. A., Ng, K. W., Mugarza, E., Moore, C., Rana, S., Caswell, D. R., Murillo, M., Hancock, D. C., Argyris, P. P., Brown, W. L., Durfee, C., Larson, L. K., Vogel, R. I., Suárez-Bonnet, A., Priestnall, S. L., East, P., Ross, S., Kassiotis, G., Molina-Arcas, M., Swanton, C., Harris, R., & Downward, J. (2022). An Immunogenic Model of KRAS-Mutant Lung Cancer Enables Evaluation of Targeted Therapy and Immunotherapy Combinations. *Cancer Research*, *82*(19), 3435–3448. https://doi.org/10.1158/0008-5472.CAN-22-0325

Boutilier, A. J., & Elsawa, S. F. (2021). Macrophage Polarization States in the Tumor Microenvironment. *International Journal of Molecular Sciences*, *22*(13), 6995. https://doi.org/10.3390/ijms22136995

Bracht, J. W. P., Karachaliou, N., Bivona, T., Lanman, R. B., Faull, I., Nagy, R. J., Drozdowskyj, A., Berenguer, J., Fernandez-Bruno, M., Molina-Vila, M. A., & Rosell, R. (2019). BRAF Mutations Classes I, II, and III in NSCLC Patients Included in the SLLIP Trial: The Need for a New Pre-Clinical Treatment Rationale. *Cancers*, *11*(9). https://doi.org/10.3390/cancers11091381

Brahmer, J., Reckamp, K. L., Baas, P., Crinò, L., Eberhardt, W. E. E., Poddubskaya, E., Antonia, S., Pluzanski, A., Vokes, E. E., Holgado, E., Waterhouse, D., Ready, N., Gainor, J., Frontera, O. A., Havel, L., Steins, M., Garassino, M. C., Aerts, J. G., Domine, M., Paz-Ares, L., Reck, M., Baudelet, C., Harbison, C. T., Lestini, B., & Spigel, D. R. (2015). Nivolumab versus docetaxel in advanced squamous-cell non-small-cell lung cancer. *New England Journal of Medicine*, *373*(2), 123–135. https://doi.org/10.1056/NEJMoa1504627

Bray, F., Laversanne, M., Sung, H., Ferlay, J., Siegel, R. L., Soerjomataram, I., & Jemal, A. (2024). Global cancer statistics 2022: GLOBOCAN estimates of incidence and mortality worldwide for 36 cancers in 185 countries. *CA: A Cancer Journal for Clinicians*, *74*(3), 229–263. https://doi.org/10.3322/caac.21834

Bronte, G., Belloni, A., Calabrò, L., & Crinò, L. (2023). The great need to overcome osimertinib resistance in advanced non-small cell lung cancer: from combination strategies to fourth-generation tyrosine kinase inhibitors. *Frontiers in Oncology*, *13*, 1308460. https://doi.org/10.3389/fonc.2023.1308460

Buchbinder, E. I., & Desai, A. (2016). CTLA-4 and PD-1 Pathways: Similarities, Differences, and Implications of Their Inhibition. *American Journal of Clinical Oncology*, *39*(1), 98–106. https://doi.org/10.1097/COC.0000000000000239

Camelliti, S., Le Noci, V., Bianchi, F., Moscheni, C., Arnaboldi, F., Gagliano, N., Balsari, A., Garassino, M. C., Tagliabue, E., Sfondrini, L., & Sommariva, M. (2020). Mechanisms of hyperprogressive disease after immune checkpoint inhibitor therapy: what we (don't) know. *Journal of Experimental & Clinical Cancer Research*, *39*(1), 236. https://doi.org/10.1186/s13046-020-01721-9

Camidge, D. R., Kim, H. R., Ahn, M.-J., Yang, J. C. H., Han, J.-Y., Hochmair, M. J., Lee, K. H., Delmonte, A., García Campelo, M. R., Kim, D.-W., Griesinger, F., Felip, E., Califano, R., Spira, A., Gettinger, S. N., Tiseo, M., Lin, H. M., Gupta, N., Hanley, M. J., Ni, Q., Zhang, P., & Popat, S. (2020). Brigatinib Versus Crizotinib in Advanced ALK Inhibitor–Naive ALK-Positive Non–Small Cell Lung Cancer: Second Interim Analysis of the Phase III ALTA-1L Trial. *Journal of Clinical Oncology*, *38*(31), 3592–3603. https://doi.org/10.1200/JCO.20.00505

Cao, H., Xiang, Y., Zhang, S., Chao, Y., Guo, J., Aurich, T., Ho, J. W., Huang, Y., Liu, P., & Sugimura, R. (2024). PD-L1 regulates inflammatory programs of macrophages from human pluripotent stem cells. *Life Science Alliance*, *7*(2). https://doi.org/10.26508/lsa.202302461

Cao, L., Fang, H., Yan, D., Wu, X. M., Zhang, J., & Chang, M. X. (2022). CD44a functions as a regulator of p53 signaling, apoptosis and autophagy in the antibacterial immune response. *Communications Biology*, *5*(1), 889. https://doi.org/10.1038/s42003-022-03856-1

Cao, Y., Wang, X., Jin, T., Tian, Y., Dai, C., Widarma, C., Song, R., & Xu, F. (2020). Immune checkpoint molecules in natural killer cells as potential targets for cancer immunotherapy. *Signal Transduction and Targeted Therapy*, *5*(1), 250. https://doi.org/10.1038/s41392-020-00348-8

Cardoso, W. V., & Whitsett, J. A. (2008). Resident Cellular Components of the Lung: Developmental Aspects. *Proceedings of the American Thoracic Society*, *5*(7), 767–771. https://doi.org/10.1513/pats.200803-026HR

Carrasco-Garcia, E., Lopez, L., Moncho-Amor, V., Carazo, F., Aldaz, P., Collado, M., Bell, D., Gaafar, A., Karamitopoulou, E., Tzankov, A., Hidalgo, M., Rubio, Á., Serrano, M., Lawrie, C. H., Lovell-Badge, R., & Matheu, A. (2022). SOX9 Triggers Different Epithelial to Mesenchymal Transition States to Promote Pancreatic Cancer Progression. *Cancers*, *14*(4), 916. https://doi.org/10.3390/cancers14040916

Cascetta, P., Marinello, A., Lazzari, C., Gregorc, V., Planchard, D., Bianco, R., Normanno, N., & Morabito, A. (2022). KRAS in NSCLC: State of the Art and Future Perspectives. *Cancers*, *14*(21), 5430. https://doi.org/10.3390/cancers14215430

Catalano, M., Iannone, L. F., Nesi, G., Nobili, S., Mini, E., & Roviello, G. (2023). Immunotherapy-related biomarkers: Confirmations and uncertainties. *Critical Reviews in Oncology/Hematology*, *192*, 104135. https://doi.org/10.1016/j.critrevonc.2023.104135

Cavazzoni, A., Digiacomo, G., Volta, F., Alfieri, R., Giovannetti, E., Gnetti, L., Bellini, L., Galetti, M., Fumarola, C., Xu, G., Bonelli, M., La Monica, S., Verzè, M., Leonetti, A., Eltayeb, K., D'Agnelli, S., Moron Dalla Tor, L., Minari, R., Petronini, P. G., & Tiseo, M. (2024). PD-L1 overexpression induces STAT signaling and promotes the secretion of pro-angiogenic cytokines in non-small cell lung cancer (NSCLC). *Lung Cancer*, *187*, 107438. https://doi.org/10.1016/j.lungcan.2023.107438

Cerami, E., Gao, J., Dogrusoz, U., Gross, B. E., Sumer, S. O., Aksoy, B. A., Jacobsen, A., Byrne, C. J., Heuer, M. L., Larsson, E., Antipin, Y., Reva, B., Goldberg, A. P., Sander, C., & Schultz, N. (2012). The cBio Cancer Genomics Portal: An Open Platform for Exploring Multidimensional Cancer Genomics Data. *Cancer Discovery*, *2*(5), 401–404. https://doi.org/10.1158/2159-8290.CD-12-0095

Cha, J.-H., Chan, L.-C., Li, C.-W., Hsu, J. L., & Hung, M.-C. (2019). Mechanisms Controlling PD-L1 Expression in Cancer. *Molecular Cell*, *76*(3), 359–370. https://doi.org/10.1016/j.molcel.2019.09.030

Chaft, J. E., Rimner, A., Weder, W., Azzoli, C. G., Kris, M. G., & Cascone, T. (2021). Evolution of systemic therapy for stages I–III non-metastatic non-small-cell lung cancer. *Nature Reviews Clinical Oncology*, *18*(9), 547–557. https://doi.org/10.1038/s41571-021-00501-4

Chai, G., Yin, Y., Zhou, X., Hu, Q., Lv, B., Li, Z., Shi, M., & Zhao, L. (2020). Pulmonary oligometastases treated by stereotactic body radiation therapy (SBRT): a single institution's experience. *Translational Lung Cancer Research*, *9*(4), 1496–1506. https://doi.org/10.21037/tlcr-20-867

Chalmers, A., Cannon, L., & Akerley, W. (2019). Adverse Event Management in Patients with BRAF V600E-Mutant Non-Small Cell Lung Cancer Treated with Dabrafenib plus Trametinib. *The Oncologist*, *24*(7), 963–972. https://doi.org/10.1634/theoncologist.2018-0296

Champiat, S., Dercle, L., Ammari, S., Massard, C., Hollebecque, A., Postel-Vinay, S., Chaput, N., Eggermont, A., Marabelle, A., Soria, J. C., & Ferté, C. (2017). Hyperprogressive disease is a new pattern of progression in cancer patients treated by anti-PD-1/PD-L1. *Clinical Cancer Research*, *23*(8), 1920–1928. https://doi.org/10.1158/1078-0432.CCR-16-1741

Champiat, S., Ferrara, R., Massard, C., Besse, B., Marabelle, A., Soria, J.-C., & Ferté, C. (2018). Hyperprogressive disease: recognizing a novel pattern to improve patient management. *Nature Reviews Clinical Oncology*, *15*(12), 748–762. https://doi.org/10.1038/s41571-018-0111-2

Chan, T. A., Yarchoan, M., Jaffee, E., Swanton, C., Quezada, S. A., Stenzinger, A., & Peters, S. (2019). Development of tumor mutation burden as an immunotherapy biomarker: utility for the oncology clinic. *Annals of Oncology*, *30*(1), 44–56. https://doi.org/10.1093/annonc/mdy495

Chang, C.-H., Qiu, J., O'Sullivan, D., Buck, M. D., Noguchi, T., Curtis, J. D., Chen, Q., Gindin, M., Gubin, M. M., van der Windt, G. J. W., Tonc, E., Schreiber, R. D., Pearce, E. J., & Pearce, E. L. (2015). Metabolic Competition in the Tumor Microenvironment Is a Driver of Cancer Progression. *Cell*, *162*(6), 1229–1241. https://doi.org/10.1016/j.cell.2015.08.016

Chang, C.-Y., Armstrong, D., Corry, D. B., & Kheradmand, F. (2023). Alveolar macrophages in lung cancer: opportunities and challenges. *Frontiers in Immunology*, *14*. https://doi.org/10.3389/fimmu.2023.1268939

Chaudhry, R., Omole, A. E., & Bordoni, B. (2024). Anatomy, Thorax, Lungs. In: *StatPearls [Internet]. Treasure Island (FL): StatPearls.* PMID: 29262068

Chen, C., Zhao, S., Karnad, A., & Freeman, J. W. (2018). The biology and role of CD44 in cancer progression: Therapeutic implications. In *Journal of Hematology and Oncology*, *11*(1). https://doi.org/10.1186/s13045-018-0605-5

Chen, H., Zheng, M., Zhang, W., Long, Y., Xu, Y., & Yuan, M. (2022). Research Status of Mouse Models for Non-Small-Cell Lung Cancer (NSCLC) and Antitumor Therapy of Traditional Chinese Medicine (TCM) in Mouse Models. *Evidence-Based Complementary and Alternative Medicine*, 1–13. https://doi.org/10.1155/2022/6404853

Chen, J. (2016). The Cell-Cycle Arrest and Apoptotic Functions of p53 in Tumor Initiation and Progression. *Cold Spring Harbor Perspectives in Medicine*, *6*(3), a026104. https://doi.org/10.1101/cshperspect.a026104

Chen, J. W., & Dhahbi, J. (2021). Lung adenocarcinoma and lung squamous cell carcinoma cancer classification, biomarker identification, and gene expression analysis using overlapping feature selection methods. *Scientific Reports*, *11*(1), 13323. https://doi.org/10.1038/s41598-021-92725-8

Chen, L., Diao, L., Yang, Y., Yi, X., Rodriguez, B. L., Li, Y., Villalobos, P. A., Cascone, T., Liu, X., Tan, L., Lorenzi, P. L., Huang, A., Zhao, Q., Peng, D., Fradette, J. J., Peng, D. H., Ungewiss, C., Roybal, J., Tong, P., Oba, J., Skoulidis, F., Peng, W., Carter, B. W., Gay, C. M., Fan, Y., Class, C. A., Zhu, J., Rodriguez-Canales, J., Kawakami, M., Byers, L. A., Woodman, S. E., Papadimitrakopoulou, V. A., Dmitrovsky, E., Wang, J., Ullrich, S. E., Wistuba, I. I., Heymach, J. V., Qin, F. X.-F., & Gibbons, D. L. (2018). CD38-Mediated

Immunosuppression as a Mechanism of Tumor Cell Escape from PD-1/PD-L1 Blockade. *Cancer Discovery*, *8*(9), 1156–1175. https://doi.org/10.1158/2159-8290.CD-17-1033

Chen, Q., Jia, G., Zhang, X., & Ma, W. (2023). Targeting HER3 to overcome EGFR TKI resistance in NSCLC. *Frontiers in Immunology*, *14*, 1332057. https://doi.org/10.3389/fimmu.2023.1332057

Chen, X., Shen, C., Wei, Z., Zhang, R., Wang, Y., Jiang, L., Chen, K., Qiu, S., Zhang, Y., Zhang, T., Chen, B., Xu, Y., Feng, Q., Huang, J., Zhong, Z., Li, H., Che, G., & Xiao, K. (2021). Patient-derived non-small cell lung cancer xenograft mirrors complex tumor heterogeneity. *Cancer Biology and Medicine*, *18*(1), 184–198. https://doi.org/10.20892/j.issn.2095-3941.2020.0012

Chen, Y., Sun, H., Deng, Y., Ma, Y., Huang, H., Liu, Y., Zhang, Y., Zhang, H., Ye, S., E, M., Guo, H., Wu, M., Wu, C., Pu, X., Chen, X., Liang, C., Ou, Q., Weng, H., Wu, X., Shao, Y., Gu, A., & Lin, T. (2023). The clinical and genomic distinctions of Class1/2/3 BRAF-mutant colorectal cancer and differential prognoses. *Biomarker Research*, *11*(1), 11. https://doi.org/10.1186/s40364-022-00443-8

Chen, Y., Zhang, R., Wang, L., Correa, A. M., Pataer, A., Xu, Y., Zhang, X., Ren, C., Wu, S., Meng, Q. H., Fujimoto, J., Jensen, V. B., Antonoff, M. B., Hofstetter, W. L., Mehran, R. J., Pisimisis, G., Rice, D. C., Sepesi, B., Vaporciyan, A. A., Walsh, G. L., Swisher, S. G., Roth, J.A., Heymach, J. V., & Fang, B. (2019). Tumor characteristics associated with engraftment of patient-derived non–small cell lung cancer xenografts in immunocompromised mice. *Cancer*, *125*(21), 3738–3748. https://doi.org/10.1002/cncr.32366

Cheon, D.-J., & Orsulic, S. (2011). Mouse Models of Cancer. *Annual Review of Pathology: Mechanisms of Disease*, *6*(1), 95–119. https://doi.org/10.1146/annurev.pathol.3.121806.154244

Chiarle, R., Voena, C., Ambrogio, C., Piva, R., & Inghirami, G. (2008). The anaplastic lymphoma kinase in the pathogenesis of cancer. *Nature Reviews Cancer*, *8*(1), 11–23. https://doi.org/10.1038/nrc2291

Chiou, V. L., & Burotto, M. (2015). Pseudoprogression and Immune-Related Response in Solid Tumors. *Journal of Clinical Oncology*, *33*(31), 3541–3543. https://doi.org/10.1200/JCO.2015.61.6870

Choi, W., Jeong, K.-C., Park, S.-Y., Kim, S., Kang, E. H., Hwang, M., & Han, J.-Y. (2022). MYC amplification-conferred primary resistance to capmatinib in a MET-amplified NSCLC patient: a case report. *Translational Lung Cancer Research*, *11*(9), 1967–1972. https://doi.org/10.21037/tlcr-22-176

Choi, Y., Lee, S., Kim, K., Kim, S.-H., Chung, Y.-J., & Lee, C. (2018). Studying cancer immunotherapy using patient-derived xenografts (PDXs) in humanized mice. *Experimental & Molecular Medicine*, *50*(8), 1–9. https://doi.org/10.1038/s12276-018-0115-0

Chubachi, S., Yasuda, H., Irie, H., Fukunaga, K., Naoki, K., Soejima, K., & Betsuyaku, T. (2016). A Case of Non-Small Cell Lung Cancer with Possible "Disease Flare" on Nivolumab Treatment. *Case Reports in Oncological Medicine*, *2016*, 1–3. https://doi.org/10.1155/2016/1075641

Clark, C. A., Gupta, H. B., Sareddy, G., Pandeswara, S., Lao, S., Yuan, B., Drerup, J. M., Padron, A., Conejo-Garcia, J., Murthy, K., Liu, Y., Turk, M. J., Thedieck, K., Hurez, V., Li, R., Vadlamudi, R., & Curiel, T. J. (2016). Tumor-Intrinsic PD-L1 Signals Regulate Cell Growth, Pathogenesis, and Autophagy in Ovarian Cancer and Melanoma. *Cancer Research*, *76*(23), 6964–6974. https://doi.org/10.1158/0008-5472.CAN-16-0258

Cognigni, V., Pecci, F., Lupi, A., Pinterpe, G., De Filippis, C., Felicetti, C., Cantini, L., & Berardi, R. (2022). The Landscape of ALK-Rearranged Non-Small Cell Lung Cancer: A Comprehensive Review of Clinicopathologic, Genomic Characteristics, and Therapeutic Perspectives. *Cancers*, *14*(19), 4765. https://doi.org/10.3390/cancers14194765

Collins, N. B., Al Abosy, R., Miller, B. C., Bi, K., Zhao, Q., Quigley, M., Ishizuka, J. J., Yates, K. B., Pope, H. W., Manguso, R. T., Shrestha, Y., Wadsworth, M., Hughes, T., Shalek, A. K., Boehm, J. S., Hahn, W. C., Doench, J. G., & Haining, W. N. (2022). PI3K activation allows immune evasion by promoting an inhibitory myeloid

tumor microenvironment. *Journal for ImmunoTherapy of Cancer*, *10*(3), e003402. https://doi.org/10.1136/jitc-2021-003402

Conde, E., Rojo, F., Gómez, J., Enguita, A. B., Abdulkader, I., González, A., Lozano, D., Mancheño, N., Salas, C., Salido, M., Salido-Ruiz, E., & de Álava, E. (2022). Molecular diagnosis in non-small-cell lung cancer: expert opinion on ALK and ROS1 testing. *Journal of Clinical Pathology*, *75*(3), 145–153. https://doi.org/10.1136/jclinpath-2021-207490

Cooper, A. J., Sequist, L. V., & Lin, J. J. (2022). Third-generation EGFR and ALK inhibitors: mechanisms of resistance and management. *Nature Reviews Clinical Oncology*, *19*(8), 499–514. https://doi.org/10.1038/s41571-022-00639-9

Cornel, A. M., Mimpen, I. L., & Nierkens, S. (2020). MHC Class I Downregulation in Cancer: Underlying Mechanisms and Potential Targets for Cancer Immunotherapy. *Cancers*, *12*(7), 1760. https://doi.org/10.3390/cancers12071760

Cortot, A. B., & Jänne, P. A. (2014). Molecular mechanisms of resistance in epidermal growth factor receptor-mutant lung adenocarcinomas. *European Respiratory Review*, *23*(133), 356–366. https://doi.org/10.1183/09059180.00004614

Cretella, D., Digiacomo, G., Giovannetti, E., & Cavazzoni, A. (2019). PTEN Alterations as a Potential Mechanism for Tumor Cell Escape from PD-1/PD-L1 Inhibition. *Cancers*, *11*(9), 1318. https://doi.org/10.3390/cancers11091318

Crosbie, P. A., Balata, H., Evison, M., Atack, M., Bayliss-Brideaux, V., Colligan, D., Duerden, R., Eaglesfield, J., Edwards, T., Elton, P., Foster, J., Greaves, M., Hayler, G., Higgins, C., Howells, J., Irion, K., Karunaratne, D., Kelly, J., King, Z., Manson, S., Mellor, S., Miller, D., Myerscough, A., Newton, T., O'Leary, M., Pearson, R., Pickford, J., Sawyer, R., Screaton, N. J., Sharman, A., Simmons, M., Smith, E., Taylor, B., Taylor, S., Walsham, A., Watts, A., Whittaker, J., Yarnell, L., Threlfall, A., Barber, P. V., Tonge, J., & Booton, R. (2019). Implementing lung cancer screening: baseline results from a community-based 'Lung Health Check' pilot in deprived areas of Manchester. *Thorax*, *74*(4), 405–409. https://doi.org/10.1136/thoraxjnl-2017-211377

Cui, J.-W., Li, Y., Yang, Y., Yang, H.-K., Dong, J.-M., Xiao, Z.-H., He, X., Guo, J.-H., Wang, R.-Q., Dai, B., & Zhou, Z.-L. (2024). Tumor immunotherapy resistance: Revealing the mechanism of PD-1 / PD-L1-mediated tumor immune escape. *Biomedicine & Pharmacotherapy*, *171*, 116203. https://doi.org/10.1016/j.biopha.2024.116203

Cunniff, B., Druso, J. E., & van der Velden, J. L. (2021). Lung organoids: advances in generation and 3D-visualization. *Histochemistry and Cell Biology*, *155*(2), 301–308. https://doi.org/10.1007/s00418-020-01955-w

Dai, J., Zhu, X., Li, D., Huang, Y., Liu, X., He, W., Duan, L., Zhao, D., Zhu, Y., Chen, C., Provencio, M., Ramirez, R. A., Antonoff, M. B., Wu, C., & Jiang, G. (2022). Sleeve resection after neoadjuvant chemoimmunotherapy in the treatment of locally advanced non-small cell lung cancer. *Translational Lung Cancer Research*, *11*(2), 188–200. https://doi.org/10.21037/tlcr-22-56

Dankner, M., Rose, A. A. N., Rajkumar, S., Siegel, P. M., & Watson, I. R. (2018). Classifying BRAF alterations in cancer: new rational therapeutic strategies for actionable mutations. *Oncogene*, *37*(24), 3183–3199. https://doi.org/10.1038/s41388-018-0171-x

Dankner, M., Rose, A. A. N., Rajkumar, S., Siegel, P. M., & Watson, I. R. (2018b). Classifying BRAF alterations in cancer: new rational therapeutic strategies for actionable mutations. *Oncogene*, *37*(24), 3183–3199. https://doi.org/10.1038/s41388-018-0171-x

Dasari, S., & Bernard Tchounwou, P. (2014). Cisplatin in cancer therapy: Molecular mechanisms of action. *European Journal of Pharmacology*, *740*, 364–378. https://doi.org/10.1016/j.ejphar.2014.07.025

Davies, E. J., Marsh Durban, V., Meniel, V., Williams, G. T., & Clarke, A. R. (2014). PTEN loss and KRAS activation leads to the formation of serrated adenomas and metastatic carcinoma in the mouse intestine. *The Journal of Pathology*, *233*(1), 27–38. https://doi.org/10.1002/path.4312

Davies, K. D., Le, A. T., Theodoro, M. F., Skokan, M. C., Aisner, D. L., Berge, E. M., Terracciano, L. M., Cappuzzo, F., Incarbone, M., Roncalli, M., Alloisio, M., Santoro, A., Camidge, D. R., Varella-Garcia, M., & Doebele, R. C. (2012). Identifying and Targeting *ROS1* Gene Fusions in Non–Small Cell Lung Cancer. *Clinical Cancer Research*, *18*(17), 4570–4579. https://doi.org/10.1158/1078-0432.CCR-12-0550

Davies, K. D., Mahale, S., Astling, D. P., Aisner, D. L., Le, A. T., Hinz, T. K., Vaishnavi, A., Bunn, P. A., Heasley, L. E., Tan, A.-C., Camidge, D. R., Varella-Garcia, M., & Doebele, R. C. (2013). Resistance to ROS1 Inhibition Mediated by EGFR Pathway Activation in Non-Small Cell Lung Cancer. *PLoS ONE*, *8*(12), e82236. https://doi.org/10.1371/journal.pone.0082236

de Alencar, V. T. L., Figueiredo, A. B., Corassa, M., Gollob, K. J., & Cordeiro de Lima, V. C. (2022). Lung cancer in never smokers: Tumor immunology and challenges for immunotherapy. *Frontiers in Immunology*, *13*, 984349. https://doi.org/10.3389/fimmu.2022.984349

De Giglio, A., Di Federico, A., Nuvola, G., Deiana, C., & Gelsomino, F. (2021). The Landscape of Immunotherapy in Advanced NSCLC: Driving Beyond PD-1/PD-L1 Inhibitors (CTLA-4, LAG3, IDO, OX40, TIGIT, Vaccines). In *Current Oncology Reports* (Vol. 23, Issue 11). Springer. https://doi.org/10.1007/s11912-021-01124-9

De Giovanni, C., Nicoletti, G., Quaglino, E., Landuzzi, L., Palladini, A., Ianzano, M. L., Dall'Ora, M., Grosso, V., Ranieri, D., Laranga, R., Croci, S., Amici, A., Penichet, M. L., Iezzi, M., Cavallo, F., Nanni, P., & Lollini, P. L. (2014). Vaccines against human HER2 prevent mammary carcinoma in mice transgenic for human HER2. *Breast Cancer Research*, *16*(1). https://doi.org/10.1186/bcr3602

de Koning, H. J., van der Aalst, C. M., de Jong, P. A., Scholten, E. T., Nackaerts, K., Heuvelmans, M. A., Lammers, J.-W. J., Weenink, C., Yousaf-Khan, U., Horeweg, N., van 't Westeinde, S., Prokop, M., Mali, W. P., Mohamed Hoesein, F. A. A., van Ooijen, P. M. A., Aerts, J. G. J. V., den Bakker, M. A., Thunnissen, E., Verschakelen, J., Vliegenthart, R., Walter, J. E., ten Haaf, K., Groen, H. J. M., & Oudkerk, M. (2020). Reduced Lung-Cancer Mortality with Volume CT Screening in a Randomized Trial. *New England Journal of Medicine*, *382*(6), 503–513. https://doi.org/10.1056/NEJMoa1911793

de Seranno, S., & Meuwissen, R. (2010). Progress and applications of mouse models for human lung cancer. *European Respiratory Journal*, *35*(2), 426–443. https://doi.org/10.1183/09031936.00124709

Dean, I., Lee, C. Y. C., Tuong, Z. K., Li, Z., Tibbitt, C. A., Willis, C., Gaspal, F., Kennedy, B. C., Matei-Rascu, V., Fiancette, R., Nordenvall, C., Lindforss, U., Baker, S. M., Stockmann, C., Sexl, V., Hammond, S. A., Dovedi, S. J., Mjösberg, J., Hepworth, M. R., Carlesso, G., Clatworthy, M. R., & Withers, D. R. (2024). Rapid functional impairment of natural killer cells following tumor entry limits anti-tumor immunity. *Nature Communications*, *15*(1), 683. https://doi.org/10.1038/s41467-024-44789-z

Del Re, M., Arrigoni, E., Restante, G., Passaro, A., Rofi, E., Crucitta, S., De Marinis, F., Di Paolo, A., & Danesi, R. (2018). Concise Review: Resistance to Tyrosine Kinase Inhibitors in Non-Small Cell Lung Cancer: The Role of Cancer Stem Cells. *Stem Cells*, *36*(5), 633–640. https://doi.org/10.1002/stem.2787

Dempke, W. C. M., Fenchel, K., & Dale, S. P. (2018). Programmed cell death ligand-1 (PD-L1) as a biomarker for non-small cell lung cancer (NSCLC) treatment—are we barking up the wrong tree? *Translational Lung Cancer Research*, *7*(S3), S275–S279. https://doi.org/10.21037/tlcr.2018.04.18

den Hollander, P., Maddela, J. J., & Mani, S. A. (2024). Spatial and Temporal Relationship between Epithelial–Mesenchymal Transition (EMT) and Stem Cells in Cancer. *Clinical Chemistry*, *70*(1), 190–205. https://doi.org/10.1093/clinchem/hvad197

Di Federico, A., De Giglio, A., Gelsomino, F., De Biase, D., Giunchi, F., Palladini, A., Sperandi, F., Melotti, B., & Ardizzoni, A. (2022). Genomic Landscape, Clinical Features and Outcomes of Non-Small Cell Lung Cancer Patients Harboring BRAF Alterations of Distinct Functional Classes. *Cancers*, *14*(14), 3472. https://doi.org/10.3390/cancers14143472

Di Federico, A., Angelicola, S., Frascino, M., Siracusa, I., Bisanti, B., Ruzzi, F., Semprini M. S., De Giglio, A., Brocchi, S., Giunchi, F., Gruppioni, E., Lollini, P. L., Ardizzoni, A., & Gelsomino, F. (2024). Clinical and Preclinical Activity of EGFR Tyrosine Kinase Inhibitors in Non–Small-Cell Lung Cancer Harboring BRAF Class 3 Mutations. *JCO Precision Oncology*, *8*, e2400240. https://doi.org/10.1200/PO.24.0024

Di Giacomo, A. M., Danielli, R., Guidoboni, M., Calabrò, L., Carlucci, D., Miracco, C., Volterrani, L., Mazzei, M. A., Biagioli, M., Altomonte, M., & Maio, M. (2009). Therapeutic efficacy of ipilimumab, an anti-CTLA-4 monoclonal antibody, in patients with metastatic melanoma unresponsive to prior systemic treatments: clinical and immunological evidence from three patient cases. *Cancer Immunology, Immunotherapy*, *58*(8), 1297–1306. https://doi.org/10.1007/s00262-008-0642-y

Dinić, J., Dragoj, M., Jovanović Stojanov, S., Stepanović, A., Lupšić, E., Pajović, M., Mohr, T., Glumac, S., Marić, D., Ercegovac, M., Podolski-Renić, A., & Pešić, M. (2024). Multidrug-Resistant Profiles in Non-Small Cell Lung Carcinoma Patient-Derived Cells: Implications for Personalized Approaches with Tyrosine Kinase Inhibitors. *Cancers*, *16*(11), 1984. https://doi.org/10.3390/cancers16111984

Dohopolski, M., Gottumukkala, S., Gomez, D., & Iyengar, P. (2021). Radiation Therapy in Non-Small-Cell Lung Cancer. *Cold Spring Harbor Perspectives in Medicine*, *11*(10), a037713. https://doi.org/10.1101/cshperspect.a037713

Dolled-Filhart, M., Locke, D., Murphy, T., Lynch, F., Yearley, J. H., Frisman, D., Pierce, R., Weiner, R., Wu, D., & Emancipator, K. (2016). Development of a Prototype Immunohistochemistry Assay to Measure Programmed Death Ligand-1 Expression in Tumor Tissue. *Archives of Pathology & Laboratory Medicine*, *140*(11), 1259–1266. https://doi.org/10.5858/arpa.2015-0544-OA

Doroshow, D. B., Bhalla, S., Beasley, M. B., Sholl, L. M., Kerr, K. M., Gnjatic, S., Wistuba, I. I., Rimm, D. L., Tsao, M. S., & Hirsch, F. R. (2021). PD-L1 as a biomarker of response to immune-checkpoint inhibitors. In *Nature Reviews Clinical Oncology* (Vol. 18, Issue 6, pp. 345–362). Nature Research. https://doi.org/10.1038/s41571-021-00473-5

Drilon, A., Camidge, D. R., Lin, J. J., Kim, S.-W., Solomon, B. J., Dziadziuszko, R., Besse, B., Goto, K., de Langen, A. J., Wolf, J., Lee, K. H., Popat, S., Springfeld, C., Nagasaka, M., Felip, E., Yang, N., Velcheti, V., Lu, S., Kao, S., Dooms, C., Krebs, M. G., Yao, W., Beg, M. S., Hu, X., Moro-Sibilot, D., Cheema, P., Stopatschinskaja, S., Mehta, M., Trone, D., Graber, A., Sims, G., Yuan, Y., & Cho, B. C. (2024). Repotrectinib in ROS1 Fusion–Positive Non–Small-Cell Lung Cancer. *New England Journal of Medicine*, *390*(2), 118–131. https://doi.org/10.1056/NEJMoa2302299

Drilon, A., Jenkins, C., Iyer, S., Schoenfeld, A., Keddy, C., & Davare, M. A. (2021). ROS1-dependent cancers — biology, diagnostics and therapeutics. *Nature Reviews Clinical Oncology*, *18*(1), 35–55. https://doi.org/10.1038/s41571-020-0408-9

Drilon, A., Lin, J. J., Filleron, T., Ni, A., Milia, J., Bergagnini, I., Hatzoglou, V., Velcheti, V., Offin, M., Li, B., Carbone, D. P., Besse, B., Mok, T., Awad, M. M., Wolf, J., Owen, D., Camidge, D. R., Riely, G. J., Peled, N., Kris, M. G., Mazieres, J., Gainor, J., & Gautschi, O. (2018). Frequency of Brain Metastases and Multikinase Inhibitor Outcomes in Patients With RET–Rearranged Lung Cancers. *Journal of Thoracic Oncology*, *13*(10), 1595–1601. https://doi.org/10.1016/j.jtho.2018.07.004

Drilon, A., Oxnard, G. R., Tan, D. S. W., Loong, H. H. F., Johnson, M., Gainor, J., McCoach, C. E., Gautschi, O., Besse, B., Cho, B. C., Peled, N., Weiss, J., Kim, Y.-J., Ohe, Y., Nishio, M., Park, K., Patel, J., Seto, T., Sakamoto, T., Rosen, E., Shah, M. H., Barlesi, F., Cassier, P. A., Bazhenova, L., De Braud, F., Garralda, E., Velcheti, V., Satouchi, M., Ohashi, K., Pennell, N. A., Reckamp, K. L., Dy, G. K., Wolf, J., Solomon, B.,

Falchook, G., Ebata, K., Nguyen, M., Nair, B., Zhu, E. Y., Yang, L., Huang, X., Olek, E., Rothenberg, S. M., Goto, K., & Subbiah, V. (2020). Efficacy of Selpercatinib in RET Fusion–Positive Non–Small-Cell Lung Cancer. *New England Journal of Medicine*, *383*(9), 813–824. https://doi.org/10.1056/NEJMoa2005653

Drosten, M., Guerra, C., & Barbacid, M. (2018). Genetically Engineered Mouse Models of K-Ras-Driven Lung and Pancreatic Tumors: Validation of Therapeutic Targets. *Cold Spring Harbor Perspectives in Medicine*, *8*(5), a031542. https://doi.org/10.1101/cshperspect.a031542

Dulos, J., Carven, G. J., van Boxtel, S. J., Evers, S., Driessen-Engels, L. J. A., Hobo, W., Gorecka, M. A., de Haan, A. F. J., Mulders, P., Punt, C. J. A., Jacobs, J. F. M., Schalken, J. A., Oosterwijk, E., van Eenennaam, H., & Boots, A. M. (2012). PD-1 Blockade Augments Th1 and Th17 and Suppresses Th2 Responses in Peripheral Blood From Patients With Prostate and Advanced Melanoma Cancer. *Journal of Immunotherapy*, *35*(2), 169–178. https://doi.org/10.1097/CJI.0b013e318247a4e7

DuPage, M., Dooley, A. L., & Jacks, T. (2009). Conditional mouse lung cancer models using adenoviral or lentiviral delivery of Cre recombinase. *Nature Protocols*, *4*(7), 1064–1072. https://doi.org/10.1038/nprot.2009.95

Duś, D., Budzyński, W., & Radzikowski, C. (1985). LL2 cell line derived from transplantable murine Lewis lung carcinoma--maintenance in vitro and growth characteristics. *Archivum Immunologiae et Therapiae Experimentalis*, *33*(6), 817–823.

El-Sayes, N., Vito, A., & Mossman, K. (2021). Tumor Heterogeneity: A Great Barrier in the Age of Cancer Immunotherapy. *Cancers*, *13*(4), 806. https://doi.org/10.3390/cancers13040806

Escors, D., Gato-Cañas, M., Zuazo, M., Arasanz, H., García-Granda, M. J., Vera, R., & Kochan, G. (2018). The intracellular signalosome of PD-L1 in cancer cells. *Signal Transduction and Targeted Therapy* 3 (1). https://doi.org/10.1038/s41392-018-0022-9

Ettinger, D. S., Wood, D. E., Akerley, W., Bazhenova, L. A., Borghaei, H., Camidge, D. R., Cheney, R. T., Chirieac, L. R., D'Amico, T. A., Demmy, T. L., Dilling, T. J., Dobelbower, M. C., Govindan, R., Grannis, F. W., Horn, L., Jahan, T. M., Komaki, R., Krug, L. M., Lackner, R. P., Lanuti, M., Lilenbaum, R., Lin, J., Loo, B. W., Martins, R., Otterson, G. A., Patel, J. D., Pisters, K. M., Reckamp, K., Riely, G. J., Rohren, E., Schild, S. E., Shapiro, T. A., Swanson, S. J., Tauer, K., Yang, S. C., Gregory, K. & Hughes, M. (2015). Non–Small Cell Lung Cancer, Version 6.2015. *Journal of the National Comprehensive Cancer Network*, *13*(5), 515–524. https://doi.org/10.6004/jnccn.2015.0071

Faria, S. L. (2014). Role of Radiotherapy in Metastatic Non-Small Cell Lung Cancer. *Frontiers in Oncology*, *4*. https://doi.org/10.3389/fonc.2014.00229

Ferrara, R., Auger, N., Auclin, E., & Besse, B. (2018). Clinical and Translational Implications of RET Rearrangements in Non–Small Cell Lung Cancer. *Journal of Thoracic Oncology*, *13*(1), 27–45. https://doi.org/10.1016/j.jtho.2017.10.021

Ferrara, R., Besse, B., Mezquita, L., Texier, M., Lahmar, J., Audigier-Valette, C., Tessonnier, L., Mazieres, J., Zalcman, G., Brosseau, S., Le Moulec, S., Leroy, L., Duchemann, B., Lefebvre, C., Veillon, R., Westeel, V., Koscielny, S., Champiat, S., Ferté, C., Planchard, D., Remon, J., Boucher, M. E., Gazzah, A., Adam, J., Bria, E., Tortora, G., Soria, J. C., & Caramella, C. (2018). Hyperprogressive Disease in Patients with Advanced Non-Small Cell Lung Cancer Treated with PD-1/PD-L1 Inhibitors or with Single-Agent Chemotherapy. *JAMA Oncology*, *4*(11), 1543–1552. https://doi.org/10.1001/jamaoncol.2018.3676

Fields, E. C., McGuire, W. P., Lin, L., & Temkin, S. M. (2017). Radiation treatment in women with ovarian cancer: Past, present, and future. In *Frontiers in Oncology 7* https://doi.org/10.3389/fonc.2017.00177

First Anti–PD-L1 Drug Approved for NSCLC. (2016). *Cancer Discovery*, *6*(12), OF1–OF1. https://doi.org/10.1158/2159-8290.CD-NB2016-143

Fitzgerald, B., Connolly, K. A., Cui, C., Fagerberg, E., Mariuzza, D. L., Hornick, N. I., Foster, G. G., William, I., Cheung, J. F., & Joshi, N. S. (2021). A mouse model for the study of anti-tumor T cell responses in Kras-driven lung adenocarcinoma. *Cell Reports Methods*, *1*(5), 100080. https://doi.org/10.1016/j.crmeth.2021.100080

Florez, N., Kiel, L., Riano, I., Patel, S., DeCarli, K., Dhawan, N., Franco, I., Odai-Afotey, A., Meza, K., Swami, N., Patel, J., & Sequist, L. V. (2024). Lung Cancer in Women: The Past, Present, and Future. *Clinical Lung Cancer*, *25*(1), 1–8. https://doi.org/10.1016/j.cllc.2023.10.007

Fois, S. S., Paliogiannis, P., Zinellu, A., Fois, A. G., Cossu, A., & Palmieri, G. (2021). Molecular Epidemiology of the Main Druggable Genetic Alterations in Non-Small Cell Lung Cancer. *International Journal of Molecular Sciences*, *22*(2), 612. https://doi.org/10.3390/ijms22020612

Fontaine, D. A., & Davis, D. B. (2016). Attention to Background Strain Is Essential for Metabolic Research: C57BL/6 and the International Knockout Mouse Consortium. *Diabetes*, *65*(1), 25–33. https://doi.org/10.2337/db15-0982

Frampton, G. M., Ali, S. M., Rosenzweig, M., Chmielecki, J., Lu, X., Bauer, T. M., Akimov, M., Bufill, J. A., Lee, C., Jentz, D., Hoover, R., Ou, S.-H. I., Salgia, R., Brennan, T., Chalmers, Z. R., Jaeger, S., Huang, A., Elvin, J. A., Erlich, R., Fichtenholtz, A., Gowen, K. A., Greenbowe, J., Johnson, A., Khaira, D., McMahon, C., Sanford, E. M., Roels, S., White, J., Greshock, J., Schlegel, R., Lipson, D., Yelensky, R., Morosini, D., Ross, J. S., Collisson, E., Peters, M., Stephens, P. J., & Miller, V. A. (2015). Activation of MET via Diverse Exon 14 Splicing Alterations Occurs in Multiple Tumor Types and Confers Clinical Sensitivity to MET Inhibitors. *Cancer Discovery*, *5*(8), 850–859. https://doi.org/10.1158/2159-8290.CD-15-0285

Friedlaender, A., Drilon, A., Banna, G. L., Peters, S., & Addeo, A. (2020). The METeoric rise of MET in lung cancer. *Cancer*, *126*(22), 4826–4837. https://doi.org/10.1002/cncr.33159

Friedlaender, A., Drilon, A., Weiss, G. J., Banna, G. L., & Addeo, A. (2020). KRAS as a druggable target in NSCLC: Rising like a phoenix after decades of development failures. *Cancer Treatment Reviews*, *85*, 101978. https://doi.org/10.1016/j.ctrv.2020.101978

Friedlaender, A., Perol, M., Banna, G. L., Parikh, K., & Addeo, A. (2024). Oncogenic alterations in advanced NSCLC: a molecular super-highway. *Biomarker Research*, *12*(1), 24. https://doi.org/10.1186/s40364-024-00566-0

Friedlaender, A., Subbiah, V., Russo, A., Banna, G. L., Malapelle, U., Rolfo, C., & Addeo, A. (2022). EGFR and HER2 exon 20 insertions in solid tumours: from biology to treatment. *Nature Reviews Clinical Oncology*, *19*(1), 51–69. https://doi.org/10.1038/s41571-021-00558-1

Fuchs, V., Sobarzo, A., Msamra, M., Kezerle, Y., Linde, L., Sevillya, G., Anoze, A., Refaely, Y., Cohen, A. Y., Melamed, I., Azriel, A., Shoukrun, R., Raviv, Y., Porgador, A., Peled, N., & Roisman, L. C. (2024). Personalizing non-small cell lung cancer treatment through patient-derived xenograft models: preclinical and clinical factors for consideration. *Clinical and Translational Oncology*, *26*(9), 2227–2239. https://doi.org/10.1007/s12094-024-03450-3

Fujiwara, Y., Mittra, A., Naqash, A. R., & Takebe, N. (2020). A review of mechanisms of resistance to immune checkpoint inhibitors and potential strategies for therapy. In *Cancer Drug Resistance* (Vol. 3, Issue 3, pp. 252–275). OAE Publishing Inc. https://doi.org/10.20517/cdr.2020.11

Fukuoka, M., Wu, Y.-L., Thongprasert, S., Sunpaweravong, P., Leong, S.-S., Sriuranpong, V., Chao, T.-Y., Nakagawa, K., Chu, D.-T., Saijo, N., Duffield, E. L., Rukazenkov, Y., Speake, G., Jiang, H., Armour, A. A., To, K.-F., Yang, J. C.-H., & Mok, T. S. K. (2011). Biomarker Analyses and Final Overall Survival Results From a Phase III, Randomized, Open-Label, First-Line Study of Gefitinib Versus Carboplatin/Paclitaxel in Clinically Selected Patients With Advanced Non–Small-Cell Lung Cancer in Asia (IPASS). *Journal of Clinical Oncology*, *29*(21), 2866–2874. https://doi.org/10.1200/JCO.2010.33.4235

Gainor, J. F., Curigliano, G., Kim, D.-W., Lee, D. H., Besse, B., Baik, C. S., Doebele, R. C., Cassier, P. A., Lopes, G., Tan, D. S. W., Garralda, E., Paz-Ares, L. G., Cho, B. C., Gadgeel, S. M., Thomas, M., Liu, S. V, Taylor, M. H., Mansfield, A. S., Zhu, V. W., Clifford, C., Zhang, H., Palmer, M., Green, J., Turner, C. D., & Subbiah, V. (2021). Pralsetinib for RET fusion-positive non-small-cell lung cancer (ARROW): a multi-cohort, open-label, phase 1/2 study. *The Lancet Oncology*, *22*(7), 959–969. https://doi.org/10.1016/S1470-2045(21)00247-3

Gainor, J. F., & Shaw, A. T. (2013). Novel Targets in Non-Small Cell Lung Cancer: ROS1 and RET Fusions. *The Oncologist*, *18*(7), 865–875. https://doi.org/10.1634/theoncologist.2013-0095

Gainor, J. F., Tseng, D., Yoda, S., Dagogo-Jack, I., Friboulet, L., Lin, J. J., Hubbeling, H. G., Dardaei, L., Farago, A. F., Schultz, K. R., Ferris, L. A., Piotrowska, Z., Hardwick, J., Huang, D., Mino-Kenudson, M., Iafrate, A. J., Hata, A. N., Yeap, B. Y., & Shaw, A. T. (2017). Patterns of Metastatic Spread and Mechanisms of Resistance to Crizotinib in ROS1-Positive Non–Small-Cell Lung Cancer. *JCO Precision Oncology*, *1*, 1–13. https://doi.org/10.1200/PO.17.00063

Gao, J., Aksoy, B. A., Dogrusoz, U., Dresdner, G., Gross, B., Sumer, S. O., Sun, Y., Jacobsen, A., Sinha, R., Larsson, E., Cerami, E., Sander, C., & Schultz, N. (2013). Integrative Analysis of Complex Cancer Genomics and Clinical Profiles Using the cBioPortal. *Science Signaling*, *6*(269). https://doi.org/10.1126/scisignal.2004088

Gao, J., Liang, Y., & Wang, L. (2022). Shaping Polarization Of Tumor-Associated Macrophages In Cancer Immunotherapy. *Frontiers in Immunology*, *13*. https://doi.org/10.3389/fimmu.2022.888713

Gao, L., Guo, Q., Li, X., Yang, X., Ni, H., Wang, T., Zhao, Q., Liu, H., Xing, Y., Xi, T., & Zheng, L. (2019). MiR-873/PD-L1 axis regulates the stemness of breast cancer cells. *EBioMedicine*, *41*, 395–407. https://doi.org/10.1016/j.ebiom.2019.02.034

Gao, Y., Yang, J., Cai, Y., Fu, S., Zhang, N., Fu, X., & Li, L. (2018). IFN-γ-mediated inhibition of lung cancer correlates with PD-L1 expression and is regulated by PI3K-AKT signaling. *International Journal of Cancer*, *143*(4), 931–943. https://doi.org/10.1002/ijc.31357

Garcia-Diaz, A., Shin, D. S., Moreno, B. H., Saco, J., Escuin-Ordinas, H., Rodriguez, G. A., Zaretsky, J. M., Sun, L., Hugo, W., Wang, X., Parisi, G., Saus, C. P., Torrejon, D. Y., Graeber, T. G., Comin-Anduix, B., Hu-Lieskovan, S., Damoiseaux, R., Lo, R. S., & Ribas, A. (2017). Interferon Receptor Signaling Pathways Regulating PD-L1 and PD-L2 Expression. *Cell Reports*, *19*(6), 1189–1201. https://doi.org/10.1016/j.celrep.2017.04.031

Garon, E. B., Rizvi, N. A., Hui, R., Leighl, N., Balmanoukian, A. S., Eder, J. P., Patnaik, A., Aggarwal, C., Gubens, M., Horn, L., Carcereny, E., Ahn, M.-J., Felip, E., Lee, J.-S., Hellmann, M. D., Hamid, O., Goldman, J. W., Soria, J.-C., Dolled-Filhart, M., Rutledge, R. Z., Zhang, J., Lunceford, J. K., Rangwala, R., Lubiniecki, G. M., Roach, C., Emancipator, K., & Gandhi, L. (2015). Pembrolizumab for the Treatment of Non–Small-Cell Lung Cancer. *New England Journal of Medicine*, *372*(21), 2018–2028. https://doi.org/10.1056/NEJMoa1501824

Garrido-Laguna, I., Uson, M., Rajeshkumar, N. V., Tan, A. C., de Oliveira, E., Karikari, C., Villaroel, M. C., Salomon, A., Taylor, G., Sharma, R., Hruban, R. H., Maitra, A., Laheru, D., Rubio-Viqueira, B., Jimeno, A., & Hidalgo, M. (2011). Tumor Engraftment in Nude Mice and Enrichment in Stroma- Related Gene Pathways Predict Poor Survival and Resistance to Gemcitabine in Patients with Pancreatic Cancer. *Clinical Cancer Research*, *17*(17), 5793–5800. https://doi.org/10.1158/1078-0432.CCR-11-0341

Gazdar, A. F. (2009). Activating and resistance mutations of EGFR in non-small-cell lung cancer: role in clinical response to EGFR tyrosine kinase inhibitors. *Oncogene*, *28*(S1), S24–S31. https://doi.org/10.1038/onc.2009.198

Gazdar, A. F., Gao, B., & Minna, J. D. (2010). Lung cancer cell lines: Useless artifacts or invaluable tools for medical science? *Lung Cancer*, *68*(3), 309–318. https://doi.org/10.1016/j.lungcan.2009.12.005

Gazdar, A. F., Girard, L., Lockwood, W. W., Lam, W. L., & Minna, J. D. (2010). Lung Cancer Cell Lines as Tools for Biomedical Discovery and Research. *JNCI: Journal of the National Cancer Institute*, *102*(17), 1310–1321. https://doi.org/10.1093/jnci/djq279

Gejman, R. S., Chang, A. Y., Jones, H. F., DiKun, K., Hakimi, A. A., Schietinger, A., & Scheinberg, D. A. (2018). Rejection of immunogenic tumor clones is limited by clonal fraction. *ELife*, *7*. https://doi.org/10.7554/eLife.41090

Gemelli, M., Noonan, D. M., Carlini, V., Pelosi, G., Barberis, M., Ricotta, R., & Albini, A. (2022). Overcoming Resistance to Checkpoint Inhibitors: Natural Killer Cells in Non-Small Cell Lung Cancer. *Frontiers in Oncology*, *12*, 886440. https://doi.org/10.3389/fonc.2022.886440

Gen, S., Tanaka, I., Morise, M., Koyama, J., Kodama, Y., Matsui, A., Miyazawa, A., Hase, T., Hibino, Y., Yokoyama, T., Kimura, T., Yoshida, N., Sato, M., & Hashimoto, N. (2022). Clinical efficacy of osimertinib in EGFR-mutant non-small cell lung cancer with distant metastasis. *BMC Cancer*, *22*(1), 654. https://doi.org/10.1186/s12885-022-09741-8

Gessi, S., Bencivenni, S., Battistello, E., Vincenzi, F., Colotta, V., Catarzi, D., Varano, F., Merighi, S., Borea, P. A., & Varani, K. (2017). Inhibition of A2A Adenosine Receptor Signaling in Cancer Cells Proliferation by the Novel Antagonist TP455. *Frontiers in Pharmacology*, *8*. https://doi.org/10.3389/fphar.2017.00888

Gettinger, S., Choi, J., Hastings, K., Truini, A., Datar, I., Sowell, R., Wurtz, A., Dong, W., Cai, G., Melnick, M. A., Du, V. Y., Schlessinger, J., Goldberg, S. B., Chiang, A., Sanmamed, M. F., Melero, I., Agorreta, J., Montuenga, L. M., Lifton, R., Rutledge, R. Z., Zhang, J., Lunceford, J. K., Rangwala, R., Lubiniecki, G. M., Roach, C., Emancipator, K., & Politi, K. (2017). Impaired HLA Class I Antigen Processing and Presentation as a Mechanism of Acquired Resistance to Immune Checkpoint Inhibitors in Lung Cancer. *Cancer Discovery*, *7*(12), 1420–1435. https://doi.org/10.1158/2159-8290.CD-17-0593

Ghandi, M., Huang, F. W., Jané-Valbuena, J., Kryukov, G. V., Lo, C. C., McDonald, E. R., Barretina, J., Gelfand, E. T., Bielski, C. M., Li, H., Hu, K., Andreev-Drakhlin, A. Y., Kim, J., Hess, J. M., Haas, B. J., Aguet, F., Weir, B. A., Rothberg, M. V., Paolella, B. R., Lawrence, M. S., Akbani, R., Lu, Y., Tiv, H. L., Gokhale, P. C., de Weck, A., Mansour, A. A., Oh, C., Shih, J., Hadi, K., Rosen, Y., Bistline, J., Venkatesan, K., Reddy, A., Sonkin, D., Liu, M., Lehar, J., Korn, J. M., Porter, D. A., Jones, M. D., Golji, J., Caponigro, G., Taylor, J. E., Dunning, C. M., Creech, A. L., Warren, A. C., McFarland, J. M., Zamanighomi, M., Kauffmann, A., Stransky, N., Imielinski, M., Maruvka, Y. E., Cherniack, A. D., Tsherniak, A., Vazquez, F. Jaffe, J. D., Lane, A. A., Weinstock, D. M., Johannessen, C. M., Morrissey, M. P., Stegmeier, F., Schlegel, R., Hahn, W. C., Getz, G., Mills, G. B., Boehm, J. S., Golub, T. R., Garraway, L. A., & Sellers, W. R. (2019). Next-generation characterization of the Cancer Cell Line Encyclopedia. *Nature*, *569*(7757), 503–508. https://doi.org/10.1038/s41586-019-1186-3

Ghimire, B., Maroni, R., Vulkan, D., Shah, Z., Gaynor, E., Timoney, M., Jones, L., Arvanitis, R., Ledson, M., Lukehirst, L., Rutherford, P., Clarke, F., Gardner, K., Marcus, M. W., Hill, S., Fidoe, D., Mason, S., Smith, S. G., Quaife, S. L., Fitzgerald, K., Poirier, V., Duffy, S. W., & Field, J. K. (2019). Evaluation of a health service adopting proactive approach to reduce high risk of lung cancer: The Liverpool Healthy Lung Programme. *Lung Cancer*, *134*, 66–71. https://doi.org/10.1016/j.lungcan.2019.05.026

Giaj-Levra, N., Borghetti, P., Bruni, A., Ciammella, P., Cuccia, F., Fozza, A., Franceschini, D., Scotti, V., Vagge, S., & Alongi, F. (2020). Current radiotherapy techniques in NSCLC: challenges and potential solutions. *Expert Review of Anticancer Therapy*, *20*(5), 387–402. https://doi.org/10.1080/14737140.2020.1760094

Gibson, A. J. W., Pabani, A., Dean, M. L., Martos, G., Cheung, W. Y., & Navani, V. (2023). Real-World Treatment Patterns and Effectiveness of Targeted and Immune Checkpoint Inhibitor-Based Systemic Therapy in BRAF Mutation-Positive NSCLC. *JTO Clinical and Research Reports*, *4*(3), 100460. https://doi.org/10.1016/j.jtocrr.2022.100460

Girard, N., Galland-Girodet, S., Avrillon, V., Besse, B., Duruisseaux, M., Cadranel, J., Otto, J., Prevost, A., Roch, B., Bennouna, J., Bouledrak, K., Coudurier, M., Egenod, T., Lamy, R., Ricordel, C., Moro-Sibilot, D., Odier, L., Tillon-Strozyk, J., Zalcman, G., Missy, P., Westeel, V., & Baldacci, S. (2022). Lorlatinib for advanced ROS1+ non-small-cell lung cancer: results of the IFCT-1803 LORLATU study. *ESMO Open*, *7*(2), 100418. https://doi.org/10.1016/j.esmoop.2022.100418

Giusti, V., Ruzzi, F., Landuzzi, L., Ianzano, M. L., Laranga, R., Nironi, E., Scalambra, L., Nicoletti, G., De Giovanni, C., Olivero, M., Arigoni, M., Calogero, R., Nanni, P., Palladini, A., & Lollini, P. L. (2021). Evolution of HER2-positive mammary carcinoma: HER2 loss reveals claudin-low traits in cancer progression. *Oncogenesis*, *10*(11). https://doi.org/10.1038/s41389-021-00360-9

Glabman, R. A., Choyke, P. L., & Sato, N. (2022). Cancer-Associated Fibroblasts: Tumorigenicity and Targeting for Cancer Therapy. *Cancers*, *14*(16), 3906. https://doi.org/10.3390/cancers14163906

Gohy, S., Carlier, F. M., Fregimilicka, C., Detry, B., Lecocq, M., Ladjemi, M. Z., Verleden, S., Hoton, D., Weynand, B., Bouzin, C., & Pilette, C. (2019). Altered generation of ciliated cells in chronic obstructive pulmonary disease. *Scientific Reports*, *9*(1), 17963. https://doi.org/10.1038/s41598-019-54292-x

Goldstraw, P., Chansky, K., Crowley, J., Rami-Porta, R., Asamura, H., Eberhardt, W. E. E., Nicholson, A. G., Groome, P., Mitchell, A., & Bolejack, V (2016). The IASLC Lung Cancer Staging Project: Proposals for Revision of the TNM Stage Groupings in the Forthcoming (Eighth) Edition of the TNM Classification for Lung Cancer. *Journal of Thoracic Oncology*, *11*(1), 39–51. https://doi.org/10.1016/j.jtho.2015.09.009

Gong, B., Oh-hara, T., Fujita, N., & Katayama, R. (2018). 3D culture system containing gellan gum restores oncogene dependence in ROS1 rearrangements non-small cell lung cancer. *Biochemical and Biophysical Research Communications*, *501*(2), 527–533. https://doi.org/10.1016/j.bbrc.2018.05.031

Goronzy, J. J., & Weyand, C. M. (2017). Successful and Maladaptive T Cell Aging. *Immunity*, *46*(3), 364–378. https://doi.org/10.1016/j.immuni.2017.03.010

Grant, M. J., Aredo, J. V., Starrett, J. H., Stockhammer, P., van Alderwerelt van Rosenburgh, I. K., Wurtz, A., Piper-Valillo, A. J., Piotrowska, Z., Falcon, C., Yu, H. A., Aggarwal, C., Scholes, D., Patil, T., Nguyen, C., Phadke, M., Li, F.-Y., Neal, J., Lemmon, M. A., Walther, Z., Politi, K., & Goldberg, S. B. (2023). Efficacy of Osimertinib in Patients with Lung Cancer Positive for Uncommon EGFR Exon 19 Deletion Mutations. *Clinical Cancer Research*, *29*(11), 2123–2130. https://doi.org/10.1158/1078-0432.CCR-22-3497

Greillier, L., Tomasini, P., & Barlesi, F. (2018). The clinical utility of tumor mutational burden in non-small cell lung cancer. *Translational Lung Cancer Research*, *7*(5), 639–646. https://doi.org/10.21037/tlcr.2018.10.08

Gristina, V., Malapelle, U., Galvano, A., Pisapia, P., Pepe, F., Rolfo, C., Tortorici, S., Bazan, V., Troncone, G., & Russo, A. (2020). The significance of epidermal growth factor receptor uncommon mutations in non-small cell lung cancer: A systematic review and critical appraisal. *Cancer Treatment Reviews*, *85*, 101994. https://doi.org/10.1016/j.ctrv.2020.101994

Grossman, J. E., Vasudevan, D., Joyce, C. E., & Hildago, M. (2021). Is PD-L1 a consistent biomarker for anti-PD-1 therapy? The model of balstilimab in a virally-driven tumor. In *Oncogene* (Vol. 40, Issue 8, pp. 1393–1395). Springer Nature. https://doi.org/10.1038/s41388-020-01611-6

Guaitoli, G., Bertolini, F., Bettelli, S., Manfredini, S., Maur, M., Trudu, L., Aramini, B., Masciale, V., Grisendi, G., Dominici, M., & Barbieri, F. (2021). Deepening the Knowledge of ROS1 Rearrangements in Non-Small Cell Lung Cancer: Diagnosis, Treatment, Resistance and Concomitant Alterations. *International Journal of Molecular Sciences*, *22*(23), 12867. https://doi.org/10.3390/ijms222312867

Guo, Q., Liu, L., Chen, Z., Fan, Y., Zhou, Y., Yuan, Z., & Zhang, W. (2022). Current treatments for non-small cell lung cancer. *Frontiers in Oncology*, *12*. https://doi.org/10.3389/fonc.2022.945102

Gutierrez, C., & Schiff, R. (2011). HER 2: Biology, Detection, and Clinical Implications. *Archives of Pathology & Laboratory Medicine*, *135*(1), 55–62. https://doi.org/10.1043/2010-0454-RAR.1

Gutierrez, W. R., Scherer, A., McGivney, G. R., Brockman, Q. R., Knepper-Adrian, V., Laverty, E. A., Roughton, G. A., & Dodd, R. D. (2021). Divergent immune landscapes of primary and syngeneic Kras-driven mouse tumor models. *Scientific Reports*, *11*(1), 1098. https://doi.org/10.1038/s41598-020-80216-1

Haddad, M., & Sharma, S. (2024). Physiology, Lung. In: *StatPearls [Internet]. Treasure Island (FL): StatPearls*. PMID: 31424761

Hamamoto, J., Yasuda, H., Aizawa, K., Nishino, M., Nukaga, S., Hirano, T., Kawada, I., Naoki, K., Betsuyaku, T., & Soejima, K. (2017). Non-small cell lung cancer PC-9 cells exhibit increased sensitivity to gemcitabine and vinorelbine upon acquiring resistance to EGFR-tyrosine kinase inhibitors. *Oncology Letters*, *14*(3), 3559–3565. https://doi.org/10.3892/ol.2017.6591

Hancock, J. F. (2003). Ras proteins: different signals from different locations. *Nature Reviews Molecular Cell Biology*, *4*(5), 373–385. https://doi.org/10.1038/nrm1105

Haut, B., Karamaoun, C., Mauroy, B., & Sobac, B. (2023). Water and heat exchanges in mammalian lungs. *Scientific Reports*, *13*(1), 6636. https://doi.org/10.1038/s41598-023-33052-y

Hayes, S. A., Hudson, A. L., Clarke, S. J., Molloy, M. P., & Howell, V. M. (2014). From mice to men: GEMMs as trial patients for new NSCLC therapies. *Seminars in Cell & Developmental Biology*, *27*, 118–127. https://doi.org/10.1016/j.semcdb.2014.04.002

Hayes, T. K., Aquilanti, E., Persky, N. S., Yang, X., Kim, E. E., Brenan, L., Goodale, A. B., Alan, D., Sharpe, T., Shue, R. E., Westlake, L., Golomb, L., Silverman, B. R., Morris, M. D., Fisher, T. R., Beyene, E., Li, Y. Y., Cherniack, A. D., Piccioni, F., Hicks, J. K., Chi, A. S., Cahill, D. P., Dietrich, J., Batchelor, T. T., Root, D. E., Johannessen, C. M., & Meyerson, M. (2024). Comprehensive mutational scanning of EGFR reveals TKI sensitivities of extracellular domain mutants. *Nature Communications*, *15*(1), 2742. https://doi.org/10.1038/s41467-024-45594-4

He, S., Gui, J., Xiong, K., Chen, M., Gao, H., & Fu, Y. (2022). A roadmap to pulmonary delivery strategies for the treatment of infectious lung diseases. *Journal of Nanobiotechnology*, *20*(1), 101. https://doi.org/10.1186/s12951-022-01307-x

Heid, J., Affolter, A., Jakob, Y., Kern, J., Rotter, N., Tenschert, E., & Lammert, A. (2022). 3D cell culture alters signal transduction and drug response in head and neck squamous cell carcinoma. *Oncology Letters*, *23*(6), 177. https://doi.org/10.3892/ol.2022.13297

Heineman, D. J., Daniels, J. M., & Schreurs, W. H. (2017). Clinical staging of NSCLC: current evidence and implications for adjuvant chemotherapy. *Therapeutic Advances in Medical Oncology*, *9*(9), 599–609. https://doi.org/10.1177/1758834017722746

Hellmann, M. D., Paz-Ares, L., Bernabe Caro, R., Zurawski, B., Kim, S.-W., Carcereny Costa, E., Park, K., Alexandru, A., Lupinacci, L., de la Mora Jimenez, E., Sakai, H., Albert, I., Vergnenegre, A., Peters, S., Syrigos, K., Barlesi, F., Reck, M., Borghaei, H., Brahmer, J. R., O'Byrne, K. J., Geese, W. J., Bhagavatheeswaran, P., Rabindran, S. K., Kasinathan, R. S., Nathan, F. E., & Ramalingam, S. S. (2019). Nivolumab plus Ipilimumab in Advanced Non–Small-Cell Lung Cancer. *New England Journal of Medicine*, *381*(21), 2020–2031. https://doi.org/10.1056/NEJMoa1910231

Herbst, R. S., Garon, E. B., Kim, D.-W., Cho, B. C., Gervais, R., Perez-Gracia, J. L., Han, J.-Y., Majem, M., Forster, M. D., Monnet, I., Novello, S., Gubens, M. A., Boyer, M., Su, W.-C., Samkari, A., Jensen, E. H., Kobie, J., Piperdi, B., & Baas, P. (2021). Five Year Survival Update From KEYNOTE-010: Pembrolizumab Versus Docetaxel for Previously Treated, Programmed Death-Ligand 1–Positive Advanced NSCLC. *Journal of Thoracic Oncology*, *16*(10), 1718–1732. https://doi.org/10.1016/j.jtho.2021.05.001

Hidalgo, M., Amant, F., Biankin, A. V., Budinská, E., Byrne, A. T., Caldas, C., Clarke, R. B., de Jong, S., Jonkers, J., Mælandsmo, G. M., Roman-Roman, S., Seoane, J., Trusolino, L., & Villanueva, A. (2014). Patient-Derived Xenograft Models: An Emerging Platform for Translational Cancer Research. *Cancer Discovery*, *4*(9), 998–1013. https://doi.org/10.1158/2159-8290.CD-14-0001

Hidalgo, M., Bruckheimer, E., Rajeshkumar, N. V., Garrido-Laguna, I., De Oliveira, E., Rubio-Viqueira, B., Strawn, S., Wick, M. J., Martell, J., & Sidransky, D. (2011). A Pilot Clinical Study of Treatment Guided by Personalized Tumorgrafts in Patients with Advanced Cancer. *Molecular Cancer Therapeutics*, *10*(8), 1311–1316. https://doi.org/10.1158/1535-7163.MCT-11-0233

Hiltbrunner, S., Cords, L., Kasser, S., Freiberger, S. N., Kreutzer, S., Toussaint, N. C., Grob, L., Opitz, I., Messerli, M., Zoche, M., Soltermann, A., Rechsteiner, M., van den Broek, M., Bodenmiller, B., & Curioni-Fontecedro, A. (2023). Acquired resistance to anti-PD1 therapy in patients with NSCLC associates with immunosuppressive T cell phenotype. *Nature Communications*, *14*(1). https://doi.org/10.1038/s41467-023-40745-5

Hoffner, B., & Benchich, K. (2018). Trametinib: A Targeted Therapy in Metastatic Melanoma. *Journal of the Advanced Practitioner in Oncology*, *9*(7), 741–745.

Horn, L., Wang, Z., Wu, G., Poddubskaya, E., Mok, T., Reck, M., Wakelee, H., Chiappori, A. A., Lee, D. H., Breder, V., Orlov, S., Cicin, I., Cheng, Y., Liu, Y., Fan, Y., Whisenant, J. G., Zhou, Y., Oertel, V., Harrow, K., Liang, C., Mao, L., Selvaggi, G., & Wu, Y.-L. (2021). Ensartinib vs Crizotinib for Patients With Anaplastic Lymphoma Kinase−Positive Non–Small Cell Lung Cancer. *JAMA Oncology*, *7*(11), 1617. https://doi.org/10.1001/jamaoncol.2021.3523

Hsu, J. L., & Hung, M.-C. (2016). The role of HER2, EGFR, and other receptor tyrosine kinases in breast cancer. *Cancer and Metastasis Reviews*, *35*(4), 575–588. https://doi.org/10.1007/s10555-016-9649-6

Huang, L., Guo, Z., Wang, F., & Fu, L. (2021). KRAS mutation: from undruggable to druggable in cancer. *Signal Transduction and Targeted Therapy*, *6*(1), 386. https://doi.org/10.1038/s41392-021-00780-4

Hudson, K., Cross, N., Jordan-Mahy, N., & Leyland, R. (2020). The Extrinsic and Intrinsic Roles of PD-L1 and Its Receptor PD-1: Implications for Immunotherapy Treatment. In *Frontiers in Immunology* (Vol. 11). Frontiers Media S.A. https://doi.org/10.3389/fimmu.2020.568931

Hui, C., Qu, V., Wang, J.-Y., von Eyben, R., Chang, Y.-C., Chiang, P.-L., Liang, C.-H., Lu, J.-T., Li, G., Hayden-Gephart, M., Wakelee, H., Neal, J., Ramchandran, K., Das, M., Nagpal, S., Soltys, S., Myall, N., & Pollom, E. (2022). Local control of brain metastases with osimertinib alone in patients with EGFR-mutant non-small cell lung cancer. *Journal of Neuro-Oncology*, *160*(1), 233–240. https://doi.org/10.1007/s11060-022-04145-x

Huo, K.-G., Notsuda, H., Fang, Z., Liu, N. F., Gebregiworgis, T., Li, Q., Pham, N.-A., Li, M., Liu, N., Shepherd, F. A., Marshall, C. B., Ikura, M., Moghal, N., & Tsao, M.-S. (2022). Lung Cancer Driven by BRAFG469V Mutation Is Targetable by EGFR Kinase Inhibitors. *Journal of Thoracic Oncology*, *17*(2), 277–288. https://doi.org/10.1016/j.jtho.2021.09.008

Hussain, M. R. M., Baig, M., Mohamoud, H. S. A., Ulhaq, Z., Hoessli, D. C., Khogeer, G. S., Al-Sayed, R. R., & Al-Aama, J. Y. (2015). BRAF gene: From human cancers to developmental syndromes. *Saudi Journal of Biological Sciences*, *22*(4), 359–373. https://doi.org/10.1016/j.sjbs.2014.10.002

Hynds, R. E., Frese, K. K., Pearce, D. R., Grönroos, E., Dive, C., & Swanton, C. (2021). Progress towards non-small-cell lung cancer models that represent clinical evolutionary trajectories. *Open Biology*, *11*(1). https://doi.org/10.1098/rsob.200247

Hynes, N. E., & Lane, H. A. (2005). ERBB receptors and cancer: the complexity of targeted inhibitors. *Nature Reviews Cancer*, *5*(5), 341–354. https://doi.org/10.1038/nrc1609

Idrisova, K. F., Simon, H.-U., & Gomzikova, M. O. (2022). Role of Patient-Derived Models of Cancer in Translational Oncology. *Cancers*, *15*(1), 139. https://doi.org/10.3390/cancers15010139

Imamura, F., Inoue, T., Kunimasa, K., Kubota, A., Kuhara, H., Tamiya, M., Nishino, K., Kimura, M., Kuno, K., Kawachi, H., & Kumagai, T. (2020). Switching from first or Second Generation EGFR-TKI to Osimertinib in *EGFR* Mutation-Positive NSCLC. *Lung Cancer Management*, *9*(2). https://doi.org/10.2217/lmt-2020-0005

Inamura, K. (2017). Lung Cancer: Understanding Its Molecular Pathology and the 2015 WHO Classification. *Frontiers in Oncology*, *7*. https://doi.org/10.3389/fonc.2017.00193

Indini, A., Rijavec, E., Bareggi, C., & Grossi, F. (2020). Novel treatment strategies for early-stage lung cancer: the oncologist's perspective. *Journal of Thoracic Disease*, *12*(6), 3390–3398. https://doi.org/10.21037/jtd.2020.02.46

Inoue, M., Toki, H., Matsui, J., Togashi, Y., Dobashi, A., Fukumura, R., Gondo, Y., Minowa, O., Tanaka, N., Mori, S., Takeuchi, K., & Noda, T. (2016). Mouse models for ROS1-fusion-positive lung cancers and their application to the analysis of multikinase inhibitor efficiency. *Carcinogenesis*, *37*(5), 452–460. https://doi.org/10.1093/carcin/bgw028

International Agency for Research on Cancer - World Health Organization. (n.d.). *GLOBOCAN - Cancer Today*. Retrieved October 25, 2024, from https://gco.iarc.fr/today/en/dataviz/pie?mode=cancer&group_populations=1

Ivashkiv, L. B. (2018). IFNγ: signalling, epigenetics and roles in immunity, metabolism, disease and cancer immunotherapy. In *Nature Reviews Immunology* (Vol. 18, Issue 9, pp. 545–558). Nature Publishing Group. https://doi.org/10.1038/s41577-018-0029-z

Jackson, E. L., Olive, K. P., Tuveson, D. A., Bronson, R., Crowley, D., Brown, M., & Jacks, T. (2005). The Differential Effects of Mutant p53 Alleles on Advanced Murine Lung Cancer. *Cancer Research*, *65*(22), 10280–10288. https://doi.org/10.1158/0008-5472.CAN-05-2193

Jackson, E. L., Willis, N., Mercer, K., Bronson, R. T., Crowley, D., Montoya, R., Jacks, T., & Tuveson, D. A. (2001). Analysis of lung tumor initiation and progression using conditional expression of oncogenic K-ras. *Genes & Development*, *15*(24), 3243–3248. https://doi.org/10.1101/gad.943001

Jänne, P. A., Riely, G. J., Gadgeel, S. M., Heist, R. S., Ou, S.-H. I., Pacheco, J. M., Johnson, M. L., Sabari, J. K., Leventakos, K., Yau, E., Bazhenova, L., Negrao, M. V., Pennell, N. A., Zhang, J., Anderes, K., Der-Torossian, H., Kheoh, T., Velastegui, K., Yan, X., Christensen, J. G., Chao, R. C., & Spira, A. I. (2022). Adagrasib in Non–Small-Cell Lung Cancer Harboring a KRAS G12C Mutation. *New England Journal of Medicine*, *387*(2), 120–131. https://doi.org/10.1056/NEJMoa2204619

Jenkins, R. W., Barbie, D. A., & Flaherty, K. T. (2018). Mechanisms of resistance to immune checkpoint inhibitors. *British Journal of Cancer*, *118*(1), 9–16. https://doi.org/10.1038/bjc.2017.434

Jeon, D. S., Kim, H. C., Kim, S. H., Kim, T.-J., Kim, H. K., Moon, M. H., Beck, K. S., Suh, Y.-G., Song, C., Ahn, J. S., Lee, J. E., Lim, J. U., Jeon, J. H., Jung, K.-W., Jung, C. Y., Cho, J. S., Choi, Y.-D., Hwang, S.-S., & Choi, C.-M. (2023). Five-Year Overall Survival and Prognostic Factors in Patients with Lung Cancer: Results from the Korean Association of Lung Cancer Registry (KALC-R) 2015. *Cancer Research and Treatment*, *55*(1), 103–111. https://doi.org/10.4143/crt.2022.264

Jeppesen, S. S., Schytte, T., Jensen, H. R., Brink, C., & Hansen, O. (2013). Stereotactic body radiation therapy versus conventional radiation therapy in patients with early stage non-small cell lung cancer: An updated retrospective study on local failure and survival rates. *Acta Oncologica*, *52*(7), 1552–1558. https://doi.org/10.3109/0284186X.2013.813635

Ji, H., Ramsey, M. R., Hayes, D. N., Fan, C., McNamara, K., Kozlowski, P., Torrice, C., Wu, M. C., Shimamura, T., Perera, S. A., Liang, M.-C., Cai, D., Naumov, G. N., Bao, L., Contreras, C. M., Li, D., Chen, L.,

Krishnamurthy, J., Koivunen, J., Chirieac, L. R., Padera, R. F., Bronson, R. T., Lindeman, N. I., Christiani, D. C., Lin, X., Shapiro, G. I., Jänne, P. A., Johnson, B. E., Meyerson, M., Kwiatkowski, D. J., Castrillon, D. H., Bardeesy, N., Sharpless, N. E., & Wong, K.-K. (2007). LKB1 modulates lung cancer differentiation and metastasis. *Nature*, *448*(7155), 807–810. https://doi.org/10.1038/nature06030

Jia, W., Gao, Q., Han, A., Zhu, H., & Yu, J. (2019). The potential mechanism, recognition and clinical significance of tumor pseudoprogression after immunotherapy. *Cancer Biology & Medicine*, *16*(4), 655–670. https://doi.org/10.20892/j.issn.2095-3941.2019.0144

Jiang, Y., Zhao, J., Zhang, Y., Li, K., Li, T., Chen, X., Zhao, S., Zhao, S., Liu, K., & Dong, Z. (2018). Establishment of lung cancer patient-derived xenograft models and primary cell lines for lung cancer study. *Journal of Translational Medicine*, *16*(1), 138. https://doi.org/10.1186/s12967-018-1516-5

Jin, J., Yoshimura, K., Sewastjanow-Silva, M., Song, S., & Ajani, J. A. (2023). Challenges and Prospects of Patient-Derived Xenografts for Cancer Research. *Cancers*, *15*(17), 4352. https://doi.org/10.3390/cancers15174352

Johnson, D. B., Nebhan, C. A., Moslehi, J. J., & Balko, J. M. (2022). Immune-checkpoint inhibitors: long-term implications of toxicity. *Nature Reviews Clinical Oncology*, *19*(4), 254–267. https://doi.org/10.1038/s41571-022-00600-w

Johnson, D. E., O'Keefe, R. A., & Grandis, J. R. (2018). Targeting the IL-6/JAK/STAT3 signalling axis in cancer. *Nature Reviews Clinical Oncology*, *15*(4), 234–248. https://doi.org/10.1038/nrclinonc.2018.8

Johnson, L., Mercer, K., Greenbaum, D., Bronson, R. T., Crowley, D., Tuveson, D. A., & Jacks, T. (2001). Somatic activation of the K-ras oncogene causes early onset lung cancer in mice. *Nature*, *410*(6832), 1111–1116. https://doi.org/10.1038/35074129

Jones-Freeman, B., & Starkey, M. R. (2020). Bronchioalveolar stem cells in lung repair, regeneration and disease. *The Journal of Pathology*, *252*(3), 219–226. https://doi.org/10.1002/path.5527

Jordan, A. R., Racine, R. R., Hennig, M. J. P., & Lokeshwar, V. B. (2015). The Role of CD44 in Disease Pathophysiology and Targeted Treatment. *Frontiers in Immunology*, *6*. https://doi.org/10.3389/fimmu.2015.00182

Jorgovanovic, D., Song, M., Wang, L., & Zhang, Y. (2020). Roles of IFN-γ in tumor progression and regression: A review. In *Biomarker Research* (Vol. 8, Issue 1). BioMed Central Ltd. https://doi.org/10.1186/s40364-020-00228-x

Joseph, D., Puttaswamy, R. K., & Krovvidi, H. (2013). Non-respiratory functions of the lung. *Continuing Education in Anaesthesia Critical Care & Pain*, *13*(3), 98–102. https://doi.org/10.1093/bjaceaccp/mks060

Judd, J., Abdel Karim, N., Khan, H., Naqash, A. R., Baca, Y., Xiu, J., VanderWalde, A. M., Mamdani, H., Raez, L. E., Nagasaka, M., Pai, S. G., Socinski, M. A., Nieva, J. J., Kim, C., Wozniak, A. J., Ikpeazu, C., de Lima Lopes, G., Spira, A. I., Korn, W. M., Kim, E. S., Liu, S. V., & Borghaei, H. (2021). Characterization of KRAS Mutation Subtypes in Non–small Cell Lung Cancer. *Molecular Cancer Therapeutics*, *20*(12), 2577–2584. https://doi.org/10.1158/1535-7163.MCT-21-0201

Juneja, V. R., McGuire, K. A., Manguso, R. T., LaFleur, M. W., Collins, N., Haining, W. N., Freeman, G. J., & Sharpe, A. H. (2017). PD-L1 on tumor cells is sufficient for immune evasion in immunogenic tumors and inhibits CD8 T cell cytotoxicity. *Journal of Experimental Medicine*, *214*(4), 895–904. https://doi.org/10.1084/jem.20160801

Jung, J. (2014). Human Tumor Xenograft Models for Preclinical Assessment of Anticancer Drug Development. *Toxicological Research*, *30*(1), 1–5. https://doi.org/10.5487/TR.2014.30.1.001

Kajiwara, N., Akata, S., Uchida, O., Usuda, J., Ohira, T., Kawate, N., & Ikeda, N. (2010). Cine MRI enables better therapeutic planning than CT in cases of possible lung cancer chest wall invasion. *Lung Cancer*, *69*(2), 203–208. https://doi.org/10.1016/j.lungcan.2009.10.016

Kalbasi, A., & Ribas, A. (2020). Tumour-intrinsic resistance to immune checkpoint blockade. *Nature Reviews Immunology*, *20*(1), 25–39. https://doi.org/10.1038/s41577-019-0218-4

Kalemkerian, G. P., Narula, N., Kennedy, E. B., Biermann, W. A., Donington, J., Leighl, N. B., Lew, M., Pantelas, J., Ramalingam, S. S., Reck, M., Saqi, A., Simoff, M., Singh, N., & Sundaram, B. (2018). Molecular Testing Guideline for the Selection of Patients With Lung Cancer for Treatment With Targeted Tyrosine Kinase Inhibitors: American Society of Clinical Oncology Endorsement of the College of American Pathologists/International Association for the Study of Lung Cancer/Association for Molecular Pathology Clinical Practice Guideline Update. *Journal of Clinical Oncology*, *36*(9), 911–919. https://doi.org/10.1200/JCO.2017.76.7293

Kalvapudi, S., Vedire, Y., Yendamuri, S., & Barbi, J. (2023). Neoadjuvant therapy in non-small cell lung cancer: basis, promise, and challenges. *Frontiers in Oncology*, *13*. https://doi.org/10.3389/fonc.2023.1286104

Karachaliou, N., Pilotto, S., Lazzari, C., Bria, E., de Marinis, F., & Rosel, R., (2016). Cellular and molecular biology of small cell lung cancer: an overview. *Translational Lung Cancer*, *5*(1).

Karoulia, Z., Wu, Y., Ahmed, T. A., Xin, Q., Bollard, J., Krepler, C., Wu, X., Zhang, C., Bollag, G., Herlyn, M., Fagin, J. A., Lujambio, A., Gavathiotis, E., & Poulikakos, P. I. (2016). An Integrated Model of RAF Inhibitor Action Predicts Inhibitor Activity against Oncogenic BRAF Signaling. *Cancer Cell*, *30*(3), 485–498. https://doi.org/10.1016/j.ccell.2016.06.024

Kas, B., Talbot, H., Ferrara, R., Richard, C., Lamarque, J.-P., Pitre-Champagnat, S., Planchard, D., Balleyguier, C., Besse, B., Mezquita, L., Lassau, N., & Caramella, C. (2020). Clarification of Definitions of Hyperprogressive Disease During Immunotherapy for Non–Small Cell Lung Cancer. *JAMA Oncology*, *6*(7). https://doi.org/10.1001/jamaoncol.2020.1634

Katayama, Y., Yamada, T., Tanimura, K., Tokuda, S., Morimoto, K., Hirai, S., Matsui, Y., Nakamura, R., Ishida, M., Kawachi, H., Yoneda, K., Hosoya, K., Tsuji, T., Ozasa, H., Yoshimura, A., Iwasaku, M., Kim, Y. H., Horinaka, M., Sakai, T., Utsumi, T., Shiotsu, S., Takeda, T., Katayama, R., & Takayama, K. (2023). Adaptive resistance to lorlatinib via EGFR signaling in ALK-rearranged lung cancer. *Npj Precision Oncology*, *7*(1), 12. https://doi.org/10.1038/s41698-023-00350-7

Kato, S., Goodman, A., Walavalkar, V., Barkauskas, D. A., Sharabi, A., & Kurzrock, R. (2017). Hyperprogressors after immunotherapy: Analysis of genomic alterations associated with accelerated growth rate. *Clinical Cancer Research*, *23*(15), 4242–4250. https://doi.org/10.1158/1078-0432.CCR-16-3133

Kazandjian, D., Blumenthal, G. M., Yuan, W., He, K., Keegan, P., & Pazdur, R. (2016). FDA Approval of Gefitinib for the Treatment of Patients with Metastatic EGFR Mutation–Positive Non–Small Cell Lung Cancer. *Clinical Cancer Research*, *22*(6), 1307–1312. https://doi.org/10.1158/1078-0432.CCR-15-2266

Kazandjian, D., Suzman, D. L., Blumenthal, G., Mushti, S., He, K., Libeg, M., Keegan, P., & Pazdur, R. (2016). FDA Approval Summary: Nivolumab for the Treatment of Metastatic Non-Small Cell Lung Cancer With Progression On or After Platinum-Based Chemotherapy. *The Oncologist*, *21*(5), 634–642. https://doi.org/10.1634/theoncologist.2015-0507

Kerr, K. M., & Hirsch, F. R. (2016). Programmed Death Ligand-1 Immunohistochemistry: Friend or Foe? *Archives of Pathology & Laboratory Medicine*, *140*(4), 326–331. https://doi.org/10.5858/arpa.2015-0522-SA

Kerr, K. M., Tsao, M.-S., Nicholson, A. G., Yatabe, Y., Wistuba, I. I., & Hirsch, F. R. (2015). Programmed Death-Ligand 1 Immunohistochemistry in Lung Cancer: In what state is this art? *Journal of Thoracic Oncology*, *10*(7), 985–989. https://doi.org/10.1097/JTO.0000000000000526

Kersten, K., de Visser, K. E., van Miltenburg, M. H., & Jonkers, J. (2017). Genetically engineered mouse models in oncology research and cancer medicine. *EMBO Molecular Medicine*, *9*(2), 137–153. https://doi.org/10.15252/emmm.201606857

Khan, F., Bell, G., Antony, J., Palmer, M., Balter, P., Bucci, K., & Chapman, M. J. (2009). The Use of 4DCT to Reduce Lung Dose: A Dosimetric Analysis. *Medical Dosimetry*, *34*(4), 273–278. https://doi.org/10.1016/j.meddos.2008.11.005

Kim, D.-S., Ji, W., Kim, D. H., Choi, Y. J., Im, K., Lee, C. W., Cho, J., Min, J., Woo, D.-C., Choi, C.-M., Lee, J. C., Sung, Y. H., & Rho, J. K. (2022). Generation of genetically engineered mice for lung cancer with mutant EGFR. *Biochemical and Biophysical Research Communications*, *632*, 85–91. https://doi.org/10.1016/j.bbrc.2022.09.104

Kim, E. S., & Salgia, R. (2009). MET Pathway as a Therapeutic Target. *Journal of Thoracic Oncology*, *4*(4), 444–447. https://doi.org/10.1097/JTO.0b013e31819d6f91

Kim, S. Y., & Halmos, B. (2020). Choosing the best first-line therapy: NSCLC with no actionable oncogenic driver. *Lung Cancer Management*, *9*(3). https://doi.org/10.2217/lmt-2020-0003

Kim, S.-Y., Lee, J. Y., Kim, D. H., Joo, H.-S., Yun, M. R., Jung, D., Yun, J., Heo, S. G., Ahn, B.-C., Park, C. W., Pyo, K. H., Chun, Y. J., Hong, M. H., Kim, H. R., & Cho, B. C. (2019). Patient-Derived Cells to Guide Targeted Therapy for Advanced Lung Adenocarcinoma. *Scientific Reports*, *9*(1), 19909. https://doi.org/10.1038/s41598-019-56356-4

Kinugasa, Y., Matsui, T., & Takakura, N. (2014). CD44 Expressed on Cancer-Associated Fibroblasts Is a Functional Molecule Supporting the Stemness and Drug Resistance of Malignant Cancer Cells in the Tumor Microenvironment. *Stem Cells*, *32*(1), 145–156. https://doi.org/10.1002/stem.1556

Kiyozumi, D., Noda, T., Yamaguchi, R., Tobita, T., Matsumura, T., Shimada, K., Kodani, M., Kohda, T., Fujihara, Y., Ozawa, M., Yu, Z., Miklossy, G., Bohren, K. M., Horie, M., Okabe, M., Matzuk, M. M., & Ikawa, M. (2020). NELL2-mediated lumicrine signaling through OVCH2 is required for male fertility. *Science*, *368*(6495), 1132–1135. https://doi.org/10.1126/science.aay5134

Kobayashi, K. (2023). Primary Resistance to EGFR Tyrosine Kinase Inhibitors (TKIs): Contexts and Comparisons in EGFR-Mutated Lung Cancer. *Journal of Respiration*, *3*(4), 223–236. https://doi.org/10.3390/jor3040021

Koizumi, F., Shimoyama, T., Taguchi, F., Saijo, N., & Nishio, K. (2005). Establishment of a human non-small cell lung cancer cell line resistant to gefitinib. *International Journal of Cancer*, *116*(1), 36–44. https://doi.org/10.1002/ijc.20985

Kong-Beltran, M., Seshagiri, S., Zha, J., Zhu, W., Bhawe, K., Mendoza, N., Holcomb, T., Pujara, K., Stinson, J., Fu, L., Severin, C., Rangell, L., Schwall, R., Amler, L., Wickramasinghe, D., & Yauch, R. (2006). Somatic Mutations Lead to an Oncogenic Deletion of Met in Lung Cancer. *Cancer Research*, *66*(1), 283–289. https://doi.org/10.1158/0008-5472.CAN-05-2749

König, D., Schär, S., Vuong, D., Guckenberger, M., Furrer, K., Opitz, I., Weder, W., Rothschild, S. I., Ochsenbein, A., Zippelius, A., Addeo, A., Mark, M., Eboulet, E. I., Hayoz, S., Thierstein, S., Betticher, D. C., Ris, H.-B., Stupp, R., Curioni-Fontecedro, A., Peters, S., Pless, M., & Früh, M. (2022). Long-term outcomes of operable stage III NSCLC in the pre-immunotherapy era: results from a pooled analysis of the SAKK 16/96, SAKK 16/00, SAKK 16/01, and SAKK 16/08 trials. *ESMO Open*, *7*(2), 100455. https://doi.org/10.1016/j.esmoop.2022.100455

Koulouris, A., Tsagkaris, C., Corriero, A. C., Metro, G., & Mountzios, G. (2022). Resistance to TKIs in EGFR-Mutated Non-Small Cell Lung Cancer: From Mechanisms to New Therapeutic Strategies. *Cancers*, *14*(14), 3337. https://doi.org/10.3390/cancers14143337

La Monica, S., Caffarra, C., Saccani, F., Galvani, E., Galetti, M., Fumarola, C., Bonelli, M., Cavazzoni, A., Cretella, D., Sirangelo, R., Gatti, R., Tiseo, M., Ardizzoni, A., Giovannetti, E., Petronini, P. G., & Alfieri, R. R. (2013). Gefitinib Inhibits Invasive Phenotype and Epithelial-Mesenchymal Transition in Drug-Resistant NSCLC Cells with MET Amplification. *PLoS ONE*, *8*(10), e78656. https://doi.org/10.1371/journal.pone.0078656

La Monica, S., Minari, R., Cretella, D., Bonelli, M., Fumarola, C., Cavazzoni, A., Galetti, M., Digiacomo, G., Riccardi, F., Petronini, P. G., Tiseo, M., & Alfieri, R. (2019). Acquired BRAF G469A Mutation as a Resistance Mechanism to First-Line Osimertinib Treatment in NSCLC Cell Lines Harboring an EGFR Exon 19 Deletion. *Targeted Oncology*, *14*(5), 619–626. https://doi.org/10.1007/s11523-019-00669-x

Lababede, O., & Meziane, M. A. (2018). The Eighth Edition of TNM Staging of Lung Cancer: Reference Chart and Diagrams. *The Oncologist*, *23*(7), 844–848. https://doi.org/10.1634/theoncologist.2017-0659

Lackey, A., & Donington, J. (2013). Surgical Management of Lung Cancer. *Seminars in Interventional Radiology*, *30*(02), 133–140. https://doi.org/10.1055/s-0033-1342954

Lake, D., Corrêa, S. A. L., & Müller, J. (2016). Negative feedback regulation of the ERK1/2 MAPK pathway. *Cellular and Molecular Life Sciences*, *73*(23), 4397–4413. https://doi.org/10.1007/s00018-016-2297-8

Lambert, J. M., Lambert, Q. T., Reuther, G. W., Malliri, A., Siderovski, D. P., Sondek, J., Collard, J. G., & Der, C. J. (2002). Tiam1 mediates Ras activation of Rac by a PI(3)K-independent mechanism. *Nature Cell Biology*, *4*(8), 621–625. https://doi.org/10.1038/ncb833

Lamberti, G., Andrini, E., Sisi, M., Rizzo, A., Parisi, C., Di Federico, A., Gelsomino, F., & Ardizzoni, A. (2020). Beyond EGFR, ALK and ROS1: Current evidence and future perspectives on newly targetable oncogenic drivers in lung adenocarcinoma. *Critical Reviews in Oncology/Hematology*, *156*. https://doi.org/10.1016/j.critrevonc.2020.103119

Lambrecht, B. N., Prins, J.-;B., & Hoogsteden, H. C. (2001). Lung dendritic cells and host immunity to infection. *European Respiratory Journal*, *18*(4), 692–704. https://doi.org/10.1183/09031936.01.18040692

Lamichhane, P., Karyampudi, L., Shreeder, B., Krempski, J., Bahr, D., Daum, J., Kalli, K. R., Goode, E. L., Block, M. S., Cannon, M. J., & Knutson, K. L. (2017). IL10 Release upon PD-1 Blockade Sustains Immunosuppression in Ovarian Cancer. *Cancer Research*, *77*(23), 6667–6678. https://doi.org/10.1158/0008-5472.CAN-17-0740

Lampreht Tratar, U., Horvat, S., & Cemazar, M. (2018). Transgenic Mouse Models in Cancer Research. *Frontiers in Oncology*, *8*. https://doi.org/10.3389/fonc.2018.00268

Landuzzi, L., Palladini, A., Ceccarelli, C., Asioli, S., Nicoletti, G., Giusti, V., Ruzzi, F., Ianzano, M. L., Scalambra, L., Laranga, R., Balboni, T., Arigoni, M., Olivero, M., Calogero, R. A., De Giovanni, C., Dall'Ora, M., Di Oto, E., Santini, D., Foschini, M. P., Cucchi, M. C., Zanotti, S., Taffurelli, M., Nanni, P., & Lollini, P. L. (2021). Early stability and late random tumor progression of a HER2-positive primary breast cancer patient-derived xenograft. *Scientific Reports*, *11*(1). https://doi.org/10.1038/s41598-021-81085-y

Łazar-Poniatowska, M., Bandura, A., Dziadziuszko, R., & Jassem, J. (2021). Concurrent chemoradiotherapy for stage III non-small-cell lung cancer: recent progress and future perspectives (a narrative review). *Translational Lung Cancer Research*, *10*(4), 2018–2031. https://doi.org/10.21037/tlcr-20-704

Le, X., Elamin, Y. Y., & Zhang, J. (2023). New Actions on Actionable Mutations in Lung Cancers. *Cancers*, *15*(11), 2917. https://doi.org/10.3390/cancers15112917

Le, X., Negrao, M. V., Reuben, A., Federico, L., Diao, L., McGrail, D., Nilsson, M., Robichaux, J., Munoz, I. G., Patel, S., Elamin, Y., Fan, Y.-H., Lee, W.-C., Parra, E., Solis Soto, L. M., Chen, R., Li, J., Karpinets, T., Khairullah, R., Kadara , H., Behrens , C., Sepesi, B., Wang, R., Zhu, M., Wang, L., Vaporciyan , A., Roth, J., Swisher, S., Haymaker, C., Zhang, J., Wang, J., Wong, K.-K., Byers, L. A., Bernatchez, C., Zhang, J., Wistuba, I. I., Gibbons, D. L., Akbay, E. A., & Heymach, J. V. (2021). Characterization of the Immune Landscape of EGFR-Mutant NSCLC Identifies CD73/Adenosine Pathway as a Potential Therapeutic Target. *Journal of Thoracic Oncology*, *16*(4), 583–600. https://doi.org/10.1016/j.jtho.2020.12.010

Lee, C., Jiang, Z. K., Planken, S., Manzuk, L. K., Ortiz, R., Hall, M., Noorbehesht, K., Ram, S., Affolter, T., Troche, G. E., Ihle, N. T., Johnson, T., Ahn, Y., Kraus, M., & Giddabasappa, A. (2023). Efficacy and Imaging-Enabled

Pharmacodynamic Profiling of KRAS G12C Inhibitors in Xenograft and Genetically Engineered Mouse Models of Cancer. *Molecular Cancer Therapeutics*, *22*(7), 891–900. https://doi.org/10.1158/1535-7163.MCT-22-0810

Lee, C. K., Brown, C., Gralla, R. J., Hirsh, V., Thongprasert, S., Tsai, C.-M., Tan, E. H., Ho, J. C.-M., Chu, D. T., Zaatar, A., Osorio Sanchez, J. A., Vu, V. Van, Au, J. S. K., Inoue, A., Lee, S. M., Gebski, V., & Yang, J. C.-H. (2013). Impact of EGFR Inhibitor in Non–Small Cell Lung Cancer on Progression-Free and Overall Survival: A Meta-Analysis. *JNCI: Journal of the National Cancer Institute*, *105*(9), 595–605. https://doi.org/10.1093/jnci/djt072

Lee, M., & Razi, S. S. (2024). Pulmonary Sleeve Resection. In: *StatPearls [Internet]. Treasure Island (FL): StatPearls.* PMID: 33232070

Lee, Y., Choi, Y.-R., Kim, K.-Y., & Shin, D. H. (2016). The impact of intermittent versus continuous exposure to EGFR tyrosine kinase inhibitor on selection of *EGFR* T790M-mutant drug-resistant clones in a lung cancer cell line carrying activating *EGFR* mutation. *Oncotarget*, *7*(28), 43315–43323. https://doi.org/10.18632/oncotarget.9703

Lei, M., Liu, J., Gao, Y., Dai, W., Huang, H., Jiang, Q., & Liu, Z. (2024). DPP Inhibition Enhances the Efficacy of PD-1 Blockade by Remodeling the Tumor Microenvironment in Lewis Lung Carcinoma Model. *Biomolecules*, *14*(4), 391. https://doi.org/10.3390/biom14040391

Leiter, A., Veluswamy, R. R., & Wisnivesky, J. P. (2023). The global burden of lung cancer: current status and future trends. *Nature Reviews Clinical Oncology*, *20*(9), 624–639. https://doi.org/10.1038/s41571-023-00798-3

Lemjabbar-Alaoui, H., Hassan, O. U., Yang, Y.-W., & Buchanan, P. (2015). Lung cancer: Biology and treatment options. *Biochimica et Biophysica Acta (BBA) - Reviews on Cancer*, *1856*(2), 189–210. https://doi.org/10.1016/j.bbcan.2015.08.002

Leonetti, A., Sharma, S., Minari, R., Perego, P., Giovannetti, E., & Tiseo, M. (2019). Resistance mechanisms to osimertinib in EGFR-mutated non-small cell lung cancer. *British Journal of Cancer*, *121*(9), 725–737. https://doi.org/10.1038/s41416-019-0573-8

Li, C., & Lu, H. (2018). Adenosquamous carcinoma of the lung. *OncoTargets and Therapy*, *Volume 11*, 4829–4835. https://doi.org/10.2147/OTT.S164574

Li, G., Choi, J. E., Kryczek, I., Sun, Y., Liao, P., Li, S., Wei, S., Grove, S., Vatan, L., Nelson, R., Schaefer, G., Allen, S. G., Sankar, K., Fecher, L. A., Mendiratta-Lala, M., Frankel, T. L., Qin, A., Waninger, J. J., Tezel, A., Alva, A., Lao, C. D., Ramnath, N., Cieslik, M., Harms, P. W., Green, M. D., Chinnaiyan, A. M., & Zou, W. (2023). Intersection of immune and oncometabolic pathways drives cancer hyperprogression during immunotherapy. *Cancer Cell*, *41*(2), 304-322.e7. https://doi.org/10.1016/j.ccell.2022.12.008

Li, H., van der Merwe, P. A., & Sivakumar, S. (2022). Biomarkers of response to PD-1 pathway blockade. *British Journal of Cancer*, *126*(12), 1663–1675. https://doi.org/10.1038/s41416-022-01743-4

Li, H. Y., McSharry, M., Bullock, B., Nguyen, T. T., Kwak, J., Poczobutt, J. M., Sippel, T. R., Heasley, L. E., Weiser-Evans, M. C., Clambey, E. T., & Nemenoff, R. A. (2017). The Tumor Microenvironment Regulates Sensitivity of Murine Lung Tumors to PD-1/PD-L1 Antibody Blockade. *Cancer Immunology Research*, *5*(9), 767–777. https://doi.org/10.1158/2326-6066.CIR-16-0365

Li, J., & Kwok, H. (2020). Current Strategies for Treating NSCLC: From Biological Mechanisms to Clinical Treatment. *Cancers*, *12*(6), 1587. https://doi.org/10.3390/cancers12061587

Li, M. S. C., Saw, S. P. L., & Addeo, A. (2024). Anti-CTLA-4 in non-small-cell lung cancer: insights from the NIPPON study. *The Lancet Respiratory Medicine*. https://doi.org/10.1016/S2213-2600(24)00218-2

Li, X., Wu, D., Liu, H., & Chen, J. (2020). Pulmonary sarcomatoid carcinoma: progress, treatment and expectations. *Therapeutic Advances in Medical Oncology*, *12*. https://doi.org/10.1177/1758835920950207

Li, Z., Shen, L., Ding, D., Huang, J., Zhang, J., Chen, Z., & Lu, S. (2018). Efficacy of Crizotinib among Different Types of ROS1 Fusion Partners in Patients with ROS1-Rearranged Non–Small Cell Lung Cancer. *Journal of Thoracic Oncology*, *13*(7), 987–995. https://doi.org/10.1016/j.jtho.2018.04.016

Lim, Z.-F., & Ma, P. C. (2019). Emerging insights of tumor heterogeneity and drug resistance mechanisms in lung cancer targeted therapy. *Journal of Hematology & Oncology*, *12*(1), 134. https://doi.org/10.1186/s13045-019-0818-2

Lin, J. J., Ritterhouse, L. L., Ali, S. M., Bailey, M., Schrock, A. B., Gainor, J. F., Ferris, L. A., Mino-Kenudson, M., Miller, V. A., Iafrate, A. J., Lennerz, J. K., & Shaw, A. T. (2017). ROS1 Fusions Rarely Overlap with Other Oncogenic Drivers in Non–Small Cell Lung Cancer. *Journal of Thoracic Oncology*, *12*(5), 872–877. https://doi.org/10.1016/j.jtho.2017.01.004

Lin, Y.-F., Liu, J.-J., Chang, Y.-J., Yu, C.-S., Yi, W., Lane, H.-Y., & Lu, C.-H. (2022). Predicting Anticancer Drug Resistance Mediated by Mutations. *Pharmaceuticals*, *15*(2), 136. https://doi.org/10.3390/ph15020136

Litvak, A. M., Paik, P. K., Woo, K. M., Sima, C. S., Hellmann, M. D., Arcila, M. E., Ladanyi, M., Rudin, C. M., Kris, M. G., & Riely, G. J. (2014). Clinical Characteristics and Course of 63 Patients with BRAF Mutant Lung Cancers. *Journal of Thoracic Oncology*, *9*(11), 1669–1674. https://doi.org/10.1097/JTO.0000000000000344

Liu, C., Zheng, S., Wang, Z., Wang, S., Wang, X., Yang, L., Xu, H., Cao, Z., Feng, X., Xue, Q., Wang, Y., Sun, N., & He, J. (2022). KRAS-G12D mutation drives immune suppression and the primary resistance of anti-PD-1/PD-L1 immunotherapy in non-small cell lung cancer. *Cancer Communications*, *42*(9), 828–847. https://doi.org/10.1002/cac2.12327

Liu, F., Wei, Y., Zhang, H., Jiang, J., Zhang, P., & Chu, Q. (2022). NTRK Fusion in Non-Small Cell Lung Cancer: Diagnosis, Therapy, and TRK Inhibitor Resistance. *Frontiers in Oncology*, *12*. https://doi.org/10.3389/fonc.2022.864666

Liu, G., & Summer, R. (2019). Cellular Metabolism in Lung Health and Disease. *Annual Review of Physiology*, *81*(1), 403–428. https://doi.org/10.1146/annurev-physiol-020518-114640

Liu, J., Li, X., Shao, Y., Guo, X., & He, J. (2020). The efficacy and safety of osimertinib in treating nonsmall cell lung cancer. *Medicine*, *99*(34), e21826. https://doi.org/10.1097/MD.0000000000021826

Liu, Q., Yu, S., Zhao, W., Qin, S., Chu, Q., & Wu, K. (2018). EGFR-TKIs resistance via EGFR-independent signaling pathways. *Molecular Cancer*, *17*(1), 53. https://doi.org/10.1186/s12943-018-0793-1

Liu, S., Ren, J., & ten Dijke, P. (2021). Targeting TGFβ signal transduction for cancer therapy. *Signal Transduction and Targeted Therapy*, *6*(1), 8. https://doi.org/10.1038/s41392-020-00436-9

Liu, W., Cui, Y., Zheng, X., Yu, K., & Sun, G. (2023). Application status and future prospects of the PDX model in lung cancer. *Frontiers in Oncology*, *13*. https://doi.org/10.3389/fonc.2023.1098581

Liu, W., Huo, G., & Chen, P. (2023). Clinical benefit of pembrolizumab in treatment of first line non-small cell lung cancer: a systematic review and meta-analysis of clinical characteristics. *BMC Cancer*, *23*(1), 458. https://doi.org/10.1186/s12885-023-10959-3

Liu, Y., Wu, W., Cai, C., Zhang, H., Shen, H., & Han, Y. (2023). Patient-derived xenograft models in cancer therapy: technologies and applications. *Signal Transduction and Targeted Therapy*, *8*(1), 160. https://doi.org/10.1038/s41392-023-01419-2

Liu, Z., & Gao, W. (2019). Overcoming acquired resistance of gefitinib in lung cancer cells without T790M by AZD9291 or Twist1 knockdown in vitro and in vivo. *Archives of Toxicology*, *93*(6), 1555–1571. https://doi.org/10.1007/s00204-019-02453-2

Lo Russo, G., Moro, M., Sommariva, M., Cancila, V., Boeri, M., Centonze, G., Ferro, S., Ganzinelli, M., Gasparini, P., Huber, V., Milione, M., Porcu, L., Proto, C., Pruneri, G., Signorelli, D., Sangaletti, S., Sfondrini, L., Storti, C., Tassi, E., Bardelli, A., Marsoni, S., Torri, V., Tripodo, C., Colombo, M. P., Anichini, A., Rivoltini, L., Balsari, A., Sozzi, G., & Garassino, M. C. (2019). Antibody-Fc/FcR interaction on macrophages as a mechanism for hyperprogressive disease in non-small cell lung cancer subsequent to PD-1/PD-L1 blockade. *Clinical Cancer Research*, *25*(3), 989–999. https://doi.org/10.1158/1078-0432.CCR-18-1390

LoPiccolo, J., Gusev, A., Christiani, D. C., & Jänne, P. A. (2024). Lung cancer in patients who have never smoked — an emerging disease. *Nature Reviews Clinical Oncology*, *21*(2), 121–146. https://doi.org/10.1038/s41571-023-00844-0

Lu, Y., Liu, Y., Oeck, S., Zhang, G. J., Schramm, A., & Glazer, P. M. (2020). Hypoxia Induces Resistance to EGFR Inhibitors in Lung Cancer Cells via Upregulation of FGFR1 and the MAPK Pathway. *Cancer Research*, *80*(21), 4655–4667. https://doi.org/10.1158/0008-5472.CAN-20-1192

Lu, Y., Zhang, X., Ning, J., & Zhang, M. (2023). Immune checkpoint inhibitors as first-line therapy for non-small cell lung cancer: A systematic evaluation and meta-analysis. *Human Vaccines & Immunotherapeutics*, *19*(1). https://doi.org/10.1080/21645515.2023.2169531

Ludin, A., & Zon, L. I. (2017). Cancer immunotherapy: The dark side of PD-1 receptor inhibition. *Nature*, *552*(7683), 41–42. https://doi.org/10.1038/nature24759

Luo, Z., Wu, R.-R., Lv, L., Li, P., Zhang, L.-Y., Hao, Q.-L., & Li, W. (2014). Prognostic value of CD44 expression in non-small cell lung cancer: a systematic review. *International Journal of Clinical and Experimental Pathology*, *7*(7), 3632–3646.

Lynch, T. J., Bell, D. W., Sordella, R., Gurubhagavatula, S., Okimoto, R. A., Brannigan, B. W., Harris, P. L., Haserlat, S. M., Supko, J. G., Haluska, F. G., Louis, D. N., Christiani, D. C., Settleman, J., & Haber, D. A. (2004). Activating Mutations in the Epidermal Growth Factor Receptor Underlying Responsiveness of Non–Small-Cell Lung Cancer to Gefitinib. *New England Journal of Medicine*, *350*(21), 2129–2139. https://doi.org/10.1056/NEJMoa040938

Ma, C., Wei, S., & Song, Y. (2011). T790M and acquired resistance of EGFR TKI: a literature review of clinical reports. *Journal of Thoracic Disease*, *3*(1), 10–18. https://doi.org/10.3978/j.issn.2072-1439.2010.12.02

Ma, L., Dong, L., & Chang, P. (2019). CD44v6 engages in colorectal cancer progression. *Cell Death & Disease*, *10*(1), 30. https://doi.org/10.1038/s41419-018-1265-7

Ma, X., Zhang, Y., Wang, S., & Yu, J. (2021). Predictive value of tumor mutation burden (TMB) with targeted next-generation sequencing in immunocheckpoint inhibitors for non-small cell lung cancer (NSCLC). *Journal of Cancer*, *12*(2), 584–594. https://doi.org/10.7150/jca.48105

Macke, R. A., Schuchert, M. J., Odell, D. D., Wilson, D. O., Luketich, J. D., & Landreneau, R. J. (2015). Parenchymal preserving anatomic resections result in less pulmonary function loss in patients with Stage I non-small cell lung cancer. *Journal of Cardiothoracic Surgery*, *10*(1), 49. https://doi.org/10.1186/s13019-015-0253-6

Mahase, E. (2023). Lung cancer screening for over 55s will be rolled out in England. *BMJ*, p1469. https://doi.org/10.1136/bmj.p1469

Maleki, A., Manhapra, A., Mousa, H. M., & Foster, C. S. (2022). Regulation of Immune Responses. In *Albert and Jakobiec's Principles and Practice of Ophthalmology* (pp. 819–835). Springer International Publishing. https://doi.org/10.1007/978-3-030-42634-7_332

Malumbres, M., & Barbacid, M. (2003). RAS oncogenes: the first 30 years. *Nature Reviews Cancer*, *3*(6), 459–465. https://doi.org/10.1038/nrc1097

Manguso, R. T., Pope, H. W., Zimmer, M. D., Brown, F. D., Yates, K. B., Miller, B. C., Collins, N. B., Bi, K., LaFleur, M. W., Juneja, V. R., Weiss, S. A., Lo, J., Fisher, D. E., Miao, D., Van Allen, E., Root, D. E., Sharpe, A. H., Doench, J. G., & Haining, W. N. (2017). In vivo CRISPR screening identifies Ptpn2 as a cancer immunotherapy target. *Nature*, *547*(7664), 413–418. https://doi.org/10.1038/nature23270

Mansour, F. A., Al-Mazrou, A., Al-Mohanna, F., Al-Alwan, M., & Ghebeh, H. (2020). PD-L1 is overexpressed on breast cancer stem cells through notch3/mTOR axis. *OncoImmunology*, *9*(1). https://doi.org/10.1080/2162402X.2020.1729299

Marchiò, C., Scaltriti, M., Ladanyi, M., Iafrate, A. J., Bibeau, F., Dietel, M., Hechtman, J. F., Troiani, T., López-Rios, F., Douillard, J.-Y., Andrè, F., & Reis-Filho, J. S. (2019). ESMO recommendations on the standard methods to detect NTRK fusions in daily practice and clinical research. *Annals of Oncology*, *30*(9), 1417–1427. https://doi.org/10.1093/annonc/mdz204

Massarelli, E., Varella-Garcia, M., Tang, X., Xavier, A. C., Ozburn, N. C., Liu, D. D., Bekele, B. N., Herbst, R. S., & Wistuba, I. I. (2007). KRAS Mutation Is an Important Predictor of Resistance to Therapy with Epidermal Growth Factor Receptor Tyrosine Kinase Inhibitors in Non–Small-Cell Lung Cancer. *Clinical Cancer Research*, *13*(10), 2890–2896. https://doi.org/10.1158/1078-0432.CCR-06-3043

Mathew, M., Safyan, R. A., & Shu, C. A. (2017). PD-L1 as a biomarker in NSCLC: challenges and future directions. *Annals of Translational Medicine*, *5*(18), 375–375. https://doi.org/10.21037/atm.2017.08.04

Mathieu, L. N., Larkins, E., Akinboro, O., Roy, P., Amatya, A. K., Fiero, M. H., Mishra-Kalyani, P. S., Helms, W. S., Myers, C. E., Skinner, A. M., Aungst, S., Jin, R., Zhao, H., Xia, H., Zirkelbach, J. F., Bi, Y., Li, Y., Liu, J., Grimstein, M., Zhang, X., Woods, S., Reece, K., Abukhdeir, A. M., Ghosh, S., Philip, R., Tang, S., Goldberg, K. B., Pazdur, R., Beaver, J. A., & Singh, H. (2022). FDA Approval Summary: Capmatinib and Tepotinib for the Treatment of Metastatic NSCLC Harboring MET Exon 14 Skipping Mutations or Alterations. *Clinical Cancer Research*, *28*(2), 249–254. https://doi.org/10.1158/1078-0432.CCR-21-1566

Mazet, J. M., Mahale, J. N., Tong, O., Watson, R. A., Lechuga-Vieco, A. V., Pirgova, G., Lau, V. W. C., Attar, M., Koneva, L. A., Sansom, S. N., Fairfax, B. P., & Gérard, A. (2023). IFNγ signaling in cytotoxic T cells restricts anti-tumor responses by inhibiting the maintenance and diversity of intra-tumoral stem-like T cells. *Nature Communications*, *14*(1), 321. https://doi.org/10.1038/s41467-023-35948-9

Mazières, J., Peters, S., Lepage, B., Cortot, A. B., Barlesi, F., Beau-Faller, M., Besse, B., Blons, H., Mansuet-Lupo, A., Urban, T., Moro-Sibilot, D., Dansin, E., Chouaid, C., Wislez, M., Diebold, J., Felip, E., Rouquette, I., Milia, J. D., & Gautschi, O. (2013). Lung Cancer That Harbors an HER2 Mutation: Epidemiologic Characteristics and Therapeutic Perspectives. *Journal of Clinical Oncology*, *31*(16), 1997–2003. https://doi.org/10.1200/JCO.2012.45.6095

McCoach, C. E., Le, A. T., Gowan, K., Jones, K., Schubert, L., Doak, A., Estrada-Bernal, A., Davies, K. D., Merrick, D. T., Bunn, P. A., Purcell, W. T., Dziadziuszko, R., Varella-Garcia, M., Aisner, D. L., Camidge, D. R., & Doebele, R. C. (2018). Resistance Mechanisms to Targeted Therapies in ROS1+ and ALK+ Non–small Cell Lung Cancer. *Clinical Cancer Research*, *24*(14), 3334–3347. https://doi.org/10.1158/1078-0432.CCR-17-2452

McFadden, D. G., Politi, K., Bhutkar, A., Chen, F. K., Song, X., Pirun, M., Santiago, P. M., Kim-Kiselak, C., Platt, J. T., Lee, E., Hodges, E., Rosebrock, A. P., Bronson, R. T., Socci, N. D., Hannon, G. J., Jacks, T., & Varmus, H. (2016). Mutational landscape of EGFR-, MYC-, and Kras-driven genetically engineered mouse models of lung adenocarcinoma. *Proceedings of the National Academy of Sciences*, *113*(42). https://doi.org/10.1073/pnas.1613601113

McKeage, M. J., Tin Tin, S., Khwaounjoo, P., Sheath, K., Dixon-McIver, A., Ng, D., Sullivan, R., Cameron, L., Shepherd, P., Laking, G. R., Kingston, N., Strauss, M., Lewis, C., Elwood, M., & Love, D. R. (2020). Screening for anaplastic lymphoma kinase (ALK) gene rearrangements in non-small-cell lung cancer in New Zealand. *Internal Medicine Journal*, *50*(6), 716–725. https://doi.org/10.1111/imj.14435

Memon, D., Schoenfeld, A. J., Ye, D., Fromm, G., Rizvi, H., Zhang, X., Keddar, M. R., Mathew, D., Yoo, K. J., Qiu, J., Lihm, J., Miriyala, J., Sauter, J. L., Luo, J., Chow, A., Bhanot, U. K., McCarthy, C., Vanderbilt, C. M., Liu, C., Abu-Akeel, M., Plodkowski, A. J., McGranahan, N., Łuksza, M., Greenbaum, B. D., Merghoub, T., Achour, I., Barrett, J. C., Stewart, R., Beltrao, P., Schreiber, T. H., Minn, A. J., Miller, M. L., & Hellmann, M. D. (2024). Clinical and molecular features of acquired resistance to immunotherapy in non-small cell lung cancer. *Cancer Cell*. https://doi.org/10.1016/j.ccell.2023.12.013

Meraz, I. M., Majidi, M., Fang, B., Meng, F., Gao, L., Shao, R., Song, R., Li, F., Lissanu, Y., Chen, H., Ha, M. J., Wang, Q., Wang, J., Shpall, E., Jung, S. Y., Haderk, F., Gui, P., Riess, J. W., Olivas, V., Bivona, T. G., & Roth, J. A. (2023). 3-Phosphoinositide-dependent kinase 1 drives acquired resistance to osimertinib. *Communications Biology*, *6*(1), 509. https://doi.org/10.1038/s42003-023-04889-w

Meyer, M.-L., Fitzgerald, B. G., Paz-Ares, L., Cappuzzo, F., Jänne, P. A., Peters, S., & Hirsch, F. R. (2024). New promises and challenges in the treatment of advanced non-small-cell lung cancer. *The Lancet*, *404*(10454), 803–822. https://doi.org/10.1016/S0140-6736(24)01029-8

Miles, B., & Mackey, J. D. (2021). Epidermal Growth Factor Receptor Tyrosine Kinase Inhibitors and Lung Cancer: History, Epidemiology, and Market Outlook. *Cureus*. https://doi.org/10.7759/cureus.13470

Milne, G. R., & Palmer, T. M. (2011). Anti-Inflammatory and Immunosuppressive Effects of the A2A Adenosine Receptor. *The Scientific World JOURNAL*, *11*, 320–339. https://doi.org/10.1100/tsw.2011.22

Minari, R., Bordi, P., & Tiseo, M. (2016). Third-generation epidermal growth factor receptor-tyrosine kinase inhibitors in T790M-positive non-small cell lung cancer: review on emerged mechanisms of resistance. *Translational Lung Cancer Research*, *5*(6), 695–608. https://doi.org/10.21037/tlcr.2016.12.02

Mini, E., Nobili, S., Caciagli, B., Landini, I., & Mazzei, T. (2006). Cellular pharmacology of gemcitabine. *Annals of Oncology*, *17*, v7–v12. https://doi.org/10.1093/annonc/mdj941

Mino-Kenudson, M., Schalper, K., Cooper, W., Dacic, S., Hirsch, F. R., Jain, D., Lopez-Rios, F., Tsao, M. S., Yatabe, Y., Beasley, M. B., Yu, H., Sholl, L. M., Brambilla, E., Chou, T.-Y., Connolly, C., Wistuba, I., Kerr, K. M., & Lantuejoul, S. (2022). Predictive Biomarkers for Immunotherapy in Lung Cancer: Perspective From the International Association for the Study of Lung Cancer Pathology Committee. *Journal of Thoracic Oncology*, *17*(12), 1335–1354. https://doi.org/10.1016/j.jtho.2022.09.109

Mirabelli, P., Coppola, L., & Salvatore, M. (2019). Cancer Cell Lines Are Useful Model Systems for Medical Research. *Cancers*, *11*(8), 1098. https://doi.org/10.3390/cancers11081098

Mirhadi, S., Tam, S., Li, Q., Moghal, N., Pham, N.-A., Tong, J., Golbourn, B. J., Krieger, J. R., Taylor, P., Li, M., Weiss, J., Martins-Filho, S. N., Raghavan, V., Mamatjan, Y., Khan, A. A., Cabanero, M., Sakashita, S., Huo, K., Agnihotri, S., Ishizawa, K., Waddell, T. K., Zadeh, G., Yasufuku, K., Liu, G., Shepherd, F. A., Moran, M. F., & Tsao, M.-S. (2022). Integrative analysis of non-small cell lung cancer patient-derived xenografts identifies distinct proteotypes associated with patient outcomes. *Nature Communications*, *13*(1), 1811. https://doi.org/10.1038/s41467-022-29444-9

Miserocchi, G., Mercatali, L., Liverani, C., De Vita, A., Spadazzi, C., Pieri, F., Bongiovanni, A., Recine, F., Amadori, D., & Ibrahim, T. (2017). Management and potentialities of primary cancer cultures in preclinical and translational studies. *Journal of Translational Medicine*, *15*(1), 229. https://doi.org/10.1186/s12967-017-1328-z

Mitsudomi, T., Morita, S., Yatabe, Y., Negoro, S., Okamoto, I., Tsurutani, J., Seto, T., Satouchi, M., Tada, H., Hirashima, T., Asami, K., Katakami, N., Takada, M., Yoshioka, H., Shibata, K., Kudoh, S., Shimizu, E., Saito, H., Toyooka, S., Nakagawa, K., & Fukuoka, M. (2010). Gefitinib versus cisplatin plus docetaxel in patients with non-small-cell lung cancer harbouring mutations of the epidermal growth factor receptor (WJTOG3405): an open label, randomised phase 3 trial. *The Lancet Oncology*, *11*(2), 121–128. https://doi.org/10.1016/S1470-2045(09)70364-X

Mok, T., Camidge, D. R., Gadgeel, S. M., Rosell, R., Dziadziuszko, R., Kim, D.-W., Pérol, M., Ou, S.-H. I., Ahn, J. S., Shaw, A. T., Bordogna, W., Smoljanović, V., Hilton, M., Ruf, T., Noé, J., & Peters, S. (2020). Updated overall survival and final progression-free survival data for patients with treatment-naive advanced ALK-positive non-small-cell lung cancer in the ALEX study. *Annals of Oncology*, *31*(8), 1056–1064. https://doi.org/10.1016/j.annonc.2020.04.478

Montagne, F., Guisier, F., Venissac, N., & Baste, J.-M. (2021). The Role of Surgery in Lung Cancer Treatment: Present Indications and Future Perspectives—State of the Art. *Cancers*, *13*(15), 3711. https://doi.org/10.3390/cancers13153711

Moore, A. M., Nooruddin, Z., Reveles, K. R., Datta, P., Whitehead, J. M., Franklin, K., Alkadimi, M., Williams, M. H., Williams, R. A., Smith, S., Reichelderfer, R., Cotarla, I., Brannman, L., Frankart, A., Mulrooney, T., Hsieh, K., Simmons, D. J., Jones, X., & Frei, C. R. (2023). Durvalumab Treatment Patterns for Patients with Unresectable Stage III Non-Small Cell Lung Cancer in the Veterans Health Administration (VHA): A Nationwide, Real-World Study. *Current Oncology*, *30*(9), 8411–8423. https://doi.org/10.3390/curroncol30090611

Motzer, R. J., Tannir, N. M., McDermott, D. F., Arén Frontera, O., Melichar, B., Choueiri, T. K., Plimack, E. R., Barthélémy, P., Porta, C., George, S., Powles, T., Donskov, F., Neiman, V., Kollmannsberger, C. K., Salman, P., Gurney, H., Hawkins, R., Ravaud, A., Grimm, M.-O., Bracarda, S., Barrios, C. H., Tomita, Y., Castellano, D., Rini, B. I., Chen, A. C., Mekan, S., McHenry, M. B., Wind-Rotolo, M., Doan, J., Sharma, P., Hammers, H. J., & Escudier, B. (2018). Nivolumab plus Ipilimumab versus Sunitinib in Advanced Renal-Cell Carcinoma. *New England Journal of Medicine*, *378*(14), 1277–1290. https://doi.org/10.1056/NEJMoa1712126

Muto, S., Enta, A., Maruya, Y., Inomata, S., Yamaguchi, H., Mine, H., Takagi, H., Ozaki, Y., Watanabe, M., Inoue, T., Yamaura, T., Fukuhara, M., Okabe, N., Matsumura, Y., Hasegawa, T., Osugi, J., Hoshino, M., Higuchi, M., Shio, Y., Hamada, K., & Suzuki, H. (2023). Wnt/β-Catenin Signaling and Resistance to Immune Checkpoint Inhibitors: From Non-Small-Cell Lung Cancer to Other Cancers. *Biomedicines*, *11*(1). https://doi.org/10.3390/biomedicines11010190

Nagasaka, M., Singh, V., Baca, Y., Sukari, A., Kim, C., Mamdani, H., Spira, A. I., Uprety, D., Bepler, G., Kim, E. S., Raez, L. E., Pai, S. G., Ikpeazu, C., Oberley, M., Feldman, R., Xiu, J., Korn, W. M., Wozniak, A. J., Borghaei, H., & Liu, S. V. (2022). The Effects of HER2 Alterations in EGFR Mutant Non-small Cell Lung Cancer. *Clinical Lung Cancer*, *23*(1), 52–59. https://doi.org/10.1016/j.cllc.2021.08.012

Nagasaki, J., Ishino, T., & Togashi, Y. (2022). Mechanisms of resistance to immune checkpoint inhibitors. *Cancer Science*, *113*(10), 3303–3312. https://doi.org/10.1111/cas.15497

Nakajima, E. C., Drezner, N., Li, X., Mishra-Kalyani, P. S., Liu, Y., Zhao, H., Bi, Y., Liu, J., Rahman, A., Wearne, E., Ojofeitimi, I., Hotaki, L. T., Spillman, D., Pazdur, R., Beaver, J. A., & Singh, H. (2022). FDA Approval Summary: Sotorasib for KRAS G12C-Mutated Metastatic NSCLC. *Clinical Cancer Research*, *28*(8), 1482–1486. https://doi.org/10.1158/1078-0432.CCR-21-3074

Nanjwade, B. K., Adichwal, S. A., Gaikwad, K. R., Parikh, K. A., & Manvi, F. V. (2011). Pulmonary Drug Delivery: Novel Pharmaceutical Technologies Breathe New Life into the Lungs. *PDA Journal of Pharmaceutical Science and Technology*, *65*(5), 513–534. https://doi.org/10.5731/pdajpst.2011.00704

Nanni, P., Landuzzi, L., Manara, M. C., Righi, A., Nicoletti, G., Cristalli, C., Pasello, M., Parra, A., Carrabotta, M., Ferracin, M., Palladini, A., Ianzano, M. L., Giusti, V., Ruzzi, F., Magnani, M., Donati, D. M., Picci, P., Lollini, P.-L., & Scotlandi, K. (2019). Bone sarcoma patient-derived xenografts are faithful and stable preclinical models for molecular and therapeutic investigations. *Scientific Reports*, *9*(1), 12174. https://doi.org/10.1038/s41598-019-48634-y

Nanni, P., Nicoletti, G., Palladini, A., Croci, S., Murgo, A., Ianzano, M. L., Grosso, V., Stivani, V., Antognoli, A., Lamolinara, A., Landuzzi, L., di Tomaso, E., Iezzi, M., De Giovanni, C., & Lollini, P.-L. (2012). Multiorgan

Metastasis of Human HER-2+ Breast Cancer in Rag2−/−;Il2rg−/− Mice and Treatment with PI3K Inhibitor. *PLoS ONE*, *7*(6), e39626. https://doi.org/10.1371/journal.pone.0039626

Navani, N., Butler, R., Ibrahimo, S., Verma, A., Evans, M., Doherty, G. J., & Ahmed, S. (2022). Optimising tissue acquisition and the molecular testing pathway for patients with non-small cell lung cancer: A UK expert consensus statement. *Lung Cancer*, *172*, 142–153. https://doi.org/10.1016/j.lungcan.2022.08.003

NCI Staff. (2015). *FDA Approves First Immunotherapy Treatment for Lung Cancer*. National Cancer Institute (NIH). https://www.cancer.gov/news-events/cancer-currents-blog/2015/fda-opdivo

Nebhan, C. A., Johnson, D. B., Sullivan, R. J., Amaria, R. N., Flaherty, K. T., Sosman, J. A., & Davies, M. A. (2021). Efficacy and Safety of Trametinib in Non-V600 BRAF Mutant Melanoma: A Phase II Study. *The Oncologist*, *26*(9), 731-e1498. https://doi.org/10.1002/onco.13795

Neel, D. S., Allegakoen, D. V., Olivas, V., Mayekar, M. K., Hemmati, G., Chatterjee, N., Blakely, C. M., McCoach, C. E., Rotow, J. K., Le, A., Karachaliou, N., Rosell, R., Riess, J. W., Nichols, R., Doebele, R. C., & Bivona, T. G. (2019). Differential Subcellular Localization Regulates Oncogenic Signaling by ROS1 Kinase Fusion Proteins. *Cancer Research*, *79*(3), 546–556. https://doi.org/10.1158/0008-5472.CAN-18-1492

Nguyen-Ngoc, T., Bouchaab, H., Adjei, A. A., & Peters, S. (2015). BRAF Alterations as Therapeutic Targets in Non–Small-Cell Lung Cancer. *Journal of Thoracic Oncology*, *10*(10), 1396–1403. https://doi.org/10.1097/JTO.0000000000000644

Ni, J., Cozzi, P. J., Hao, J. L., Beretov, J., Chang, L., Duan, W., Shigdar, S., Delprado, W. J., Graham, P. H., Bucci, J., Kearsley, J. H., & Li, Y. (2014). CD44 variant 6 is associated with prostate cancer metastasis and chemo-/radioresistance. *The Prostate*, *74*(6), 602–617. https://doi.org/10.1002/pros.22775

Nicholson, A. G., Tsao, M. S., Beasley, M. B., Borczuk, A. C., Brambilla, E., Cooper, W. A., Dacic, S., Jain, D., Kerr, K. M., Lantuejoul, S., Noguchi, M., Papotti, M., Rekhtman, N., Scagliotti, G., van Schil, P., Sholl, L., Yatabe, Y., Yoshida, A., & Travis, W. D. (2022). The 2021 WHO Classification of Lung Tumors: Impact of Advances Since 2015. *Journal of Thoracic Oncology*, *17*(3), 362–387. https://doi.org/10.1016/j.jtho.2021.11.003

Nieto, C., Miller, B., Alzofon, N., Chimed, T., Himes, J., Joshi, M., Gomez, K., Chowdhury, F. N., Le, P. N., Weaver, A., Somerset, H., Morton, J. J., Wang, J. H., Wang, X. J., Gao, D., Hansen, K., Keysar, S. B., & Jimeno, A. (2023). The programmed death ligand 1 interactome demonstrates bidirectional signaling coordinating immune suppression and cancer progression in head and neck squamous cell carcinoma. *Journal of the National Cancer Institute*, *115*(11), 1392–1403. https://doi.org/10.1093/jnci/djad126

Ning, T., Yan, X., Lu, Z.-J., Wang, G.-P., Zhang, N.-G., Yang, J.-L., Jiang, S.-S., Wu, Y., Yang, L., Guan, Y.-S., & Luo, F. (2009). Gene Therapy with the Angiogenesis Inhibitor Endostatin in an Orthotopic Lung Cancer Murine Model. *Human Gene Therapy*, *20*(2), 103–111. https://doi.org/10.1089/hum.2008.098

Nishino, K., Yamasaki, S., Nakashima, R., Zwama, M., & Hayashi-Nishino, M. (2021). Function and Inhibitory Mechanisms of Multidrug Efflux Pumps. *Frontiers in Microbiology*, *12*. https://doi.org/10.3389/fmicb.2021.737288

Nomura, T., Tamaoki, N., Takakura, A., & Suemizu, H. (2008). Basic Concept of Development and Practical Application of Animal Models for Human Diseases. In *Humanized Mice* (Vol. 324, pp. 1–24).

Okada, S., Vaeteewoottacharn, K., & Kariya, R. (2019). Application of Highly Immunocompromised Mice for the Establishment of Patient-Derived Xenograft (PDX) Models. *Cells*, *8*(8), 889. https://doi.org/10.3390/cells8080889

Okwundu, N., Grossman, D., Hu-Lieskovan, S., Grossmann, K. F., & Swami, U. (2021). The dark side of immunotherapy. *Annals of Translational Medicine*, *9*(12), 1041–1041. https://doi.org/10.21037/atm-20-4750

Olivares-Hernández, A., González del Portillo, E., Tamayo-Velasco, Á., Figuero-Pérez, L., Zhilina-Zhilina, S., Fonseca-Sánchez, E., & Miramontes-González, J. P. (2023). Immune checkpoint inhibitors in non-small cell lung cancer: from current perspectives to future treatments—a systematic review. *Annals of Translational Medicine*, *11*(10), 354–354. https://doi.org/10.21037/atm-22-4218

Olivo Pimentel, V., Marcus, D., van der Wiel, A. M., Lieuwes, N. G., Biemans, R., Lieverse, R. I., Neri, D., Theys, J., Yaromina, A., Dubois, L. J., & Lambin, P. (2021). Releasing the brakes of tumor immunity with anti-PD-L1 and pushing its accelerator with L19–IL2 cures poorly immunogenic tumors when combined with radiotherapy. *Journal for ImmunoTherapy of Cancer*, *9*(3), e001764. https://doi.org/10.1136/jitc-2020-001764

Olmedo, M. E., Cervera, R., Cabezon-Gutierrez, L., Lage, Y., Corral de la Fuente, E., Gómez Rueda, A., Mielgo-Rubio, X., Trujillo, J. C., & Couñago, F. (2022). New horizons for uncommon mutations in non-small cell lung cancer: BRAF, KRAS, RET, MET, NTRK, HER2. *World Journal of Clinical Oncology*, *13*(4), 276–286. https://doi.org/10.5306/wjco.v13.i4.276

Olson, B., Li, Y., Lin, Y., Liu, E. T., & Patnaik, A. (2018). Mouse Models for Cancer Immunotherapy Research. *Cancer Discovery*, *8*(11), 1358–1365. https://doi.org/10.1158/2159-8290.CD-18-0044

Orian-Rousseau, V. (2015). CD44 Acts as a Signaling Platform Controlling Tumor Progression and Metastasis. *Frontiers in Immunology*, *6*. https://doi.org/10.3389/fimmu.2015.00154

Ortega, M. A., Boaru, D. L., De Leon-Oliva, D., Fraile-Martinez, O., García-Montero, C., Rios, L., Garrido-Gil, M. J., Barrena-Blázquez, S., Minaya-Bravo, A. M., Rios-Parra, A., Álvarez-Mon, M., Jiménez-Álvarez, L., López-González, L., Guijarro, L. G., Diaz, R., & Saez, M. A. (2024). PD-1/PD-L1 axis: implications in immune regulation, cancer progression, and translational applications. *Journal of Molecular Medicine*, *102*(8), 987–1000. https://doi.org/10.1007/s00109-024-02463-3

Oser, M. G., Niederst, M. J., Sequist, L. V, & Engelman, J. A. (2015). Transformation from non-small-cell lung cancer to small-cell lung cancer: molecular drivers and cells of origin. *The Lancet Oncology*, *16*(4), e165–e172. https://doi.org/10.1016/S1470-2045(14)71180-5

Ou, S.-H. I., & Nagasaka, M. (2020). A Catalog of 5' Fusion Partners in ROS1-Positive NSCLC Circa 2020. *JTO Clinical and Research Reports*, *1*(3), 100048. https://doi.org/10.1016/j.jtocrr.2020.100048

Oudkerk, M., Liu, S., Heuvelmans, M. A., Walter, J. E., & Field, J. K. (2021). Lung cancer LDCT screening and mortality reduction — evidence, pitfalls and future perspectives. *Nature Reviews Clinical Oncology*, *18*(3), 135–151. https://doi.org/10.1038/s41571-020-00432-6

Oxnard, G. R., Lo, P. C., Nishino, M., Dahlberg, S. E., Lindeman, N. I., Butaney, M., Jackman, D. M., Johnson, B. E., & Jänne, P. A. (2013). Natural History and Molecular Characteristics of Lung Cancers Harboring EGFR Exon 20 Insertions. *Journal of Thoracic Oncology*, *8*(2), 179–184. https://doi.org/10.1097/JTO.0b013e3182779d18

Özgü, E., Kaplan, B. G., Sivakumar, S., Sokol, E. S., Aydın, E., Tokat, Ü. M., Adibi, A., Karakoç, E. G., Hu, J., Kurzrock, R., & Demiray, M. (2024). Therapeutic vulnerabilities and pan-cancer landscape of BRAF class III mutations in epithelial solid tumors. *BJC Reports*, *2*(1), 77. https://doi.org/10.1038/s44276-024-00086-2

Özgüroğlu, M., Kilickap, S., Sezer, A., Gümüş, M., Bondarenko, I., Gogishvili, M., Nechaeva, M., Schenker, M., Cicin, I., Ho, G. F., Kulyaba, Y., Zyuhal, K., Scheusan, R.-I., Garassino, M. C., He, X., Kaul, M., Okoye, E., Li, Y., Li, S., Pouliot, J.-F., Seebach, F., Lowy, I., Gullo, G., & Rietschel, P. (2023). First-line cemiplimab monotherapy and continued cemiplimab beyond progression plus chemotherapy for advanced non-small-cell lung cancer with PD-L1 50% or more (EMPOWER-Lung 1): 35-month follow-up from a mutlicentre, open-label, randomised, phase 3 trial. *The Lancet Oncology*, *24*(9), 989–1001. https://doi.org/10.1016/S1470-2045(23)00329-7

Pagliarini, R., Shao, W., & Sellers, W. R. (2015). Oncogene addiction: pathways of therapeutic response, resistance, and road maps toward a cure. *EMBO Reports*, *16*(3), 280–296. https://doi.org/10.15252/embr.201439949

Paik, P. K., Arcila, M. E., Fara, M., Sima, C. S., Miller, V. A., Kris, M. G., Ladanyi, M., & Riely, G. J. (2011). Clinical Characteristics of Patients With Lung Adenocarcinomas Harboring *BRAF* Mutations. *Journal of Clinical Oncology*, *29*(15), 2046–2051. https://doi.org/10.1200/JCO.2010.33.1280

Palladini, A., Nicoletti, G., Lamolinara, A., Dall'ora, M., Balboni, T., Ianzano, M. L., Laranga, R., Landuzzi, L., Giusti, V., Ceccarelli, C., Santini, D., Taffurelli, M., Oto, E. Di, Asioli, S., Amici, A., Pupa, S. M., De Giovanni, C., Tagliabue, E., Iezzi, M., … Lollini, P.-L. (2017). HER2 isoforms co-expression differently tunes mammary tumor phenotypes affecting onset, vasculature and therapeutic response. *Oncotarget*, *8*(33), 54444–54458. www.impactjournals.com/oncotarget

Palladini, A., Thrane, S., Janitzek, C. M., Pihl, J., Clemmensen, S. B., de Jongh, W. A., Clausen, T. M., Nicoletti, G., Landuzzi, L., Penichet, M. L., Balboni, T., Ianzano, M. L., Giusti, V., Theander, T. G., Nielsen, M. A., Salanti, A., Lollini, P. L., Nanni, P., & Sander, A. F. (2018). Virus-like particle display of HER2 induces potent anti-cancer responses. *OncoImmunology*, *7*(3). https://doi.org/10.1080/2162402X.2017.1408749

Palma, D., Visser, O., Lagerwaard, F. J., Belderbos, J., Slotman, B. J., & Senan, S. (2010). Impact of Introducing Stereotactic Lung Radiotherapy for Elderly Patients With Stage I Non–Small-Cell Lung Cancer: A Population-Based Time-Trend Analysis. *Journal of Clinical Oncology*, *28*(35), 5153–5159. https://doi.org/10.1200/JCO.2010.30.0731

Parisi, F., Rossi, G., Biello, F., Tagliamento, M., Barletta, G., Zullo, L., Cella, E., Sacco, G., Dellepiane, C., Bennicelli, E., Favero, D., Alama, A., Coco, S., Marconi, S., Zinoli, L., Tanda, E. T., Pronzato, P., Rijavec, E., & Genova, C. (2022). Current state of the art on the diagnosis and the role of target therapy for treatment of ROS1-rearranged non-small cell lung cancer: a narrative review. *Precision Cancer Medicine*, *5*, 25–25. https://doi.org/10.21037/pcm-22-6

Park, M.-Y., Jung, M. H., Eo, E. Y., Kim, S., Lee, S. H., Lee, Y. J., Park, J. S., Cho, Y. J., Chung, J. H., Kim, C. H., Il Yoon, H., Lee, J. H., & Lee, C.-T. (2017). Generation of lung cancer cell lines harboring EGFR T790M mutation by CRISPR/Cas9-mediated genome editing. *Oncotarget*, *8*(22), 36331–36338. https://doi.org/10.18632/oncotarget.16752

Park, S., Ahn, B.-C., Lim, S. W., Sun, J.-M., Kim, H. R., Hong, M. H., Lee, S.-H., Ahn, J. S., Park, K., Choi, Y. La, Cho, B. C., & Ahn, M.-J. (2018). Characteristics and Outcome of ROS1-Positive Non–Small Cell Lung Cancer Patients in Routine Clinical Practice. *Journal of Thoracic Oncology*, *13*(9), 1373–1382. https://doi.org/10.1016/j.jtho.2018.05.026

Parvez, A., Choudhary, F., Mudgal, P., Khan, R., Qureshi, K. A., Farooqi, H., & Aspatwar, A. (2023). PD-1 and PD-L1: architects of immune symphony and immunotherapy breakthroughs in cancer treatment. *Frontiers in Immunology*, *14*. https://doi.org/10.3389/fimmu.2023.1296341

Patel, B., Gupta, N., & Ahsan, F. (2015). Particle engineering to enhance or lessen particle uptake by alveolar macrophages and to influence the therapeutic outcome. *European Journal of Pharmaceutics and Biopharmaceutics*, *89*, 163–174. https://doi.org/10.1016/j.ejpb.2014.12.001

Patel, M. R., Jay-Dixon, J., Sadiq, A. A., Jacobson, B. A., & Kratzke, R. A. (2013). Resistance to EGFR-TKI Can Be Mediated through Multiple Signaling Pathways Converging upon Cap-Dependent Translation in EGFR-Wild Type NSCLC. *Journal of Thoracic Oncology*, *8*(9), 1142–1147. https://doi.org/10.1097/JTO.0b013e31829ce963

Patel, S. A., Nilsson, M. B., Yang, Y., Le, X., Tran, H. T., Elamin, Y. Y., Yu, X., Zhang, F., Poteete, A., Ren, X., Shen, L., Wang, J., Moghaddam, S. J., Cascone, T., Curran, M., Gibbons, D. L., & Heymach, J. V. (2023). IL6 Mediates Suppression of T- and NK-cell Function in EMT-associated TKI-resistant EGFR-mutant NSCLC. *Clinical Cancer Research*, *29*(7), 1292–1304. https://doi.org/10.1158/1078-0432.CCR-22-3379

Pelosi, G., Barbareschi, M., Cavazza, A., Graziano, P., Rossi, G., & Papotti, M. (2015). Large cell carcinoma of the lung: A tumor in search of an author. A clinically oriented critical reappraisal. *Lung Cancer*, *87*(3), 226–231. https://doi.org/10.1016/j.lungcan.2015.01.008

Peng, W., Liu, C., Xu, C., Lou, Y., Chen, J., Yang, Y., Yagita, H., Overwijk, W. W., Lizee, G., Radvanyi, L., & Hwu, P. (2012). PD-1 Blockade Enhances T-cell Migration to Tumors by Elevating IFN-γ Inducible Chemokines. *Cancer Research*, *72*(20), 5209–5218. https://doi.org/10.1158/0008-5472.CAN-12-1187

Peters, S., Camidge, D. R., Shaw, A. T., Gadgeel, S., Ahn, J. S., Kim, D.-W., Ou, S.-H. I., Pérol, M., Dziadziuszko, R., Rosell, R., Zeaiter, A., Mitry, E., Golding, S., Balas, B., Noe, J., Morcos, P. N., & Mok, T. (2017). Alectinib versus Crizotinib in Untreated ALK-Positive Non–Small-Cell Lung Cancer. *New England Journal of Medicine*, *377*(9), 829–838. https://doi.org/10.1056/NEJMoa1704795

Petrella, F., Rizzo, S., Attili, I., Passaro, A., Zilli, T., Martucci, F., Bonomo, L., Del Grande, F., Casiraghi, M., De Marinis, F., & Spaggiari, L. (2023). Stage III Non-Small-Cell Lung Cancer: An Overview of Treatment Options. *Current Oncology*, *30*(3), 3160–3175. https://doi.org/10.3390/curroncol30030239

Pham, D., Bhandari, S., Pinkston, C., Oechsli, M., & Kloecker, G. (2020). Lung Cancer Screening Registry Reveals Low-dose CT Screening Remains Heavily Underutilized. *Clinical Lung Cancer*, *21*(3), e206–e211. https://doi.org/10.1016/j.cllc.2019.09.002

Phillips, T., Simmons, P., Inzunza, H. D., Cogswell, J., Novotny, J., Taylor, C., & Zhang, X. (2015). Development of an Automated PD-L1 Immunohistochemistry (IHC) Assay for Non–Small Cell Lung Cancer. *Applied Immunohistochemistry & Molecular Morphology*, *23*(8), 541–549. https://doi.org/10.1097/PAI.0000000000000256

Pinto, S., Pahl, J., Schottelius, A., Carter, P. J., & Koch, J. (2022). Reimagining antibody-dependent cellular cytotoxicity in cancer: the potential of natural killer cell engagers. *Trends in Immunology*, *43*(11), 932–946. https://doi.org/10.1016/j.it.2022.09.007

Planchard, D., Sanborn, R. E., Negrao, M. V., Vaishnavi, A., & Smit, E. F. (2024). BRAFV600E-mutant metastatic NSCLC: disease overview and treatment landscape. *Npj Precision Oncology*, *8*(1), 90. https://doi.org/10.1038/s41698-024-00552-7

Platanias, L. C. (2005). Mechanisms of type-I- and type-II-interferon-mediated signalling. In *Nature Reviews Immunology* (Vol. 5, Issue 5, pp. 375–386). https://doi.org/10.1038/nri1604

Politi, K., Zakowski, M. F., Fan, P.-D., Schonfeld, E. A., Pao, W., & Varmus, H. E. (2006). Lung adenocarcinomas induced in mice by mutant EGF receptors foundin human lung cancers respondto a tyrosine kinase inhibitor orto down-regulation of the receptors. *Genes & Development*, *20*(11), 1496–1510. https://doi.org/10.1101/gad.1417406

Pons-Tostivint, E., Latouche, A., Vaflard, P., Ricci, F., Loirat, D., Hescot, S., Sablin, M.-P., Rouzier, R., Kamal, M., Morel, C., Lecerf, C., Servois, V., Paoletti, X., & Le Tourneau, C. (2019). Comparative Analysis of Durable Responses on Immune Checkpoint Inhibitors Versus Other Systemic Therapies: A Pooled Analysis of Phase III Trials. *JCO Precision Oncology*, *3*, 1–10. https://doi.org/10.1200/PO.18.00114

Ponta, H., Sherman, L., & Herrlich, P. A. (2003). CD44: From adhesion molecules to signalling regulators. In *Nature Reviews Molecular Cell Biology* (Vol. 4, Issue 1, pp. 33–45). https://doi.org/10.1038/nrm1004

Pottier, C., Fresnais, M., Gilon, M., Jérusalem, G., Longuespée, R., & Sounni, N. E. (2020). Tyrosine Kinase Inhibitors in Cancer: Breakthrough and Challenges of Targeted Therapy. *Cancers*, *12*(3), 731. https://doi.org/10.3390/cancers12030731

Puri, M., Gawri, K., & Dawar, R. (2023). Therapeutic strategies for BRAF mutation in non-small cell lung cancer: a review. *Frontiers in Oncology*, *13*. https://doi.org/10.3389/fonc.2023.1141876

Puri, S., & Shafique, M. (2020). Combination checkpoint inhibitors for treatment of non-small-cell lung cancer: an update on dual anti-CTLA-4 and anti-PD-1/PD-L1 therapies. *Drugs in Context*, *9*, 1–11. https://doi.org/10.7573/dic.2019-9-2

Pyo, K. H., Lim, S. M., Kim, H. R., Sung, Y. H., Yun, M. R., Kim, S.-M., Kim, H., Kang, H. N., Lee, J. M., Kim, S. G., Park, C. W., Chang, H., Shim, H. S., Lee, H.-W., & Cho, B. C. (2017). Establishment of a Conditional Transgenic Mouse Model Recapitulating EML4-ALK –Positive Human Non–Small Cell Lung Cancer. *Journal of Thoracic Oncology*, *12*(3), 491–500. https://doi.org/10.1016/j.jtho.2016.10.022

Qiao, M., Zhou, F., Liu, X., Jiang, T., Wang, H., Li, X., Zhao, C., Cheng, L., Chen, X., Ren, S., Wang, Z., & Zhou, C. (2024). Targeting focal adhesion kinase boosts immune response in KRAS/LKB1 co-mutated lung adenocarcinoma via remodeling the tumor microenvironment. *Experimental Hematology & Oncology*, *13*(1), 11. https://doi.org/10.1186/s40164-023-00471-6

Qin, K., Hong, L., Zhang, J., & Le, X. (2023). MET Amplification as a Resistance Driver to TKI Therapies in Lung Cancer: Clinical Challenges and Opportunities. *Cancers*, *15*(3), 612. https://doi.org/10.3390/cancers15030612

Quint, L. E. (2007). Staging non-small cell lung cancer. *Cancer Imaging*, *7*(1), 148–159. https://doi.org/10.1102/1470-7330.2007.0026

Raedler, L. A. (2015). Opdivo (Nivolumab): Second PD-1 Inhibitor Receives FDA Approval for Unresectable or Metastatic Melanoma. *American Health & Drug Benefits*, *8*(Spec Feature), 180–183.

Ramalingam, S., & Belani, C. (2008). Systemic Chemotherapy for Advanced Non-Small Cell Lung Cancer: Recent Advances and Future Directions. *The Oncologist*, *13*(S1), 5–13. https://doi.org/10.1634/theoncologist.13-S1-5

Raman, V., Yang, C.-F. J., Deng, J. Z., & D'Amico, T. A. (2018). Surgical treatment for early stage non-small cell lung cancer. *Journal of Thoracic Disease*, *10*(S7), S898–S904. https://doi.org/10.21037/jtd.2018.01.172

Rangachari, D., Yamaguchi, N., VanderLaan, P. A., Folch, E., Mahadevan, A., Floyd, S. R., Uhlmann, E. J., Wong, E. T., Dahlberg, S. E., Huberman, M. S., & Costa, D. B. (2015). Brain metastases in patients with EGFR -mutated or ALK -rearranged non-small-cell lung cancers. *Lung Cancer*, *88*(1), 108–111. https://doi.org/10.1016/j.lungcan.2015.01.020

Reck, M., Rodríguez-Abreu, D., Robinson, A. G., Hui, R., Csőszi, T., Fülöp, A., Gottfried, M., Peled, N., Tafreshi, A., Cuffe, S., O'Brien, M., Rao, S., Hotta, K., Leiby, M. A., Lubiniecki, G. M., Shentu, Y., Rangwala, R., & Brahmer, J. R. (2016). Pembrolizumab versus Chemotherapy for PD-L1–Positive Non–Small-Cell Lung Cancer. *New England Journal of Medicine*, *375*(19), 1823–1833. https://doi.org/10.1056/NEJMoa1606774

Recondo, G., Che, J., Jänne, P. A., & Awad, M. M. (2020). Targeting MET Dysregulation in Cancer. *Cancer Discovery*, *10*(7), 922–934. https://doi.org/10.1158/2159-8290.CD-19-1446

Remon, J., Hendriks, L. E. L., Mountzios, G., García-Campelo, R., Saw, S. P. L., Uprety, D., Recondo, G., Villacampa, G., & Reck, M. (2023). MET alterations in NSCLC—Current Perspectives and Future Challenges. *Journal of Thoracic Oncology*, *18*(4), 419–435. https://doi.org/10.1016/j.jtho.2022.10.015

Reshetnyak, A. V., Rossi, P., Myasnikov, A. G., Sowaileh, M., Mohanty, J., Nourse, A., Miller, D. J., Lax, I., Schlessinger, J., & Kalodimos, C. G. (2021). Mechanism for the activation of the anaplastic lymphoma kinase receptor. *Nature*, *600*(7887), 153–157. https://doi.org/10.1038/s41586-021-04140-8

Rho, J. K., Choi, Y. J., Lee, J. K., Ryoo, B.-Y., Na, I. Il, Yang, S. H., Kim, C. H., & Lee, J. C. (2009). Epithelial to mesenchymal transition derived from repeated exposure to gefitinib determines the sensitivity to EGFR inhibitors in A549, a non-small cell lung cancer cell line. *Lung Cancer*, *63*(2), 219–226. https://doi.org/10.1016/j.lungcan.2008.05.017

Riccardo, F., Arigoni, M., Buson, G., Zago, E., Iezzi, M., Longo, D. L., Carrara, M., Fiore, A., Nuzzo, S., Bicciato, S., Nanni, P., Landuzzi, L., Cavallo, F., Calogero, R., & Quaglino, E. (2014). Characterization of a genetic mouse model of lung cancer: a promise to identify Non-Small Cell Lung Cancer therapeutic targets and biomarkers. *BMC Genomics*, *15*(S3), S1. https://doi.org/10.1186/1471-2164-15-S3-S1

Richter, M., Piwocka, O., Musielak, M., Piotrowski, I., Suchorska, W. M., & Trzeciak, T. (2021). From Donor to the Lab: A Fascinating Journey of Primary Cell Lines. *Frontiers in Cell and Developmental Biology*, *9*. https://doi.org/10.3389/fcell.2021.711381

Ríos-Hoyo, A., Moliner, L., & Arriola, E. (2022). Acquired Mechanisms of Resistance to Osimertinib—The Next Challenge. *Cancers*, *14*(8), 1931. https://doi.org/10.3390/cancers14081931

Rittmeyer, A., Barlesi, F., Waterkamp, D., Park, K., Ciardiello, F., von Pawel, J., Gadgeel, S. M., Hida, T., Kowalski, D. M., Dols, M. C., Cortinovis, D. L., Leach, J., Polikoff, J., Barrios, C., Kabbinavar, F., Frontera, O. A., De Marinis, F., Turna, H., Lee, J.-S., Ballinger, M., Kowanetz, M., He, P., Chen, D. S., Sandler, A., & Gandara, D. R. (2017). Atezolizumab versus docetaxel in patients with previously treated non-small-cell lung cancer (OAK): a phase 3, open-label, multicentre randomised controlled trial. *The Lancet*, *389*(10066), 255–265. https://doi.org/10.1016/S0140-6736(16)32517-X

Rivera-Concepcion, J., Uprety, D., & Adjei, A. A. (2022). Challenges in the Use of Targeted Therapies in Non–Small Cell Lung Cancer. *Cancer Research and Treatment*, *54*(2), 315–329. https://doi.org/10.4143/crt.2022.078

Robey, R. W., Pluchino, K. M., Hall, M. D., Fojo, A. T., Bates, S. E., & Gottesman, M. M. (2018). Revisiting the role of ABC transporters in multidrug-resistant cancer. *Nature Reviews Cancer*, *18*(7), 452–464. https://doi.org/10.1038/s41568-018-0005-8

Rodríguez De Dios, N., Navarro-Martin, A., Cigarral, C., Chicas-Sett, R., García, R., Garcia, V., Gonzalez, J. A., Gonzalo, S., Murcia-Mejía, M., Robaina, R., Sotoca, A., Vallejo, C., Valtueña, G., & Couñago, F. (2022). GOECP/SEOR radiotheraphy guidelines for non-small-cell lung cancer. *World Journal of Clinical Oncology*, *13*(4), 237–266. https://doi.org/10.5306/wjco.v13.i4.237

Rodríguez-Hernández, M. A., Chapresto-Garzón, R., Cadenas, M., Navarro-Villarán, E., Negrete, M., Gómez-Bravo, M. A., Victor, V. M., Padillo, F. J., & Muntané, J. (2020). Differential effectiveness of tyrosine kinase inhibitors in 2D/3D culture according to cell differentiation, p53 status and mitochondrial respiration in liver cancer cells. *Cell Death & Disease*, *11*(5), 339. https://doi.org/10.1038/s41419-020-2558-1

Rogers, A. B. (2019). Stress of Strains: Inbred Mice in Liver Research. *Gene Expression*, *19*(1), 61–67. https://doi.org/10.3727/105221618X15337408678723

Rogers, D. F. (1994). Airway goblet cells: responsive and adaptable front-line defenders. *The European Respiratory Journal*, *7*(9), 1690–1706.

Rosell, R., Moran, T., Queralt, C., Porta, R., Cardenal, F., Camps, C., Majem, M., Lopez-Vivanco, G., Isla, D., Provencio, M., Insa, A., Massuti, B., Gonzalez-Larriba, J. L., Paz-Ares, L., Bover, I., Garcia-Campelo, R., Moreno, M. A., Catot, S., Rolfo, C., Reguart, N., Palmero, R., Sánchez, J. M., Bastus, R., Mayo, C., Bertran-Alamillo, J., Molina, M. A., Sanchez, J. J., & Taron, M. (2009). Screening for Epidermal Growth Factor Receptor Mutations in Lung Cancer. *New England Journal of Medicine*, *361*(10), 958–967. https://doi.org/10.1056/NEJMoa0904554

Rosen, R. D., & Sapra, A. (2024). TNM Classification. In: StatPearls [Internet]. Treasure Island (FL): StatPearls. PMID: 31985980

Ru Zhao, Y., Xie, X., de Koning, H. J., Mali, W. P., Vliegenthart, R., & Oudkerk, M. (2011). NELSON lung cancer screening study. *Cancer Imaging: The Official Publication of the International Cancer Imaging Society*, *11 Spec No A*(1A), S79-84. https://doi.org/10.1102/1470-7330.2011.9020

Ruge, C. A., Kirch, J., & Lehr, C.-M. (2013). Pulmonary drug delivery: from generating aerosols to overcoming biological barriers—therapeutic possibilities and technological challenges. *The Lancet Respiratory Medicine*, *1*(5), 402–413. https://doi.org/10.1016/S2213-2600(13)70072-9

Ruzzi, F., Angelicola, S., Landuzzi, L., Nironi, E., Semprini, M. S., Scalambra, L., Altimari, A., Gruppioni, E., Fiorentino, M., Giunchi, F., Ferracin, M., Astolfi, A., Indio, V., Ardizzoni, A., Gelsomino, F., Nanni, P., Lollini, P. L., & Palladini, A. (2022). ADK-VR2, a cell line derived from a treatment-naïve patient with SDC4-ROS1 fusion-positive primarily crizotinib-resistant NSCLC: a novel preclinical model for new drug development of ROS1-rearranged NSCLC. *Translational Lung Cancer Research*, *11*(11), 2216–2229. https://doi.org/10.21037/tlcr-22-163

Ryu, R., & Ward, K. E. (2018). Atezolizumab for the First-Line Treatment of Non-small Cell Lung Cancer (NSCLC): Current Status and Future Prospects. *Frontiers in Oncology*, *8*. https://doi.org/10.3389/fonc.2018.00277

Saâda-Bouzid, E., Defaucheux, C., Karabajakian, A., Coloma, V. P., Servois, V., Paoletti, X., Even, C., Fayette, J., Guigay, J., Loirat, D., Peyrade, F., Alt, M., Gal, J., & Le Tourneau, C. (2017). Hyperprogression during anti-PD-1/PD-L1 therapy in patients with recurrent and/or metastatic head and neck squamous cell carcinoma. *Annals of Oncology*, *28*(7), 1605–1611. https://doi.org/10.1093/annonc/mdx178

Saada-Bouzid, E., Defaucheux, C., Karabajakian, A., Palomar Coloma, V., Servois, V., Paoletti, X., Even, C., Fayette, J., Guigay, J., Loirat, D., Romano, E., & Le Tourneau, C. (2016). Tumor's flare-up and patterns of recurrence in patients (pts) with recurrent and/or metastatic (R/M) head and neck squamous cell carcinoma (HNSCC) treated with anti-PD1/PD-L1 inhibitors. *Journal of Clinical Oncology*, *34*(15_suppl), 6072–6072. https://doi.org/10.1200/JCO.2016.34.15_suppl.6072

Sahin, I. H., & Klostergaard, J. (2021). BRAF Mutations as Actionable Targets: A Paradigm Shift in the Management of Colorectal Cancer and Novel Avenues. *JCO Oncology Practice*, *17*(12), 723–730. https://doi.org/10.1200/OP.21.00160

Salehi-Rad, R., Li, R., Tran, L. M., Lim, R. J., Abascal, J., Momcilovic, M., Park, S. J., Ong, S. L., Shabihkhani, M., Huang, Z. L., Paul, M., Shackelford, D. B., Krysan, K., Liu, B., & Dubinett, S. M. (2021). Novel Kras-mutant murine models of non-small cell lung cancer possessing co-occurring oncogenic mutations and increased tumor mutational burden. *Cancer Immunology, Immunotherapy*, *70*(8), 2389–2400. https://doi.org/10.1007/s00262-020-02837-9

Salemme, V., Centonze, G., Avalle, L., Natalini, D., Piccolantonio, A., Arina, P., Morellato, A., Ala, U., Taverna, D., Turco, E., & Defilippi, P. (2023). The role of tumor microenvironment in drug resistance: emerging technologies to unravel breast cancer heterogeneity. *Frontiers in Oncology*, *13*. https://doi.org/10.3389/fonc.2023.1170264

Sanmamed, M. F., Chester, C., Melero, I., & Kohrt, H. (2016). Defining the optimal murine models to investigate immune checkpoint blockers and their combination with other immunotherapies. *Annals of Oncology*, *27*(7), 1190–1198. https://doi.org/10.1093/annonc/mdw041

Santarpia, M., Massafra, M., Gebbia, V., D'Aquino, A., Garipoli, C., Altavilla, G., & Rosell, R. (2021). A narrative review of MET inhibitors in non-small cell lung cancer with MET exon 14 skipping mutations. *Translational Lung Cancer Research*, *10*(3), 1536–1556. https://doi.org/10.21037/tlcr-20-1113

Santhanakrishnan, J., Meganathan, P., & Vedagiri, H. (2024). Structural biology of HER2/ERBB2 dimerization: mechanistic insights and differential roles in healthy versus cancerous cells. *Exploration of Medicine*, 530–543. https://doi.org/10.37349/emed.2024.00237

Sarfaty, M., Moore, A., Neiman, V., Dudnik, E., Ilouze, M., Gottfried, M., Katznelson, R., Nechushtan, H., Sorotsky, H. G., Paz, K., Katz, A., Saute, M., Wolner, M., Moskovitz, M., Miller, V., Elvin, J., Lipson, D., Ali, S., Gutman, L. S., Dvir, A., Gordon, N., & Peled, N. (2017). RET Fusion Lung Carcinoma: Response to Therapy and Clinical Features in a Case Series of 14 Patients. *Clinical Lung Cancer*, *18*(4), e223–e232. https://doi.org/10.1016/j.cllc.2016.09.003

Sartore-Bianchi, A., Trusolino, L., Martino, C., Bencardino, K., Lonardi, S., Bergamo, F., Zagonel, V., Leone, F., Depetris, I., Martinelli, E., Troiani, T., Ciardiello, F., Racca, P., Bertotti, A., Siravegna, G., Torri, V., Amatu,

A., Ghezzi, S., Marrapese, G., Palmeri, L., Valtorta, E., Cassingena, A., Lauricella, C., Vanzulli, A., Regge, D., Veronese, S., Comoglio, P. M., Bardelli, A., Marsoni, S., & Siena, S. (2016). Dual-targeted therapy with trastuzumab and lapatinib in treatment-refractory, KRAS codon 12/13 wild-type, HER2-positive metastatic colorectal cancer (HERACLES): a proof-of-concept, multicentre, open-label, phase 2 trial. *The Lancet Oncology*, *17*(6), 738–746. https://doi.org/10.1016/S1470-2045(16)00150-9

Saxena, M., & Christofori, G. (2013). Rebuilding cancer metastasis in the mouse. *Molecular Oncology*, *7*(2), 283–296. https://doi.org/10.1016/j.molonc.2013.02.009

Scheffler, M., Bos, M., Gardizi, M., König, K., Michels, S., Fassunke, J., Heydt, C., Künstlinger, H., Ihle, M., Ueckeroth, F., Albus, K., Serke, M., Gerigk, U., Schulte, W., Töpelt, K., Nogova, L., Zander, T., Engel-Riedel, W., Stoelben, E., Ko, Y.-D., Randerath, W., Kaminsky, B., Panse, J., Becker, C., Hellmich, M., Merkelbach-Bruse, S., Heukamp, L. C., Büttner, R., & Wolf, J. (2015). PIK3CA mutations in non-small cell lung cancer (NSCLC): Genetic heterogeneity, prognostic impact and incidence of prior malignancies. *Oncotarget*, *6*(2), 1315–1326. https://doi.org/10.18632/oncotarget.2834

Schmidt, A., Oberle, N., & Krammer, P. H. (2012). Molecular Mechanisms of Treg-Mediated T Cell Suppression. *Frontiers in Immunology*, *3*. https://doi.org/10.3389/fimmu.2012.00051

Schmitt, M., Metzger, M., Gradl, D., Davidson, G., & Orian-Rousseau, V. (2015). CD44 functions in Wnt signaling by regulating LRP6 localization and activation. *Cell Death & Differentiation*, *22*(4), 677–689. https://doi.org/10.1038/cdd.2014.156

Schneeberger, V. E., Allaj, V., Gardner, E. E., Poirier, J. T., & Rudin, C. M. (2016). Quantitation of Murine Stroma and Selective Purification of the Human Tumor Component of Patient-Derived Xenografts for Genomic Analysis. *PLOS ONE*, *11*(9), e0160587. https://doi.org/10.1371/journal.pone.0160587

Schoenfeld, A. J., & Hellmann, M. D. (2020). Acquired Resistance to Immune Checkpoint Inhibitors. In *Cancer Cell* (Vol. 37, Issue 4, pp. 443–455). Cell Press. https://doi.org/10.1016/j.ccell.2020.03.017

Scobie, M. R., Zhou, K. I., Ahmed, S., & Kelley, M. J. (2023). Utility of Tumor Mutational Burden as a Biomarker for Response to Immune Checkpoint Inhibition in the VA Population. *JCO Precision Oncology*, *7*. https://doi.org/10.1200/PO.23.00176

Sculier, J.-P., & Moro-Sibilot, D. (2009). First- and second-line therapy for advanced nonsmall cell lung cancer. *European Respiratory Journal*, *33*(4), 915–930. https://doi.org/10.1183/09031936.00132008

Semenova, E. A., Nagel, R., & Berns, A. (2015). Origins, genetic landscape, and emerging therapies of small cell lung cancer. *Genes & Development*, *29*(14), 1447–1462. https://doi.org/10.1101/gad.263145.115

Senbanjo, L. T., & Chellaiah, M. A. (2017). CD44: A Multifunctional Cell Surface Adhesion Receptor Is a Regulator of Progression and Metastasis of Cancer Cells. *Frontiers in Cell and Developmental Biology*, *5*. https://doi.org/10.3389/fcell.2017.00018

Sezer, A., Kilickap, S., Gümüş, M., Bondarenko, I., Özgüroğlu, M., Gogishvili, M., Turk, H. M., Cicin, I., Bentsion, D., Gladkov, O., Clingan, P., Sriuranpong, V., Rizvi, N., Gao, B., Li, S., Lee, S., McGuire, K., Chen, C.-I., Makharadze, T., Paydas, S., Nechaeva, M., Seebach, F., Weinreich, D. M., Yancopoulos, G. D., Gullo, G., Lowy, I., & Rietschel, P. (2021). Cemiplimab monotherapy for first-line treatment of advanced non-small-cell lung cancer with PD-L1 of at least 50%: a multicentre, open-label, global, phase 3, randomised, controlled trial. *The Lancet*, *397*(10274), 592–604. https://doi.org/10.1016/S0140-6736(21)00228-2

Sharma, S. V., & Settleman, J. (2010). Exploiting the balance between life and death: Targeted cancer therapy and "oncogenic shock." *Biochemical Pharmacology*, *80*(5), 666–673. https://doi.org/10.1016/j.bcp.2010.03.001

Sharpe, A. H., & Pauken, K. E. (2018). The diverse functions of the PD1 inhibitory pathway. *Nature Reviews Immunology*, *18*(3), 153–167. https://doi.org/10.1038/nri.2017.108

Shaw, A. T., Kim, D.-W., Nakagawa, K., Seto, T., Crinó, L., Ahn, M.-J., De Pas, T., Besse, B., Solomon, B. J., Blackhall, F., Wu, Y.-L., Thomas, M., O'Byrne, K. J., Moro-Sibilot, D., Camidge, D. R., Mok, T., Hirsh, V., Riely, G. J., Iyer, S., Tassell, V., Polli, A., Wilner, K. D., & Jänne, P. A. (2013). Crizotinib versus Chemotherapy in Advanced ALK-Positive Lung Cancer. *New England Journal of Medicine*, *368*(25), 2385–2394. https://doi.org/10.1056/NEJMoa1214886

Shaw, A. T., Riely, G. J., Bang, Y.-J., Kim, D.-W., Camidge, D. R., Solomon, B. J., Varella-Garcia, M., Iafrate, A. J., Shapiro, G. I., Usari, T., Wang, S. C., Wilner, K. D., Clark, J. W., & Ou, S.-H. I. (2019). Crizotinib in ROS1-rearranged advanced non-small-cell lung cancer (NSCLC): updated results, including overall survival, from PROFILE 1001. *Annals of Oncology*, *30*(7), 1121–1126. https://doi.org/10.1093/annonc/mdz131

Shaw, A. T., Yeap, B. Y., Mino-Kenudson, M., Digumarthy, S. R., Costa, D. B., Heist, R. S., Solomon, B., Stubbs, H., Admane, S., McDermott, U., Settleman, J., Kobayashi, S., Mark, E. J., Rodig, S. J., Chirieac, L. R., Kwak, E. L., Lynch, T. J., & Iafrate, A. J. (2009). Clinical Features and Outcome of Patients With Non–Small-Cell Lung Cancer Who Harbor EML4-ALK. *Journal of Clinical Oncology*, *27*(26), 4247–4253. https://doi.org/10.1200/JCO.2009.22.6993

Shi, Y., Fu, X., Hua, Y., Han, Y., Lu, Y., & Wang, J. (2012). The Side Population in Human Lung Cancer Cell Line NCI-H460 Is Enriched in Stem-Like Cancer Cells. *PLoS ONE*, *7*(3), e33358. https://doi.org/10.1371/journal.pone.0033358

Sholl, L. (2017). Molecular diagnostics of lung cancer in the clinic. *Translational Lung Cancer Research*, *6*(5), 560–569. https://doi.org/10.21037/tlcr.2017.08.03

Sia, J., Szmyd, R., Hau, E., & Gee, H. E. (2020). Molecular Mechanisms of Radiation-Induced Cancer Cell Death: A Primer. *Frontiers in Cell and Developmental Biology*, *8*. https://doi.org/10.3389/fcell.2020.00041

Simasi, J., Schubert, A., Oelkrug, C., Gillissen, A., & Nieber, K. (2014). Primary and secondary resistance to tyrosine kinase inhibitors in lung cancer. *Anticancer Research*, *34*(6), 2841–2850.

Simond, A. M., & Muller, W. J. (2020). *In vivo modeling of the EGFR family in breast cancer progression and therapeutic approaches* (pp. 189–228). https://doi.org/10.1016/bs.acr.2020.04.004

Singavi, A. K., Menon, S., Kilari, D., Alqwasmi, A., Ritch, P. S., Thomas, J. P., Martin, A. L., Oxencis, C., Ali, S., & George, B. (2017). Predictive biomarkers for hyper-progression (HP) in response to immune checkpoint inhibitors (ICI) – analysis of somatic alterations (SAs). *Annals of Oncology*, *28*, v405. https://doi.org/10.1093/annonc/mdx376.006

Singh, B., Carpenter, G., & Coffey, R. J. (2016). EGF receptor ligands: recent advances. *F1000Research*, *5*, 2270. https://doi.org/10.12688/f1000research.9025.1

Singh, N., Temin, S., Baker, S., Blanchard, E., Brahmer, J. R., Celano, P., Duma, N., Ellis, P. M., Elkins, I. B., Haddad, R. Y., Hesketh, P. J., Jain, D., Johnson, D. H., Leighl, N. B., Mamdani, H., Masters, G., Moffitt, P. R., Phillips, T., Riely, G. J., Robinson, A. G., Rosell, R., Schiller, J. H., Schneider, B. J., Spigel, D. R., & Jaiyesimi, I. A. (2022). Therapy for Stage IV Non–Small-Cell Lung Cancer Without Driver Alterations: ASCO Living Guideline. *Journal of Clinical Oncology*, *40*(28), 3323–3343. https://doi.org/10.1200/JCO.22.00825

Skaper, S. D. (2012). The neurotrophin family of neurotrophic factors: an overview. *Methods in Molecular Biology*, *846*, 1-12. https://doi.org/10.1007/978-1-61779-536-7_1

Skoulidis, F., Li, B. T., Dy, G. K., Price, T. J., Falchook, G. S., Wolf, J., Italiano, A., Schuler, M., Borghaei, H., Barlesi, F., Kato, T., Curioni-Fontecedro, A., Sacher, A., Spira, A., Ramalingam, S. S., Takahashi, T., Besse, B., Anderson, A., Ang, A., Tran, Q., Mather, O., Henary, H., Ngarmchamnanrith, G., Friberg, G., Velcheti, V., & Govindan, R. (2021). Sotorasib for Lung Cancers with KRAS p.G12C Mutation. *New England Journal of Medicine*, *384*(25), 2371–2381. https://doi.org/10.1056/NEJMoa2103695

Śmiech, M., Leszczyński, P., Kono, H., Wardell, C., & Taniguchi, H. (2020). Emerging BRAF Mutations in Cancer Progression and Their Possible Effects on Transcriptional Networks. *Genes*, *11*(11), 1342. https://doi.org/10.3390/genes11111342

Solana, R., Tarazona, R., Gayoso, I., Lesur, O., Dupuis, G., & Fulop, T. (2012). Innate immunosenescence: Effect of aging on cells and receptors of the innate immune system in humans. *Seminars in Immunology*, *24*(5), 331–341. https://doi.org/10.1016/j.smim.2012.04.008

Solomon, B. J., Besse, B., Bauer, T. M., Felip, E., Soo, R. A., Camidge, D. R., Chiari, R., Bearz, A., Lin, C.-C., Gadgeel, S. M., Riely, G. J., Tan, E. H., Seto, T., James, L. P., Clancy, J. S., Abbattista, A., Martini, J.-F., Chen, J., Peltz, G., Thurm, H., Ou, S.-H. I., & Shaw, A. T. (2018). Lorlatinib in patients with ALK-positive non-small-cell lung cancer: results from a global phase 2 study. *The Lancet Oncology*, *19*(12), 1654–1667. https://doi.org/10.1016/S1470-2045(18)30649-1

Solomon, B. J., Mok, T., Kim, D.-W., Wu, Y.-L., Nakagawa, K., Mekhail, T., Felip, E., Cappuzzo, F., Paolini, J., Usari, T., Iyer, S., Reisman, A., Wilner, K. D., Tursi, J., & Blackhall, F. (2014). First-Line Crizotinib versus Chemotherapy in ALK-Positive Lung Cancer. *New England Journal of Medicine*, *371*(23), 2167–2177. https://doi.org/10.1056/NEJMoa1408440

Son, B., Lee, S., Youn, H., Kim, E., Kim, W., & Youn, B. (2017). The role of tumor microenvironment in therapeutic resistance. *Oncotarget*, *8*(3), 3933–3945. https://doi.org/10.18632/oncotarget.13907

Song, H., Yao, E., Lin, C., Gacayan, R., Chen, M.-H., & Chuang, P.-T. (2012). Functional characterization of pulmonary neuroendocrine cells in lung development, injury, and tumorigenesis. *Proceedings of the National Academy of Sciences*, *109*(43), 17531–17536. https://doi.org/10.1073/pnas.1207238109

Song, M., Ping, Y., Zhang, K., Yang, L., Li, F., Zhang, C., Cheng, S., Yue, D., Maimela, N. R., Qu, J., Liu, S., Sun, T., Li, Z., Xia, J., Zhang, B., Wang, L., & Zhang, Y. (2019). Low-dose IFNγ induces tumor cell stemness in tumor microenvironment of non–small cell lung cancer. *Cancer Research*, *79*(14), 3737–3748. https://doi.org/10.1158/0008-5472.CAN-19-0596

Song, Y.-A., Ma, T., Zhang, X.-Y., Cheng, X.-S., Olajuyin, A.-M., Sun, Z.-F., & Zhang, X.-J. (2019). Apatinib preferentially inhibits PC9 gefitinib-resistant cancer cells by inducing cell cycle arrest and inhibiting VEGFR signaling pathway. *Cancer Cell International*, *19*(1), 117. https://doi.org/10.1186/s12935-019-0836-8

Sperk, M., Domselaar, R. van, & Neogi, U. (2018). Immune Checkpoints as the Immune System Regulators and Potential Biomarkers in HIV-1 Infection. *International Journal of Molecular Sciences*, *19*(7), 2000. https://doi.org/10.3390/ijms19072000

Spigel, D. R., Faivre-Finn, C., Gray, J. E., Vicente, D., Planchard, D., Paz-Ares, L., Vansteenkiste, J. F., Garassino, M. C., Hui, R., Quantin, X., Rimner, A., Wu, Y.-L., Özgüroğlu, M., Lee, K. H., Kato, T., de Wit, M., Kurata, T., Reck, M., Cho, B. C., Senan, S., Naidoo, J., Mann, H., Newton, M., Thiyagarajah, P., & Antonia, S. J. (2022). Five-Year Survival Outcomes From the PACIFIC Trial: Durvalumab After Chemoradiotherapy in Stage III Non–Small-Cell Lung Cancer. *Journal of Clinical Oncology*, *40*(12), 1301–1311. https://doi.org/10.1200/JCO.21.01308

Spitaleri, G., Trillo Aliaga, P., Attili, I., Del Signore, E., Corvaja, C., Corti, C., Uliano, J., Passaro, A., & de Marinis, F. (2023). MET in Non-Small-Cell Lung Cancer (NSCLC): Cross 'a Long and Winding Road' Looking for a Target. *Cancers*, *15*(19), 4779. https://doi.org/10.3390/cancers15194779

Spranger, S., Spaapen, R. M., Zha, Y., Williams, J., Meng, Y., Ha, T. T., & Gajewski, T. F. (2013). Up-Regulation of PD-L1, IDO, and Tregs in the Melanoma Tumor Microenvironment Is Driven by CD8+ T Cells. *Science Translational Medicine*, *5*(200). https://doi.org/10.1126/scitranslmed.3006504

Stewart, E. L., Zhixing Tan, S., Liu, G., & Tsao, M.-S. (2015). Known and putative mechanisms of resistance to EGFR targeted therapies in NSCLC patients with EGFR mutations—a review. *Translational Lung Cancer*, *4*(1), 67–81. https://doi.org/10.3978/j.issn.2218-6751.2014.11.06

Straub, M., Drecoll, E., Pfarr, N., Weichert, W., Langer, R., Hapfelmeier, A., Götz, C., Wolff, K.-D., Kolk, A., & Specht, K. (2016). CD274/PD-L1 gene amplification and PD-L1 protein expression are common events in squamous cell carcinoma of the oral cavity. *Oncotarget*, *7*(11), 12024–12034. https://doi.org/10.18632/oncotarget.7593

Suda, K., Mizuuchi, H., Maehara, Y., & Mitsudomi, T. (2012). Acquired resistance mechanisms to tyrosine kinase inhibitors in lung cancer with activating epidermal growth factor receptor mutation—diversity, ductility, and destiny. *Cancer and Metastasis Reviews*, *31*(3–4), 807–814. https://doi.org/10.1007/s10555-012-9391-7

Suda, K., Murakami, I., Yu, H., Kim, J., Tan, A.-C., Mizuuchi, H., Rozeboom, L., Ellison, K., Rivard, C. J., Mitsudomi, T., & Hirsch, F. R. (2018). CD44 Facilitates Epithelial-to-Mesenchymal Transition Phenotypic Change at Acquisition of Resistance to EGFR Kinase Inhibitors in Lung Cancer. *Molecular Cancer Therapeutics*, *17*(10), 2257–2265. https://doi.org/10.1158/1535-7163.MCT-17-1279

Sudo, M., Chin, T. M., Mori, S., Doan, N. B., Said, J. W., Akashi, M., & Koeffler, H. P. (2013). Inhibiting proliferation of gefitinib-resistant, non-small cell lung cancer. *Cancer Chemotherapy and Pharmacology*, *71*(5), 1325–1334. https://doi.org/10.1007/s00280-013-2132-y

Sun, C., Mezzadra, R., & Schumacher, T. N. (2018). Regulation and Function of the PD-L1 Checkpoint. *Immunity*, *48*(3), 434–452. https://doi.org/10.1016/j.immuni.2018.03.014

Sun, J., Hu, R., Han, M., Tan, Y., Xie, M., Gao, S., & Hu, J.-F. (2024). Mechanisms underlying therapeutic resistance of tyrosine kinase inhibitors in chronic myeloid leukemia. *International Journal of Biological Sciences*, *20*(1), 175–181. https://doi.org/10.7150/ijbs.86305

Sun, Z., Fourcade, J., Pagliano, O., Chauvin, J.-M., Sander, C., Kirkwood, J. M., & Zarour, H. M. (2015). IL10 and PD-1 Cooperate to Limit the Activity of Tumor-Specific CD8+ T Cells. *Cancer Research*, *75*(8), 1635–1644. https://doi.org/10.1158/0008-5472.CAN-14-3016

Sunil, H. S., & O'Donnell, K. A. (2024). Capturing heterogeneity in PDX models: representation matters. *Nature Communications*, *15*(1), 4652. https://doi.org/10.1038/s41467-024-47607-8

Sutherland, K. D., & Berns, A. (2010). Cell of origin of lung cancer. *Molecular Oncology*, *4*(5), 397–403. https://doi.org/10.1016/j.molonc.2010.05.002

Syed, Y. Y. (2017). Durvalumab: First Global Approval. *Drugs*, *77*(12), 1369–1376. https://doi.org/10.1007/s40265-017-0782-5

Takahashi, M. (2022). RET receptor signaling: Function in development, metabolic disease, and cancer. *Proceedings of the Japan Academy, Series B*, *98*(3), PJA9803B-02. https://doi.org/10.2183/pjab.98.008

Takase, M., Yamada, M., Nakamura, T., Nakaya, N., Kogure, M., Hatanaka, R., Nakaya, K., Chiba, I., Kanno, I., Nochioka, K., Tsuchiya, N., Hirata, T., Hamanaka, Y., Sugawara, J., Kobayashi, T., Fuse, N., Uruno, A., Kodama, E. N., Kuriyama, S., Tsuji, I., & Hozawa, A. (2023). Association between lung function and hypertension and home hypertension in a Japanese population: the Tohoku Medical Megabank Community-Based Cohort Study. *Journal of Hypertension*, *41*(3), 443–452. https://doi.org/10.1097/HJH.0000000000003356

Takeuchi, K., Soda, M., Togashi, Y., Suzuki, R., Sakata, S., Hatano, S., Asaka, R., Hamanaka, W., Ninomiya, H., Uehara, H., Lim Choi, Y., Satoh, Y., Okumura, S., Nakagawa, K., Mano, H., & Ishikawa, Y. (2012). RET, ROS1 and ALK fusions in lung cancer. *Nature Medicine*, *18*(3), 378–381. https://doi.org/10.1038/nm.2658

Tan, A. C. (2020). Targeting the PI3K/Akt/mTOR pathway in non-small cell lung cancer (NSCLC). *Thoracic Cancer*, *11*(3), 511–518. https://doi.org/10.1111/1759-7714.13328

Tan, A. C., Tan, S. H., Ang, M.-K., & Tan, D. S. W. (2023). First-line ALK inhibitors in treatment-naive advanced ALK rearranged non-small cell lung cancer: systematic review and network meta-analysis. *Precision Cancer Medicine*, *6*, 3–3. https://doi.org/10.21037/pcm-22-54

Tan, N., Malek, M., Zha, J., Yue, P., Kassees, R., Berry, L., Fairbrother, W. J., Sampath, D., & Belmont, L. D. (2011). Navitoclax Enhances the Efficacy of Taxanes in Non–Small Cell Lung Cancer Models. *Clinical Cancer Research*, *17*(6), 1394–1404. https://doi.org/10.1158/1078-0432.CCR-10-2353

Tang, S., Qin, C., Hu, H., Liu, T., He, Y., Guo, H., Yan, H., Zhang, J., Tang, S., & Zhou, H. (2022). Immune Checkpoint Inhibitors in Non-Small Cell Lung Cancer: Progress, Challenges, and Prospects. *Cells*, *11*(3), 320. https://doi.org/10.3390/cells11030320

Tang, Y., Pu, X., Yuan, X., Pang, Z., Li, F., & Wang, X. (2024). Targeting KRASG12D mutation in non-small cell lung cancer: molecular mechanisms and therapeutic potential. *Cancer Gene Therapy*, *31*(7), 961–969. https://doi.org/10.1038/s41417-024-00778-4

Tang, Z.-H., Jiang, X.-M., Guo, X., Fong, C. M. V., Chen, X., & Lu, J.-J. (2016). Characterization of osimertinib (AZD9291)-resistant non-small cell lung cancer NCI-H1975/OSIR cell line. *Oncotarget*, *7*(49), 81598–81610. https://doi.org/10.18632/oncotarget.13150

ten Berge, D. M. H. J., Damhuis, R. A. M., Aerts, J. G. J. V., & Dingemans, A.-M. C. (2023). Real-world treatment patterns and survival of patients with ROS1 rearranged stage IV non-squamous NSCLC in the Netherlands. *Lung Cancer*, *181*, 107253. https://doi.org/10.1016/j.lungcan.2023.107253

Terrones, M., de Beeck, K. O., Van Camp, G., & Vandeweyer, G. (2023). Pre-clinical modelling of ROS1+ non-small cell lung cancer. *Lung Cancer*, *180*, 107192. https://doi.org/10.1016/j.lungcan.2023.107192

Terrones, M., Deben, C., Rodrigues-Fortes, F., Schepers, A., de Beeck, K. O., Van Camp, G., & Vandeweyer, G. (2024). CRISPR/Cas9-edited ROS1 + non-small cell lung cancer cell lines highlight differential drug sensitivity in 2D vs 3D cultures while reflecting established resistance profiles. *Journal of Translational Medicine*, *22*(1), 234. https://doi.org/10.1186/s12967-024-04988-0

Testa, U., Castelli, G., & Pelosi, E. (2023). ROS1-Rearranged Lung Adenocarcinoma: From Molecular Genetics to Target Therapy. *Onco*, *3*(3), 189–204. https://doi.org/10.3390/onco3030014

Thai, A. A., Solomon, B. J., Sequist, L. V., Gainor, J. F., & Heist, R. S. (2021). Lung cancer. *The Lancet 398*(10299), 535–554). https://doi.org/10.1016/S0140-6736(21)00312-3

Thapa, R., & Wilson, G. D. (2016). The Importance of CD44 as a Stem Cell Biomarker and Therapeutic Target in Cancer. In *Stem Cells International* (Vol. 2016). Hindawi Limited. https://doi.org/10.1155/2016/2087204

The Cancer Genome Atlas Research Network. (2014). Comprehensive molecular profiling of lung adenocarcinoma. *Nature*, *511*(7511), 543–550. https://doi.org/10.1038/nature13385

Theivanthiran, B., Evans, K. S., DeVito, N. C., Plebanek, M., Sturdivant, M., Wachsmuth, L. P., Salama, A. K. S., Kang, Y., Hsu, D., Balko, J. M., Johnson, D. B., Starr, M., Nixon, A., Holtzhausen, A., & Hanks, B. A. (2020). A tumor-intrinsic PD-L1/NLRP3 inflammasome signaling pathway drives resistance to anti–PD-1 immunotherapy. *Journal of Clinical Investigation*, *130*(5), 2570–2586. https://doi.org/10.1172/JCI133055

Timmerman, R. D., Paulus, R., Pass, H. I., Gore, E. M., Edelman, M. J., Galvin, J., Straube, W. L., Nedzi, L. A., McGarry, R. C., Robinson, C. G., Schiff, P. B., Chang, G., Loo, B. W., Bradley, J. D., & Choy, H. (2018). Stereotactic Body Radiation Therapy for Operable Early-Stage Lung Cancer. *JAMA Oncology*, *4*(9), 1263. https://doi.org/10.1001/jamaoncol.2018.1251

Travis, W. D., Brambilla, E., Burke, A. P., Marx, A., & Nicholson, A. G. (2015). Introduction to The 2015 World Health Organization Classification of Tumors of the Lung, Pleura, Thymus, and Heart. *Journal of Thoracic Oncology*, *10*(9), 1240–1242. https://doi.org/10.1097/JTO.0000000000000663

Travis, W. D., Brambilla, E., Nicholson, A. G., Yatabe, Y., Austin, J. H. M., Beasley, M. B., Chirieac, Lucian. R., Dacic, S., Duhig, E., Flieder, D. B., Geisinger, K., Hirsch, F. R., Ishikawa, Y., Kerr, K. M., Noguchi, M., Pelosi, G., Powell, C. A., Tsao, M. S., & Wistuba, I. (2015). The 2015 World Health Organization

Classification of Lung Tumors. *Journal of Thoracic Oncology*, *10*(9), 1243–1260. https://doi.org/10.1097/JTO.0000000000000630

Tsang, M. W. K. (2016). Stereotactic body radiotherapy: current strategies and future development. *Journal of Thoracic Disease*, *8*(S6), S517–S527. https://doi.org/10.21037/jtd.2016.03.14

Tsukumo, Y., Naito, M., & Suzuki, T. (2020). Influence of EGFR-activating mutations on sensitivity to tyrosine kinase inhibitors in a KRAS mutant non-small cell lung cancer cell line. *PLOS ONE*, *15*(3), e0229712. https://doi.org/10.1371/journal.pone.0229712

Tunali, I., Gray, J. E., Qi, J., Abdalah, M., Jeong, D. K., Guvenis, A., Gillies, R. J., & Schabath, M. B. (2019). Novel clinical and radiomic predictors of rapid disease progression phenotypes among lung cancer patients treated with immunotherapy: An early report. *Lung Cancer*, *129*, 75–79. https://doi.org/10.1016/j.lungcan.2019.01.010

Ushio, R., Murakami, S., & Saito, H. (2022). Predictive Markers for Immune Checkpoint Inhibitors in Non-Small Cell Lung Cancer. *Journal of Clinical Medicine*, *11*(7), 1855. https://doi.org/10.3390/jcm11071855

Vaishnavi, A., Capelletti, M., Le, A. T., Kako, S., Butaney, M., Ercan, D., Mahale, S., Davies, K. D., Aisner, D. L., Pilling, A. B., Berge, E. M., Kim, J., Sasaki, H., Park, S., Kryukov, G., Garraway, L. A., Hammerman, P. S., Haas, J., Andrews, S. W., Lipson, D., Stephens, P. L., Miller, V. A., Varella-Garcia, M., Jänne, P. A., & Doebele, R. C. (2013). Oncogenic and drug-sensitive NTRK1 rearrangements in lung cancer. *Nature Medicine*, *19*(11), 1469–1472. https://doi.org/10.1038/nm.3352

van der Aalst, C. M., ten Haaf, K., & de Koning, H. J. (2021). Implementation of lung cancer screening: what are the main issues? *Translational Lung Cancer Research*, *10*(2), 1050–1063. https://doi.org/10.21037/tlcr-20-985

van Staveren, W. C. G., Solís, D. Y. W., Hébrant, A., Detours, V., Dumont, J. E., & Maenhaut, C. (2009). Human cancer cell lines: Experimental models for cancer cells in situ? For cancer stem cells? *Biochimica et Biophysica Acta (BBA) - Reviews on Cancer*, *1795*(2), 92–103. https://doi.org/10.1016/j.bbcan.2008.12.004

Vathiotis, I. A., Bafaloukos, D., Syrigos, K. N., & Samonis, G. (2023). Evolving Treatment Landscape of HER2-mutant Non-Small Cell Lung Cancer: Trastuzumab Deruxtecan and Beyond. *Cancers*, *15*(4), 1286. https://doi.org/10.3390/cancers15041286

Vella, V., De Francesco, E. M., Bonavita, E., Lappano, R., & Belfiore, A. (2022). IFN-I signaling in cancer: the connection with dysregulated Insulin/IGF axis. In *Trends in Endocrinology and Metabolism* (Vol. 33, Issue 8, pp. 569–586). Elsevier Inc. https://doi.org/10.1016/j.tem.2022.04.009

Verusingam, N. D., Chen, Y.-C., Lin, H.-F., Liu, C.-Y., Lee, M.-C., Lu, K.-H., Cheong, S.-K., Han-Kiat Ong, A., Chiou, S.-H., & Wang, M.-L. (2021). Generation of osimertinib-resistant cells from epidermal growth factor receptor L858R/T790M mutant non-small cell lung carcinoma cell line. *Journal of the Chinese Medical Association*, *84*(3), 248–254. https://doi.org/10.1097/JCMA.0000000000000438

Vesely, M. D., & Schreiber, R. D. (2013). Cancer immunoediting: antigens, mechanisms, and implications to cancer immunotherapy. *Annals of the New York Academy of Sciences*, *1284*(1), 1–5. https://doi.org/10.1111/nyas.12105

Vicencio, J. M., Evans, R., Green, R., An, Z., Deng, J., Treacy, C., Mustapha, R., Monypenny, J., Costoya, C., Lawler, K., Ng, K., De-Souza, K., Coban, O., Gomez, V., Clancy, J., Chen, S. H., Chalk, A., Wong, F., Gordon, P., Savage, C., Gomes, C., Pan, T., Alfano, G., Dolcetti, L., Chan, J. N. E., Flores-Borja, F., Barber, P. R., Weitsman, G., Sosnowska, D., Capone, E., Iacobelli, S., Hochhauser, D., Hartley, J. A., Parsons, M., Arnold, J. N., Ameer-Beg, S., Quezada, S. A., Yarden, Y., Sala, G. & Ng, T. (2022). Osimertinib and anti-HER3 combination therapy engages immune dependent tumor toxicity via STING activation in trans. *Cell Death & Disease*, *13*(3), 274. https://doi.org/10.1038/s41419-022-04701-3

Vinod, S. K., & Hau, E. (2020). Radiotherapy treatment for lung cancer: Current status and future directions. *Respirology*, *25*(S2), 61–71. https://doi.org/10.1111/resp.13870

Virbel, G., Le Fèvre, C., Noël, G., & Antoni, D. (2021). Stereotactic Body Radiotherapy for Patients with Lung Oligometastatic Disease: A Five-Year Systematic Review. *Cancers*, *13*(14), 3623. https://doi.org/10.3390/cancers13143623

Volta, F., La Monica, S., Leonetti, A., Gnetti, L., Bonelli, M., Cavazzoni, A., Fumarola, C., Galetti, M., Eltayeb, K., Minari, R., Petronini, P. G., Tiseo, M., & Alfieri, R. (2023). Intrinsic Resistance to Osimertinib in EGFR Mutated NSCLC Cell Lines Induced by Alteration in Cell-Cycle Regulators. *Targeted Oncology*, *18*(6), 953–964. https://doi.org/10.1007/s11523-023-01005-0

Walter, A. O., Sjin, R. T. T., Haringsma, H. J., Ohashi, K., Sun, J., Lee, K., Dubrovskiy, A., Labenski, M., Zhu, Z., Wang, Z., Sheets, M., St Martin, T., Karp, R., van Kalken, D., Chaturvedi, P., Niu, D., Nacht, M., Petter, R. C., Westlin, W., Lin, K., Jaw-Tsai, S., Raponi, M., Van Dyke, T., Etter, J., Weaver, Z., Pao, W., Singh, J., Simmons, A. D., Harding, T. C., & Allen, A. (2013). Discovery of a Mutant-Selective Covalent Inhibitor of EGFR that Overcomes T790M-Mediated Resistance in NSCLC. *Cancer Discovery*, *3*(12), 1404–1415. https://doi.org/10.1158/2159-8290.CD-13-0314

Wan, P. T. C., Garnett, M. J., Roe, S. M., Lee, S., Niculescu-Duvaz, D., Good, V. M., Project, C. G., Jones, C. M., Marshall, C. J., Springer, C. J., Barford, D., & Marais, R. (2004). Mechanism of Activation of the RAF-ERK Signaling Pathway by Oncogenic Mutations of B-RAF. *Cell*, *116*(6), 855–867. https://doi.org/10.1016/S0092-8674(04)00215-6

Wang, B., Han, Y., Zhang, Y., Zhao, Q., Wang, H., Wei, J., Meng, L., Xin, Y., & Jiang, X. (2023). Overcoming acquired resistance to cancer immune checkpoint therapy: potential strategies based on molecular mechanisms. *Cell & Bioscience*, *13*(1), 120. https://doi.org/10.1186/s13578-023-01073-9

Wang, C., Tan, J. Y. M., Chitkara, N., & Bhatt, S. (2024). TP53 Mutation-Mediated Immune Evasion in Cancer: Mechanisms and Therapeutic Implications. *Cancers*, *16*(17), 3069. https://doi.org/10.3390/cancers16173069

Wang, S., Wang, Q., Zhu, W., Wei, J., Feng, D., Lv, X., & Liu, M. (2022). Role of Pneumonectomy in T1–4N2M0 Non-Small Cell Lung Cancer: A Propensity Score Matching Analysis. *Frontiers in Oncology*, *12*. https://doi.org/10.3389/fonc.2022.880515

Wang, X., Yang, X., Zhang, C., Wang, Y., Cheng, T., Duan, L., Tong, Z., Tan, S., Zhang, H., Saw, P. E., Gu, Y., Wang, J., Zhang, Y., Shang, L., Liu, Y., Jiang, S., Yan, B., Li, R., Yang, Y., Yu, J., Chen, Y., Gao, G. F., Ye, Q. & Gao, S. (2020). Tumor cell-intrinsic PD-1 receptor is a tumor suppressor and mediates resistance to PD-1 blockade therapy. *Proceedings of the National Academy of Sciences*, *117*(12), 6640–6650. https://doi.org/10.1073/pnas.1921445117

Wee, P., & Wang, Z. (2017). Epidermal Growth Factor Receptor Cell Proliferation Signaling Pathways. *Cancers*, *9*(5), 52. https://doi.org/10.3390/cancers9050052

Wei, S. C., Duffy, C. R., & Allison, J. P. (2018). Fundamental Mechanisms of Immune Checkpoint Blockade Therapy. *Cancer Discovery*, *8*(9), 1069–1086. https://doi.org/10.1158/2159-8290.CD-18-0367

Wolf, N. K., Kissiov, D. U., & Raulet, D. H. (2023). Roles of natural killer cells in immunity to cancer, and applications to immunotherapy. *Nature Reviews Immunology*, *23*(2), 90–105. https://doi.org/10.1038/s41577-022-00732-1

Wu, C.-E., Chang, C.-F., Kou-Sheng, L., Chiang, J., Lee, S.-W., & Chiu, Y.-C. (2020). PD-L1 Immunohistochemistry Comparability and Their Correlation with Clinical Characteristics in NSCLC. *Analytical Cellular Pathology*, *2020*, 1–7. https://doi.org/10.1155/2020/3286139

Wu, J., Savooji, J., & Liu, D. (2016). Second- and third-generation ALK inhibitors for non-small cell lung cancer. *Journal of Hematology & Oncology*, *9*(1), 19. https://doi.org/10.1186/s13045-016-0251-8

Wu, J., Zhao, X., Sun, Q., Jiang, Y., Zhang, W., Luo, J., & Li, Y. (2020). Synergic effect of PD-1 blockade and endostar on the PI3K/AKT/mTOR-mediated autophagy and angiogenesis in Lewis lung carcinoma mouse model. *Biomedicine & Pharmacotherapy*, *125*, 109746. https://doi.org/10.1016/j.biopha.2019.109746

Wu, S.-G., Chang, T.-H., Tsai, M.-F., Liu, Y.-N., Huang, Y.-L., Hsu, C.-L., Jheng, H.-N., & Shih, J.-Y. (2024). miR-204 suppresses cancer stemness and enhances osimertinib sensitivity in non-small cell lung cancer by targeting CD44. *Molecular Therapy - Nucleic Acids*, *35*(1), 102091. https://doi.org/10.1016/j.omtn.2023.102091

Wu, X., Giobbie-Hurder, A., Liao, X., Connelly, C., Connolly, E. M., Li, J., Manos, M. P., Lawrence, D., McDermott, D., Severgnini, M., Zhou, J., Gjini, E., Lako, A., Lipschitz, M., Pak, C. J., Abdelrahman, S., Rodig, S., & Hodi, F. S. (2017). Angiopoietin-2 as a Biomarker and Target for Immune Checkpoint Therapy. *Cancer Immunology Research*, *5*(1), 17–28. https://doi.org/10.1158/2326-6066.CIR-16-0206

Wuerdemann, N., Pütz, K., Eckel, H., Jain, R., Wittekindt, C., Huebbers, C. U., Sharma, S. J., Langer, C., Gattenlöhner, S., Büttner, R., Speel, E.-J., Suchan, M., Wagner, S., Quaas, A., & Klussmann, J. P. (2020). LAG-3, TIM-3 and VISTA Expression on Tumor-Infiltrating Lymphocytes in Oropharyngeal Squamous Cell Carcinoma—Potential Biomarkers for Targeted Therapy Concepts. *International Journal of Molecular Sciences*, *22*(1), 379. https://doi.org/10.3390/ijms22010379

Wujanto, C., Vellayappan, B., Siva, S., Louie, A. V., Guckenberger, M., Slotman, B. J., Onishi, H., Nagata, Y., Liu, M., & Lo, S. S. (2019). Stereotactic Body Radiotherapy for Oligometastatic Disease in Non-small Cell Lung Cancer. *Frontiers in Oncology*, *9*. https://doi.org/10.3389/fonc.2019.01219

Xie, M., Xu, X., & Fan, Y. (2021). KRAS-Mutant Non-Small Cell Lung Cancer: An Emerging Promisingly Treatable Subgroup. *Frontiers in Oncology*, *11*. https://doi.org/10.3389/fonc.2021.672612

Xu, P., & Le Pechoux, C. (2015). Chemoradiotherapy for stage III non-small cell lung cancer: have we reached the limit? *Chinese Clinical Oncology*, *4*(4), 45. https://doi.org/10.3978/j.issn.2304-3865.2015.11.04

Yadollahi, P., Jeon, Y. K., Ng, W. L., & Choi, I. (2021). Current understanding of cancer-intrinsic PD-L1: regulation of expression and its protumoral activity. *BMB Reports*, *54*(1), 12–20. https://doi.org/10.5483/BMBRep.2021.54.1.241

Yaeger, R., Kotani, D., Mondaca, S., Parikh, A. R., Bando, H., Van Seventer, E. E., Taniguchi, H., Zhao, H., Thant, C. N., de Stanchina, E., Rosen, N., Corcoran, R. B., Yoshino, T., Yao, Z., & Ebi, H. (2019). Response to Anti-EGFR Therapy in Patients with BRAF non-V600-Mutant Metastatic Colorectal Cancer. *Clinical Cancer Research : An Official Journal of the American Association for Cancer Research*, *25*(23), 7089–7097. https://doi.org/10.1158/1078-0432.CCR-19-2004

Yan, N., Guo, S., Zhang, H., Zhang, Z., Shen, S., & Li, X. (2022). BRAF-Mutated Non-Small Cell Lung Cancer: Current Treatment Status and Future Perspective. *Frontiers in Oncology*, *12*. https://doi.org/10.3389/fonc.2022.863043

Yan, S., Gritsiuta, A. I., Medrano del Rosal, G., Jones, G., Rocco, G., & Jones, D. R. (2020). Pneumonectomy for lung cancer. *Shanghai Chest*, *4*, 25–25. https://doi.org/10.21037/shc.2019.12.05

Yanagimura, N., Takeuchi, S., Fukuda, K., Arai, S., Tanimoto, A., Nishiyama, A., Ogo, N., Takahashi, H., Asai, A., Watanabe, S., Kikuchi, T., & Yano, S. (2022). STAT3 inhibition suppresses adaptive survival of ALK-rearranged lung cancer cells through transcriptional modulation of apoptosis. *NPJ Precision Oncology*, *6*(1), 11. https://doi.org/10.1038/s41698-022-00254-y

Yang, Y., Huang, J., Xie, N., Huang, H., Xu, S., Cai, J., & Qi, S. (2018). lincROR influences the stemness and crizotinib resistance in EML/ALK+ non-small-cell lung cancer cells. *OncoTargets and Therapy*, *Volume 11*, 3649–3657. https://doi.org/10.2147/OTT.S165290

Yang, Y., Li, C., Liu, T., Dai, X., & Bazhin, A. V. (2020). Myeloid-Derived Suppressor Cells in Tumors: From Mechanisms to Antigen Specificity and Microenvironmental Regulation. *Frontiers in Immunology*, *11*. https://doi.org/10.3389/fimmu.2020.01371

Yang, Y., Li, S., Wang, Y., Zhao, Y., & Li, Q. (2022). Protein tyrosine kinase inhibitor resistance in malignant tumors: molecular mechanisms and future perspective. *Signal Transduction and Targeted Therapy*, *7*(1), 329. https://doi.org/10.1038/s41392-022-01168-8

Yano, T., Miura, N., Takenaka, T., Haro, A., Okazaki, H., Ohba, T., Kouso, H., Kometani, T., Shoji, F., & Maehara, Y. (2008). Never-smoking nonsmall cell lung cancer as a separate entity. *Cancer*, *113*(5), 1012–1018. https://doi.org/10.1002/cncr.23679

Yao, Z., Torres, N. M., Tao, A., Gao, Y., Luo, L., Li, Q., de Stanchina, E., Abdel-Wahab, O., Solit, D. B., Poulikakos, P. I., & Rosen, N. (2015). BRAF Mutants Evade ERK-Dependent Feedback by Different Mechanisms that Determine Their Sensitivity to Pharmacologic Inhibition. *Cancer Cell*, *28*(3), 370–383. https://doi.org/10.1016/j.ccell.2015.08.001

Yao, Z., Yaeger, R., Rodrik-Outmezguine, V. S., Tao, A., Torres, N. M., Chang, M. T., Drosten, M., Zhao, H., Cecchi, F., Hembrough, T., Michels, J., Baumert, H., Miles, L., Campbell, N. M., de Stanchina, E., Solit, D. B., Barbacid, M., Taylor, B. S., & Rosen, N. (2017). Tumours with class 3 BRAF mutants are sensitive to the inhibition of activated RAS. *Nature*, *548*(7666), 234–238. https://doi.org/10.1038/nature23291

Yarden, Y. (2001). Biology of HER2 and Its Importance in Breast Cancer. *Oncology*, *61*(Suppl. 2), 1–13. https://doi.org/10.1159/000055396

Yasuda, H., de Figueiredo-Pontes, L. L., Kobayashi, S., & Costa, D. B. (2012). Preclinical Rationale for Use of the Clinically Available Multitargeted Tyrosine Kinase Inhibitor Crizotinib in ROS1-Translocated Lung Cancer. *Journal of Thoracic Oncology*, *7*(7), 1086–1090. https://doi.org/10.1097/JTO.0b013e3182570919

Yasuda, H., Kobayashi, S., & Costa, D. B. (2012). EGFR exon 20 insertion mutations in non-small-cell lung cancer: preclinical data and clinical implications. *The Lancet Oncology*, *13*(1), e23–e31. https://doi.org/10.1016/S1470-2045(11)70129-2

Yi, M., Niu, M., Xu, L., Luo, S., & Wu, K. (2021). Regulation of PD-L1 expression in the tumor microenvironment. *Journal of Hematology & Oncology*, *14*(1), 10. https://doi.org/10.1186/s13045-020-01027-5

Yoshida, G. J. (2020). Applications of patient-derived tumor xenograft models and tumor organoids. *Journal of Hematology & Oncology*, *13*(1), 4. https://doi.org/10.1186/s13045-019-0829-z

Yu, H. A., Arcila, M. E., Rekhtman, N., Sima, C. S., Zakowski, M. F., Pao, W., Kris, M. G., Miller, V. A., Ladanyi, M., & Riely, G. J. (2013). Analysis of Tumor Specimens at the Time of Acquired Resistance to EGFR-TKI Therapy in 155 Patients with EGFR-Mutant Lung Cancers. *Clinical Cancer Research*, *19*(8), 2240–2247. https://doi.org/10.1158/1078-0432.CCR-12-2246

Yuan, M., Huang, L.-L., Chen, J.-H., Wu, J., & Xu, Q. (2019). The emerging treatment landscape of targeted therapy in non-small-cell lung cancer. *Signal Transduction and Targeted Therapy*, *4*(1), 61. https://doi.org/10.1038/s41392-019-0099-9

Zaman, A., Wu, W., & Bivona, T. G. (2019). Targeting Oncogenic BRAF: Past, Present, and Future. *Cancers*, *11*(8), 1197. https://doi.org/10.3390/cancers11081197

Zapata, L., Caravagna, G., Williams, M. J., Lakatos, E., AbdulJabbar, K., Werner, B., Chowell, D., James, C., Gourmet, L., Milite, S., Acar, A., Riaz, N., Chan, T. A., Graham, T. A., & Sottoriva, A. (2023). Immune selection determines tumor antigenicity and influences response to checkpoint inhibitors. *Nature Genetics*, *55*(3), 451–460. https://doi.org/10.1038/s41588-023-01313-1

Zaretsky, J. M., Garcia-Diaz, A., Shin, D. S., Escuin-Ordinas, H., Hugo, W., Hu-Lieskovan, S., Torrejon, D. Y., Abril-Rodriguez, G., Sandoval, S., Barthly, L., Saco, J., Homet Moreno, B., Mezzadra, R., Chmielowski, B.,

Ruchalski, K., Shintaku, I. P., Sanchez, P. J., Puig-Saus, C., Cherry, G., … Ribas, A. (2016). Mutations Associated with Acquired Resistance to PD-1 Blockade in Melanoma. *New England Journal of Medicine*, *375*(9), 819–829. https://doi.org/10.1056/NEJMoa1604958

Zhang, A., Miao, K., Sun, H., & Deng, C.-X. (2022). Tumor heterogeneity reshapes the tumor microenvironment to influence drug resistance. *International Journal of Biological Sciences*, *18*(7), 3019–3033. https://doi.org/10.7150/ijbs.72534

Zhang, C., Fei, Y., Wang, H., Hu, S., Liu, C., Hu, R., & Du, Q. (2023). CAFs orchestrates tumor immune microenvironment—A new target in cancer therapy? *Frontiers in Pharmacology*, *14*. https://doi.org/10.3389/fphar.2023.1113378

Zhang, D., Liu, X., Shen, F., Zhao, D., Shi, Y., Zhang, H., Liu, J., Gao, X., Chen, M., Zhao, J., Zhong, W., Gao, J., He, M., Liu, Y., Yang, X., Qin, J., Tang, Y., Mu, X., Gu, Y., Zhang, S., Chen, X., Pang, L., Meng, Q., Guo, Y., Zhang, Y., Li, W., Xing, P., Cheng, Y., Xin, T., Li, Q., Li, Y., Chen, J., Gao, F., Jin, B., Rossi, A., Adachi, H., Guerrera, F., Husain, H., Xu, Y., & Wang, M. (2023). Osimertinib versus comparator first-generation epidermal growth factor receptor tyrosine kinase inhibitors as first-line treatment in patients with advanced EGFR-mutated non-small cell lung cancer: a Chinese, multicenter, real-world cohort study. *Translational Lung Cancer Research*, *12*(11), 2229–2244. https://doi.org/10.21037/tlcr-23-577

Zhang, L., Zheng, L., Yang, Q., & Sun, J. (2022). The Evolution of BRAF Activation in Non-Small-Cell Lung Cancer. *Frontiers in Oncology*, *12*. https://doi.org/10.3389/fonc.2022.882940

Zhang, T., Wan, B., Zhao, Y., Li, C., Liu, H., Lv, T., Zhan, P., & Song, Y. (2019). Treatment of uncommon EGFR mutations in non-small cell lung cancer: new evidence and treatment. *Translational Lung Cancer Research*, *8*(3), 302–316. https://doi.org/10.21037/tlcr.2019.04.12

Zhang, X., Huang, Y., & Yang, X. (2021). The complex role of PD-L1 in antitumor immunity: a recent update. *Cellular & Molecular Immunology*, *18*(8), 2067–2068. https://doi.org/10.1038/s41423-021-00702-y

Zhang, Y., & Zhang, Z. (2020). The history and advances in cancer immunotherapy: understanding the characteristics of tumor-infiltrating immune cells and their therapeutic implications. *Cellular & Molecular Immunology*, *17*(8), 807–821. https://doi.org/10.1038/s41423-020-0488-6

Zhao, J., Kim, J. E., Reed, E., & Li, Q. Q. (2005). Molecular mechanism of antitumor activity of taxanes in lung cancer (Review). *International Journal of Oncology*, *27*(1), 247–256.

Zhao, J., Li, X., Fan, R., Qin, Y., Wang, Z., Wang, B., Li, S., Fan, J., Wu, X., Liu, H., Guan, Y., Liang, Y., Zhang, X., & Guo, Y. (2022). Primary resistance to first- and second-generation ALK inhibitors in a non-small cell lung cancer patient with coexisting ALK rearrangement and an ALK F1174L-cis-S1189C de novo mutation: A case report. *Frontiers in Pharmacology*, *13*. https://doi.org/10.3389/fphar.2022.1060460

Zhao, R., Hu, Z., Zhang, X., Huang, S., Yu, G., Wu, Z., Yu, W., Lu, J., & Ruan, B. (2024). The oncogenic mechanisms of the Janus kinase-signal transducer and activator of transcription pathway in digestive tract tumors. *Cell Communication and Signaling*, *22*(1), 68. https://doi.org/10.1186/s12964-023-01421-9

Zhao, Z.-Q., Yu, Z.-Y., Li, J., & Ouyang, X.-N. (2016). Gefitinib induces lung cancer cell autophagy and apoptosis via blockade of the PI3K/AKT/mTOR pathway. *Oncology Letters*, *12*(1), 63–68. https://doi.org/10.3892/ol.2016.4606

Zheng, C., Sun, Y., Ye, X., Chen, H., & Ji, H. (2011). Establishment and characterization of primary lung cancer cell lines from Chinese population. *Acta Pharmacologica Sinica*, *32*(3), 385–392. https://doi.org/10.1038/aps.2010.214

Zhong, W., Myers, J. S., Wang, F., Wang, K., Lucas, J., Rosfjord, E., Lucas, J., Hooper, A. T., Yang, S., Lemon, L. A., Guffroy, M., May, C., Bienkowska, J. R., & Rejto, P. A. (2020). Comparison of the molecular and cellular

phenotypes of common mouse syngeneic models with human tumors. *BMC Genomics*, *21*(1), 2. https://doi.org/10.1186/s12864-019-6344-3

Zhou, J. X., Lee, C. H., Qi, C. F., Wang, H., Naghashfar, Z., Abbasi, S., & Morse, H. C. (2009). IFN Regulatory Factor 8 Regulates MDM2 in Germinal Center B Cells. *The Journal of Immunology*, *183*(5), 3188–3194. https://doi.org/10.4049/jimmunol.0803693

Zhou, K., Li, S., Zhao, Y., & Cheng, K. (2023). Mechanisms of drug resistance to immune checkpoint inhibitors in non-small cell lung cancer. *Frontiers in Immunology*, *14*. https://doi.org/10.3389/fimmu.2023.1127071

Zhou, Y., Yu, F., Zhao, Y., Zeng, Y., Yang, X., Chu, L., Chu, X., Li, Y., Zou, L., Guo, T., Zhu, Z., & Ni, J. (2020). A narrative review of evolving roles of radiotherapy in advanced non-small cell lung cancer: from palliative care to active player. *Translational Lung Cancer Research*, *9*(6), 2479–2493. https://doi.org/10.21037/tlcr-20-1145

Zhou, Z., Liu, Z., Ou, Q., Wu, X., Wang, X., Shao, Y., Liu, H., & Yang, Y. (2021). Targeting FGFR in non-small cell lung cancer: implications from the landscape of clinically actionable aberrations of FGFR kinases. *Cancer Biology and Medicine*, *18*(2), 490–501. https://doi.org/10.20892/j.issn.2095-3941.2020.0120

Zhu, L., Jiang, M., Wang, H., Sun, H., Zhu, J., Zhao, W., Fang, Q., Yu, J., Chen, P., Wu, S., Zheng, Z., & He, Y. (2021). A narrative review of tumor heterogeneity and challenges to tumor drug therapy. *Annals of Translational Medicine*, *9*(16), 1351–1351. https://doi.org/10.21037/atm-21-1948

Zhu, M., Kim, J., Deng, Q., Ricciuti, B., Alessi, J. V., Eglenen-Polat, B., Bender, M. E., Huang, H.-C., Kowash, R. R., Cuevas, I., Bennett, Z. T., Gao, J., Minna, J. D., Castrillon, D. H., Awad, M. M., Xu, L., & Akbay, E. A. (2023). Loss of p53 and mutational heterogeneity drives immune resistance in an autochthonous mouse lung cancer model with high tumor mutational burden. *Cancer Cell*, *41*(10), 1731-1748.e8. https://doi.org/10.1016/j.ccell.2023.09.006

Zhu, Q., Zhan, P., Zhang, X., Lv, T., & Song, Y. (2015). Clinicopathologic characteristics of patients with ROS1 fusion gene in non-small cell lung cancer: a meta-analysis. *Translational Lung Cancer Research*, *4*(3), 300–309.

Zhu, X., Chen, L., Liu, L., & Niu, X. (2019). EMT-Mediated Acquired EGFR-TKI Resistance in NSCLC: Mechanisms and Strategies. *Frontiers in Oncology*, *9*. https://doi.org/10.3389/fonc.2019.01044

Zhu, Z., Ni, J., Cai, X., Su, S., Zhuang, H., Yang, Z., Chen, M., Ma, S., Xie, C., Xu, Y., Li, J., Ge, H., Liu, A., Zhao, L., Rao, C., Xie, C., Bi, N., Hui, Z., Zhu, G., Yuan, Z., Wang, J., Zhao, L., Zhou, W., Rim, C. H., Navarro-Martin, A., Vanneste, B. G. L., De Ruysscher, D., Choi, J. I., Jassem, J., Chang3, J. Y., Kepka, L., Käsmann, L., Milano, M. T., Van Houtte, P., Suwinski, R., Traverso, A., Doi, H., Suh, Y.-G., Noël, G., Tomita, N., , Kowalchuk, R. O., Sio, T. T., Li, B., Lu, B., & Fu, X. (2022). International consensus on radiotherapy in metastatic non-small cell lung cancer. *Translational Lung Cancer Research*, *11*(9), 1763–1795. https://doi.org/10.21037/tlcr-22-644

Zou, H. Y., Friboulet, L., Kodack, D. P., Engstrom, L. D., Li, Q., West, M., Tang, R. W., Wang, H., Tsaparikos, K., Wang, J., Timofeevski, S., Katayama, R., Dinh, D. M., Lam, H., Lam, J. L., Yamazaki, S., Hu, W., Patel, B., Bezwada, D., Frias, R. L., Lifshits, E., Mahmood, S., Gainor, J. F., Affolter, T., Lappin, P. B., Gukasyan, H., Lee, N., Deng, S., Jain, R. K., Johnson, T. W., Shaw, A. T., Fantin, V. R., & Smeal, T. (2015). PF-06463922, an ALK/ROS1 Inhibitor, Overcomes Resistance to First and Second Generation ALK Inhibitors in Preclinical Models. *Cancer Cell*, *28*(1), 70–81. https://doi.org/10.1016/j.ccell.2015.05.010